Identifying and Characterizing Type 1 and Type 2 Eosinophil Subtypes

by

Christopher Daniel Nazaroff

A Dissertation Presented in Partial Fulfillment
of the Requirements for the Degree
Doctor of Philosophy

Approved April 2020 by the
Graduate Supervisory Committee:

Jia Guo, Co-Chair
Mathew Rank, Co-Chair
Joshua LaBaer
Peter Williams

ARIZONA STATE UNIVERSITY

May 2020

ABSTRACT

Eosinophils are innate immune cells that are most commonly associated with parasite infection and allergic responses. Recent studies, though, have identified eosinophils as cells with diverse effector functions at baseline and in disease. Eosinophils in specific tissue immune environments are proposed to promote unique and specific effector functions, suggesting these cells have the capacity to differentiate into unique subtypes. The studies here focus on defining these subtypes using functional, molecular, and genetic analysis as well as using novel techniques to image these subtypes *in situ*.

To characterized these subtypes, an *in vitro* cytokine induced type 1 (E1) and type 2 (E2) eosinophil model was developed that display features and functions of eosinophils found *in vivo*. For example, E1 eosinophils secrete type 1 mediators (e.g., IL-12, CXCL9 and CXCL10), express iNOS and express increased levels of the surface molecules PDL1 and MHC-I. Conversely, E2 eosinophils release type 2 mediators (e.g., IL4, IL13, CCL17, and CCL22), degranulate and express increased surface molecules CD11b, ST2 and Siglec-F. Completion of differential expression analysis of RNAseq on these subtypes revealed 500 and 655 unique genes were upregulated in E1 and E2 eosinophils, respectively. Functional enrichment studies showed interferon regulatory factor (IRF) transcription factors were uniquely regulated in both mouse and human E1 and E2 eosinophils. These subtypes are sensitive to their environment, modulating their IRF and cell surface expression when stimulated with opposing cytokines, suggesting plasticity.

To identify and study these subtypes *in situ*, chromogenic and fluorescent eosinophil-specific immunostaining protocols were developed. Methods were created and optimized, here, to identify eosinophils by their granule proteins in formalin fixed mouse

tissues. Yet, eosinophil-specific antibodies alone are not enough to identify and study the complex interactions eosinophil subtypes perform within a tissue. Therefore, as part of this thesis, a novel highly-multiplexed immunohistochemistry technique was developed utilizing cleavable linkers to address these concerns. This technique is capable of analyzing up to 22 markers within a single biopsy with single-cell resolution. With this approach, eosinophil subtypes can be studied *in situ* in routine patient biopsies.

ACKNOWLEDGMENTS

I want to thank everyone in my labs for all their hard work and dedication to helping me complete this dissertation. I also want to thank the late Dr. James “Jamie” Lee for his uplifting motivational talks and creative ideas. Finally, I want to thank all of my funding sources and the people who helped to secure it so I could continue my research.

TABLE OF CONTENTS

Page

LIST OF TABLES

Table Page

LIST OF FIGURES

CHAPTER 1

INTRODUCTION

The contribution of our immune system to our health and well-being is still a subject of great mystery. An orchestrated set of events sets stage for the development and response of the adaptive and the innate immune systems. These events are not in isolation, but interact with each other and the local stromal cells amplifying or suppressing molecular and cellular activities. The work completed in this dissertation is an effort to define the role and contribution of eosinophils to the body. Eosinophils are highly evolutionarily conserved cells that have classic functions of killing parasites and creating havoc in allergy. Yet, eosinophils are diverse cells with an underappreciated wide variety of immune functions that are important in homeostasis and disease. The work here dives into the novelty of unique functions of eosinophil subtypes in specific environments and the methods available to view these complex cells.

1.1 Mouse Eosinophil Biology

1.1.1 Eosinophil Hematopoiesis and Differentiation

Eosinophils are a white blood cell named after the dye eosin which stains their basic granule proteins a reddish color. Although described by Paul Ehrlich in 1879 for their staining capabilities in blood films, “granule” cells were described previously [1]. Eosinophils develop in the bone marrow from hematopoietic stem cells (HSC). HSC differentiate into multi-potent progenitors (MPP) cells before becoming common myeloid progenitor (CMP) cells then granulocyte macrophage progenitor (GMP) cells in mice. From here GMPs are differentiated into eosinophil progenitor (EoP) cells which lock the

cells into an eosinophil lineage until the fully mature eosinophil is formed. After maturation, the eosinophil either stays in the bone marrow or is released into circulation where it will migrate into various tissues [2]. The development of eosinophils from stem cells to mature eosinophils is driven by soluble mediators and transcription factors.

Many transcription factors have been described to be important in eosinophil development. C/EBPα, PU.1, GATA-1and Xbp1, in particular, are important in eosinophil lineage commitment [3, 4]. Genetic deletions of C/EBP isoforms resulted in deficits in maturation of myeloblasts into granulocytes, eosinophil maturation and macrophage activation [5-7]. PU.1 is an important transcription factor for determining myeloid lineages as well as eosinophil commitment. The most important transcription factor for eosinophil development seems to be GATA-1 which determines eosinophil commitment from GMPs [8, 9]. Xbp1 is a recently described transcription factor that is important for eosinophil maturation and survival but it's exact role remains unknown. From mouse models deletion of Xbp1 results in an absence of mature eosinophils in circulation but EoP's are still present in bone marrow [10]. All transcription factors work in harmony to push commitment and maturation of eosinophils.

Cytokines are a second factor needed for the survival, expansion, and differentiation of eosinophils from EoP to mature eosinophils. IL-5 and GM-CSF work in unison with the transcription factors to promote myeloid and eosinophil lineages [11]. In hematopoiesis, GM-CSF promotes the myeloid lineage which includes neutrophil, macrophage, and eosinophil precursors whereas IL-5 specifically promotes the expansion of the eosinophil lineage [12]. IL-3, which shares the common beta chain with IL-5 and GM-CSF receptors, has been shown to have similar functions for survival and

differentiation in humans [13]. The importance of IL-5 has been shown in mouse models where the lack of IL-5 or IL-5Rα results in a drastic reduction of eosinophils and the overexpression of IL-5 produces elevated eosinophil counts [14-17]. This is true for humans as well, as recently approved biologics that target IL-5/IL-5Rα deplete eosinophils in allergic or hypereosinophilic patients [18]. The effects of IL-5 and GM-CSF are not limited to hematopoiesis, they also have pro-survival and activating properties on mature eosinophils outside of the bone marrow [19, 20].

1.1.2 Eosinophil Survival and Death

After development and migration out of the bone marrow eosinophils can be found in circulation and within tissues. In circulation eosinophils have a relatively short half-life between 8-18hrs [3]. Once in tissues the local immune microenvironment promotes the survival of eosinophils. It is believed that survival is promoted mainly through IL-5, as survival is extended *in vitro* [19] and eosinophils are reduced by anti-IL5 neutralization *in vivo* [21]. IL-5 is mainly produced by T cells and innate lymphoid cells but activated eosinophils are also capable of producing their own IL-5 as well as GM-CSF [22-24]. Without these cytokines eosinophils have increased apoptosis which allows the efficient clearance of these cells without promoting inflammation.

Many different agents can stimulate apoptosis in eosinophils, but death can be attributed to a few common pathways. For example, exposure to specific cytokines, extracellular matrix molecules, or other factors such as glucocorticoids alter the expression of specific cell surface receptors, such as Fas (CD95), Siglec-8(human), CD300a, CD30, leading to signal transduction pathways that may promote apoptosis. Although the exact pathways are not fully understood many have been shown to induce

apoptosis by activation of caspases and mitochondrial dysfunction by reactive-oxygen species [3, 25].

1.1.3 Degranulation

Degranulation is the process by which eosinophils release their secondary granule proteins. This is the classical marker of activation in eosinophils. The secondary granules contain the proteins eosinophil peroxidase (EPX) (mouse and human), major basic protein (MBP) (mouse and human), eosinophil associated ribonucleases (mEARs (mice)/EDN (human)) and eosinophilic cationic protein (ECP (humans)) [26, 27]. EPX is highly specific to both mouse and human eosinophils and not expressed by other cells while the other granule proteins are expressed by other cells such as basophils, neutrophils and macrophages [28].

The structure of the secondary granules is comprised of an electron dense crystalline core, as seen by electron micrograph, which is surrounded by a mixture of granule proteins, cytokines, and other mediators. Several mechanisms of granule protein release have been described to date [27]. 1) Classical exocytosis involves fusion between the granules and the plasma membrane resulting in entire granule release. This can also occur by compound exocytosis where multiple granules will fuse into a super granule before fusion to the plasma membrane [2]. 2) Piecemeal degranulation (PMD) involves granule proteins being mobilized into small vesicles, called sombrero vesicles, which migrate to the plasma membrane where they fuse and are released into the extracellular space. This is believed to be the main mechanism that controls selective release of immune mediators [29]. 3) Cytolysis occurs with the rupture of the plasma membrane from necrosis resulting in the release of intact granules. These cell-free granules can be

triggered to release their contents in response to specific stimuli, acting like an organelle [30].

The cationic proteins are the most abundant proteins found in these granules. MBP is an extremely basic protein with an isoelectric point greater than 11 [31]. It is the most abundant protein within the secondary granules and forms the crystalline core [32, 33]. MBP is expressed as two different homologs MBP-1 and MBP-2 with MBP-2 being exclusive to eosinophils along with EPX [34]. *In vitro* studies show that MBP is cytotoxic to helminths and mammalian cells [35]. The mechanism involves MPB increasing the membrane permeability through surface charge interactions [36]. MBP has activities against basophils, mast cells, neutrophils, platelets, and alveolar macrophages [34]. Lung instillation induces airway hyperresponsiveness in rats, rabbits, and monkeys and airway remodeling in mice [37, 38]. MBP also has antagonistic effects on the M2 muscarinic receptor [39].

EPX is the most abundant protein within the granule matrix [34]. It is a peroxidase that uses hydrogen peroxide and either bromide, chloride or thiocyanate to generate reactive oxygen species (ROS) [34]. These ROS induce oxidative stress and damage on cells which can result in cell death [11]. EPX has also been shown, like MBP, to have direct toxic effects on parasites on its cationic properties [40, 41]. However, EPX has additional non-cytotoxic activities as shown by reduced collagen deposition and mucus production in EPX deficient mouse models [42, 43].

mEARs are ribonucleases that are divergent from ECP and EDN in humans. Although 50% protein sequence identity occurs between these proteins, their functions are not fully known and their expression varies significantly between eosinophils and

other cells such as macrophages [44]. To date more than 13 related mEARs have been identified in mice. These proteins reside in the cytoplasm, and thus can be released in the absence of degranulation. For example, mEAR11 has been demonstrated to promote type 2 immune responses in macrophage, as a distinct function from eosinophils activities potentially [45].

1.1.4 Secreted Eosinophil Mediators

Eosinophils produce an extensive number of mediators that promote or suppress functions in other cells as well as eosinophils. They may do this through rapid release of pre-formed biomolecules found in granules and secretory vesicles [46] or through transcription and translational responses. Eosinophils have the capacity to produce cytokines, chemokines, lipids, enzymes, and small molecules in response to various stimuli [29, 47]. Cytokines and chemokines are important cell signaling proteins that govern the type of immune responses that are initiated through the recruitment and activation of specific immune cells. These signaling molecules make up the immune microenvironments that can be classified into various pathways. For example, IFNγ/CXCL10 are part of type 1 pathways and IL-13/CCL24 are part of type 2 [48]. Although normally associated with type 2 immune responses, eosinophils are capable of producing type 1, type 17, regulatory, and suppressive cytokines [49-52].

Eosinophil immune modulating abilities are not limited to the proteins mentioned above. Eosinophils can also produce lipid mediators such as HETES, leukotrienes, resolvins and prostaglandins which can be inflammatory (Leukotriene C4 [53]) or anti-inflammatory (Protectin D1 [54]) as well as enzymes such as matrix metalloproteinases (MMPs) that are important in tissue remodeling/repair [55].

1.1.5 Eosinophil-specific Mouse Models

Various genetically modified mouse models have been developed that specifically target eosinophils. Three strains have been developed that utilize the eosinophil specific EPX promoter. The PHIL transgenic mouse expresses diphtheria toxin A (DTA) under the eosinophil peroxidase promoter (EPX) [56]. DTA expressed from behind the EPX promoter binds the protein translational machinery creating an eosinophil-specific cell death. iPHIL is a conditional knockout mouse where eosinophils specifically express human diphtheria toxin receptor (DTR) from the natural EPX locus, using the EPX promoter to regulate DTR expression. This allows the selective elimination of eosinophils by the administration of diphtheria toxin [57]. Finally, eoCre is a knockin model that allows the modulation of specific genes in eosinophils. In these mice, mammalianized Cre recombinase was inserted into the natural locus behind the EPX promoter which when crossed with a floxed transgenic mouse allows the specific knock-out (specific gene is floxed) or knock-in (specific gene has a floxed stop cassette) [58]. These mice can be used to study how eosinophil functions change in the absence of specific genes.

dblΔGATA-1 mice were created by the deletion of the high-affinity GATA-binding site in the GATA-1 promoter which as mentioned earlier is important in eosinophil as well as erythroid, megakaryocytes, and mast cell lineages [9]. GATA-1 can recognize multiple binding sites and it was discovered that deletion of the palindromic "double-GATA" binding site specifically blocked the eosinophil lineage and left the other myeloid cells untouched. These mice have provided unique tools to study what happens when eosinophils are missing under homeostasis and during disease.

Two strains of mice with peripheral circulating hypereosinophilia were created by the transgenic over-expression of IL-5. N.J. 1628 mice utilize the CD3δ promoter to over express IL-5 in thymocytes and T cells. All white blood cell population are increased in circulation, but eosinophils make up >60% of total circulating white blood cells [15]. The other IL-5 transgenic mouse induced overexpression of IL-5 from the CD2 promoter found on T cells, natural killer cells, and B cells [14, 59]. These mice also present with higher white blood cell counts and have elevated eosinophils equivalent to parasite-infected animals. Both models showed that overexpression of IL-5 was sufficient to promote eosinophil differentiation in the bone marrow and hypereosinophilia. These mice are important tools in understanding eosinophil biology and have expanded are knowledge on the roles eosinophils play in health and disease. They are no longer seen as cytotoxic end stage effector cells.

1.1.6 Differences between Human and Mice Eosinophils

Animal models are an essential tool in understanding human biology and pathology [60]. Although animal biology does not match human biology exactly there are many conserved mechanisms between them as a result of them sharing 99% of their genes [60]. In the case of eosinophils, human and mouse are very similar but they do have some distinct differences [2]. Morphologically the human eosinophil is bigger, 12-15μm (human) vs 8-10μm (mouse), and the nucleus is bi-lobed versus the segmented circular or ring-like shape of the mouse eosinophil [61]. They share many cell surface markers such as IL-5Rα and CCR3, although in humans CCR3 is found on other cells, such as T cells or mast cells, whereas in mice it is quite specific [2]. There are additional distinctions such as Siglec-8 (human)/Siglec-F (mouse), EMR1 (human)/F4/80 (mouse), and GR1

(mouse), [2]. They both chemoattract towards eotaxin-1 (CCL11) and -2 (CCL24) but only human eosinophils respond to eotaxin-3 (CCL26), mice only express a CCL26 pseudogene [62]. RANTES (CCL5) is another chemokine that attracts both human and mouse eosinophils *in vivo* but in vitro mouse eosinophils do not respond [62-67]. Suggesting migration *in vivo* is secondary to RANTES in mice. Finally differences in release of mediators have been shown where human eosinophils are more sensitive to degranulation *in vivo* and *in vitro* (mediator stimulated) compared to mouse as well as some differences in other immune mediators such as cytokines and chemokines [2].

Of note many studies do not directly compare human and mouse so just because one is reported in human studies does not negate its expression in mice. However, from a genomic perspective we can say that certain genes are specific to one or the other species such as CCL6 being a mouse only gene with only homologs identified in humans [68].

Although there are known differences, many significant similarities exist between human and mice allowing mice to be a model system. Eosinophils are found throughout the body in the same locations: thymus, GI tract, adipose tissue, uterus, blood and bone marrow, for example. The half-life of circulating eosinophils is similar between mouse [57] and human [69], and they similarly respond to type 1 and type 2 environments by releasing type 1 and type 2 cytokines, chemokines, and expressing cell surface molecules. For example, both human and mouse eosinophils express CCL17, IL-4 and IL-13 and upregulate CD11b in response to IL-33/GM-CSF as well as express CXCL10, iNOS, and ICAM-1 in response to IFNγ/TNFα [23, 46, 49, 70-73].

1.2 Roles in Health and Disease

Eosinophils were traditionally thought to be important in type 2 responses such as helminth infections and allergic asthma as a result of eosinophilia being present in both patients with either a parasite infection [74] or asthma [75]. However, as a result of mouse models it is now appreciated that eosinophils not only play a role in parasitic infections and allergic asthma but play many roles in health and disease as described below.

1.2.1 Allergy

Asthma is the most common condition associated with eosinophilia in the airways. Allergic asthma is characterized by goblet metaplasia/mucus hypersecretion and airway hyperresponsiveness (AHR) [76]. Eosinophils are thought to be a major player in asthma pathology where studies have shown correlation between disease severity and eosinophil mediators [77]. Their secondary granule proteins can be found in the bronchial alveolar lavage (BAL) fluid and sputum of patients [78, 79]. Patients also display elevated levels of IL-5 which directly increases hematopoiesis and eosinophil survival [75]. Even though there is significant infiltration of eosinophils in the airways of patients, it is still unclear what their role is. Studying mechanisms in patients has its challenges so much of the literature is primarily from allergen-challenged mouse models of allergic airway disease [80, 81]. These models display characteristics of asthma including mucus hypersecretion, AHR, and airway remodeling [76], but in general there is very little eosinophil degranulation [82, 83]. More recently, studies suggest the role of eosinophils as immune regulatory cells is of greater significance than as mediators of destruction through secondary granule protein release [43, 84]. Interestingly, several studies have shown that

eosinophils modulate T cell activities through the recruitment of allergen-specific T cells, activation of memory T cells, M2 macrophage increases, modulation of dendritic cell (DC) activation, T cell polarization in the lymph node and the suppression of Th1/Th17 responses [85-90]. One study by Jacobsen *et al.* showed that IL-13 from eosinophils and not the granule proteins is responsible for eosinophil-dependent effects [91]. Studies manipulating eosinophils supported their role as a pro-inflammatory destructive cell but therapies targeting eosinophils in patients have not resulted in great success [90]

Eosinophils are found resident in the gastrointestinal (GI) tract from the stomach to the colon during steady-state condition, but they are not found within the esophagus. Eosinophils can infiltrate various parts of the GI during conditions such as eosinophilic esophagitis (EoE), Crohn's disease and ulcerative colitis [90, 92]. EoE is a disease characterized by eosinophil infiltration into the esophagus, esophageal fibrosis and food impaction. IL-5, IL-13, and CCL26 (eotaxin-3) are all prominent molecular features of this disease which drives the recruitment of eosinophils to the esophagus [76, 93]. Therapies targeting eosinophils reduce eosinophilia, but symptoms do not improve much [94]. Crohn's and colitis are both inflammatory bowel diseases where eosinophils contribute to inflammation and remodeling [95, 96]. Again, the roles of these cells are not clear even though they are associated with disease pathologies.

1.2.2 Homeostasis

Eosinophils have many roles in health and homeostatic functions [76, 90, 97, 98]. Eosinophils are found resident in many tissues including the thymus, uterus, adipose tissue, intestine, skin and lung. In the thymus eosinophils localize to the cortico-medullary region where it is thought they play a role in T cell negative selection [99]. In

the uterus eosinophil populations can vary with estrus [100], infiltrate the cervix during pregnancy [101] and are thought to promote postpartum remodeling [102]. In adipose tissue, eosinophil derived IL-4/13 has been shown to modulate alternatively activated macrophages (AAMs) which are important in promoting insulin sensitivity through glucose homeostasis and development of brown fat [103-105]. In the intestine, they are attributed to maintaining homeostasis through immune modulation. Eosinophils have been shown to promote B cell class switching to IgA, maintain gut microbiota composition, and regulate T cell responses [106-109].

They also play a role in mammary gland development. During postnatal development, macrophages and eosinophils are recruited to the growing terminal end buds [110]. When eosinophils are deleted, mammary gland epithelial development is impaired suggesting a role for eosinophils.

More recently in the lungs a resident population of eosinophils has been implicated to the maintenance of lung immune homeostasis. Through interactions with dendritic cells, these resident eosinophils were shown to reduce the type 2 responses during allergen challenge [111].

These studies expand on our knowledge of the roles of eosinophils which are no longer seen as the traditional end stage destructive cell. All these various functions and roles can be attributed to the various mediator eosinophils are able to release.

1.3 Eosinophil Subtypes

1.3.1 LIAR Hypothesis

The paradigm that eosinophils are innate end stage destructive cells has been challenged by the many studies. Although eosinophils and their granule proteins can be found in the lung tissue of asthmatics, there is a lack of evidence to support their direct role in causing damage. Also, eosinophils as previously mentioned have been shown to play roles in adaptive immunity, development and are found resident in various tissues at baseline. All of this evidence supports the idea that eosinophil are a complex cell with pleiotropic functions.

Nearly a decade ago, J. Lee *et al.* proposed that eosinophils are attracted to specific sites that contain cell turnover or stem cell activity(ies) [97]. Once accumulated they believed that instead of reacting by degranulating their cytotoxic proteins they instead regulate the **L**ocal **I**mmunity **A**nd/or **R**emodeling/Repair in both health and disease (The LIAR Hypothesis). They also suggest that eosinophils do not dominate the immune response but instead respond and contribute to the microenvironment present. The local microenvironment is made up of the immune signaling biomolecules that coordinate specific immune responses. Within a type 2 microenvironment they believe that eosinophils exacerbate the immune response by promoting type 2 mediators and inhibiting type 1 responses. Within a Th1/Th17 microenvironment they suggest that eosinophils help suppress immune responses by modulating Th1/Th17 responses. Finally, in a neutral microenvironment they believe that eosinophils neither suppress nor exacerbate local immune responses instead, they help to promote a balance in homeostasis.

As more studies have occurred over the last decade these roles of eosinophils have become more distinct and specialized per immune microenvironment where even type 1 and type 17 environments have unique activities, for example. This suggests that accumulating eosinophils at specific locations will have specific functions based on the local immune microenvironment. Moreover, this suggests that eosinophils may have unique subtype activities based upon their localization.

1.3.2 Leukocyte Subtype Model

Cells with unique functions may be defined by morphology, ontogeny, phenotype, subtype, molecular profiling, and/or activation state/functions depending on the view of the definition and literature [112]. Here subtype is meant as a definition inclusive of cell origin, transcription factor regulation, and functional activities that are unique for the conditions placed on the cell.

The subtype model can be traced back to the early 1970s where T cells were first separated into $CD4^+$ and $CD8^+$ cells [113]. As research progressed studies demonstrated that $CD4^+$ T cell functions were heterogeneous [114-116]. It was later shown that in mice the $CD4^+$ cells could be separated based on the cytokines they produced into Th1 (IL-2, INFγ, GM-CSF, and IL-3) and Th2 (IL-3, IL-4, and IL-5) cells [117]. These subtypes were shown to develop through cytokine stimulation from a common precursor [118, 119]. IL-12 induces Th1 cells through the activation of STAT4 and T-bet transcriptions factors which are responsible for the upregulation of IFNγ and the downregulation of IL-4 and IL5 [120-123]. While IL-4 induces Th2 cells through the activation of transcription factors STAT6, GATA3, and c-Maf which increases IL-4 and IL-5 cytokine production and decreases IFNγ [124]. Interestingly, the cytokines produced by each subtype

promotes their own population in an autocrine fashion while simultaneously inhibiting the expansion of the opposite population [125, 126]. The dependence on cytokine stimulation suggests that the immune microenvironment plays a key role in the activation of these subtypes.

Now T cells can be stratified into Th1, Th2, Th9, Th17, Th22, Treg, and Tfh. All of these subtype develop by specific cytokine stimulation and can be characterized by their cell surface proteins, cytokine production and transcription factors [127]. Similar to T cells, other lymphocytes discovered 12 years ago, termed innate lymphoid cells (ILCs), were registered with the International Union of Immunological Sciences and the Nomenclature Committee (iuis.org) due to their wide range of reported functions and activation states [128]. These were classified into subtype groups: Group 1, Group 2, or Group 3 ILCs. In brief, ILCs were classified by their ontology, transcription factors and cytokine expression: ILC1s express transcription factor T-bet and produce INFγ; ILC2s express transcription factor GATA-3 and produce IL-5 and IL-13, ILC3 express transcription factor RORγt and produce IL-17 [129]. Within these groups there are variations of these subtypes. In part, these variations are due to plasticity of the subtypes. Identification of subtypes by transcription factor regulation was a significant advantage in defining these various groups and subtypes, but also provided demonstrations of plasticity in lymphocytes [130]. For example, ILC2s may be pushed into ILC-1 like subtype upon exposure to IL-12, resulting in reduced GATA-3:T-bet ratio and increased production of INFγ. Thus, cytokine environment, transcription factor expression, and immune functions are key ingredients of defining subtypes.

Myeloid cells, such as dendritic cells and macrophage were originally defined by ontology, the mediators that influence the cytokine release, cell surface expression, and function of these cells in tissues and *ex vivo* [131]. For example, macrophages were originally stratified into M1 and M2 [132]. M1 were activated by IFNγ, LPS and GM-CSF and produced IL1β, TNFα, IL-12, IL-18 and IL-23. M2 were induced by IL-4 and IL-13 and produced IL-10 and TGFβ [133]. It is now appreciated that these cells are more complicated than originally thought and further subtypes have been identified such as M2a, M2b, M2c, M2d and tumor associated macrophages (TAMS) [134-136]. DCs were particularly stratified by cell surface molecules and immune activities (e.g., plasmacytoid vs conventional) and are now being reorganized based on -omics sequencing and functions associated with transcription factor expression [137-139]. This difficulty of defining myeloid cell subtypes is in part due to T-bet, GATA-3, and RORγt being a less significant influencer of subtype function as compared to lymphocytes. Rather, ongoing studies are still defining the roles of other transcription factors, such as PPARs, BCLs, and IRFs that are highly relevant to the functions of these cells. Interferon Regulatory Factor (IRF) in particular appears to be relevant for DC [140] and Macrophage subtype choices [141]. Eosinophils, being in the myeloid family, appear to follow the same pattern. To date a significant regulatory role for T-bet, GATA-3, and RORγt have not been reported for eosinophils, yet these cells respond to unique cytokine environments by expressing unique cell surface molecules and releasing specific mediators.

Subtypes are a very complex system that to this day is still evolving with new discoveries. Although not perfect it allows investigators to have a starting point for which they can branch out and modify as new evidence is uncovered.

1.3.3 Eosinophils Subtypes Identified *in vivo*

Eosinophils are similar to other myeloid cells, such as DCs and macrophage, whereby they have been characterized by activation states including density, morphology, cell surface proteins, released mediators, and location.

The basic definition of eosinophil activation for decades included the identification that degranulated eosinophils were found in the lungs of asthmatics. As blood eosinophils contained granules and eosinophils in asthma did not, this was identified as a state of activation. To define these activated eosinophils, measures of density were completed (i.e., less granules means less density and therefore an activated form). Hypodense eosinophils from patient were more activated compared to the normal-dense eosinophils [142-144]. The hypodense phenotype was shown to be a result of prior eosinophil activation with inflammatory mediators in which eosinophil degranulation occurs [145, 146].A classic method of identifying eosinophils and activation states included taking advantage of the new (at that time) technique of flow cytometry. This permitted multiple cell surface parameters to be tested at once on an individual cell [147-149]. Classic identifiers for both mouse and human eosinophils were IL-5Rα and CCR3. As mentioned previously, IL-5Rα is expressed on EoP to fully differentiated eosinophils, although may be lowered in times of chronic IL-5 exposure [150-153]. Interestingly, IL-5Rα has also been identified on neutrophils with no known function, i.e., it does not appear to signal [154]. In addition, siglec-F (mouse) and siglec-8 (human) are highly expressed by eosinophils but can be expressed by alveolar macrophages and mast cells, respectively [155-157]

Several cell surface molecules are found on eosinophils that may be found on additional myeloid cells, potentially creating overlap during analysis and identification by flow cytometry. For example, F4/80 is a common macrophage marker that is readily identified on eosinophils, albeit at a lower level of intensity [158], yet its ortholog EMR1 in human is highly specific for eosinophils [159]. Similarly, both mouse eosinophils and neutrophils are recognized by antibodies to Gr1 and CD11b yet, eosinophils tend to have lower expression of Gr1 rendering them as a separate population from neutrophils [160]. Thus, a combination of cell surface molecules generates a panel that is eosinophil specific by flow cytometry. In brief, mouse eosinophils are often described as side-scatter^{hi}, IL-5Rα^{+}, CCR3^{+}, Siglec-F^{+}, F4/80^{med,} Gr1$^{low/med,}$ Cd11b^{med} in the standard literature. Human eosinophils are often defined as side-scatter^{hi}, CD14^{-}CD16^{-}Siglec-8^{+}C-kit^{-}, CD11b^{+}CCR3^{+} [161]. Of note, the expression level of cell surface proteins can in different microenvironments. These and additional molecules on the surface of eosinophils can be found here (Review [2]).

When evaluating eosinophils in various tissues at homeostasis investigators described different features of eosinophils. For example, in mice thymic eosinophils were described as being CD11c^{+}, hypodense, released high levels of superoxide anion, and expressed CD25 and CD69 on their cell surface [99]. Within the uterus eosinophils can be described as CD11b+ F4/80+ MHC-II- [162]. In addition, intestinal eosinophils are shown to produce IL-1β, and express increased levels of CD11b, CD11c, MHC-II, and CD80 compared to blood [107, 163, 164].

1.3.4 Eosinophil Subtypes in Allergic Type 2 Microenvironments

Allergic type 2 microenvironments are characterized by elevated expression of type 2 cytokines (e.g., IL-4, IL-5, IL-9, IL-13), chemokines (e.g., CCL11, CCL17, CCL22, CCL24), and prostaglandin D2 [165, 166]. This correlates with an influx of eosinophils, Th2 CD4 T cells, ILC2s, and M2 macrophages. In mice, eosinophils have been found to express these mediators and modulate these pathways, in particular with co-exposure to innate cytokine IL-33, which is a member of the IL-1 family of cytokines. In both human and mouse, eosinophil exposure to IL-33 promotes the release of IL-13 and type 2 chemokines. In mice, IL-13 from eosinophils has been shown to polarize macrophages into a M2 phenotype and to be the major mediator in Th2 pulmonary pathologies [23, 91]. The central role of these cytokines in the pathogenesis of asthma has been the focus of recent therapeutics [18].

Correlating these immune functions with cell surface expression has been the primary means of identifying eosinophil subtypes to date. In asthma, eosinophils have been divided into compartments by the expression of various surface molecules. Circulating eosinophils in patients display variations in CD45, CD45R0, CD48, CD137, IL-17RA and -B, αL integrin, and some of the Fc receptors compared to healthy controls [73, 167]. In BAL fluid eosinophil surface proteins CD11b, CD11c, and CD69 are upregulated and CD62L and IL5rα are found downregulated. Sputum eosinophils were similar where they were shown to increase CD69, PDL1, CD11b, CBRM1/5 [168, 169].

Mouse models of allergic airway disease have been fruitful in identifying and advancing the subtype field. Multiple populations have been described from the lungs of allergen mouse models. Abdala *et al*. described an eosinophil population whose CD11c

and siglec-F expression increased and morphology changed when the population migrated from the lung into the airways [170]. Of note, the nuclei became more segmented and there were cytoplasmic vacuoles present. Ochkur *et al.* identified a $CD69^{+}$ subpopulation within the BAL of an allergen challenged mouse model as well as a severe asthma model, yet this CD69 expression was not correlated with degranulation of eosinophils as previously thought [171]. Mesnil *et al.* recently characterized the lung resident population in detail [111]. These resident eosinophils (rEos) were characterized as Siglec-F^{int} $CD62L^{+}$ $CD101^{lo}$ cells with a ring-shaped nucleus and were IL-5 independent as they were unaffected by IL-5 neutralization. The inflammatory eosinophil population that is recruited after allergen challenge was characterized as Siglec-F^{hi} $CD62L^{-}CD101^{hi}$ cells with a segmented nucleus. They also suggested that the rEos were there to control inflammation by their ability to inhibit DCs from propagating Th2 inflammation. Interestingly, they found evidence for a resident eosinophil population in humans as well. These rEos were less segmented and contained no cytoplasmic vacuoles.

In addition to the models above, models of mixed type 2 and type 17 asthma that include exposure to fungal antigen (*Aspergillus fumigates*) demonstrate some unique features of eosinophils as well. A fourth group identified another population within the lung that they characterized as Siglec-$F^{+}CD11c^{-}GR\text{-}1^{+}$ [160]. GR-1 is a commonly used neutrophil marker that is usually absence or low expressing in eosinophils. GR-1 is unique in which the antibody commonly used RB6-8C5 reacts both Ly6C and Ly6G antigens. It was shown that this sub-population was specifically $Ly6G^{Hi}$ and $Ly6C^{-}$ different from the dual positive neutrophils. They were also shown to produce the B cell chemoattractant CXCL13 as well as IL-27 suggesting a unique role in B cell recruitment.

Additionally, Guerra, et al., showed eosinophils exposed to *Aspergillus* uniquely expressed IL-17 and IL-23 [52].

Within EoE, investigators have described various populations with different functions. Le-Carlson *et al.* described a subpopulation of $CD40^+$ and $CD80^+$ eosinophils that were identified in esophageal biopsies compared to healthy controls suggestion an important antigen presentation role [172]. Multiple populations of circulating eosinophils have described as $PDL1^+$[173] and $CD66b^+$p-$STAT1^+$p-$STAT6^+$ [174] suggesting different roles in inflammation.

Roth *et al.* performed a comprehensive study looking at the distinct cytokine profiles eosinophils produce in various skin diseases to try and characterize functionally different subpopulations [175]. They examined allergic/reactive, infectious, autoimmune, and tumors/lymphomas (LY) and found that the cytokines expressed varied between diseases. Tumor eosinophils mainly expressed IL6, TGF-β, and CCL24; autoimmune eosinophils produced MMP-9 and the allergic and infectious disease eosinophils produced IL-5 as expected.

1.3.5 Eosinophil Subtypes in Type 1 Microenvironments

Type 1 environments are found in situations of viral exposure, cancer, autoimmunity, and transplant rejection. A common theme is a microenvironment rich in IFN-γ and TNFα. IFNγ has a direct anti-viral function but can also modulate the functions of macrophages, B cells, granulocytes and induces activation of subsets of T cells [176]. In response to these stimulations, eosinophils also produce type 1 cytokines such as IL-12, IFNγ, and TNFα [46]. Studies have shown ex vivo in mice and humans exposure to these type 1 cytokines have the capacity to induce type 1 chemokine production by eosinophils as

well as either activate or suppress T cell activity, depending on context [47, 49, 70, 164, 177].

Eosinophil exposure to type 1 environments stimulates expression of toll-like receptors for viral recognition and various enzymes for viral inactivation [76]. Studies into eosinophil interactions with viruses have revealed distinct phenotypes. When exposed to rhinovirus type 16, eosinophils were shown to increase CD18 and ICAM-1 expression which allowed eosinophils to bind the viral particles [178]. When exposed to respiratory syncytial virus eosinophils increase their expression of IRF-7, IFNγ, and NOS2 [179]. During influenza A infection, eosinophils upregulated MHC-I and CD86 and were shown to reduce morbidity and viral burden by recruiting and activating $CD8^+$ T cells [180]. Additionally, in a parainfluenza model, eosinophils increased TLR7 and NOS2 [181] while in a pneumonia virus model eosinophils were shown to release IL-6, CXCL10, CCL2, and CCL3 [182].

In another model of type 1 responses, eosinophils were also found to induce activation of CD8 T cells, produce chemokines, and promote tumor rejection[49]. These eosinophils expressed elevated levels of MHC I as an identifier of their activation state.

Conversely, eosinophils in type 1 environments can potentially have immune suppressive activities. During bacterial infection with H. pylori, Arnold *et al.* found that gastric eosinophils at baseline are $CD45^+CD11b^+$MHC $II^-Ly6G^-SiglecF^+CCR3^+$IL-$5R\alpha^+F4/80^+CD44^+$ but display increased CD11b and siglec-F expression as well as granularity during infection [164]. Interestingly, they found that these eosinophils physically contact bacterium (or bacterial particles) and suppress Th1 activities through the upregulation of PDL1. In a model of lung transplant eosinophils were also found to

have increased expression of PDL1, which was found to be needed for eosinophil inhibition of the T cell receptor [183, 184]. Future work is needed to distinguish these differing functions of type 1 eosinophils as well as the relevant expression and importance of PDL1 as it is found in both type 1 and type 2 environments.

1.4 Imaging Immune Cells

1.4.1 In situ Imaging

Standard methods to visualize eosinophils within tissue is based on histological techniques on thinly sliced (5-10μm thick) formalin fixed paraffin embedded (FFPE) biopsies. Hematoxylin and eosin (H&E) is a commonly used stain that allows the visualization of cytoplasmic, nuclear, and extracellular matrix (ECM) features [185]. On eosinophils hematoxylin stains the nuclei a blue-purple color and eosin stains the cationic granule proteins a reddish-pink in the cytoplasm. The unique pattern of a purple bi-lobed (human) or multi-lobed (mouse) nucleus along with the reddish cytoplasmic granules allows the distinction of eosinophils from other cells within the tissue. H&E is beneficial in being able to simultaneously visualize multiple cell types as well as ECM features but it is limited when evaluating eosinophils. Although eosinophils can be counted it has to be done manually and requires a trained eye. In addition, eosinophils that have fully degranulated or lysed are not stained and in turn are missed in the quantification [186, 187]. Alternatively, eosinophil specific antibodies were developed to overcome these limitations.

Immunostaining assays such as IHC and immunofluorescence (IF) use antibodies that recognize proteins of interest [188]. Antibodies against the granule proteins EPX and

MBP have been developed for eosinophil assessments in mice and humans [189]. EPX is a mouse monoclonal and MBP is a rat monoclonal antibody that specifically recognized only eosinophils. With these antibodies, we are able to employ IHC and IF methods to tissues as well as isolated cells. These methods result in high contrast/isolated staining which allows eosinophils to be quantified by automated image analysis software [190].

1.4.2 Multiplex Imaging

The immune system is composed of a diverse network of cells that are constantly interacting and responding to external stimuli. The interactions and spatial organization of these cells control the outcomes of the specific immune response [191, 192]. Understanding this network will reveal novel insight into how the immune system responds and progresses during disease helping to develop preventative and modulating therapies. Understanding his network is important in predicting immune responses, understanding immune initiation, and developing diagnostics and therapies. This concept is most popular in the cancer community where Galon *et al.* in 2006 showed that the type, density, and location of immune cells within tumors predicted clinical outcome [193].

Although there is a need for gathering all this information within a single section, imaging techniques are limited. Traditional IHC is limited to 1-2 markers for chromogenic detection and 3-5 markers for fluorescent based detection. Chromogenic detection is limited to 2 enzymes and spatial overlap. To stain two markers the two antibodies must be from a different species and located in spate compartments. Two overlapping chromogens cannot be visually separated so co-localization studies are impossible. With these challenges, 1 color IHC is the most commonly technique. To overcome these issues fluorescent techniques can be used but immunofluorescent

imaging is limited to 3-5 markers depending on the microscope setup. Fluorescent imaging is limited by the spectral overlap between fluorophores. The emission spectrums of fluorophores are fairly broad and there are only a limited number of dyes that can be spectrally resolved.

To effectively phenotype multiple cell populations in situ many more markers are necessary. To expand beyond 5 markers many multiplexed methods have been developed that rely on multi-spectral imaging, mass spectrometry imaging, or iterative/sequential staining.

1.4.3 Multispectral Imaging

Multispectral imaging is a technique that uses special equipment to image a multiplexed sample and "unmix" the resulting image into individual signals [194]. To be able to unmix a multiplex image, single color controls as well as an autofluorescence control are first imaged and the spectrums are registered into a spectral library. Once registered, software can perform linear unmixing to separate the individual signals from a multiplexed image [195, 196]. One benefit of this approach is an increased signal-to-noise ratio because the autofluorescence background can be efficiently separated from each signal. This technique has been made popular by Perkin Elmer who developed the Opal system that allows the visualization of up to 7 colors (6 antibodies + DAPI). While 7 colors is an improvement over traditional techniques, to fully phenotype multiple cell types a greater number of makers need to be imaged simultaneously. The specialized equipment and extensive optimization has limited its use in standard biology labs.

1.4.4 Mass Spectrometry-Based

A huge advancement of multiplexing came with the advent of mass cytometry that uses rare earth metals instead of fluorophores as the reporters on antibodies. By relying on isotopically pure non-biological elemental metals, multiplexing up to 100-markers is capable in principle [197]. This approach sends ionized single cells through a mass spectrometer where the individual metals can be quantified. Although originally developed for analysis of isolated single cells two groups have recently combined mass cytometry with IHC to perform highly multiplex imaging on FFPE tissues [198, 199]. Giesen *et al*. described imaging mass cytometry where they use laser ablation coupled to mass cytometry to image 32 proteins simultaneously with 1µm resolution [199]. The image is achieved by advance software that maps the ions back to where the laser was located. Angelo *et al*. imaged 10 markers simultaneously by generating secondary ions with a rasterized oxygen duoplasmatron primary ion beam [198]. Again, similar software is used to map the ions back to the location of the laser. With this technique they achieved 200-300nm resolution which is comparable to traditional immunofluorescence [200]. Each technique has its own advantages. Imaging mass cytometry has the potential to detect up 135 distinct antibodies simultaneously and is not effected by matrix composition while MIBI is currently limited to 7 detectors per acquisition and is sensitive to matrix effects [200]. MIBI on the other hand has higher resolution (~200nm) than imaging mass cytometry and can scan the same area multiple times [198]. Both techniques have extremely slow acquisition times (~8hr/mm^2) and are dependent on expensive reagents and equipment which hinders the widespread use of this approach.

1.4.5 Sequential Staining

These techniques involve serial cycles of staining, imaging, and removal of the signal by heat, pH, osmaolarity, chemicals, and/or photobleaching [201-205]. A sequential staining technique using directly conjugated primary antibodies was first shown by Schubert *et al.* where they developed a technique call multi-epitope-ligand cartography (MELC). MELC involved staining single cells with 1 or 2 antibodies that were conjugated to either FITC or PE. After imaging the signal was removed be photobleaching. Other groups have developed similar techniques where the fluorophores are inactivated by sodium borohydride or alkaline solutions [203, 206, 207]. In practice, these techniques have shown up to 61 markers within a single biopsy. The limitations of these techniques are the cost of labeled primary antibodies, epitope damage from bleaching solution, and the low sensitivity for low abundant proteins [208].

Alternatively, indirect staining avoids the expensive conjugated primaries and instead uses cheaper conjugated secondary antibodies. Not only is this approach cheaper but these techniques are more sensitive because multiple secondaries can bind to the primary amplifying the signal. Further amplification can be achieved by using an enzyme conjugated secondary. Species overlap is the major limitation with this approach, where the secondary cannot distinguish between two primaries from the same species. To overcome this, many methods of antibody removal or stripping have been developed. Although the methods vary slightly the principle is to interrupt the non-covalent interaction between antibody and epitope using a combination of heat, pH, osmolarity, detergents, and/or denaturing reagents. A very common technique involves boiling samples in antigen retrieval buffers such as citrate or tris [209-213] but this has been

shown to not work with every antibody [214]. Lin *et al.* proposed protease degradation of the antibodies between cycles but this can lead to extensive degradation to latter epitopes [215]. Pirici *et al.* found that glycine/SDS pH2 was the best elution buffer when tested against high salt, glycine pH 2, glycine pH 10, Tris/SDS pH 6.75, and Tris/SDS/2-mercaptoethanol pH 6.75 on 14 antibodies [202]. Whereas when Gendusa *et al*. compared glycine/SDS pH2 against 2-Mercaptoethanol/SDS, and 6M urea on multiple antibodies, they found that 2-Mercaptoethanol/SDS had the best overall performance [214]. This raises the concern that the performance of the elution buffer is dependent on the specific antibody and all antibodies need to be tested when developing a new panel [214]. Using indirect immunofluorescence with elution, Bolognesi *et al*. demonstrated more than 30 antibodies could be applied to a single slide [208]. Alternatively, Glas *et al.* developed a brightfield method that they coined SIMPLE for sequential immunoperoxidase labeling and erasing which uses elution with the alcohol soluble chromogen AEC [201]. In this case since the dye/signal is not removed by elution but instead by its solubility in alcohol. This method has been shown to stain up to 12 markers on routine FFPE tissues [212].

Although elution methods allow the use of commercially available unmodified primary antibodies, extensive testing must be performed to check antibody elution efficiency and epitope/tissue damage.

1.4.6 DNA conjugates

Several groups have taken advantage of the properties of DNA to extend multiplexing capabilities. Instead of having antibodies conjugated directly to fluorophores, antibodies are conjugated to known short DNA sequences. Knowing the sequence of each individual

antibody allows each cycle of signal development to be attributed to a specific antibody. After applying conjugated antibodies to tissue the signal is develop by hybridization of fluorophore tagged oligonucleotides [216, 217] or by PCR extension with fluorophore tagged dNTPs [192]. After the images are taken the signal is removed either by removing fluorescent oligonucleotides with low ionic strength elution buffer [216], displacing the strands with non-fluorescent strands, or by cleavage of the fluorophore [192]. This is done in a reiterative fashion and the images are registered and combined together to form a final multiplexed image. Despite the high multiplexing capabilities and minimal tissue damage the primary antibodies are modified which can alter their staining performance [218], most of the conjugated antibodies are not commercially available so conjugation has to be done in-house, and non-specific binding of the labeled oligonucleotides can cause background issues [216] restricting the widespread use of these techniques.

1.4.7 Cleavage

A more novel approach to sequential staining was developed utilizing cleavable linkers. Mondal *et al.* modified the conjugation chemistry so that the link between fluorophores and antibodies could be cleaved using the reducing agent tris(2-carboxyethyl)phosphine (TCEP) [219]. TCEP reduces the azide bond within the linker cleaving the linker and releasing the fluorophores [220]. The use of TCEP over harsher chemicals used in other techniques avoids the issues of tissue damage reducing antigenicity in subsequent cycles as well as being quick, only taking 30 minutes to remove fluorophores. The cleavable linker is not only compatible with individual histological staining techniques such as DNA/RNA FISH, direct and indirect immunofluorescence, and enzyme based IHC techniques (fluorophore conjugated tyramide) but these technique can also be combined

to visualize gene loci (DNA FISH), transcript copies (RNA-FISH), and protein expression (IF) within a single-cell [221]. This allows genomic, transcriptomic, and proteomic studies to be conducted in situ with single-cell resolution. In theory this technique is capable of visualizing hundreds of markers on a single biopsy however, the cleavage is not 100% efficient leaving behind a small amount of signal which compounds with each cycle [219]. In practice 12 cycles have been demonstrated but the maximum number of cycles has not been shown [219].

1.5 Summary and Future Prospective

In summary, we hypothesize that eosinophils can develop into functionally distinct subtypes as a result of the immune microenvironment. Many techniques to immunophenotype cells involve isolating the cells, losing spatial information. To understand the role eosinophil subtypes play in tissues, understanding the microenvironment they are located in is pertinent. To be able to study eosinophils *in situ*, imaging techniques need to be developed to be able to simultaneously identify eosinophils, their subtypes, as well as the other cells within their vicinity. To accomplish this, a novel multiplex imaging approach needs to be taken.

1.6 References

1. Kay, A.B., *The* early *history of the eosinophil.* Clin Exp Allergy, 2015. 45(3): p. 575-82.

2. Lee, J.J., et al., *Human versus mouse eosinophils: "that which we call an eosinophil, by any other name would stain as red".* J Allergy Clin Immunol, 2012. 130(3): p. 572-84.

3. Park, Y.M. and B.S. Bochner, *Eosinophil survival and apoptosis in health and disease.* Allergy Asthma Immunol Res, 2010. 2(2): p. 87-101.

4. Fulkerson, P.C., *Transcription Factors in Eosinophil Development and As Therapeutic Targets.* Frontiers in Medicine, 2017. 4(115).

5. Zhang, D.-E., et al., *Absence of granulocyte colony-stimulating factor signaling and neutrophil development in CCAAT enhancer binding protein α-deficient mice.* Proceedings of the National Academy of Sciences, 1997. 94(2): p. 569-574.

6. Yamanaka, R., et al., *Impaired granulopoiesis, myelodysplasia, and early lethality in CCAAT/enhancer binding protein epsilon-deficient mice.* Proc Natl Acad Sci U S A, 1997. 94(24): p. 13187-92.

7. Tanaka, T., et al., *Targeted disruption of the NF-IL6 gene discloses its essential role in bacteria killing and tumor cytotoxicity by macrophages.* Cell, 1995. 80(2): p. 353-361.

8. Hirasawa, R., et al., *Essential and instructive roles of GATA factors in eosinophil development.* J Exp Med, 2002. 195(11): p. 1379-86.

9. Yu, C., et al., *Targeted deletion of a high-affinity GATA-binding site in the GATA-1 promoter leads to selective loss of the eosinophil lineage in vivo.* J Exp Med, 2002. 195(11): p. 1387-95.

10. Bettigole, S.E., et al., *The transcription factor XBP1 is selectively required for eosinophil differentiation.* Nature Immunology, 2015. 16(8): p. 829-837.

11. Rothenberg, M.E. and S.P. Hogan, *The eosinophil.* Annu Rev Immunol, 2006. 24: p. 147-74.

12. Sanderson, C.J., *Interleukin-5, eosinophils, and disease.* Blood, 1992. 79(12): p. 3101-9.

13. Geijsen, N., L. Koenderman, and P.J. Coffer, *Specificity in cytokine signal transduction: lessons learned from the IL-3/IL-5/GM-CSF receptor family.* Cytokine & Growth Factor Reviews, 2001. 12(1): p. 19-25.

14. Dent, L.A., et al., *Eosinophilia in transgenic mice expressing interleukin 5.* J Exp Med, 1990. 172(5): p. 1425-31.

15. Lee, N.A., et al., *Expression of IL-5 in thymocytes/T cells leads to the development of a massive eosinophilia, extramedullary eosinophilopoiesis, and unique histopathologies.* J Immunol, 1997. 158(3): p. 1332-44.

16. Yoshida, T., et al., *Defective B-1 cell development and impaired immunity against Angiostrongylus cantonensis in IL-5R alpha-deficient mice.* Immunity, 1996. 4(5): p. 483-94.

17. Kopf, M., et al., *IL-5-deficient mice have a developmental defect in CD5+ B-1 cells and lack eosinophilia but have normal antibody and cytotoxic T cell responses.* Immunity, 1996. 4(1): p. 15-24.

18. McGregor, M.C., et al., *Role of Biologics in Asthma.* American journal of respiratory and critical care medicine, 2019. 199(4): p. 433-445.

19. Yamaguchi, Y., et al., *Highly purified murine interleukin 5 (IL-5) stimulates eosinophil function and prolongs in vitro survival. IL-5 as an eosinophil chemotactic factor.* J Exp Med, 1988. 167(5): p. 1737-42.

20. Coeffier, E., D. Joseph, and B.B. Vargaftig, *Role of interleukin-5 in enhanced migration of eosinophils from airways of immunized guinea-pigs.* Br J Pharmacol, 1994. 113(3): p. 749-56.

21. Herndon, F.J. and S.G. Kayes, *Depletion of eosinophils by anti-IL-5 monoclonal antibody treatment of mice infected with Trichinella spiralis does not alter parasite burden or immunologic resistance to reinfection.* The Journal of Immunology, 1992. 149(11): p. 3642.

22. Johnston, L.K. and P.J. Bryce, *Understanding Interleukin 33 and Its Roles in Eosinophil Development.* Frontiers in Medicine, 2017. 4: p. 51.

23. Stolarski, B., et al., *IL-33 Exacerbates Eosinophil-Mediated Airway Inflammation.* The Journal of Immunology, 2010. 185(6): p. 3472-3480.

24. Dubucquoi, S., et al., *Interleukin 5 synthesis by eosinophils: association with granules and immunoglobulin-dependent secretion.* J Exp Med, 1994. 179(2): p. 703-8.

25. Shen, Z.J. and J.S. Malter, *Determinants of eosinophil survival and apoptotic cell death.* Apoptosis, 2015. 20(2): p. 224-34.

26. Rosenberg, H.F., *Eosinophil-Derived Neurotoxin (EDN/RNase 2) and the Mouse Eosinophil-Associated RNases (mEars): Expanding Roles in Promoting Host Defense.* Int J Mol Sci, 2015. 16(7): p. 15442-55.

27. Weller, P.F. and L.A. Spencer, *Functions of tissue-resident eosinophils.* Nature reviews. Immunology, 2017. 17(12): p. 746-760.

28. Schmitz, J., et al., *IL-33, an interleukin-1-like cytokine that signals via the IL-1 receptor-related protein ST2 and induces T helper type 2-associated cytokines.* Immunity, 2005. 23(5): p. 479-90.

29. Davoine, F. and P. Lacy, *Eosinophil Cytokines, Chemokines, and Growth Factors: Emerging Roles in Immunity.* Frontiers in Immunology, 2014. 5: p. 570.

30. Spencer, L.A., et al., *Eosinophil secretion of granule-derived cytokines.* Front Immunol, 2014. 5: p. 496.

31. Hamann, K.J., et al., *The molecular biology of eosinophil granule proteins.* Int Arch Allergy Appl Immunol, 1991. 94(1-4): p. 202-9.

32. Macias, M.P., et al., *Identification of a new murine eosinophil major basic protein (mMBP) gene: cloning and characterization of mMBP-2.* J Leukoc Biol, 2000. 67(4): p. 567-76.

33. Plager, D.A., et al., *A novel and highly divergent homolog of human eosinophil granule major basic protein.* J Biol Chem, 1999. 274(20): p. 14464-73.

34. Acharya, K.R. and S.J. Ackerman, *Eosinophil granule proteins: form and function.* J Biol Chem, 2014. 289(25): p. 17406-15.

35. G J Gleich, a. C R Adolphson, and K.M. Leiferman, *The Biology of the Eosinophilic Leukocyte.* Annual Review of Medicine, 1993. 44(1): p. 85-101.

36. Wasmoen, T.L., et al., *Biochemical and amino acid sequence analysis of human eosinophil granule major basic protein.* J Biol Chem, 1988. 263(25): p. 12559-63.

37. Gundel, R.H., L.G. Letts, and G.J. Gleich, *Human eosinophil major basic protein induces airway constriction and airway hyperresponsiveness in primates.* The Journal of Clinical Investigation, 1991. 87(4): p. 1470-1473.

38. Pégorier, S., et al., *Eosinophil-Derived Cationic Proteins Activate the Synthesis of Remodeling Factors by Airway Epithelial Cells.* The Journal of Immunology, 2006. 177(7): p. 4861-4869.

39. Jacoby, D.B., R.M. Costello, and A.D. Fryer, *Eosinophil recruitment to the airway nerves.* Journal of Allergy and Clinical Immunology, 2001. 107(2): p. 211-218.

40. Auriault, C., M. Capron, and A. Capron, *Activation of rat and human eosinophils by soluble factor(s) released by Schistosoma mansoni schistosomula.* Cellular Immunology, 1982. 66(1): p. 59-69.

41. Locksley, R.M., C.B. Wilson, and S.J. Klebanoff, *Role for Endogenous and Acquired Peroxidase in the Toxoplasmacidal Activity of Murine and Human Mononuclear Phagocytes.* The Journal of Clinical Investigation, 1982. 69(5): p. 1099-1111.

42. Colon, S., et al., *Peroxidasin and eosinophil peroxidase, but not myeloperoxidase, contribute to renal fibrosis in the murine unilateral ureteral obstruction model.* Am J Physiol Renal Physiol, 2019. 316(2): p. F360-f371.

43. Jacobsen, E.A., et al., *Lung Pathologies in a Chronic Inflammation Mouse Model Are Independent of Eosinophil Degranulation.* American Journal of Respiratory and Critical Care Medicine, 2017. 195(10): p. 1321-1332.

44. Zhang, J., K.D. Dyer, and H.F. Rosenberg, *Evolution of the rodent eosinophil-associated RNase gene family by rapid gene sorting and positive selection.* Proc Natl Acad Sci U S A, 2000. 97(9): p. 4701-6.

45. Yamada, K.J., et al., *Eosinophil-associated ribonuclease 11 is a macrophage chemoattractant.* J Biol Chem, 2015. 290(14): p. 8863-75.

46. Spencer, L.A., et al., *Human eosinophils constitutively express multiple Th1, Th2, and immunoregulatory cytokines that are secreted rapidly and differentially.* J Leukoc Biol, 2009. 85(1): p. 117-23.

47. Bandeira-Melo, C. and P.F. Weller, *Mechanisms of eosinophil cytokine release.* Mem Inst Oswaldo Cruz, 2005. 100 Suppl 1: p. 73-81.

48. Annunziato, F., C. Romagnani, and S. Romagnani, *The 3 major types of innate and adaptive cell-mediated effector immunity.* Journal of Allergy and Clinical Immunology, 2015. 135(3): p. 626-635.

49. Carretero, R., et al., *Eosinophils orchestrate cancer rejection by normalizing tumor vessels and enhancing infiltration of CD8(+) T cells.* Nat Immunol, 2015. 16(6): p. 609-17.

50. Willebrand, R. and D. Voehringer, *IL-33-Induced Cytokine Secretion and Survival of Mouse Eosinophils Is Promoted by Autocrine GM-CSF.* PLOS ONE, 2016. 11(9): p. e0163751.

51. Huang, L., et al., *Eosinophil-Derived IL-10 Supports Chronic Nematode Infection.* The Journal of Immunology, 2014. 193(8): p. 4178-4187.

52. Guerra, E.S., et al., *Central Role of IL-23 and IL-17 Producing Eosinophils as Immunomodulatory Effector Cells in Acute Pulmonary Aspergillosis and Allergic Asthma.* PLoS Pathog, 2017. 13(1): p. e1006175.

53. Oyoshi, M.K., et al., *Eosinophil-derived leukotriene C4 signals via type 2 cysteinyl leukotriene receptor to promote skin fibrosis in a mouse model of atopic dermatitis.* Proceedings of the National Academy of Sciences of the United States of America, 2012. 109(13): p. 4992-4997.

54. Isobe, Y., T. Kato, and M. Arita, *Emerging roles of eosinophils and eosinophil-derived lipid mediators in the resolution of inflammation.* Frontiers in immunology, 2012. 3: p. 270-270.

55. Ohno, I., et al., *Eosinophils as a source of matrix metalloproteinase-9 in asthmatic airway inflammation.* Am J Respir Cell Mol Biol, 1997. 16(3): p. 212-9.

56. Lee, J.J., et al., *Defining a link with asthma in mice congenitally deficient in eosinophils.* Science, 2004. 305(5691): p. 1773-6.

57. Jacobsen, E.A., et al., *Eosinophil activities modulate the immune/inflammatory character of allergic respiratory responses in mice.* Allergy, 2014. 69(3): p. 315-27.

58. Doyle, A.D., et al., *Homologous recombination into the eosinophil peroxidase locus generates a strain of mice expressing Cre recombinase exclusively in eosinophils.* Journal of leukocyte biology, 2013. 94(1): p. 17-24.

59. Ortaldo, J.R., et al., *Modulation of lymphocyte function with inhibitory CD2: Loss of NK and NKT cells.* Cellular Immunology, 2007. 249(1): p. 8-19.

60. Rosenthal, N. and S. Brown, *The mouse ascending: perspectives for human-disease models.* Nat Cell Biol, 2007. 9(9): p. 993-9.

61. McGarry, M.P., C.A. Protheroe, and J.J. Lee, *Mouse Hematology: A Laboratory Manual*. 2010: Cold Spring Harbor Laboratory Press.

62. Borchers, M.T., et al., *In vitro assessment of chemokine receptor-ligand interactions mediating mouse eosinophil migration.* J Leukoc Biol, 2002. 71(6): p. 1033-41.

63. Rot, A., et al., *RANTES and macrophage inflammatory protein 1 alpha induce the migration and activation of normal human eosinophil granulocytes.* The Journal of experimental medicine, 1992. 176(6): p. 1489-1495.

64. Das, A.M., et al., *Contrasting roles for RANTES and macrophage inflammatory protein-1 alpha (MIP-1 alpha) in a murine model of allergic peritonitis.* Clinical and experimental immunology, 1999. 117(2): p. 223-229.

65. Gonzalo, J.A., et al., *The coordinated action of CC chemokines in the lung orchestrates allergic inflammation and airway hyperresponsiveness.* The Journal of experimental medicine, 1998. 188(1): p. 157-167.

66. Lee, J.B., et al., *The role of RANTES in a murine model of food allergy.* Immunol Invest, 2004. 33(1): p. 27-38.

67. Schall, T.J., N.J. Simpson, and J.Y. Mak, *Molecular cloning and expression of the murine RANTES cytokine: structural and functional conservation between mouse and man.* Eur J Immunol, 1992. 22(6): p. 1477-81.

68. Coelho, A.L., et al., *The Chemokine CCL6 Promotes Innate Immunity via Immune Cell Activation and Recruitment.* The Journal of Immunology, 2007. 179(8): p. 5474-5482.

69. Lukawska, J.J., et al., *Real-time differential tracking of human neutrophil and eosinophil migration in vivo.* The Journal of allergy and clinical immunology, 2014. 133(1): p. 233-9.e1.

70. Liu, L.Y., et al., *Generation of Th1 and Th2 chemokines by human eosinophils: evidence for a critical role of TNF-alpha.* J Immunol, 2007. 179(7): p. 4840-8.

71. Esnault, S. and E.A. Kelly, *Essential Mechanisms of Differential Activation of Eosinophils by IL-3 Compared to GM-CSF and IL-5.* Critical reviews in immunology, 2016. 36(5): p. 429-444.

72. Bouffi, C., et al., *IL-33 markedly activates murine eosinophils by an NF-kappaB-dependent mechanism differentially dependent upon an IL-4-driven autoinflammatory loop.* J Immunol, 2013. 191(8): p. 4317-25.

73. Johansson, M.W., *Activation states of blood eosinophils in asthma.* Clin Exp Allergy, 2014. 44(4): p. 482-98.

74. Huang, L. and J.A. Appleton, *Eosinophils in Helminth Infection: Defenders and Dupes.* Trends in parasitology, 2016. 32(10): p. 798-807.

75. Lambrecht, B.N. and H. Hammad, *The immunology of asthma.* Nat Immunol, 2015. 16(1): p. 45-56.

76. Rosenberg, H.F., K.D. Dyer, and P.S. Foster, *Eosinophils: changing perspectives in health and disease.* Nat Rev Immunol, 2013. 13(1): p. 9-22.

77. McBrien, C.N. and A. Menzies-Gow, *The Biology of Eosinophils and Their Role in Asthma.* Frontiers in Medicine, 2017. 4(93).

78. Wardlaw, A.J., et al., *Eosinophils and Mast Cells in Bronchoalveolar Lavage in Subjects with Mild Asthma: Relationship to Bronchial Hyperreactivity.* American Review of Respiratory Disease, 1988. 137(1): p. 62-69.

79. Nair, P., et al., *Eosinophil peroxidase in sputum represents a unique biomarker of airway eosinophilia.* Allergy, 2013. 68(9): p. 1177-1184.

80. Blanchet, M.R., M.J. Gold, and K.M. McNagny, *Mouse models to evaluate the function of genes associated with allergic airway disease.* Curr Opin Allergy Clin Immunol, 2012. 12(5): p. 467-74.

81. Kumar, R.K., C. Herbert, and P.S. Foster, *Mouse models of acute exacerbations of allergic asthma.* Respirology, 2016. 21(5): p. 842-9.

82. Denzler, K.L., et al., *Eosinophil major basic protein-1 does not contribute to allergen-induced airway pathologies in mouse models of asthma.* J Immunol, 2000. 165(10): p. 5509-17.

83. Denzler, K.L., et al., *Extensive eosinophil degranulation and peroxidase-mediated oxidation of airway proteins do not occur in a mouse ovalbumin-challenge model of pulmonary inflammation.* J Immunol, 2001. 167(3): p. 1672-82.

84. Jacobsen, E.A., N.A. Lee, and J.J. Lee, *Re-defining the unique roles for eosinophils in allergic respiratory inflammation.* Clin Exp Allergy, 2014. 44(9): p. 1119-36.

85. Jacobsen, E.A., et al., *Allergic pulmonary inflammation in mice is dependent on eosinophil-induced recruitment of effector T cells.* Journal of Experimental Medicine, 2008. 205(3): p. 699-710.

86. Walsh, E.R., et al., *Strain-specific requirement for eosinophils in the recruitment of T cells to the lung during the development of allergic asthma.* J Exp Med, 2008. 205(6): p. 1285-92.

87. Akuthota, P., H.B. Wang, and P.F. Weller, *Eosinophils as antigen-presenting cells in allergic upper airway disease.* Current Opinion in Allergy and Clinical Immunology, 2010. 10(1): p. 14-19.

88. Shi, H.-Z., et al., *Lymph node trafficking and antigen presentation by endobronchial eosinophils.* The Journal of Clinical Investigation, 2000. 105(7): p. 945-953.

89. Jacobsen, E.A., et al., *Eosinophils Regulate Dendritic Cells and Th2 Pulmonary Immune Responses following Allergen Provocation.* The Journal of Immunology, 2011: p. 1102299.

90. Jacobsen, E.A., et al., *The expanding role(s) of eosinophils in health and disease.* Blood, 2012. 120(19): p. 3882-90.

91. Jacobsen, E.A., et al., *Differential activation of airway eosinophils induces IL-13-mediated allergic Th2 pulmonary responses in mice.* Allergy, 2015. 70(9): p. 1148-59.

92. Rothenberg, M.E., *Eosinophilic gastrointestinal disorders (EGID).* Journal of Allergy and Clinical Immunology, 2004. 113(1): p. 11-28.

93. Blanchard, C., et al., *Eotaxin-3 and a uniquely conserved gene-expression profile in eosinophilic esophagitis.* J Clin Invest, 2006. 116(2): p. 536-47.

94. Straumann, A., et al., *Anti-interleukin-5 antibody treatment (mepolizumab) in active eosinophilic oesophagitis: a randomised, placebo-controlled, double-blind trial.* Gut, 2010. 59(1): p. 21-30.

95. Takedatsu, H., et al., *Interleukin-5 participates in the pathogenesis of ileitis in SAMP1/Yit mice.* European journal of immunology, 2004. 34: p. 1561-9.

96. Lampinen, M., et al., *Different regulation of eosinophil activity in Crohn's disease compared with ulcerative colitis.* J Leukoc Biol, 2008. 84(6): p. 1392-9.

97. Lee, J.J., et al., *Eosinophils in health and disease: the LIAR hypothesis.* Clin Exp Allergy, 2010. 40(4): p. 563-75.

98. Marichal, T., C. Mesnil, and F. Bureau, *Homeostatic Eosinophils: Characteristics and Functions.* Frontiers in medicine, 2017. 4: p. 101-101.

99. Throsby, M., et al., *CD11c+ Eosinophils in the Murine Thymus: Developmental Regulation and Recruitment upon MHC Class I-Restricted Thymocyte Deletion.* The Journal of Immunology, 2000. 165(4): p. 1965-1975.

100. Ross , R. and S.J. Klebanoff *THE EOSINOPHILIC LEUKOCYTE : FINE STRUCTURE STUDIES OF CHANGES IN THE UTERUS DURING THE ESTROUS CYCLE.* Journal of Experimental Medicine, 1966. 124(4): p. 653-660.

101. Wang, D., et al., *Eosinophils are cellular targets of the novel uteroplacental heparin-binding cytokine decidual/trophoblast prolactin-related protein.* Journal of Endocrinology, 2000. 167(1): p. 15-28.

102. Timmons, B.C., A.-M. Fairhurst, and M.S. Mahendroo, *Temporal Changes in Myeloid Cells in the Cervix during Pregnancy and Parturition.* The Journal of Immunology, 2009. 182(5): p. 2700-2707.

103. Wu, D., et al., *Eosinophils Sustain Adipose Alternatively Activated Macrophages Associated with Glucose Homeostasis.* Science, 2011. 332(6026): p. 243-247.

104. Qiu, Y., et al., *Eosinophils and type 2 cytokine signaling in macrophages orchestrate development of functional beige fat.* Cell, 2014. 157(6): p. 1292-308.

105. Molofsky, A.B., et al., *Innate lymphoid type 2 cells sustain visceral adipose tissue eosinophils and alternatively activated macrophages.* J Exp Med, 2013. 210(3): p. 535-49.

106. Chu, V.T., et al., *Eosinophils promote generation and maintenance of immunoglobulin-A-expressing plasma cells and contribute to gut immune homeostasis.* Immunity, 2014. 40(4): p. 582-93.

107. Jung, Y., et al., *IL-1beta in eosinophil-mediated small intestinal homeostasis and IgA production.* Mucosal Immunol, 2015. 8(4): p. 930-42.

108. Sugawara, R., et al., *Small intestinal eosinophils regulate Th17 cells by producing IL-1 receptor antagonist.* Journal of Experimental Medicine, 2016. 213(4): p. 555-567.

109. Chen, H.H., et al., *Eosinophils from Murine Lamina Propria Induce Differentiation of Naive T Cells into Regulatory T Cells via TGF-beta1 and Retinoic Acid.* PLoS One, 2015. 10(11): p. e0142881.

110. Gouon-Evans, V., M.E. Rothenberg, and J.W. Pollard, *Postnatal mammary gland development requires macrophages and eosinophils.* Development, 2000. 127(11): p. 2269-82.

111. Mesnil, C., et al., *Lung-resident eosinophils represent a distinct regulatory eosinophil subset.* J Clin Invest, 2016. 126(9): p. 3279-95.

112. Fang, P., et al., *Immune cell subset differentiation and tissue inflammation.* J Hematol Oncol, 2018. 11(1): p. 97.

113. Cantor, H. and E.A. Boyse, *Functional subclasses of T-lymphocytes bearing different Ly antigens. I. The generation of functionally distinct T-cell subclasses is a differentiative process independent of antigen.* Journal of Experimental Medicine, 1975. 141(6): p. 1376-1389.

114. Marrack, P.C. and J.W. Kappler, *Antigen-specific and nonspecific mediators of T cell/B cell cooperation. I. Evidence for their production by different T cells.* J Immunol, 1975. 114(3): p. 1116-25.

115. Liew, F.Y. and C.R. Parish, *Lack of a correlation between cell-mediated immunity to the carrier and the carrier-hapten helper effect.* J Exp Med, 1974. 139(3): p. 779-84.

116. Janeway, C.A., Jr., *Cellular cooperation during in vivo anti-hapten antibody responses. I. The effect of cell number on the response.* J Immunol, 1975. 114(4): p. 1394-401.

117. Mosmann, T.R., et al., *Two types of murine helper T cell clone. I. Definition according to profiles of lymphokine activities and secreted proteins.* J Immunol, 1986. 136(7): p. 2348-57.

118. Seder, R.A., et al., *The presence of interleukin 4 during in vitro priming determines the lymphokine-producing potential of CD4+ T cells from T cell receptor transgenic mice.* Journal of Experimental Medicine, 1992. 176(4): p. 1091-1098.

119. Hsieh, C.S., et al., *Differential regulation of T helper phenotype development by interleukins 4 and 10 in an alpha beta T-cell-receptor transgenic system.* Proceedings of the National Academy of Sciences, 1992. 89(13): p. 6065-6069.

120. Hsieh, C., et al., *Development of TH1 CD4+ T cells through IL-12 produced by Listeria-induced macrophages.* Science, 1993. 260(5107): p. 547-549.

121. Seder, R.A., et al., *Interleukin 12 acts directly on CD4+ T cells to enhance priming for interferon gamma production and diminishes interleukin 4 inhibition of such priming.* Proceedings of the National Academy of Sciences, 1993. 90(21): p. 10188-10192.

122. Jacobson, N.G., et al., *Interleukin 12 signaling in T helper type 1 (Th1) cells involves tyrosine phosphorylation of signal transducer and activator of transcription (Stat)3 and Stat4.* Journal of Experimental Medicine, 1995. 181(5): p. 1755-1762.

123. Szabo, S.J., et al., *A Novel Transcription Factor, T-bet, Directs Th1 Lineage Commitment.* Cell, 2000. 100(6): p. 655-669.

124. Liew, F.Y., *T(H)1 and T(H)2 cells: a historical perspective.* Nat Rev Immunol, 2002. 2(1): p. 55-60.

125. Gajewski, T.F. and F.W. Fitch, *Anti-proliferative effect of IFN-gamma in immune regulation. I. IFN-gamma inhibits the proliferation of Th2 but not Th1 murine helper T lymphocyte clones.* J Immunol, 1988. 140(12): p. 4245-52.

126. Fernandez-Botran, R., et al., *Lymphokine-mediated regulation of the proliferative response of clones of T helper 1 and T helper 2 cells.* Journal of Experimental Medicine, 1988. 168(2): p. 543-558.

127. Golubovskaya, V. and L. Wu, *Different Subsets of T Cells, Memory, Effector Functions, and CAR-T Immunotherapy.* Cancers, 2016. 8(3): p. 36.

128. Vivier, E., et al., *Innate Lymphoid Cells: 10 Years On.* Cell, 2018. 174(5): p. 1054-1066.

129. Spits, H., et al., *Innate lymphoid cells--a proposal for uniform nomenclature.* Nat Rev Immunol, 2013. 13(2): p. 145-9.

130. Robinette, M.L., et al., *Transcriptional programs define molecular characteristics of innate lymphoid cell classes and subsets.* Nat Immunol, 2015. 16(3): p. 306-17.

131. Fang, P., et al., *Immune cell subset differentiation and tissue inflammation.* Journal of hematology & oncology, 2018. 11(1): p. 97-97.

132. Mills, C.D., et al., *M-1/M-2 Macrophages and the Th1/Th2 Paradigm.* The Journal of Immunology, 2000. 164(12): p. 6166-6173.

133. Murray, P.J. and T.A. Wynn, *Protective and pathogenic functions of macrophage subsets.* Nature Reviews Immunology, 2011. 11(11): p. 723-737.

134. Qian, B.Z. and J.W. Pollard, *Macrophage diversity enhances tumor progression and metastasis.* Cell, 2010. 141(1): p. 39-51.

135. Mantovani, A., et al., *The chemokine system in diverse forms of macrophage activation and polarization.* Trends Immunol, 2004. 25(12): p. 677-86.

136. Roszer, T., *Understanding the Mysterious M2 Macrophage through Activation Markers and Effector Mechanisms.* Mediators Inflamm, 2015. 2015: p. 816460.

137. Vu Manh, T.P., et al., *Investigating Evolutionary Conservation of Dendritic Cell Subset Identity and Functions.* Front Immunol, 2015. 6: p. 260.

138. Galli, S.J., N. Borregaard, and T.A. Wynn, *Phenotypic and functional plasticity of cells of innate immunity: macrophages, mast cells and neutrophils.* Nat Immunol, 2011. 12(11): p. 1035-44.

139. Villani, A.-C., et al., *Single-cell RNA-seq reveals new types of human blood dendritic cells, monocytes, and progenitors.* Science, 2017. 356(6335): p. eaah4573.

140. Gabriele, L. and K. Ozato, *The role of the interferon regulatory factor (IRF) family in dendritic cell development and function.* Cytokine Growth Factor Rev, 2007. 18(5-6): p. 503-10.

141. Chistiakov, D.A., et al., *The impact of interferon-regulatory factors to macrophage differentiation and polarization into M1 and M2.* Immunobiology, 2018. 223(1): p. 101-111.

142. Prin, L., et al., *Heterogeneity of human eosinophils. II. Variability of respiratory burst activity related to cell density.* Clinical and experimental immunology, 1984. 57(3): p. 735-742.

143. Prin, L., et al., *Heterogeneity of human peripheral blood eosinophils: variability in cell density and cytotoxic ability in relation to the level and the origin of hypereosinophilia.* Int Arch Allergy Appl Immunol, 1983. 72(4): p. 336-46.

144. Capron, M., et al., *Functional role of the alpha-chain of complement receptor type 3 in human eosinophil-dependent antibody-mediated cytotoxicity against schistosomes.* J Immunol, 1987. 139(6): p. 2059-65.

145. Rothenberg, M.E., et al., *Human eosinophils have prolonged survival, enhanced functional properties, and become hypodense when exposed to human interleukin 3.* J Clin Invest, 1988. 81(6): p. 1986-92.

146. Caulfield, J.P., et al., *A morphometric study of normodense and hypodense human eosinophils that are derived in vivo and in vitro.* Am J Pathol, 1990. 137(1): p. 27-41.

147. Ruhle, P.F., et al., *Development of a Modular Assay for Detailed Immunophenotyping of Peripheral Human Whole Blood Samples by Multicolor Flow Cytometry.* Int J Mol Sci, 2016. 17(8).

148. Ethier, C., P. Lacy, and F. Davoine, *Identification of human eosinophils in whole blood by flow cytometry.* Methods Mol Biol, 2014. 1178: p. 81-92.

149. Geslewitz, W.E., C.M. Percopo, and H.F. Rosenberg, *FACS isolation of live mouse eosinophils at high purity via a protocol that does not target Siglec F*. J Immunol Methods, 2018. 454: p. 27-31.

150. Dyer, K.D., et al., *Functionally competent eosinophils differentiated ex vivo in high purity from normal mouse bone marrow.* J Immunol, 2008. 181(6): p. 4004-9.

151. Liu, L.Y., et al., *Decreased expression of membrane IL-5 receptor alpha on human eosinophils: I. Loss of membrane IL-5 receptor alpha on airway eosinophils and increased soluble IL-5 receptor alpha in the airway after allergen challenge.* J Immunol, 2002. 169(11): p. 6452-8.

152. Wang, P., et al., *Selective inhibition of IL-5 receptor alpha-chain gene transcription by IL-5, IL-3, and granulocyte-macrophage colony-stimulating factor in human blood eosinophils.* J Immunol, 1998. 160(9): p. 4427-32.

153. Tomaki, M., et al., *Eosinophilopoiesis in a murine model of allergic airway eosinophilia: involvement of bone marrow IL-5 and IL-5 receptor alpha.* J Immunol, 2000. 165(7): p. 4040-50.

154. Gorski, S.A., et al., *Expression of IL-5 receptor alpha by murine and human lung neutrophils.* PLoS One, 2019. 14(8): p. e0221113.

155. Tateyama, H., et al., *Siglec-F is induced by granulocyte-macrophage colony-stimulating factor and enhances interleukin-4-induced expression of arginase-1 in mouse macrophages.* Immunology, 2019. 158(4): p. 340-352.

156. Bochner, B.S., *Siglec-8 on human eosinophils and mast cells, and Siglec-F on murine eosinophils, are functionally related inhibitory receptors.* Clin Exp Allergy, 2009. 39(3): p. 317-24.

157. Tateno, H., P.R. Crocker, and J.C. Paulson, *Mouse Siglec-F and human Siglec-8 are functionally convergent paralogs that are selectively expressed on eosinophils and recognize 6'-sulfo-sialyl Lewis X as a preferred glycan ligand.* Glycobiology, 2005. 15(11): p. 1125-35.

158. McGarry, M.P. and C.C. Stewart, *Murine eosinophil granulocytes bind the murine macrophage-monocyte specific monoclonal antibody F4/80.* J Leukoc Biol, 1991. 50(5): p. 471-8.

159. Hamann, J., et al., *EMR1, the human homolog of F4/80, is an eosinophil-specific receptor.* Eur J Immunol, 2007. 37(10): p. 2797-802.

160. Percopo, C.M., et al., *SiglecF+Gr1hi eosinophils are a distinct subpopulation within the lungs of allergen-challenged mice.* J Leukoc Biol, 2017. 101(1): p. 321-328.

161. Johansson, M.W., et al., *Characterization of Siglec-8 Expression on Lavage Cells after Segmental Lung Allergen Challenge.* Int Arch Allergy Immunol, 2018. 177(1): p. 16-28.

162. Diener, K.R., et al., *Multi-parameter flow cytometric analysis of uterine immune cell fluctuations over the murine estrous cycle.* Journal of Reproductive Immunology, 2016. 113: p. 61-67.

163. Xenakis, J.J., et al., *Resident intestinal eosinophils constitutively express antigen presentation markers and include two phenotypically distinct subsets of eosinophils.* Immunology, 2018. 154(2): p. 298-308.

164. Arnold, I.C., et al., *Eosinophils suppress Th1 responses and restrict bacterially induced gastrointestinal inflammation.* J Exp Med, 2018.

165. Boonpiyathad, T., et al., *Immunologic mechanisms in asthma.* Semin Immunol, 2019. 46: p. 101333.

166. Lambrecht, B.N., H. Hammad, and J.V. Fahy, *The Cytokines of Asthma.* Immunity, 2019. 50(4): p. 975-991.

167. Metcalfe, D.D., et al., *Biomarkers of the involvement of mast cells, basophils and eosinophils in asthma and allergic diseases.* World Allergy Organization Journal, 2016. 9(1): p. 7.

168. Johansson, M.W., *Eosinophil Activation Status in Separate Compartments and Association with Asthma.* Frontiers in Medicine, 2017. 4: p. 75.

169. Tak, T., et al., *Similar activation state of neutrophils in sputum of asthma patients irrespective of sputum eosinophilia.* Clin Exp Immunol, 2015. 182(2): p. 204-12.

170. Abdala Valencia, H., et al., *Phenotypic plasticity and targeting of Siglec-F(high) CD11c(low) eosinophils to the airway in a murine model of asthma.* Allergy, 2016. 71(2): p. 267-71.

171. Ochkur, S.I., et al., *Coexpression of IL-5 and Eotaxin-2 in Mice Creates an Eosinophil-Dependent Model of Respiratory Inflammation with Characteristics of Severe Asthma.* The Journal of Immunology, 2007. 178(12): p. 7879.

172. Le-Carlson, M., et al., *Markers of antigen presentation and activation on eosinophils and T cells in the esophageal tissue of patients with eosinophilic esophagitis.* J Pediatr Gastroenterol Nutr, 2013. 56(3): p. 257-62.

173. Venkateshaiah, S.U., et al., *Possible Noninvasive Biomarker of Eosinophilic Esophagitis: Clinical and Experimental Evidence.* Case reports in gastroenterology, 2016. 10(3): p. 685-692.

174. Nguyen, T., et al., *Immunophenotyping of peripheral eosinophils demonstrates activation in eosinophilic esophagitis.* J Pediatr Gastroenterol Nutr, 2011. 53(1): p. 40-7.

175. N., R., et al., *Distinct eosinophil cytokine expression patterns in skin diseases – the possible existence of functionally different eosinophil subpopulations.* Allergy, 2011. 66(11): p. 1477-1486.

176. Ryffel, B., *Introduction*, in *International Review of Experimental Pathology*, G.W. Richter and K. Solez, Editors. 1993, Academic Press. p. 3-6.

177. Velazquez, J.R., et al., *Effects of interferon-gamma on mobilization and release of eosinophil-derived RANTES.* Int Arch Allergy Immunol, 1999. 118(2-4): p. 447-9.

178. Handzel, Z.T., et al., *Eosinophils bind rhinovirus and activate virus-specific T cells.* J Immunol, 1998. 160(3): p. 1279-84.

179. Phipps, S., et al., *Eosinophils contribute to innate antiviral immunity and promote clearance of respiratory syncytial virus.* Blood, 2007. 110(5): p. 1578-86.

180. Samarasinghe, A.E., et al., *Eosinophils Promote Antiviral Immunity in Mice Infected with Influenza A Virus.* J Immunol, 2017. 198(8): p. 3214-3226.

181. Drake, M.G., et al., *Human and Mouse Eosinophils Have Antiviral Activity against Parainfluenza Virus.* Am J Respir Cell Mol Biol, 2016. 55(3): p. 387-94.

182. Dyer, K.D., et al., *Pneumoviruses infect eosinophils and elicit MyD88-dependent release of chemoattractant cytokines and interleukin-6.* Blood, 2009. 114(13): p. 2649-56.

183. Onyema, O.O., et al., *Eosinophils promote inducible NOS-mediated lung allograft acceptance.* JCI Insight, 2017. 2(24).

184. Onyema, O.O., et al., *Eosinophils downregulate lung alloimmunity by decreasing TCR signal transduction.* JCI Insight, 2019. 4(11).

185. Fischer, A.H., et al., *Hematoxylin and eosin staining of tissue and cell sections.* CSH Protoc, 2008. 2008: p. pdb.prot4986.

186. Wright, B.L., et al., *Normalized serum eosinophil peroxidase levels are inversely correlated with esophageal eosinophilia in eosinophilic esophagitis.* Diseases of the Esophagus, 2017. 31(2).

187. Martin, L.J., et al., *Pediatric Eosinophilic Esophagitis Symptom Scores (PEESS v2.0) identify histologic and molecular correlates of the key clinical features of disease.* J Allergy Clin Immunol, 2015. 135(6): p. 1519-28.e8.

188. Magaki, S., et al., *An Introduction to the Performance of Immunohistochemistry.* Methods Mol Biol, 2019. 1897: p. 289-298.

189. Protheroe, C., et al., *A novel histologic scoring system to evaluate mucosal biopsies from patients with eosinophilic esophagitis.* Clin Gastroenterol Hepatol, 2009. 7(7): p. 749-755.e11.

190. Wright, B.L., et al., *Baseline Gastrointestinal Eosinophilia Is Common in Oral Immunotherapy Subjects With IgE-Mediated Peanut Allergy.* Frontiers in Immunology, 2018. 9(2624).

191. Sonnenberg, G.F. and M.R. Hepworth, *Functional interactions between innate lymphoid cells and adaptive immunity.* Nature Reviews Immunology, 2019. 19(10): p. 599-613.

192. Goltsev, Y., et al., *Deep Profiling of Mouse Splenic Architecture with CODEX Multiplexed Imaging.* Cell, 2018.

193. Galon, J., et al., *Type, density, and location of immune cells within human colorectal tumors predict clinical outcome.* Science, 2006. 313(5795): p. 1960-4.

194. Stack, E.C., et al., *Multiplexed immunohistochemistry, imaging, and quantitation: a review, with an assessment of Tyramide signal amplification, multispectral imaging and multiplex analysis.* Methods, 2014. 70(1): p. 46-58.

195. Dickinson, M.E., et al., *Multi-spectral imaging and linear unmixing add a whole new dimension to laser scanning fluorescence microscopy.* Biotechniques, 2001. 31(6): p. 1272, 1274-6, 1278.

196. Mansfield, J.R., *Multispectral Imaging: A Review of Its Technical Aspects and Applications in Anatomic Pathology.* Veterinary Pathology, 2013. 51(1): p. 185-210.

197. Bandura, D.R., et al., *Mass cytometry: technique for real time single cell multitarget immunoassay based on inductively coupled plasma time-of-flight mass spectrometry.* Anal Chem, 2009. 81(16): p. 6813-22.

198. Angelo, M., et al., *Multiplexed ion beam imaging of human breast tumors.* Nat Med, 2014. 20(4): p. 436-42.

199. Giesen, C., et al., *Highly multiplexed imaging of tumor tissues with subcellular resolution by mass cytometry.* Nat Methods, 2014. 11(4): p. 417-22.

200. Bodenmiller, B., *Multiplexed Epitope-Based Tissue Imaging for Discovery and Healthcare Applications.* Cell Syst, 2016. 2(4): p. 225-38.

201. Glass, G., J.A. Papin, and J.W. Mandell, *SIMPLE: a sequential immunoperoxidase labeling and erasing method.* J Histochem Cytochem, 2009. 57(10): p. 899-905.

202. Pirici, D., et al., *Antibody elution method for multiple immunohistochemistry on primary antibodies raised in the same species and of the same subtype.* J Histochem Cytochem, 2009. 57(6): p. 567-75.

203. Gerdes, M.J., et al., *Highly multiplexed single-cell analysis of formalin-fixed, paraffin-embedded cancer tissue.* Proc Natl Acad Sci U S A, 2013. 110(29): p. 11982-7.

204. Schubert, W., et al., *Analyzing proteome topology and function by automated multidimensional fluorescence microscopy.* Nat Biotechnol, 2006. 24(10): p. 1270-8.

205. Wahlby, C., et al., *Sequential immunofluorescence staining and image analysis for detection of large numbers of antigens in individual cell nuclei.* Cytometry, 2002. 47(1): p. 32-41.

206. Adams, D.L., et al., *Multi-Phenotypic subtyping of circulating tumor cells using sequential fluorescent quenching and restaining.* Scientific Reports, 2016. 6: p. 33488.

207. Lin, J.R., et al., *Highly multiplexed immunofluorescence imaging of human tissues and tumors using t-CyCIF and conventional optical microscopes.* Elife, 2018. 7.

208. Bolognesi, M.M., et al., *Multiplex Staining by Sequential Immunostaining and Antibody Removal on Routine Tissue Sections.* Journal of Histochemistry & Cytochemistry, 2017. 65(8): p. 431-444.

209. Toth, Z.E. and E. Mezey, *Simultaneous visualization of multiple antigens with tyramide signal amplification using antibodies from the same species.* J Histochem Cytochem, 2007. 55(6): p. 545-54.

210. Carstens, J.L., et al., *Spatial computation of intratumoral T cells correlates with survival of patients with pancreatic cancer.* Nat Commun, 2017. 8: p. 15095.

211. Parra, E.R., et al., *Validation of multiplex immunofluorescence panels using multispectral microscopy for immune-profiling of formalin-fixed and paraffin-embedded human tumor tissues.* Scientific Reports, 2017. 7: p. 13380.

212. Tsujikawa, T., et al., *Quantitative multiplex immunohistochemistry reveals myeloid-inflamed tumor-immune complexity associated with poor prognosis.* Cell reports, 2017. 19(1): p. 203-217.

213. Lan, H.Y., et al., *A novel, simple, reliable, and sensitive method for multiple immunoenzyme staining: use of microwave oven heating to block antibody crossreactivity and retrieve antigens.* Journal of Histochemistry & Cytochemistry, 1995. 43(1): p. 97-102.

214. Gendusa, R., et al., *Elution of High-affinity (>10(-9) K(D)) Antibodies from Tissue Sections: Clues to the Molecular Mechanism and Use in Sequential Immunostaining.* Journal of Histochemistry and Cytochemistry, 2014. 62(7): p. 519-531.

215. Lin, J.R., M. Fallahi-Sichani, and P.K. Sorger, *Highly multiplexed imaging of single cells using a high-throughput cyclic immunofluorescence method.* Nat Commun, 2015. 6: p. 8390.

216. Wang, Y., et al., *Rapid Sequential in Situ Multiplexing with DNA Exchange Imaging in Neuronal Cells and Tissues.* Nano Lett, 2017. 17(10): p. 6131-6139.

217. Schweller, R.M., et al., *Multiplexed in situ immunofluorescence using dynamic DNA complexes.* Angew Chem Int Ed Engl, 2012. 51(37): p. 9292-6.

218. Vira, S., et al., *Fluorescent-labeled antibodies: Balancing functionality and degree of labeling.* Analytical Biochemistry, 2010. 402(2): p. 146-150.

219. Mondal, M., et al., *Highly Multiplexed Single-Cell In Situ Protein Analysis with Cleavable Fluorescent Antibodies.* Angew Chem Int Ed Engl, 2017. 56(10): p. 2636-2639.

220. Guo, J., *System and method for iterative detection of biological molecules*. 2018, Google Patents.

221. Mondal, M., et al., *Highly multiplexed single-cell in situ RNA and DNA analysis with bioorthogonal cleavable fluorescent oligonucleotides.* Chem Sci, 2018. 9(11): p. 2909-2917.

CHAPTER 2

EOSINOPHIL SUBTYPES AND PLASTICITY INDUCED BY TYPE 1 AND TYPE 2 CYTOKINES

2.1 Introduction/Abstract

Eosinophils are commonly thought to be a rare granulocyte mainly associated with parasitic infections and allergic disease. Although traditionally known as end-stage destructive cells by the release of their cytotoxic granules new studies show they have many functions in both health and disease [90, 98]. The diversity of eosinophil tissue localization and functional activities is extensive and only recently being characterized. Eosinophils participate in intestinal and metabolic homeostasis as well as organ development, for example [27]. Eosinophils are associated with many diseases such as atopic dermatitis, asthma, eosinophilic esophagitis, nasal polyposis, myocarditis, muscle injury, inflammatory bowel diseases, cancer, allograft rejection/tolerance, and viral infections where they are found in various tissues [49, 183, 222]. Their associated functions in these diseases and at homeostasis have recently led to the hypothesis that eosinophils have the capacity to differentiate into subtypes similar to the activities of other leukocytes.

Cell subtypes have been defined in the literature by a wide array of factors including ontology, activating molecules, expression of specific mediators, cell-cell interactions, transcription factors, signaling pathways, tissue localization, and many additional metrics [124, 129, 136, 137, 140, 141, 223]. Many of these features are poorly defined for eosinophils as a means of classifying eosinophil subtypes. Earlier attempts at stratifying eosinophil subtypes started with the observations of normaldense vs.

hypodense eosinophils in humans where the hypodense eosinophils were associated with allergic disease states and the release of specific mediators (e.g., granule proteins) [142-146]. Additionally, activation states of eosinophils have only been related to allergic or type 2 immune responses and examining the expression of a few cell surface molecules per study. Although *in vitro* work with human eosinophils demonstrated these cells may be polarized by type 1 and type 2 cytokines to express some unique mediators, much remained undefined and further clarification did not arrive until studies with mouse models [46, 70, 71, 224]. With use of mouse models of disease, eosinophils have been found to promote specific and contrasting immune pathways in type 1 microenvironments as compared to the classic type 2 microenvironments. For example, immune responses to intracellular pathogens, lung transplant, and cancer are dominated by type 1 cytokines such as IFNγ and TNFα where eosinophils have been shown *in vivo* to release type 1 chemokines (e.g., CXCL10), increase expression of cell surface molecules such as MHC I and PDL1, and modulate CD8 T cell activities [49, 164, 178, 180, 181, 183, 184]. Many studies of allergic asthma have demonstrated that IL-33 and type 2 cytokines IL-4 and IL-5 induce eosinophils to release type 2 cytokines (e.g., IL-4 and IL-13) and chemokines (e.g., CCL22) to polarize M2 macrophage and recruit T cells, respectively [23, 85, 89, 91, 225]. The comparisons of type 1 and type 2 functions of eosinophils are currently disjointed, and little data exists demonstrating a direct comparison of type 1 and type 2 polarized eosinophils. Compounding this issue are technical difficulties whereby techniques such as scRNA-seq have been unable to define eosinophils both from tissue and *in vitro*, most likely because of the assumed low

abundance of RNA and high amount of RNAses [226]. As such, the composition and role of type 1 and type 2 eosinophils are not well characterized.

We developed an *in vitro* model of type 1 and type 2 eosinophils, E1 and E2, respectively, using eosinophils isolated from blood that are treated with specific cytokine activation. By mimicking the cytokine microenvironments found in type 1 [49, 164, 178, 180, 181, 183, 184] and type 2 immune responses [49, 91], eosinophils were successfully polarized into differential subtypes that correlated significantly with the reported *in vivo* characteristics of type 1 and type 2 eosinophils in mice [23, 85, 89, 91, 225]. This included predicted and novel findings in cell surface expression, morphological characteristics, viability, effector functions and gene expression. Furthermore, we identified transcriptional regulators known as interferon regulatory factors (IRFs) that were differentially regulated in E1 and E2 eosinophils and modulated by cytokine exposure indicating eosinophil subtype plasticity. The IRF transcription factors are classic modulators of other myeloid subtype differentiation and activities, and here we show for the first time IRF1 and IRF4 differential expression in eosinophil subtypes for both mouse and humans. Altogether, our results demonstrate unique insight into eosinophil biology under various disease related conditions.

2.2 Results

2.2.1 Type 1 and type 2 *in vitro* activated eosinophils and cell surface molecules.

We developed an *in vitro* model of eosinophil subtypes based on cytokine cocktails that represent the type 1 and type 2 microenvironments that eosinophils encounter in diseases such as cancer and allergic asthma, respectively. In particular, eosinophil activation by

the type 1 cytokine cocktail of IFNγ and TNFα was previously shown to induce unique downstream expression and anti-tumor activities in a model of melanoma [49]. Conversely, activation of eosinophils with type 2 associated cytokines IL-33, GM-CSF and IL-4 has previously shown to be necessary for eosinophils to express type 2 cytokines and chemokines and induce lung pathologies in a model of allergic asthma [91]. Blood eosinophils isolated from IL-5 transgenic mice NJ1638 were cultured *in vitro* for 18hrs using these type 1 or type 2 cytokines. E1 eosinophils were generated using a type 1 cocktail containing IFNγ and TNFα. E2 eosinophils were generated using a type 2 cocktail containing IL-33, GM-CSF, and IL-4. As a control, E0 eosinophils were cells cultured without activating type 1 or type 2 cytokines.

To be able to discriminate subtype populations, we screened cell surface markers by flow cytometry. We first tested the common eosinophil identification markers CCR3, CD11b, Siglec-F, F4/80, and IL-5Rα (Figure 2.4.1a, b). E0 eosinophils displayed the highest expression of CCR3 with decreasing expression in E1 eosinophils and even lower expression in E2. E2 eosinophils expressed more CD11b, Siglec-F, and F4/80 surface markers compared to E1 eosinophils. GR-1 expression is commonly used to distinguish eosinophils from neutrophils however, GR-1 has recently been shown to identify sub-populations of eosinophils in an allergic mouse model [160]. E1 eosinophils displayed high expression of GR-1 compared to E0 and E2 (Figure 2.4.1c, d). GR-1 (clone RB6-8C5) is known to recognize both Ly6C and Ly6G. Using clones specific for Ly6G and Ly6C it was determined the increase in GR-1 in E1 eosinophils was due to increased expression of Ly6C.

Next we screened a panel of cell surface markers that have been previously reported *in vivo* on eosinophils in type 1 [164, 180, 183, 184, 227] and type 2 polarized environments of disease [23, 73, 111, 156, 170, 171, 228]. *In vivo*, the presence of IFNγ and TNFα has been found to associate with increased PDL1 and MHC-I expression. *In vitro* this is recapitulated as E1 eosinophils express increased PDL1 and MHC-I in addition to higher levels of ICAM1 as compared to E0 or E2 eosinophils (Figure 2.4.1e, f). Similarly, E2 eosinophils express higher levels of ST2, CD80, CD11c and CD69 (Figure 2.4.1g, h) as reported before for mouse eosinophils in allergic models [23, 163, 170, 171]. Cell surface molecules IL-5Rα, CD44, and CD101 were unchanged between groups (Figure 2.4.2). Altogether these data demonstrate *in vitro* cytokine activation is sufficient to polarize eosinophils into cell surface expression phenotypes similar to those found *in vivo*.

2.2.2 Eosinophils exposed to type 1 and type 2 cytokines have unique morphology, viability, and mediator release.

Eosinophils have been shown *in vitro* and *in vivo* to display morphological changes such as increased hypersegementation of the nuclei and presence of vacuole-like structures in response to various stimulants [111, 170, 229-232]. After activation, morphology was evaluated on cyto-centrifuged cells with Hema 3 staining (Figure 2.4.3a, b). There were no apparent morphological differences between E0 and E1, both containing circular or figure eight nuclei and the absence of vacuoles. Similar to previous reports [111, 170, 232], the type 2 cytokines induced E2 eosinophils to develop a distinct morphological change. Approximately 50% of the E2 eosinophil population exhibited nuclear

hypersegmentation and increased numbers of optically clear vacuole-like structures in the cytoplasm (Figure 2.4.3c).

The presence of vacuole-like structure has been reported to associate with increased cell lysis and degranulation [230], yet cytokines such as IL-3, IL-5, GM-CSF, and IL-33 have been shown to increase eosinophil survival ([50, 71]. To investigate how these cocktails effected survival we evaluated cell viability by Annexin V/PI flow cytometry. No significant difference in viability is seen between the three subtypes at 24 hours. After 48 hours of stimulation with cytokines, E1 eosinophils were found to have poorer viability than E0 eosinophils (Figure 2.4.3d). This suggests the morphology of the eosinophil is disconnected to the viability of the cell *ex vivo.*

Eosinophils in type 2 disease models have been demonstrated to undergo degranulation [171], yet little is known regarding the degranulation of eosinophils in type 1 environments. Granule protein eosinophil peroxidase (EPX) was released into the culture supernatant of E2 eosinophils at significantly higher levels than E0 or E1 eosinophils after 18 hours of culture (Figure 2.4.3e). As E2 eosinophils are similar in viability to E0 and E1 eosinophils at this time point, it is unlikely the increase in EPX is due to release from dead cells.

Eosinophils produce a plethora of mediators in response to various stimuli. To confirm our subtypes follow the same pattern as found *in vivo* and reported previously, we examined their cytokine and chemokine expression (Figure 2.4.4). E1 eosinophils secreted CXCL9, CXCL10, CCL5, and IL-12a although IL-12a was the only protein that was not secreted at the highest level compared to E0 and E2 eosinophils. E2 cells secreted a specific profile with high levels of IL-6, IL-9, IL-13, CCL2, CCL3, CCL22,

and CCL17. Therefore *in vitro* cytokine induction is sufficient to induce many of the features seen *in vivo* in type 1 and type 2 environments.

2.2.3 RNAseq reveals subtype specific gene expression profiles of type 1 and type 2 eosinophils.

Having shown that these different polarized eosinophils displayed distinct characteristics relevant to their reported *in vivo* features, we performed RNAseq to identify novel gene expression profiles and pathways in mouse E0, E1, and E2 eosinophils. Gene expression profiling identified genes in common and distinct from each subtype. After differential expression analysis, E1 displayed 1001 dysregulated genes, with 697 genes being upregulated compared to E0 (Figure 2.4.5a). Similarly, E2 displayed a total of 1772 dysregulated genes ($-2 \geq \log FC \geq 2$, adjusted p-value <0.05) compared to E0, with 852 being up-regulated (Figure 2.4.5b). When E1 and E2 are compared directly to each other they share 142 up-regulated genes and 55 down-regulated genes leaving 500 and 655 unique upregulated genes in E1 and E2 respectively (Figure 2.4.5c). To validate RNAseq, we performed RT-PCR on genes elevated in each subtype and relevant to type 1 and type 2 responses. E2 highly upregulated GM-CSF, CCL24, CCL17, CCL22 and IL-13 all of which have been shown to be expressed by eosinophils in a type 2 allergic environment [23, 50, 72, 91, 233, 234], in addition to S1PR3, which has not been demonstrated previously to be increased in eosinophils upon IL-33 exposure (Figure 2.4.6a). On the other hand E1 highly upregulated CXCL9, CXCL10, CCL5, Nos2, and IL-12b that have been shown to be important in Th1 related diseases [29, 49, 181, 183, 235] (Figure 2.4.6b).

Functional enrichment analysis was completed using several software packages on genes uniquely upregulated (FC≥2 excluding genes with a FC≥2 in the other subtype, adjusted p-value <0.05) in E1 or E2 eosinophils. Using ToppGene, which calculates numerous functional enrichment and gene analyses, we found several differences (Tables 2.4.1, 2). In particular, GO analysis revealed E1 eosinophils had increased innate immune responses and defense to organisms and biotic stimulus. The MHC-I class peptide binding loading complex was increased along with increased lysosome function. GO analysis of E2, conversely revealed increased kinase activity, regulation to immune and cytokine pathways, as well as increased cell surface cellular components. Pathway analysis, which relies significantly on REACTOME and KEGG for this program, showed E1 eosinophils were highly upregulated in interferon signaling pathways (IFNα/IFNβ/IFNγ) while E2 eosinophils were highly upregulated in interleukin signaling, including IL-4/-13 and IL-10. Transcription factor (TF) interactions indicated STAT1, IFNAR2 and PSMB8, and STAT5 were up regulated in E1. E2 was predominated by MyD88, FYN, IRAK1, and MAPK interactions. Altogether these profiles pointed toward patterns recognized with genes in the DisGeNET database. E1 eosinophils were associated with viral and autoimmune diseases, which are often characterized with type 1 environments. E2 eosinophils were associated with asthma, B cell lymphomas, and multiple sclerosis.

2.2.4 Transcription factors of the IRF family are differentially regulated in mouse and human eosinophils.

ToppGene analysis revealed the STAT1 pathway was highly upregulated in E1 eosinophils and MyD88 in E2 eosinophils. Noted in the gene sets for these two

interactions was the presence of a TF group known as interferon regulatory factors (IRF(s)) [236]. IRF1 and IRF9 were found to be highly elevated genes in the STAT1 interaction in ToppGene for E1 (Table 2.4.3a). IRF4 was found upregulated in the MyD88 interaction in ToppGene for E2 (Table 2.4.3b). This class of TFs includes IRF1-9 and are associated with features of subtype differentiation in other cells, such as macrophage [141] or T cells [236], but has never been described in eosinophils. Therefore we confirmed the expression of these IRFs by RT-PCR in E1 and E2 eosinophil subtypes. RT-PCR assessments showed increases in IRF1, -5, and -8 in E1 eosinophils (Figure 2.4.7). Similarly, IRF4, often in opposing pathways to IRF1 according to the literature [236], was increased in E2 eosinophils. IRF3 remained unchanged between E1 and E2 eosinophils. These results suggest the identification of novel transcriptional regulation pathways in eosinophils promoting subtype features.

To determine if these novel subtype-associated IRF transcription factors are relevant to human eosinophils, we isolated human eosinophils and cultured them in E0, E1, and E2 cytokine conditions (with the caveat here only 1ng/mL of IL-5 was added to the human eosinophil cultures) for 18 hours. Of note, human E2 eosinophils did not appear to undergo the same morphological changes as mouse eosinophils, indicating a species difference (Figure 2.4.8a). We decided to test the IRFs that are opposed most often in the literature and specific to E1 and E2 eosinophils in mice. By RT-PCR human E1 eosinophils were found to have significantly elevated IRF1 and as well as some expression of IRF4. The human E2 expression of IRF4 was no different between E1 and E2 in this dataset, yet the downstream genes regulated by IRF4 [237] (e.g., IL-4) were uniquely up in E2 indicating the kinetics of the transcription factors might be slightly

different in mouse and human eosinophils (Figure 2.4.8b). Similarly, BAL allergen challenge in asthmatics increases IRF4, and allergen challenge in mice specifically upregulated IRF4 in mice [238, 239].

2.2.5 Type 1 and type 2 eosinophils display plasticity based on transcription factor expression of IRFs and cell surface markers.

Subtype plasticity is regulated in part by transcription factor expression [240]. In particular, IRFs are very important in regulating subtype and differentiation of many cell types, including myeloid cells [141, 241]. To test the ability of the microenvironment to modulate IRF1 and IRF4 transcription factor expression we evaluated the responses of eosinophil subtypes to switch polarized states similar to methods reported previously [242]. First, eosinophils were cultured in E1 or E2 cytokine cocktails for 18 hrs. This was followed by switching their conditions and evaluating their IRF1 and IRF4 expression 24 hrs later. As shown in Figure 2.4.9, E1 eosinophils highly upregulate IRF1 as well as binding co-factor Batf2 compared to E0 and E2. Upon switching E1 eosinophils to E2 media (E1-E2), IRF1 and Batf2 are downregulated to E2 levels. Conversely, E2 eosinophils that do not highly upregulate IRF1 and Batf2, increased their expression dramatically upon switching to E1 media (E2-E1), equivalent to E1 eosinophils. IRF4 expression in E1 eosinophils is weak, yet it too is increased in cells that are transitioned from E1 to E2 (E1-E2) as compared to those as E1 eosinophils only. The level of IRF4 expression is comparable between E2 alone and E2-E1 switched cultures, again, indicating the kinetics or regulation of IRF4 might be more complex than that of IRF1 in eosinophils. Importantly, the culture conditions above were not a result of increased cell

death (not shown) as cells remained >90% viable for the 48 hour time period (data not shown).

To further define markers of plasticity, cell surface molecules tested previously were measured on these cells. The markers with the most significant plastic changes were CD11b and PDL1 (Figure 2.4.10). Other markers were variable in their response (not shown), likely due to timing of culture conditions and receptor turnover rates.

2.3 Discussion

Eosinophils have traditionally been known as a source of inflammation and damage in response to helminths and allergens. Although, still damaging and inflammatory in allergic diseases such as asthma many studies have shined a light on the alternative functions of eosinophils. Eosinophils have been shown to play many roles in both health, where they are implicated in homeostasis and development, and in disease where functions vary between inflammatory and anti-inflammatory [90, 222, 243, 244]. Eosinophils produce a wide array of proteins, enzymes and lipid mediators [76]. Although eosinophils have the capacity to release a wide range of effector molecules, several studies have demonstrated both human and mouse eosinophils respond to specific stimuli to release selective mediators. For example, it has been suggested one mechanism of specific cytokine release is through piecemeal degranulation leading to selective release of cytokines in response to inducing agents [46, 233]. Eosinophils though, have the potential to induce transcription [29, 151, 245] and production of proteins upon cytokine stimuli as well [23, 246, 247]. Together these studies and the evidence of eosinophils in a wide variety of immune environments *in vivo* [27, 90, 97, 248], led to the hypothesis that eosinophils may be considered similar to other leukocytes; having the

ability to differentiate into specific subtypes. This concept has been proposed by others [97, 226, 249, 250] and here we continue the process of defining these subtypes in part dependent on their activation by type 2 and type 1 cytokines found in disease environments such as asthma as compared to cancer or infection.

We believe that the differential functions of eosinophils exposed to various microenvironments are a result of subtype activation. Newer single-cell sequencing technologies have gathered extensive amounts of data resulting in the discovery of many more versions of subtypes than what was traditionally thought [139, 251, 252]. Single-cell sequencing has remained a challenge for eosinophils making it difficult to identify and characterize subtypes *in vivo*. To overcome this limitation we characterized eosinophil subtypes by *in vitro* exposure to type 1 and type 2 cytokines. This technique has been utilized by many as a means to identify T cells, dendritic cells, macrophages, and other immune cells into subtypes as a reductionist starting point for clarity [118, 119, 124, 129, 133, 136, 137, 140, 141, 223, 253]. We chose to study cytokine microenvironments relevant to *in vivo* findings that improved on single cytokine comparisons [23, 46, 70-72, 254] . The type 1 and type 2 cytokine cocktails are based on the cytokines present *in vivo* in either type 1 [49, 183] or type 2 [23, 91] microenvironments.

Culture of eosinophils with type 1 and type 2 cytokines to generate E1 and E2 subtype eosinophils resulted in phenotypic and effector functions consistent with *in vivo* and *in vitro* findings. The E2 eosinophils expressed the same cytokines reported by others. These include IL-6, IL-4, IL-13, and chemokines CCL17 and CCL22 [23, 70, 72, 91]. Similarly, E1 eosinophils expressed CXCL10, CXCL9, Nos2, CCL5 and IL-12 as

reported previously [46, 49, 181, 183, 235, 255]. These cytokines and chemokines are correlated with immune activities for eosinophils. Eosinophil release of IL-4 and IL-13 is correlated with M2 macrophage polarization and release of CCL17 with CD4 T cell recruitment in allergen asthma models [23, 85, 225]. Studies by Bouffi *et al.* differentiate the functions of IL-33 and IL-4 on eosinophils, indicating the expression of IL-6, IL-13 and CCL17 is IL-33 dependent [72]. Eosinophil release of CXCL10 and CXCL9 is associated with chemoattraction of CD8 T cells in cancer models [49]. iNOS (Nos2) production, on the other hand is found as a viral killing mechanism in human and mouse eosinophils as well as inhibition of CD8 T cell activities in lung allograft acceptance [181, 183]. Thus, specific type 1 and type 2 cytokine inductions of eosinophils is correlative with unique immune cytokine and chemokine pathways that are type 1 and type 2 specific.

Cell surface molecules of eosinophils have recently been described as relevant to both eosinophil identification and eosinophil function *in vivo*. We measured the classic cell surface molecules used to identify eosinophils. These included CCR3, CD11b, Siglec-F, F4/80, and GR-1 for example. Although all subtypes express these molecules, their expression varies upon cytokine stimulation. We found E2 eosinophils were Siglec-F high and consistent with findings from Abdala-Valencia *et al*. where they showed Siglec-F expression increased with activation from the lung tissue to airways [170]. It is known that eosinophils upregulate CD11b in allergic lung [256] and IL-33 has been shown to stimulate this response in tissue [22] and E2 eosinophils were particularly upregulated in this expression. On the other hand, adhesion molecule CD62L was reduced in E2 eosinophils, suggesting alternative adhesion activation by type 1 and type 2

inducing cytokines. This is comparable to studies showing CD62L is downregulated on BAL and sputum eosinophils [257, 258] as well as stimulated by IFNγ *in vitro* [259].

IL-5Rα and CCR3 were not significantly altered by cytokine exposure and instead were slightly lower in type 1 and type 2 conditions. IL5Rα is known to be downregulated on eosinophils exposed to IL-5 and in allergen challenged lungs on both mice [153] and humans [151]. These studies show IL5Rα being sufficiently downregulated where it is no longer detectable by flow. Strikingly, we found the GR-1 high population in our subtypes consisted of the E1 subtype expressing the Ly6C antigen. This is different than findings by others where Ly6G is elevated in the airway eosinophils [160]. The difference here may be the cytokine environment as the eosinophils with high Ly6G were in an *Aspergillus* model; a model which is known to have high IL-17 cytokine expression as well. We did not test eosinophil responses to IL-17, indicating this may yet be another novel subtype of eosinophils.

Many cell surface molecules not traditionally associated as classical eosinophil markers of identity are measured as a way to identify disease correlation or effector functions. For example, CD11c, which is slightly higher in E2 eosinophils, has been previously shown to be expressed on thymus, intestine, and allergic lung airway eosinophils [99, 170, 260, 261]. ST2 has been previously shown to be expressed on eosinophils and it is known that they upregulate the receptor when exposed to IL-33 [23, 224]. CD69 has been commonly used as a generic activation marker [262] and can be upregulated by cytokines [263] on eosinophils but here we show that it is actually subtype specific and solely expressed on E2. This may differ from human eosinophils where CD69 expression is more diverse [263]. It has been reported before that ICAM-1

has been shown to increase on eosinophils exposed to Th2 cytokines IL-3, GM-CSF and TSLP as well as the BAL and sputum of Th2 dominating asthmatic patients [73]. We found both E2 and E1 eosinophils express ICAM-1, yet the expression is higher in E1 eosinophils. This may be in agreement with additional studies showing human eosinophils stimulated with IFNγ and/or TNFα has been shown to stimulate ICAM-1 expression on [227].

Overall E1 eosinophils had a pattern of increased expression of ICAM-1, MCH-I, and PDL1 as compared to E2 eosinophils. Recently MHC-I on eosinophils was correlated with antigen presentation to CD8 T cells to inhibit cancer growth, and to present viral particles to CD8 T cells to kill viral containing cells [180]. Conversely two studies demonstrate a CD8 T cell suppressive function for eosinophils in the same cytokine cocktail of IFNγ and TNFα [183, 184]. This suggests additional unknown factors modulate eosinophils from activators of CD8 T cells to suppressive mediators of CD8 T cells. One surface molecule relevant to this pathway may be PDL1. In both a gut infection model of *H. pylori* and an allograft lung transplant model, PDL1 on eosinophils was found to be critical to suppressing CD8 T cell activities [164, 184]. Despite these variances, both forms of *in vivo* conditions appear to follow the E1 subtype of utilizing iNOS (Nos2) and NO for virus killing in humans and mice and allograft acceptance in mice [181, 183].

The morphological features and degranulation of eosinophil subtypes also gave an indication of unique activities. Morphologically E2 eosinophils displayed nuclear hypersegmentation and cytoplasmic vacuolization. Although the mechanism of hypersegmentation is unknown, this characteristic correlates with type 2 cytokine

exposure both in our studies and under allergic conditions *in vivo* [111, 170]. More interesting is the development of cytoplasmic vacuoles. Vacuoles have been described in leukocytes to develop after exposure to bacterial or viral pathogens as well as weakly basic lipophilic compounds [264]. In eosinophils, evidence of vacuoles (optically clear structures) can be found on eosinophils from an allergic mouse lung [170, 234] and in circulation from allergic and hypereosinophilic patients [231, 232, 265]. In addition, these optically clear vacuoles could potentially be enlarged lipid bodies (LBs). Large LBs have been shown in human eosinophils to be sites of synthesis of inflammatory mediators such as eicosanoids and storage of inflammatory cytokines such as TNFα [266].

These results as a whole led us to complete RNAseq analysis on the E1 and E2 eosinophils. In particular identifying transcription factor pathways relevant to the regulation of these subtypes would provide novel insight to their differentiation and plasticity. Functional enrichment analysis confirmed that E1 eosinophils predominantly expressed genes related to interferon signaling, host protection and associated with viral and autoimmune disease. E2 eosinophils predominantly expressed cytokine IL-4/-13 pathways, signaling kinase pathways, and correlated with asthma, B-cell and multiple sclerosis disease. The disease profiles of E1 and E2 eosinophils are striking. Recently, eosinophils have been shown to have anti-viral activities in type 1 immune environments [179-181, 267]. Moreover, eosinophils are being studied in autoimmune diseases like lupus [268]. E2 eosinophils are already well known to play a role in asthma, but the correlation with B cell lymphoma and multiple sclerosis is interesting as eosinophils enhance B-cell survival [106, 269, 270] and are associated with multiple myeloma B cell expansion [271, 272]and a form of multiple sclerosis called neuromyelitis optica [273].

The RNAseq analysis, also, highlighted a novel transcriptional regulatory pathway that correlates with the type 1 and type 2 characteristics of E1 and E2 eosinophils. Unlike T cells and ILCs which rely heavily on T-bet and GATA-3 for type 1 and type 2, respectively, myeloid cells like eosinophils appear to respond to alternative transcription regulators [140, 141]. It has been reported previously that eosinophils induce STAT1 and STAT6 phosphorylation in type 1 and type 2 environments [70, 174], yet the role of additional transcriptional factors were unknown. Functional enrichment analysis demonstrated that STAT1 was indeed upregulated in E1 eosinophils as well as IRFs associated with STAT1 activities and type 1 immune responses. IRF1 in particular is associated with STAT1 activities and upregulates the functions of Nos2 [274]. Conversely IRF4 was modestly and specifically upregulated in mouse E2 eosinophils and found increased in human E2 eosinophils. This may be due to the dynamics of expression and DNA binding competition required by IRF4 against other IRFs, such as IRF1 and IRF5 [236]. For example, IRF4 competes with other IRFs in order to induce M2 polarization in type 2 environments, suggesting a parallel pathway to eosinophils [275]. Relative ratios of IRFs may be equally important as total expression. Other studies though demonstrate type 2 responses with increased IRF4 expression in eosinophils [238] and airways [239]. Studies showing IRF4 knockout mice exposed to ovalbumin models of asthma, suggest this transcription factor is critical to the type 2 responses in the lung [276]. IRF8 and IRF4 are classically involved in myeloid differentiation. Studies have shown IRF8 deficiency leads to eosinophil deficiency, yet IRF4 does not deplete eosinophils in mice [277]. IRF4 in particular is important in type 2 cytokine production in T cells and ILC2s, indicating this may be a positive regulator of the IL-4 production in

eosinophils [237, 278, 279]. It is to be determined what role IRF4 in eosinophils has in these models as well as the role of IRF1 in E1 eosinophil effector functions. These transcription factors are well known to be subtype defining in myeloid cells in particular and relate to plasticity. We found eosinophils displayed plasticity when stimulated with appropriate cytokines, such as switching from type 1 to type 2 cytokine exposures, resulting in up or down regulation of these IRFs. These studies are the first to define transcriptional regulation of eosinophil subtypes in both human and mouse eosinophils. Future studies to clarify the importance of these genes will include specific eosinophil knockouts of IRFs in models of health and disease.

2.4 Figures

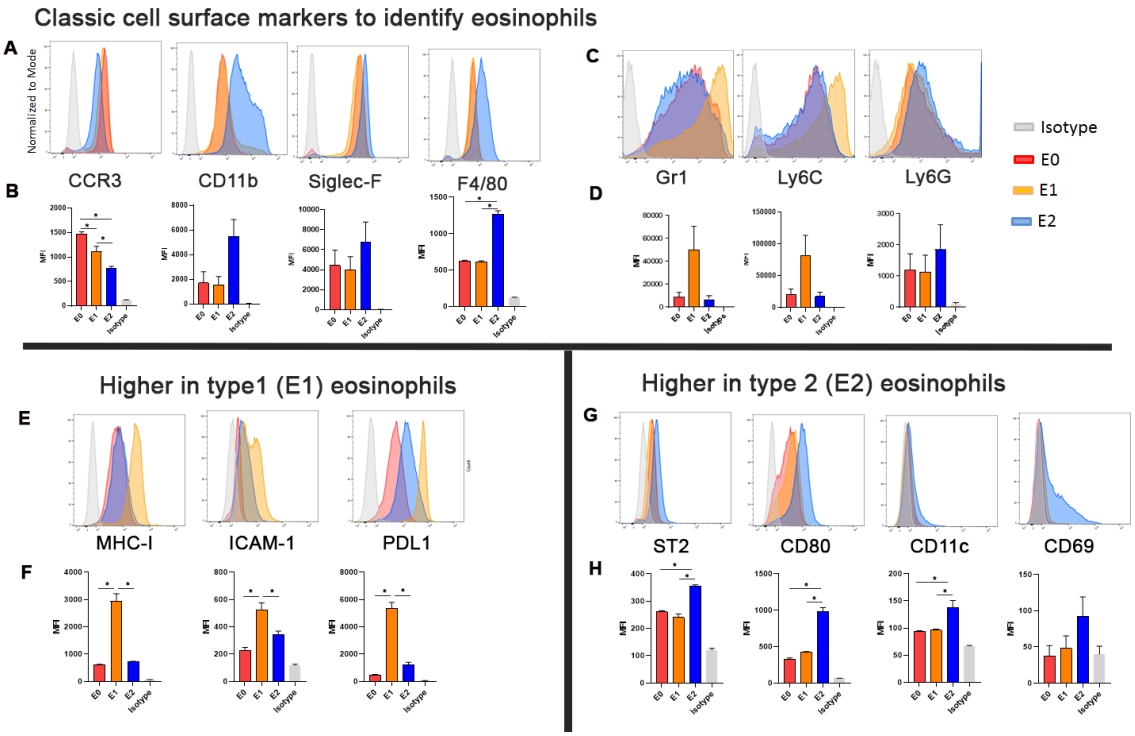

Figure 2.4.1. Expression of Cell Surface Proteins on Eosinophils After *in vitro* Activation with Type 1 and Type 2 Cytokines. Flow cytometry of cell surface molecules of E0 (red), E1 (orange), and E2 (Blue) showing differential expression by flow cytometry histograms and corresponding median fluorescence intensity (MFI). (A, B) standard markers of eosinophil identification. (C, D) Gr1 total and Ly6C and Ly6G. (E,

F) Cell surface molecules that are higher on E1 eosinophils than E2 eosinophils. (G, H) Cell surface molecules that are higher on E2 eosinophils than E1 eosinophils. MFI n≥3 with the exception of CD11b, Siglec-F, GR-1, CD80 n=2. * denotes p-value<0.05. Error bars=Mean with SEM.

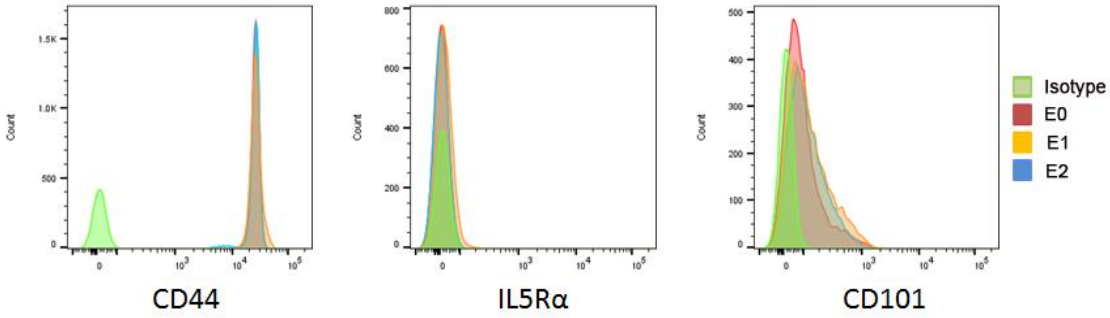

Figure 2.4.2. Expression of Cell Surface Proteins on Eosinophil Subtypes After *in vitro* Activation That Did Not Change. Flow cytometry histograms showing the expression of CD44, IL5Rα and CD101 on eosinophil subtypes E0 (red), E1 (orange), E2 (blue).

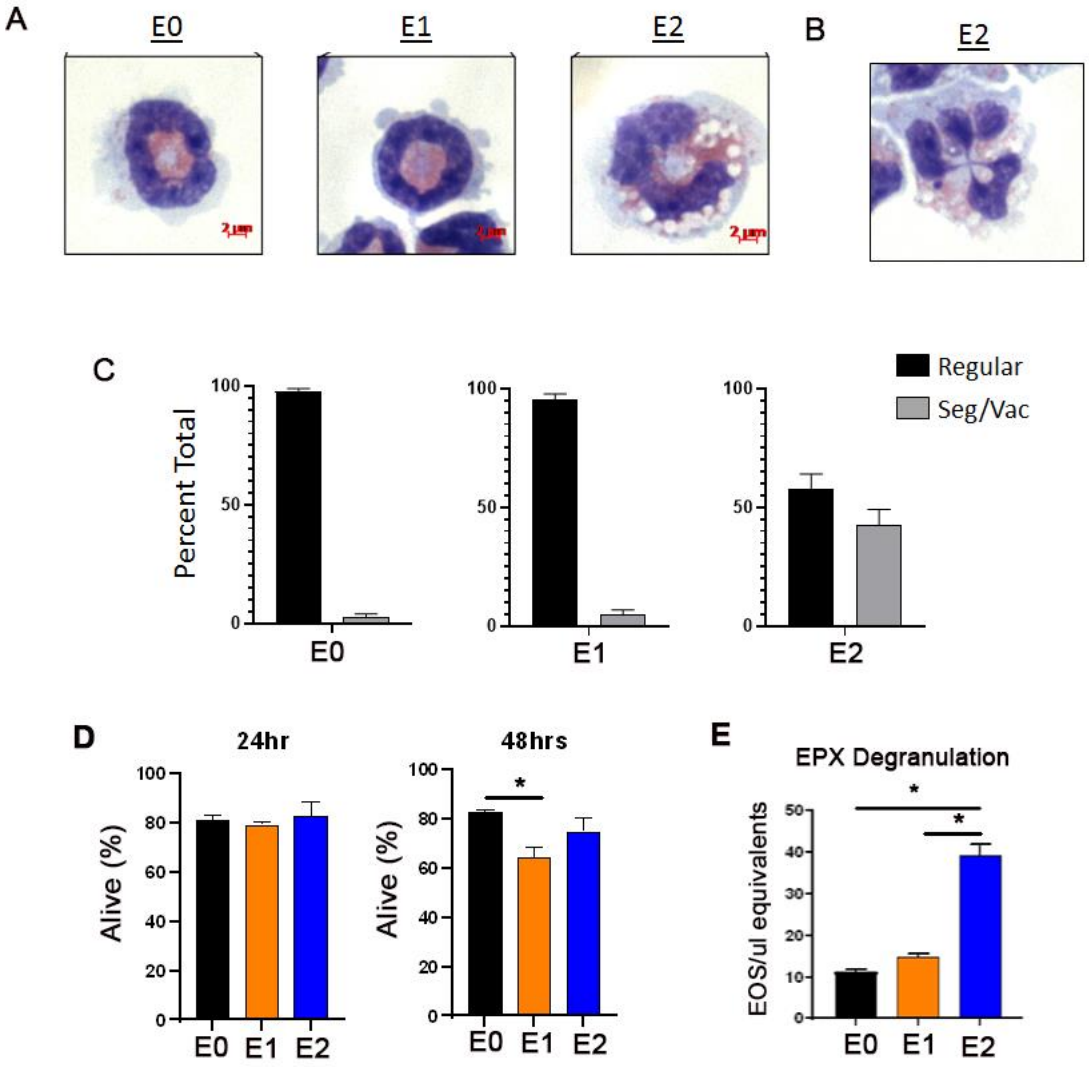

Figure 2.4.3. Eosinophils Subtypes with Unique Morphology, Viability, and Mediator Release. (A) Morphology analysis on eosinophil subtypes prepped by cytospin and Hema 3 stain. Representative images of E0, E1and E2 cells displaying cytoplasmic vacuoles and nuclear hypersegmentation. (B) E2 eosinophil displaying more extreme nuclear hypersegmentation. (C) Quantification of eosinophils that present with hypersegmented nucleus and cytoplasmic vacuoles (Seg/Vav). N=3 separate experiments. (D) Viability by annexin V/PI of eosinophil subtypes over 48 hours. Eosinophil subtypes E0 (black), E1 (orange), E2 (blue) were cultured for the indicated time. (D) EPX degranulation was measured by EPX ELISA of cell culture supernatant after 18hr incubation. N=3. Error bars=Mean with SEM. * denotes p-value<0.05.

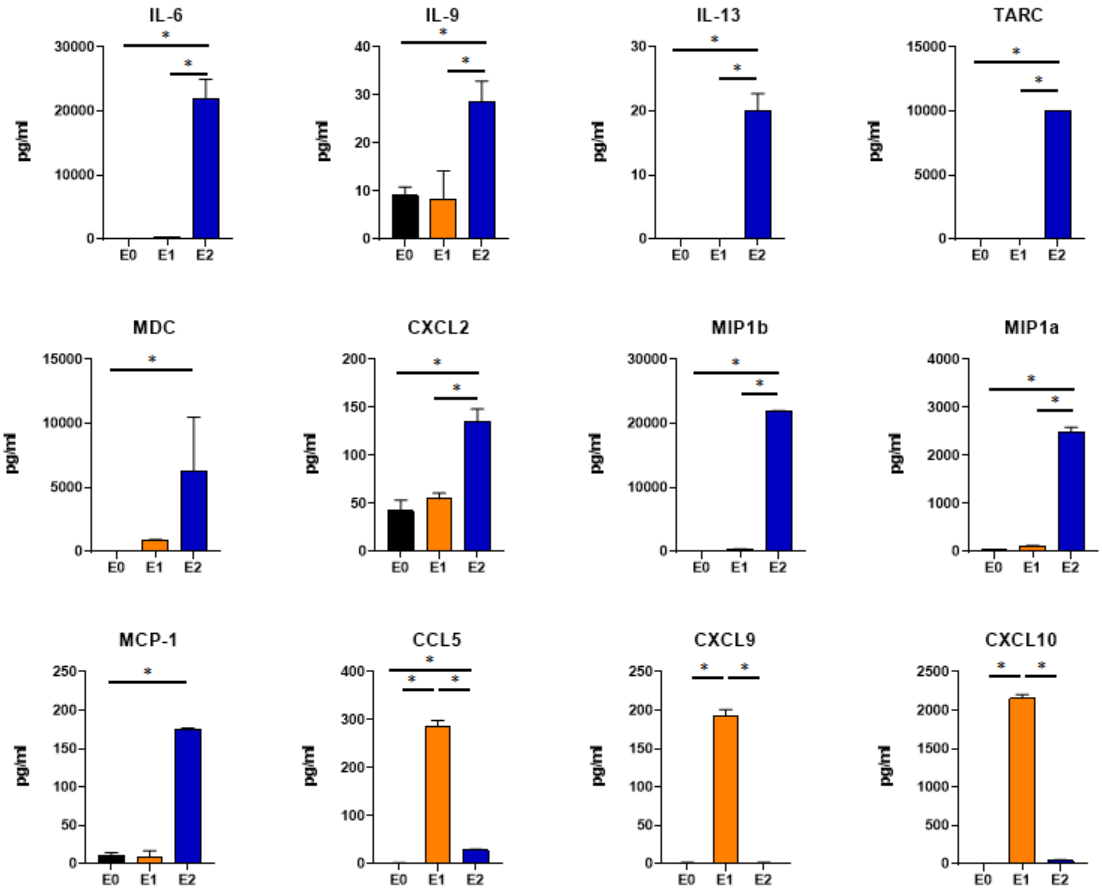

Figure 2.4.4. Eosinophils Subtypes with Unique Cytokine and Chemokine Release. Multiplex cytokine/chemokine assay was performed on eosinophil subtype cell culture supernatant. Eosinophil subtypes E0 (black), E1 (orange), E2 (blue) were cultured for 18 hrs. N=3. Error bars=Mean with SEM. * denotes p-value<0.05.

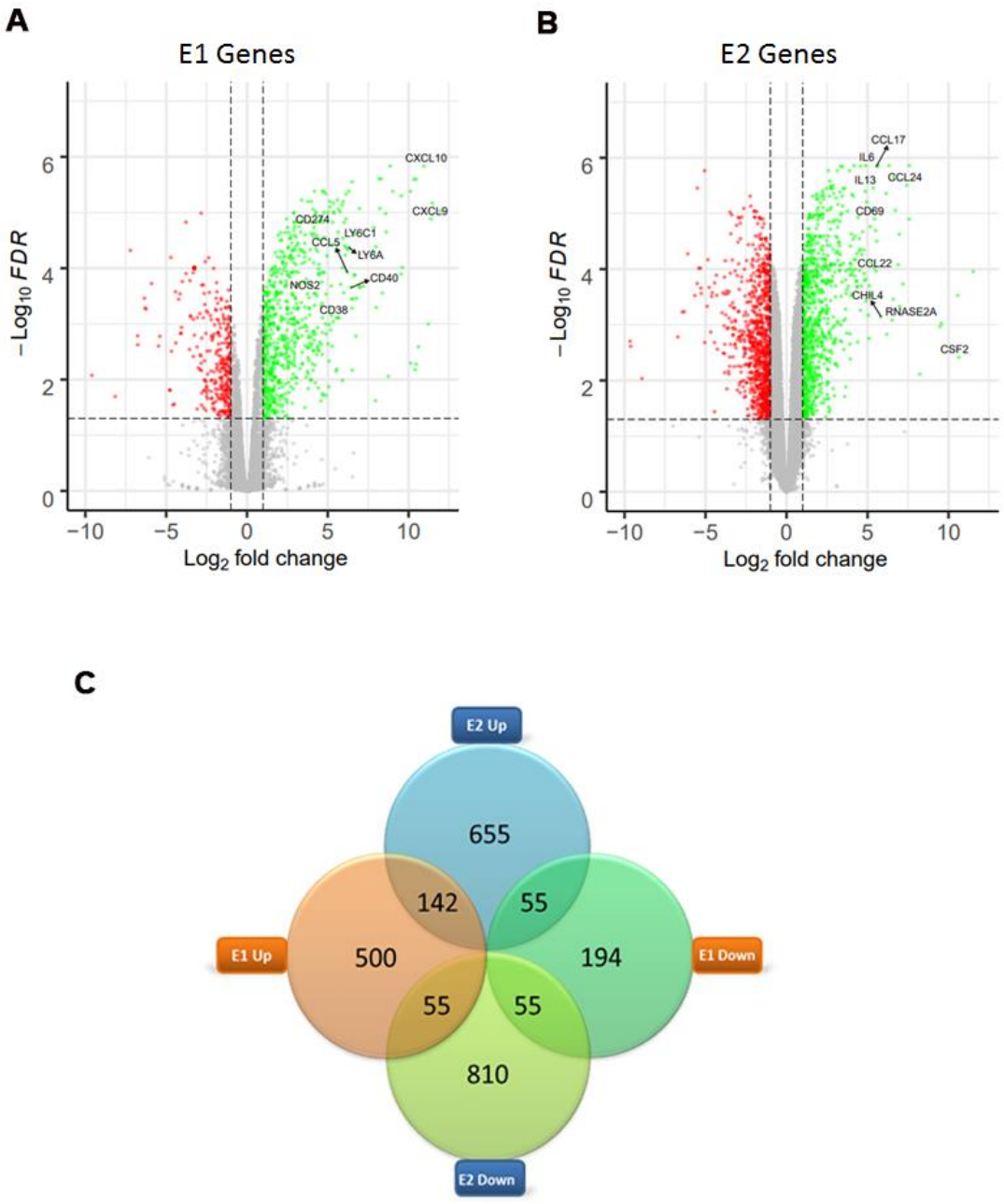
A
E1 Genes
CXCL10
CXCL9
CD274
LY6C1
CCL5
LY6A
CD40
NOS2
CD38
−Log10 FDR
Log2 fold change
B
E2 Genes
CCL17
IL6
IL13
CCL24
CD69
CCL22
CHIL4
RNASE2A
CSF2
−Log10 FDR
Log2 fold change
C
E2 Up
655
142
55
E1 Up
500
194
E1 Down
55
55
810
E2 Down

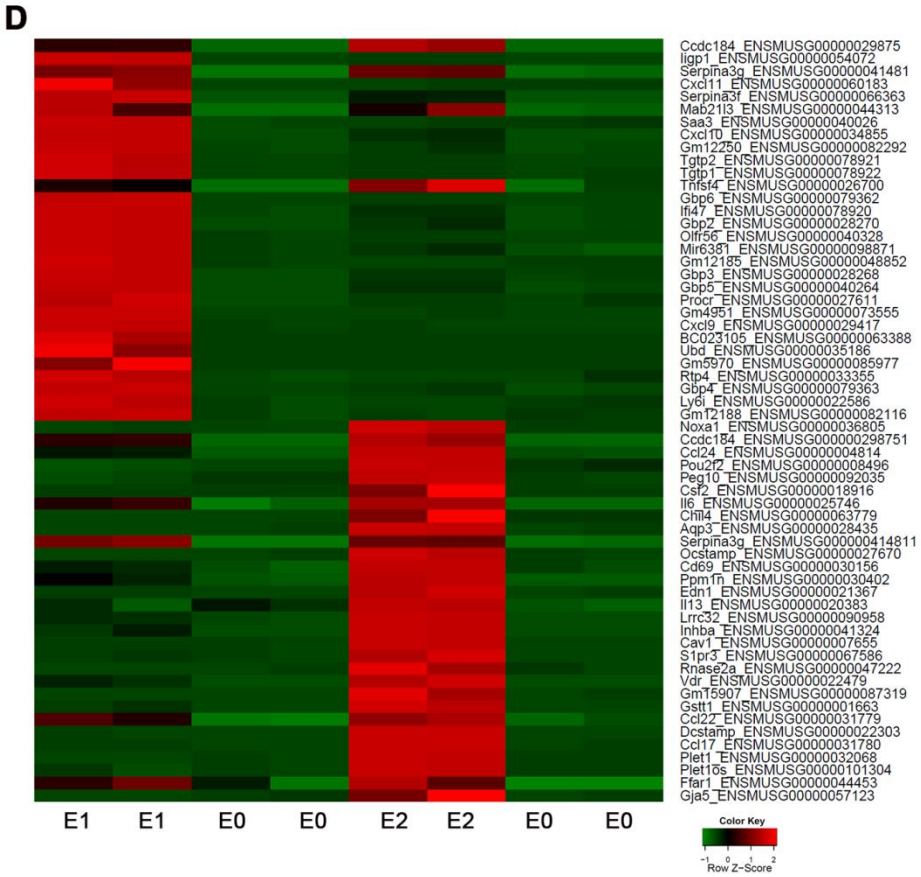

Figure 2.4.5. Differential Expression of Genes by RNAseq of Eosinophil Subtypes. Graphic representation of differentially expressed genes compared between E0, E1 and E2. (A) Volcano plot of E1 upregulated (green) and downregulated (red) genes. (B) Volcano plot of E2 upregulated (green) and downregulated genes. (C) Venn diagram comparison of dysregulated genes between E1 and E2. (D) Heat map showing the top 30 upregulated genes in E1 and E2 eosinophils as compared to E0 that underwent RNAseq analysis using (-2≥logFC≥2, adjusted p-value <0.05) parameters.

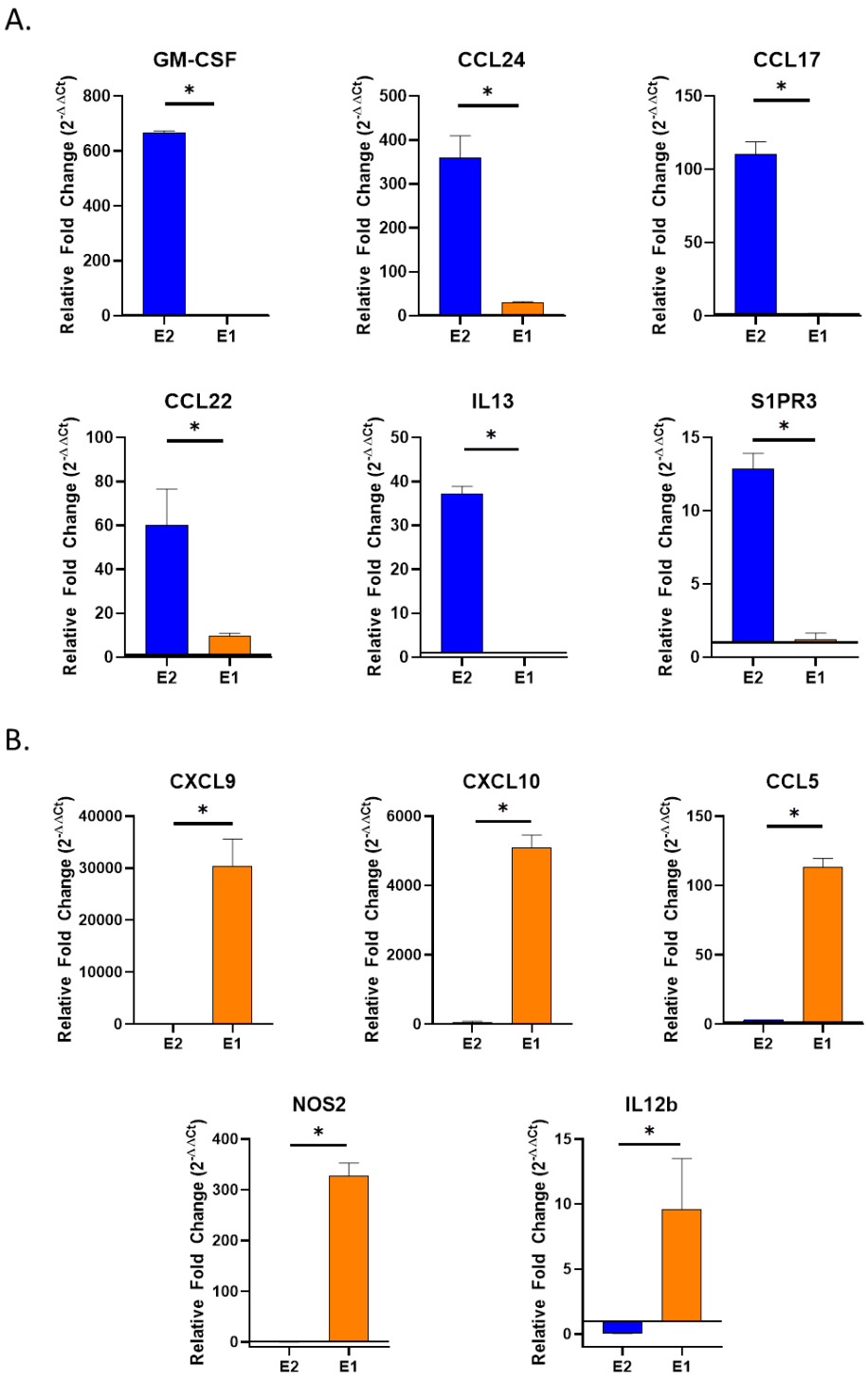

Figure 2.4.6. RT-PCR Confirmation of Genes Highly Upregulated in Eosinophil Subtypes. Highly upregulated genes in both eosinophil subtypes. (A). Genes highly upregulated in E2 eosinophils. (B) Genes highly upregulated in E1 eosinophils. Samples are relative to E0 eosinophils. Error bars=Mean with SEM. * denotes p-value<0.05.

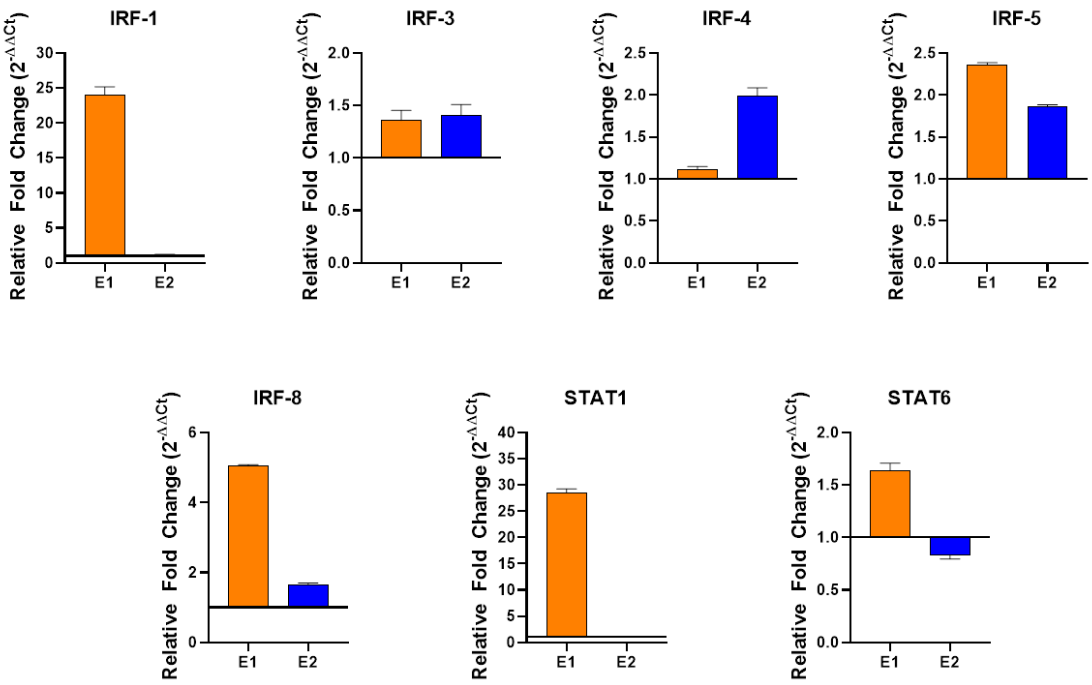

Figure 2.4.7. IRF Transcription Factors are Specifically Upregulated in Eosinophil Subtypes. Eosinophil subtypes E1 (orange) and E2 (blue) were cultured for 18 hrs. Data is normalized to E0 eosinophils. Error bars=Mean with SEM.

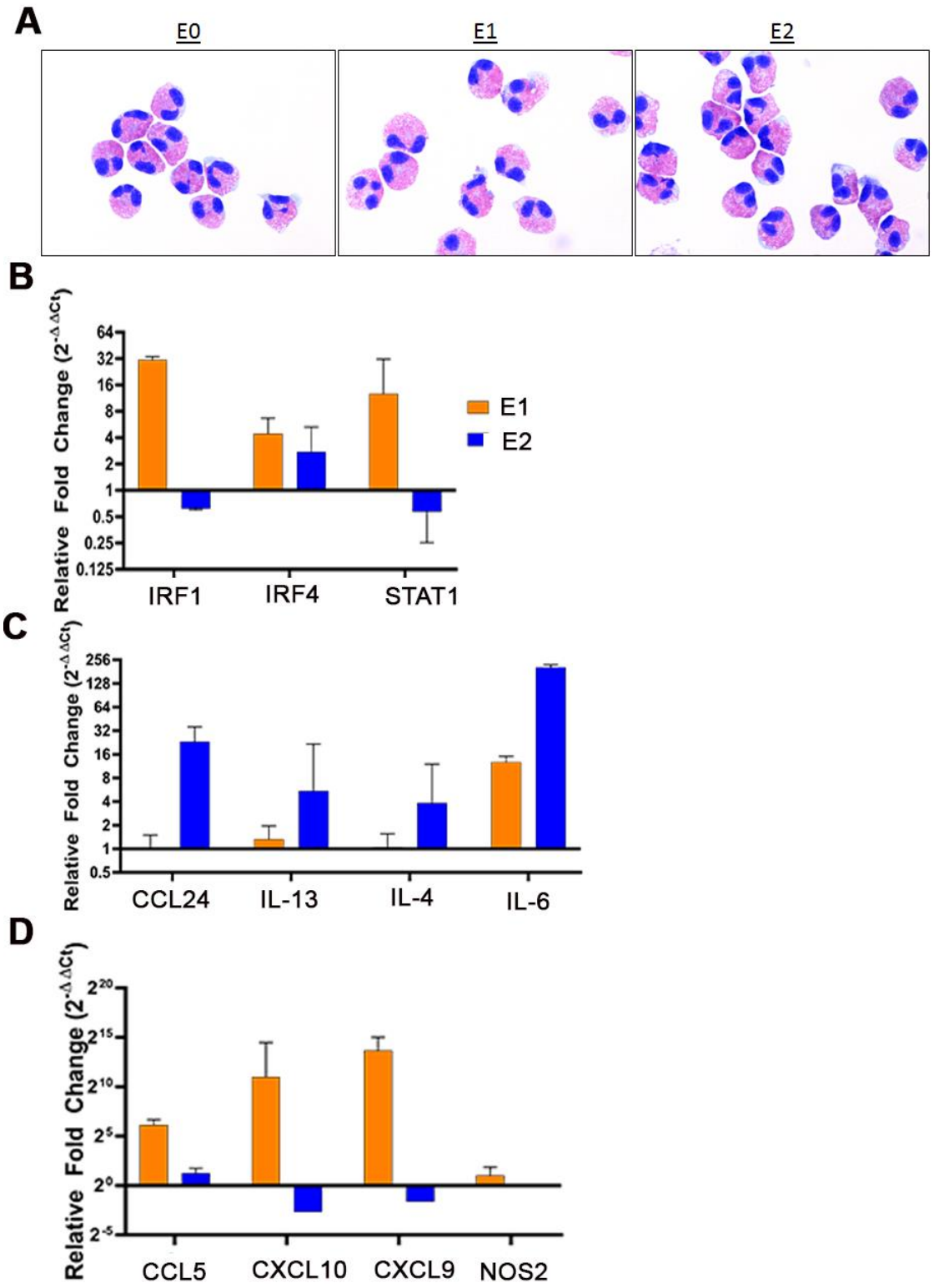

Figure 2.4.8. Human Eosinophils Demonstrate Similar Gene Regulation to Mouse Subtypes. Human eosinophils were cultured as E0, E1, or E2 for 18 hrs. (A) Morphology analysis on eosinophil subtypes prepped by cytospin and Hema 3 stain. Representative

images of E0, E1, and E2 cells display very similar morphology, unlike mouse eosinophils. (B) RT-PCR of IRF1 and STAT1 demonstrate these are increased in human E1 while IRF4 is not significantly different at this time point. (C) RT-PCR of genes found to be increased in mouse E2 as well. (D) RT-PCR of cytokines and genes found to be increased in mouse E1 as well. Data is normalized to E0 eosinophils. Error bars=Mean with SEM.

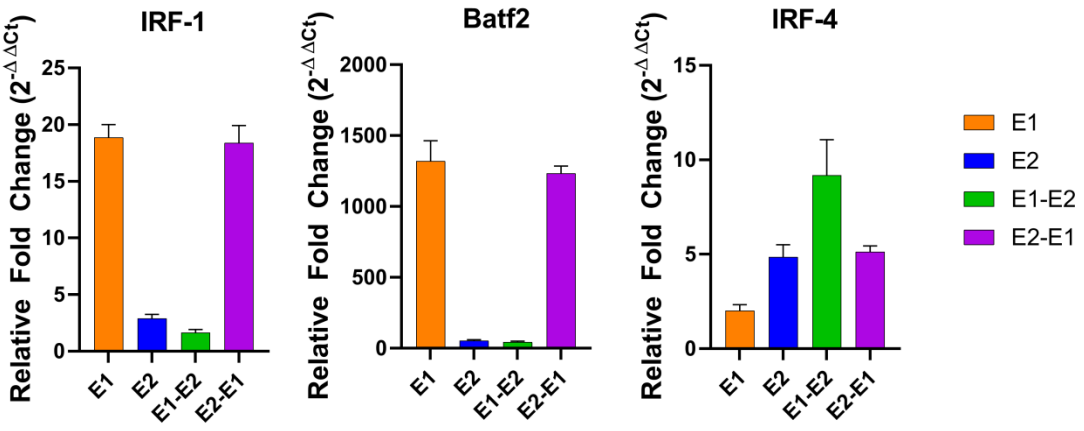

Figure 2.4.9. IRF Transcription Factors are Plastic in Eosinophil Subtypes. Eosinophil subtypes E1 (orange) and E2 (blue) were cultured for 18 hrs. These were either kept in those conditions for another 24 hrs (E1) or (E2) or washed and placed in culture such that E1 were placed in E2 media (E1-2) or E2 were placed in E1 media (E2-1) to determine if the cells had the capacity to alter their transcription factor expression. RT-PCR of IRF1 and IRF4 were completed as well as Batf2. Data is normalized to E0 eosinophils. Error bars=Mean with SEM.

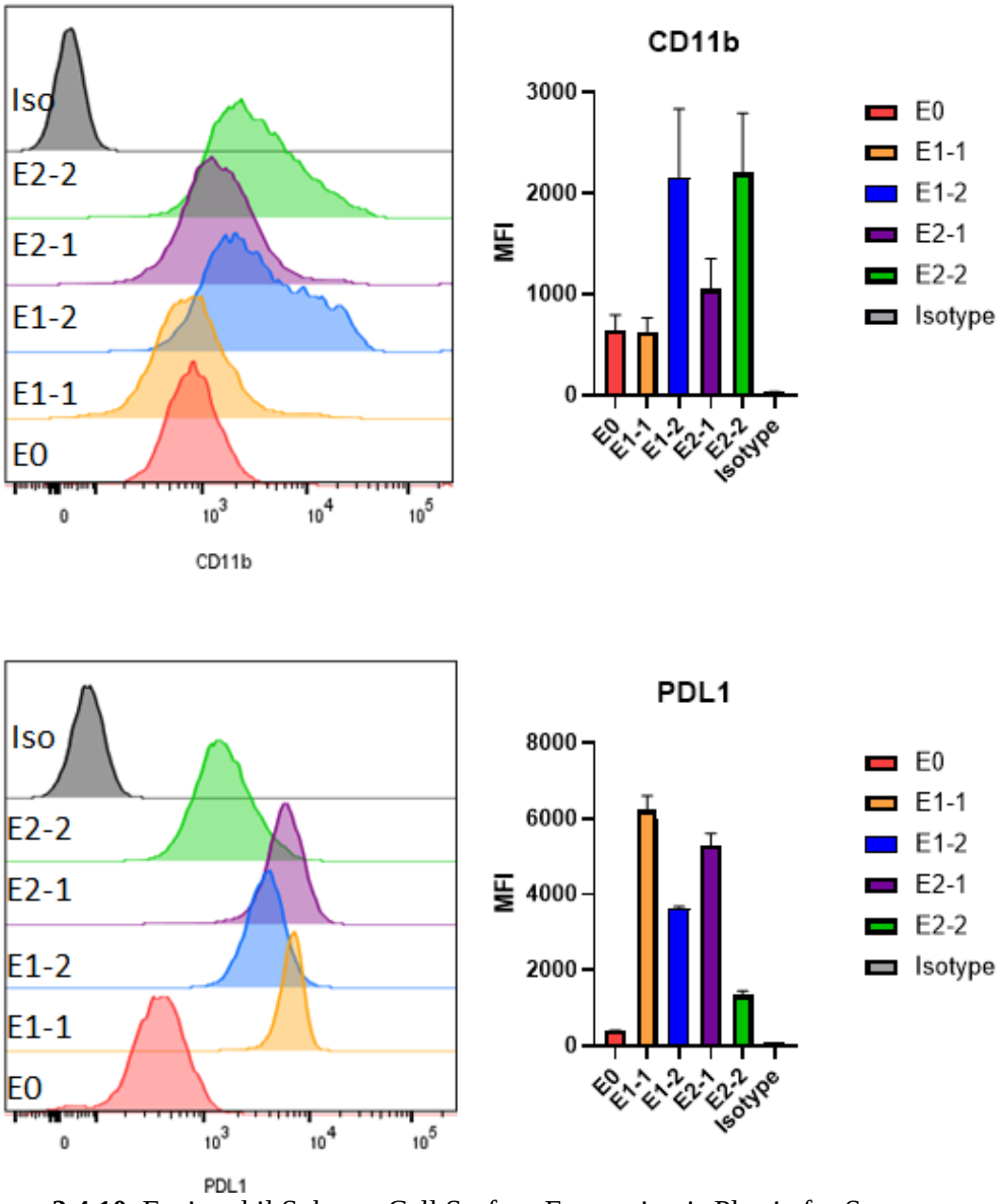

Figure 2.4.10. Eosinophil Subtype Cell Surface Expression is Plastic for Some Molecules. Eosinophil subtypes E1 (orange) and E2 (blue) were cultured for 18 hrs. These were either kept in those conditions for another 24 hrs (E1-1) or (E2-2) or washed and placed in culture such that E1 were placed in E2 media (E1-2) or E2 were placed in E1 media (E2-1) to determine if the cells had the capacity to alter their transcription factor expression. Flow cytometry of Cd11b or PDL1 are shown as histograms and mean fluorescent intensity (MFI). Error bars=Mean with SEM. * denotes p-value<0.05 compared to E0.

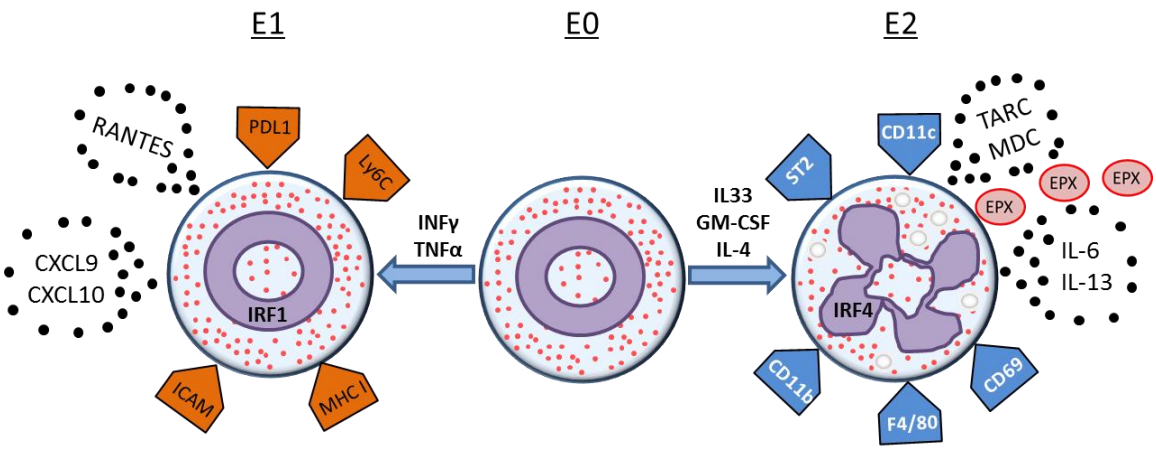

Figure 2.4.11. Schematic Summary of Our Results.

Table 1 E1 ToppGene

1: GO: Molecular Function [Display Chart] 304 input genes in category / 940 annotations before applied cutoff / 19242 genes in category

	ID	Name	Source	pValue	FDR B&H	FDR B&Y	Bonferroni	Genes from Input	Genes in Annotation
1	GO:0042802	identical protein binding		3.468E-11	3.260E-8	2.420E-7	3.260E-8	71	1995
2	GO:0003725	double-stranded RNA binding		3.823E-6	1.200E-3	8.912E-3	3.593E-3	9	78
3	GO:0015433	ATPase-coupled peptide antigen transmembrane transporter activity		3.968E-6	1.200E-3	8.912E-3	3.730E-3	3	3
4	GO:0042803	protein homodimerization activity		5.309E-6	1.200E-3	8.912E-3	4.991E-3	36	1018
5	GO:0003950	NAD+ ADP-ribosyltransferase activity		6.386E-6	1.200E-3	8.912E-3	6.002E-3	6	30

Show 28 more annotations

2: GO: Biological Process [Display Chart] 305 input genes in category / 4861 annotations before applied cutoff / 20146 genes in category

	ID	Name	Source	pValue	FDR B&H	FDR B&Y	Bonferroni	Genes from Input	Genes in Annotation
1	GO:0045087	innate immune response		2.457E-45	1.194E-41	1.083E-40	1.194E-41	92	1045
2	GO:0098542	defense response to other organism		5.864E-45	1.425E-41	1.292E-40	2.850E-41	99	1250
3	GO:0051707	response to other organism		2.134E-44	2.927E-41	2.654E-40	1.037E-40	110	1604
4	GO:0043207	response to external biotic stimulus		2.409E-44	2.927E-41	2.654E-40	1.171E-40	110	1606
5	GO:0009607	response to biotic stimulus		1.212E-43	1.179E-40	1.069E-39	5.893E-40	110	1633

Show 45 more annotations

3: GO: Cellular Component [Display Chart] 307 input genes in category / 500 annotations before applied cutoff / 20584 genes in category

	ID	Name	Source	pValue	FDR B&H	FDR B&Y	Bonferroni	Genes from Input	Genes in Annotation
1	GO:0042824	MHC class I peptide loading complex		7.110E-7	3.471E-4	2.358E-3	3.555E-4	4	6
2	GO:0005764	lysosome		2.028E-6	3.471E-4	2.358E-3	1.014E-3	29	735
3	GO:0000323	lytic vacuole		2.083E-6	3.471E-4	2.358E-3	1.041E-3	29	736
4	GO:0009986	cell surface		1.437E-5	1.796E-3	1.220E-2	7.183E-3	34	1036
5	GO:1990111	spermatoproteasome complex		3.213E-5	3.213E-3	2.183E-2	1.607E-2	3	5

Show 34 more annotations

4: Human Phenotype [Display Chart] 93 input genes in category / 2766 annotations before applied cutoff / 4707 genes in category

	ID	Name	Source	pValue	FDR B&H	FDR B&Y	Bonferroni	Genes from Input	Genes in Annotation
1	HP:0002788	Recurrent upper respiratory tract infections		1.185E-7	3.277E-4	2.787E-3	3.277E-4	16	168
2	HP:0001739	Abnormality of the nasopharynx		5.650E-7	7.813E-4	6.643E-3	1.563E-3	16	188
3	HP:0000600	Abnormality of the pharynx		5.842E-6	5.386E-3	4.580E-2	1.616E-2	16	224

5: Mouse Phenotype [Display Chart] 207 input genes in category / 3535 annotations before applied cutoff / 10724 genes in category

	ID	Name	Source	pValue	FDR B&H	FDR B&Y	Bonferroni	Genes from Input	Genes in Annotation
1	MP:0001835	abnormal antigen presentation		2.378E-21	8.406E-18	7.353E-17	8.406E-18	22	70
2	MP:0005025	abnormal response to infection		1.147E-20	2.027E-17	1.773E-16	4.055E-17	51	580
3	MP:0001793	altered susceptibility to infection		2.749E-20	3.239E-17	2.833E-16	9.717E-17	49	544
4	MP:0002406	increased susceptibility to infection		4.768E-20	4.214E-17	3.686E-16	1.685E-16	44	438
5	MP:0001836	abnormal antigen presentation via MHC class I		8.411E-19	5.947E-16	5.202E-15	2.973E-15	12	15

Show 45 more annotations

Table 1 E1 ToppGene

6: Domain [Display Chart] 308 input genes in category / 1710 annotations before applied cutoff / 18735 genes in category

	ID	Name	Source	pValue	FDR B&H	FDR B&Y	Bonferroni	Genes from Input	Genes in Annotation
1	IPR021673	RIG-I C-RD	InterPro	4.475E-6	1.446E-3	1.160E-2	7.652E-3	3	3
2	PS51789	RLR CTR	PROSITE	4.475E-6	1.446E-3	1.160E-2	7.652E-3	3	3
3	PF11648	RIG-I C-RD	Pfam	4.475E-6	1.446E-3	1.160E-2	7.652E-3	3	3
4	PS50835	IG LIKE	PROSITE	7.464E-6	1.446E-3	1.160E-2	1.276E-2	23	492
5	PS51507	IRF 2	PROSITE	8.458E-6	1.446E-3	1.160E-2	1.446E-2	4	9

Show 45 more annotations

7: Pathway [Display Chart] 223 input genes in category / 1367 annotations before applied cutoff / 12450 genes in category

	ID	Name	Source	pValue	FDR B&H	FDR B&Y	Bonferroni	Genes from Input	Genes in Annotation
1	1269311	Interferon Signaling	BioSystems: REACTOME	1.665E-29	2.275E-26	1.774E-25	2.275E-26	39	202
2	1269312	Interferon alpha/beta signaling	BioSystems: REACTOME	1.134E-26	7.751E-24	6.044E-23	1.550E-23	25	69
3	1269310	Cytokine Signaling in Immune system	BioSystems: REACTOME	9.068E-26	4.132E-23	3.222E-22	1.240E-22	63	763
4	1269314	Interferon gamma signaling	BioSystems: REACTOME	3.289E-15	1.124E-12	8.766E-12	4.496E-12	19	94
5	217173	Influenza A	BioSystems: KEGG	3.328E-11	9.099E-9	7.095E-8	4.550E-8	20	173

Show 45 more annotations

8: Pubmed [Display Chart] 309 input genes in category / 47747 annotations before applied cutoff / 38578 genes in category

	ID	Name	Source	pValue	FDR B&H	FDR B&Y	Bonferroni	Genes from Input	Genes in Annotation
1	26116899	Genome-wide transcriptional profiling reveals that HIV-1 Vpr differentially regulates interferon-stimulated genes in human monocyte-derived dendritic cells.	Pubmed	1.012E-28	4.831E-24	5.484E-23	4.831E-24	20	53
2	20237496	New genetic associations detected in a host response study to hepatitis B vaccine.	Pubmed	2.867E-23	6.844E-19	7.768E-18	1.369E-18	44	825
3	24742347	HIV-1 Tat second exon limits the extent of Tat-mediated modulation of interferon-stimulated genes in antigen presenting cells.	Pubmed	2.035E-22	3.238E-18	3.676E-17	9.714E-18	15	37
4	25170834	HIV-1 Vpr induces interferon-stimulated genes in human monocyte-derived macrophages.	Pubmed	9.661E-21	1.153E-16	1.309E-15	4.613E-16	11	15
5	22647704	Vpu-deficient HIV strains stimulate innate immune signaling responses in target cells.	Pubmed	9.140E-19	8.728E-15	9.907E-14	4.364E-14	10	14

Show 45 more annotations

9: Interaction [Display Chart] 291 input genes in category / 5754 annotations before applied cutoff / 18137 genes in category

	ID	Name	Source	pValue	FDR B&H	FDR B&Y	Bonferroni	Genes from Input	Genes in Annotation
1	int:STAT1	STAT1 interactions		3.633E-9	2.091E-5	1.931E-4	2.091E-5	19	223
2	int:IFNAR2	IFNAR2 interactions		2.558E-7	7.359E-4	6.796E-3	1.472E-3	6	18
3	int:PSMB8	PSMB8 interactions		5.201E-7	9.975E-4	9.211E-3	2.992E-3	9	61
4	int:STAT5B	STAT5B interactions		1.049E-6	1.315E-3	1.214E-2	6.038E-3	10	85
5	int:MAVS	MAVS interactions		1.143E-6	1.315E-3	1.214E-2	6.575E-3	12	129

Show 39 more annotations

10: Cytoband [Display Chart] 307 input genes in category / 229 annotations before applied cutoff / 34661 genes in category

	ID	Name	Source	pValue	FDR B&H	FDR B&Y	Bonferroni	Genes from Input	Genes in Annotation
1	6p21.3	6p21.3		3.652E-6	8.363E-4	5.029E-3	8.363E-4	12	257
2	12q24.2	12q24.2		3.537E-4	2.655E-2	1.596E-1	8.101E-2	3	16
3	12p13-p12	12p13-p12		4.637E-4	2.655E-2	1.596E-1	1.062E-1	2	4
4	7p15-p14	7p15-p14		4.637E-4	2.655E-2	1.596E-1	1.062E-1	2	4

Table 1 E1 ToppGene

11: Transcription Factor Binding Site [Display Chart] 165 input genes in category / 514 annotations before applied cutoff / 9770 genes in category

	ID	Name	Source	pValue	FDR B&H	FDR B&Y	Bonferroni	Genes from Input	Genes in Annotation
1	STTTCRNTTT V$IRF Q6	STTTCRNTTT V$IRF Q6		9.300E-18	4.780E-15	3.260E-14	4.780E-15	25	158
2	V$ICSBP Q6	V$ICSBP Q6		2.915E-12	7.492E-10	5.110E-9	1.498E-9	22	203
3	V$IRF7 01	V$IRF7 01		7.707E-12	1.320E-9	9.006E-9	3.961E-9	22	213
4	V$IRF2 01	V$IRF2 01		2.348E-10	3.017E-8	2.058E-7	1.207E-7	15	106
5	V$IRF Q6	V$IRF Q6		2.412E-9	2.480E-7	1.691E-6	1.240E-6	18	188

Show 2 more annotations

12: Gene Family [Display Chart] 213 input genes in category / 147 annotations before applied cutoff / 18194 genes in category

	ID	Name	Source	pValue	FDR B&H	FDR B&Y	Bonferroni	Genes from Input	Genes in Annotation
1	471	CD molecules|Tumor necrosis factor superfamily	genenames.org	4.269E-11	6.276E-9	3.496E-8	6.276E-9	24	394
2	198	Formyl peptide receptors	genenames.org	1.601E-6	1.177E-4	6.556E-4	2.353E-4	3	3
3	591	Histocompatibility complex|C1-set domain containing	genenames.org	8.855E-6	3.745E-4	2.087E-3	1.302E-3	6	42
4	690	Proteasome	genenames.org	1.019E-5	3.745E-4	2.087E-3	1.498E-3	6	43
5	594	Immunoglobulin like domain containing|Interleukin receptors|TIR domain containing	genenames.org	1.767E-5	5.195E-4	2.894E-3	2.597E-3	11	193

Show 5 more annotations

13: Coexpression [Display Chart] 310 input genes in category / 9327 annotations before applied cutoff / 23137 genes in category

	ID	Name	Source	pValue	FDR B&H	FDR B&Y	Bonferroni	Genes from Input	Genes in Annotation
1	M5913	Genes up-regulated in response to IFNG [GeneID=3458].	MSigDB H: Hallmark Gene Sets (v6.0)	1.723E-100	1.607E-96	1.562E-95	1.607E-96	81	200
2	M7320	Genes up-regulated in HMC-1 (mast leukemia) cells: incubated with the peptide ALL1 and then treated with Cl-IB-MECA [PubChem=3035850] versus stimulation by T cell membranes.	MSigDB C7: Immunologic Signatures (v6.0)	2.928E-93	1.365E-89	1.327E-88	2.731E-89	77	200
3	M7322	Genes up-regulated in HMC-1 (mast leukemia) cells incubated the peptide ALL1 versus those followed by treatment with Cl-IB-MECA [PubChem=3035850].	MSigDB C7: Immunologic Signatures (v6.0)	1.231E-72	3.826E-69	3.718E-68	1.148E-68	65	200
4	M5911	Genes up-regulated in response to alpha interferon proteins.	MSigDB H: Hallmark Gene Sets (v6.0)	2.635E-68	6.144E-65	5.970E-64	2.457E-64	50	97
5	M9572	Genes up-regulated in cells from peripheral lymph nodes: T reg versus T conv.	MSigDB C7: Immunologic Signatures (v6.0)	1.568E-64	2.925E-61	2.843E-60	1.463E-60	60	200

Show 45 more annotations

14: Coexpression Atlas [Display Chart] 309 input genes in category / 3430 annotations before applied cutoff / 21555 genes in category

	ID	Name	Source	pValue	FDR B&H	FDR B&Y	Bonferroni	Genes from Input	Genes in Annotation
1	gudmap RNAseq p2 Glomerlular Endothelial 2500	gudmap RNAseq p2 Glomerlular Endothelial 2500	Gudmap RNAseq	5.646E-55	1.936E-51	1.688E-50	1.936E-51	122	1686
2	GSM854291 500	Myeloid Cells, DC.8-4-11b-.SLN, CD11b-FITC CD4-PE CD11c-eFluor780 CD8a-eFluor450 C, Lymph Node, avg-3	Immgen.org, GSE15907	7.162E-52	1.228E-48	1.071E-47	2.457E-48	68	418
3	gudmap kidney adult CortVasc Tie2 1000	kidney adult CortVasc Tie2 top-relative-expression-ranked 1000	Gudmap Mouse MOE430.2	6.115E-51	6.991E-48	6.095E-47	2.097E-47	88	847
4	GSM538262 500	Myeloid Cells, DC.8-4-11b+.MLN, CD11b-FITC CD4-PE CD11c-Alexa750 CD8a-PacificBlue, Lymph Node, avg-1	Immgen.org, GSE15907	1.032E-49	8.850E-47	7.715E-46	3.540E-46	66	414
5	gudmap kidney adult CortVasc Tie2 k4 1000	kidney adult CortVasc Tie2 k-means-cluster#4 top-relative-expression-ranked 1000	Gudmap Mouse MOE430.2	9.002E-46	6.175E-43	5.384E-42	3.088E-42	43	138

Show 45 more annotations

Table 1 E1 ToppGene

15: ToppCell Atlas [Display Chart] 289 input genes in category / 2204 annotations before applied cutoff / 19604 genes in category

	ID	Name	Source	pValue	FDR B&H	FDR B&Y	Bonferroni	Genes from Input	Genes in Annotation
1	d942b27909c52a74d33064c8d88d37d8d43505d2	Hematopoietic-MACROPHAGE of Hematopoietic	BrainMap; Mouse Adult Brain Overview - NCRCRG; cells hierarchically compared	6.442E-16	1.420E-12	1.175E-11	1.420E-12	22	151
2	53c72e39f912e964775d21ea2b24a66e817b443e	ts14 Kidney-ImmunoHematopoietic of ts14 Kidney	Mouse Atlas; Mouse Adult Overview - TabulaMuris; lineage hierarchy compared within sample groups	1.344E-14	1.482E-11	1.226E-10	2.963E-11	22	174
3	904486d4462fad6afb3696bdbdf31ecbc8513e0e	ts11 Pancreas-ImmunoHematopoietic-Leukocyte-leuk 1 of ts11 Pancreas	Mouse Atlas; Mouse Adult Overview - TabulaMuris; lineage hierarchy compared within sample groups	6.871E-14	3.786E-11	3.133E-10	1.514E-10	21	168
4	70af1fee58f2a1651cee1be6e36bb33ac4abd0a3	ts11 Pancreas-ImmunoHematopoietic-Leukocyte-leuk 1--leukocyte of ts11 Pancreas	Mouse Atlas; Mouse Adult Overview - TabulaMuris; lineage hierarchy compared within sample groups	6.871E-14	3.786E-11	3.133E-10	1.514E-10	21	168
5	PND07-28-group|World of World	PND07-28-group|World of World	LungMap	1.692E-13	7.458E-11	6.171E-10	3.729E-10	20	156

Show 45 more annotations

16: Computational [Display Chart] 205 input genes in category / 540 annotations before applied cutoff / 10037 genes in category

	ID	Name	Source	pValue	FDR B&H	FDR B&Y	Bonferroni	Genes from Input	Genes in Annotation
1	M8838 MODULE 84	Immune (humoral) and inflammatory response.	MSigDb: C4 - CM: Cancer Modules (v6.0)	2.036E-15	1.100E-12	7.554E-12	1.100E-12	44	549
2	M12401 MODULE 75	Immune response.	MSigDb: C4 - CM: Cancer Modules (v6.0)	8.292E-13	2.239E-10	1.538E-9	4.478E-10	34	398
3	M4595 MODULE 436	Genes in the cancer module 436.	MSigDb: C4 - CM: Cancer Modules (v6.0)	5.321E-12	9.578E-10	6.580E-9	2.873E-9	20	139
4	M786 MODULE 345	Immune response and Ag processing and presentation.	MSigDb: C4 - CM: Cancer Modules (v6.0)	9.152E-12	1.236E-9	8.488E-9	4.942E-9	19	127
5	M15983 MODULE 46	Genes in the cancer module 46.	MSigDb: C4 - CM: Cancer Modules (v6.0)	1.636E-11	1.766E-9	1.213E-8	8.832E-9	32	394

Show 45 more annotations

17: MicroRNA [Display Chart] 310 input genes in category / 4669 annotations before applied cutoff / 72241 genes in category

	ID	Name	Source	pValue	FDR B&H	FDR B&Y	Bonferroni	Genes from Input	Genes in Annotation
1	hsa-miR-579:mirSVR highEffct	hsa-miR-579:mirSVR nonconserved highEffect-0.5	MicroRNA.org	1.092E-24	5.100E-21	4.604E-20	5.100E-21	50	1892
2	hsa-miR-302e:mirSVR lowEffct	hsa-miR-302e:mirSVR conserved lowEffect-0.1-0.5	MicroRNA.org	2.502E-20	5.842E-17	5.273E-16	1.168E-16	44	1817
3	hsa-miR-3189:mirSVR lowEffct	hsa-miR-3189:mirSVR nonconserved lowEffect-0.1-0.5	MicroRNA.org	3.857E-20	6.002E-17	5.418E-16	1.801E-16	41	1571
4	hsa-miR-4292:mirSVR lowEffct	hsa-miR-4292:mirSVR nonconserved lowEffect-0.1-0.5	MicroRNA.org	1.464E-19	1.709E-16	1.542E-15	6.834E-16	41	1631
5	hsa-miR-26b-5p:Functional MTI (Weak)	Functional MTI (Weak)	miRTarbase	5.087E-19	4.750E-16	4.288E-15	2.375E-15	43	1874

Show 45 more annotations

Table 1 E1 ToppGene

18: Drug [Display Chart] 310 input genes in category / 25044 annotations before applied cutoff / 22832 genes in category

	ID	Name	Source	pValue	FDR B&H	FDR B&Y	Bonferroni	Genes from Input	Genes in Annotation
1	1297 UP	Suloctidil [54063-56-8]; Up 200; 11.8uM; HL60; HT HG-U133A	Broad Institute CMAP Up	1.527E-40	3.825E-36	4.095E-35	3.825E-36	41	161
2	ctd:D010416	Pentachlorophenol	CTD	4.415E-26	5.529E-22	5.919E-21	1.106E-21	79	1510
3	ctd:D010081	Oxazolone	CTD	7.469E-25	6.235E-21	6.675E-20	1.871E-20	35	256
4	ctd:D014640	Vancomycin	CTD	5.215E-24	3.265E-20	3.496E-19	1.306E-19	59	906
5	ctd:D058185	Magnetite Nanoparticles	CTD	9.319E-23	4.668E-19	4.997E-18	2.334E-18	69	1313

Show 45 more annotations

19: Disease [Display Chart] 273 input genes in category / 3371 annotations before applied cutoff / 16284 genes in category

	ID	Name	Source	pValue	FDR B&H	FDR B&Y	Bonferroni	Genes from Input	Genes in Annotation
1	C0042769	Virus Diseases	DisGeNET Curated	3.287E-19	1.108E-15	9.641E-15	1.108E-15	57	872
2	C0004364	Autoimmune Diseases	DisGeNET Curated	2.118E-17	3.571E-14	3.106E-13	7.141E-14	59	1018
3	C0021400	Influenza	DisGeNET Curated	4.876E-15	5.479E-12	4.767E-11	1.644E-11	41	581
4	C0026769	Multiple Sclerosis	DisGeNET Curated	1.084E-14	9.131E-12	7.945E-11	3.653E-11	52	931
5	C0003873	Rheumatoid Arthritis	DisGeNET Curated	2.425E-14	1.635E-11	1.422E-10	8.174E-11	71	1633

Show 45 more annotations

Table 2.4.1. E1 Unique Upregulated Genes Functional Pathway Analysis by ToppGene.

Table 2 E2 ToppGene

1: GO: Molecular Function [Display Chart] 471 input genes in category / 1205 annotations before applied cutoff / 19242 genes in category

	ID	Name	Source	pValue	FDR B&H	FDR B&Y	Bonferroni	Genes from Input	Genes in Annotation
1	GO:0016301	kinase activity		1.218E-11	1.467E-8	1.126E-7	1.467E-8	85	1621
2	GO:0016773	phosphotransferase activity, alcohol group as acceptor		1.548E-10	9.326E-8	7.155E-7	1.865E-7	76	1444
3	GO:0016772	transferase activity, transferring phosphorus-containing groups		4.355E-10	1.749E-7	1.342E-6	5.248E-7	89	1859
4	GO:0004672	protein kinase activity		1.413E-9	4.257E-7	3.266E-6	1.703E-6	69	1315
5	GO:0004674	protein serine/threonine kinase activity		1.341E-8	3.233E-6	2.480E-5	1.616E-5	52	913

Show 45 more annotations

2: GO: Biological Process [Display Chart] 471 input genes in category / 6713 annotations before applied cutoff / 20146 genes in category

	ID	Name	Source	pValue	FDR B&H	FDR B&Y	Bonferroni	Genes from Input	Genes in Annotation
1	GO:0002682	regulation of immune system process		2.403E-19	1.613E-15	1.515E-14	1.613E-15	105	1776
2	GO:0042325	regulation of phosphorylation		9.113E-19	3.059E-15	2.872E-14	6.117E-15	104	1781
3	GO:0034097	response to cytokine		5.882E-18	1.145E-14	1.075E-13	3.949E-14	84	1287
4	GO:0071345	cellular response to cytokine stimulus		6.821E-18	1.145E-14	1.075E-13	4.579E-14	80	1188
5	GO:0019220	regulation of phosphate metabolic process		1.373E-17	1.365E-14	1.282E-13	9.214E-14	109	1994

Show 45 more annotations

3: GO: Cellular Component [Display Chart] 475 input genes in category / 659 annotations before applied cutoff / 20584 genes in category

	ID	Name	Source	pValue	FDR B&H	FDR B&Y	Bonferroni	Genes from Input	Genes in Annotation
1	GO:0009986	cell surface		1.401E-10	9.234E-8	6.528E-7	9.234E-8	59	1036
2	GO:0098552	side of membrane		9.910E-8	2.177E-5	1.539E-4	6.530E-5	39	663
3	GO:0097478	leaflet of membrane bilayer		9.910E-8	2.177E-5	1.539E-4	6.530E-5	39	663
4	GO:0016323	basolateral plasma membrane		1.704E-7	2.807E-5	1.984E-4	1.123E-4	22	259
5	GO:0031226	intrinsic component of plasma membrane		2.896E-7	3.816E-5	2.698E-4	1.908E-4	75	1790

Show 32 more annotations

4: Human Phenotype [Display Chart] 136 input genes in category / 3401 annotations before applied cutoff / 4707 genes in category

	ID	Name	Source	pValue	FDR B&H	FDR B&Y	Bonferroni	Genes from Input	Genes in Annotation
1	HP:0002037	Inflammation of the large intestine		1.196E-5	2.538E-2	2.211E-1	4.068E-2	18	198
2	HP:0012332	Abnormal autonomic nervous system physiology		1.493E-5	2.538E-2	2.211E-1	5.077E-2	17	182
3	HP:0004386	Gastrointestinal inflammation		4.780E-5	4.281E-2	3.729E-1	1.626E-1	20	261
4	HP:0011840	Abnormality of T cell physiology		5.294E-5	4.281E-2	3.729E-1	1.801E-1	13	125
5	HP:0003496	Increased circulating IgM level		6.773E-5	4.281E-2	3.729E-1	2.304E-1	9	63

Table 2 E2 ToppGene

5: Mouse Phenotype [Display Chart] 358 input genes in category / 4897 annotations before applied cutoff / 10724 genes in category

	ID	Name	Source	pValue	FDR B&H	FDR B&Y	Bonferroni	Genes from Input	Genes in Annotation
1	MP:0001545	abnormal hematopoietic system physiology		2.453E-19	1.201E-15	1.090E-14	1.201E-15	123	1664
2	MP:0002421	abnormal cell-mediated immunity		8.197E-19	2.007E-15	1.821E-14	4.014E-15	113	1473
3	MP:0001819	abnormal immune cell physiology		1.330E-18	2.171E-15	1.970E-14	6.513E-15	112	1461
4	MP:0002442	abnormal leukocyte physiology		2.274E-18	2.697E-15	2.447E-14	1.114E-14	110	1429
5	MP:0002420	abnormal adaptive immunity		2.753E-18	2.697E-15	2.447E-14	1.348E-14	113	1496

Show 45 more annotations

6: Domain [Display Chart] 468 input genes in category / 2400 annotations before applied cutoff / 18735 genes in category

	ID	Name	Source	pValue	FDR B&H	FDR B&Y	Bonferroni	Genes from Input	Genes in Annotation
1	PF00018	SH3 1	Pfam	3.692E-6	8.860E-3	7.407E-2	8.860E-3	16	164
2	IPR017348	PIM1/2/3	InterPro	1.589E-5	1.907E-2	1.595E-1	3.815E-2	3	3
3	SM00326	SH3	SMART	3.401E-5	2.571E-2	2.150E-1	8.162E-2	17	217
4	IPR001452	SH3 domain	InterPro	4.285E-5	2.571E-2	2.150E-1	1.028E-1	17	221
5	IPR008343	MKP	InterPro	7.163E-5	3.438E-2	2.875E-1	1.719E-1	4	10

Show 2 more annotations

7: Pathway [Display Chart] 358 input genes in category / 1822 annotations before applied cutoff / 12450 genes in category

	ID	Name	Source	pValue	FDR B&H	FDR B&Y	Bonferroni	Genes from Input	Genes in Annotation
1	1269318	Signaling by Interleukins	BioSystems: REACTOME	1.703E-11	1.912E-8	1.546E-7	3.103E-8	46	531
2	1269310	Cytokine Signaling in Immune system	BioSystems: REACTOME	2.098E-11	1.912E-8	1.546E-7	3.823E-8	57	763
3	1470923	Interleukin-4 and 13 signaling	BioSystems: REACTOME	2.522E-8	1.532E-5	1.238E-4	4.595E-5	17	114
4	523016	Transcriptional misregulation in cancer	BioSystems: KEGG	2.318E-7	1.056E-4	8.538E-4	4.224E-4	20	180
5	1470924	Interleukin-10 signaling	BioSystems: REACTOME	1.031E-6	3.758E-4	3.038E-3	1.879E-3	10	49

Show 45 more annotations

8: Pubmed [Display Chart] 479 input genes in category / 93706 annotations before applied cutoff / 38578 genes in category

	ID	Name	Source	pValue	FDR B&H	FDR B&Y	Bonferroni	Genes from Input	Genes in Annotation
1	20237496	New genetic associations detected in a host response study to hepatitis B vaccine.	Pubmed	1.481E-26	1.388E-21	1.669E-20	1.388E-21	58	825
2	19692168	Genetic susceptibility to distinct bladder cancer subphenotypes.	Pubmed	1.878E-20	8.797E-16	1.058E-14	1.759E-15	37	422
3	24952961	A high-resolution spatiotemporal atlas of gene expression of the developing mouse brain.	Pubmed	1.574E-19	4.918E-15	5.914E-14	1.475E-14	75	1849
4	25241761	Using an in situ proximity ligation assay to systematically profile endogenous protein-protein interactions in a pathway network.	Pubmed	1.478E-18	3.462E-14	4.163E-13	1.385E-13	33	371
5	19625176	PTEN identified as important risk factor of chronic obstructive pulmonary disease.	Pubmed	1.804E-17	3.050E-13	3.667E-12	1.690E-12	32	376

Show 45 more annotations

9: Interaction [Display Chart] 451 input genes in category / 8558 annotations before applied cutoff / 18137 genes in category

	ID	Name	Source	pValue	FDR B&H	FDR B&Y	Bonferroni	Genes from Input	Genes in Annotation
1	int:MYD88	MYD88 interactions		1.833E-8	1.569E-4	1.511E-3	1.569E-4	14	84
2	int:FYN	FYN interactions		5.382E-8	2.303E-4	2.218E-3	4.606E-4	24	265
3	int:IRAK1	IRAK1 interactions		8.860E-7	2.528E-3	2.435E-2	7.583E-3	16	148
4	int:MAPK14	MAPK14 interactions		1.703E-6	2.892E-3	2.785E-2	1.457E-2	22	276
5	int:MAPK8	MAPK8 interactions		1.785E-6	2.892E-3	2.785E-2	1.527E-2	19	214

Show 31 more annotations

Table 2 E2 ToppGene

10: Cytoband [Display Chart] 474 input genes in category / 326 annotations before applied cutoff / 34661 genes in category

	ID	Name	Source	pValue	FDR B&H	FDR B&Y	Bonferroni	Genes from Input	Genes in Annotation
1	22q11.23	22q11.23		9.390E-5	2.056E-2	1.309E-1	3.061E-2	6	54
2	3p21.3	3p21.3		1.699E-4	2.056E-2	1.309E-1	5.538E-2	6	60
3	3q13.13-q13.2	3q13.13-q13.2		1.892E-4	2.056E-2	1.309E-1	6.169E-2	2	2
4	7q31.2	7q31.2		5.100E-4	4.013E-2	2.554E-1	1.663E-1	3	12
5	17q12	17q12		6.155E-4	4.013E-2	2.554E-1	2.006E-1	7	105

11: Transcription Factor Binding Site [Display Chart] 301 input genes in category / 588 annotations before applied cutoff / 9770 genes in category

	ID	Name	Source	pValue	FDR B&H	FDR B&Y	Bonferroni	Genes from Input	Genes in Annotation
1	V$ETS1 B	V$ETS1 B		1.554E-5	9.139E-3	6.356E-2	9.139E-3	19	203
2	CCCNNGGGAR V$OLF1 01	CCCNNGGGAR V$OLF1 01		1.445E-4	4.249E-2	2.955E-1	8.498E-2	20	259

12: Gene Family [Display Chart] 304 input genes in category / 198 annotations before applied cutoff / 18194 genes in category

	ID	Name	Source	pValue	FDR B&H	FDR B&Y	Bonferroni	Genes from Input	Genes in Annotation
1	471	CD molecules|Tumor necrosis factor superfamily	genenames.org	4.628E-12	9.164E-10	5.377E-9	9.164E-10	30	394
2	594	Immunoglobulin like domain containing|Interleukin receptors|TIR domain containing	genenames.org	2.285E-5	1.517E-3	8.903E-3	4.525E-3	13	193
3	895	MAP kinase phosphatases	genenames.org	2.299E-5	1.517E-3	8.903E-3	4.552E-3	4	11
4	583	Heat shock 70kDa proteins	genenames.org	1.532E-4	7.581E-3	4.449E-2	3.033E-2	4	17
5	580	GTPases, IMAP	genenames.org	2.431E-4	9.625E-3	5.648E-2	4.813E-2	3	8

Show 18 more annotations

13: Coexpression [Display Chart] 477 input genes in category / 10538 annotations before applied cutoff / 23137 genes in category

	ID	Name	Source	pValue	FDR B&H	FDR B&Y	Bonferroni	Genes from Input	Genes in Annotation
1	16166618-SuppTable4	Mouse Lung not cancer Woodruff05 2371genes	GeneSigDB	4.034E-29	4.251E-25	4.183E-24	4.251E-25	105	1505
2	16166618-SuppTable3	Mouse Lung not cancer Woodruff05 2037genes	GeneSigDB	2.221E-28	1.170E-24	1.151E-23	2.340E-24	96	1301
3	11823860-SuppTable3	Human Breast van'tVeer02 2460genes Ergenes	GeneSigDB	1.837E-21	6.453E-18	6.350E-17	1.936E-17	106	1910
4	M13984	Genes up-regulated by IL2 [GeneID=3558] in cells derived from CD4+ [GeneID=920] cutaneous T-cell lymphoma (CTCL).	MSigDB C2: CGP Curated Gene Sets (v6.0)	3.986E-21	1.050E-17	1.033E-16	4.200E-17	27	115
5	M7631	Genes up-regulated in CD8 T cells: naïve versus 2' memory.	MSigDB C7: Immunologic Signatures (v6.0)	7.948E-20	1.675E-16	1.648E-15	8.375E-16	31	180

Show 45 more annotations

14: Coexpression Atlas [Display Chart] 474 input genes in category / 3864 annotations before applied cutoff / 21555 genes in category

	ID	Name	Source	pValue	FDR B&H	FDR B&Y	Bonferroni	Genes from Input	Genes in Annotation
1	GSM605823500	Myeloid Cells, DC.103-11b+.PolyIC.Lu, CD45 MHCII CD11c CD103 CD11b, Lung, avg-3	Immgen.org, GSE15907	4.955E-31	1.914E-27	1.692E-26	1.914E-27	59	409
2	GSM605761500	alpha beta T cells, T.4.Sp.B16, 4+ 8- TCR+ 45+, B16 Melanoma Spleen, avg-2	Immgen.org, GSE15907	5.952E-27	1.150E-23	1.016E-22	2.300E-23	49	322
3	GSM854269500	Myeloid Cells, DC.103-11b+24+.Lu, MHCII+ CD11c+ CD103- CD11b+ CD24+, Lung, avg-2	Immgen.org, GSE15907	8.960E-27	1.154E-23	1.020E-22	3.462E-23	54	404
4	GSM538309500	NK cells, NK.MCMV1.Sp, CD3-,NK1.1+, Spleen, avg-3	Immgen.org, GSE15907	3.162E-25	3.054E-22	2.699E-21	1.222E-21	50	367
5	GSM605820500	Myeloid Cells, DC.103+11b-.PolyIC.Lu, CD45 MHCII CD11c CD103 CD11b, Lung, avg-3	Immgen.org, GSE15907	2.557E-24	1.976E-21	1.746E-20	9.881E-21	50	384

Show 45 more annotations

Table 2 E2 ToppGene

15: ToppCell Atlas [Display Chart] 461 input genes in category / 2481 annotations before applied cutoff / 19604 genes in category

	ID	Name	Source	pValue	FDR B&H	FDR B&Y	Bonferroni	Genes from Input	Genes in Annotation
1	0ed6eb821b660b95193311a0946c276bf5e198ec	ImmunoHematopoietic-Lymphoid-natural killer cell of ImmunoHematopoietic	Mouse Atlas; Mouse Adult Overview - TabulaMuris; sample groups compared within lineage hierarchy	2.160E-17	4.100E-14	3.441E-13	5.360E-14	28	152
2	2e5168c4734e25be9f8c2037c3f3c442c22f92f5	ts04 Fat-ImmunoHematopoietic-Lymphoid-natural killer cell--natural killer cell of ts04 Fat	Mouse Atlas; Mouse Adult Overview - TabulaMuris; lineage hierarchy compared within sample groups	7.418E-17	4.100E-14	3.441E-13	1.840E-13	28	159
3	ad261b429aacc41a3175be442bbaa6d685c964b3	ts04 Fat-ImmunoHematopoietic-Lymphoid-natural killer cell of ts04 Fat	Mouse Atlas; Mouse Adult Overview - TabulaMuris; lineage hierarchy compared within sample groups	7.418E-17	4.100E-14	3.441E-13	1.840E-13	28	159
4	1755817839766478e1b273875c9a75110ba679ac	ts05 Lung-ImmunoHematopoietic-Natural killer cell-NK cell c19 of ts05 Lung	Mouse Atlas; Mouse Adult Overview - TabulaMuris; lineage hierarchy compared within sample groups	1.233E-16	4.100E-14	3.441E-13	3.059E-13	28	162
5	73050ab10f2e7c4347b5621c6c7343025d279c24	ts05 Lung-ImmunoHematopoietic-Natural killer cell-NK cell c19--natural killer cell of ts05 Lung	Mouse Atlas; Mouse Adult Overview - TabulaMuris; lineage hierarchy compared within sample groups	1.233E-16	4.100E-14	3.441E-13	3.059E-13	28	162

Show 45 more annotations

16: Computational [Display Chart] 327 input genes in category / 676 annotations before applied cutoff / 10037 genes in category

	ID	Name	Source	pValue	FDR B&H	FDR B&Y	Bonferroni	Genes from Input	Genes in Annotation
1	M16071 MODULE 38	Placenta genes.	MSigDb: C4 - CM: Cancer Modules (v6.0)	4.068E-10	2.750E-7	1.951E-6	2.750E-7	43	464
2	M7383 MODULE 5	Lung genes.	MSigDb: C4 - CM: Cancer Modules (v6.0)	2.078E-9	7.023E-7	4.982E-6	1.405E-6	40	434
3	M12401 MODULE 75	Immune response.	MSigDb: C4 - CM: Cancer Modules (v6.0)	6.988E-9	1.575E-6	1.117E-5	4.724E-6	37	398
4	M10899 MODULE 64	Membranal receptors.	MSigDb: C4 - CM: Cancer Modules (v6.0)	3.335E-8	5.637E-6	3.999E-5	2.255E-5	42	517
5	M15983 MODULE 46	Genes in the cancer module 46.	MSigDb: C4 - CM: Cancer Modules (v6.0)	5.824E-8	7.875E-6	5.586E-5	3.937E-5	35	394

Show 39 more annotations

Table 2 E2 ToppGene

17: MicroRNA [Display Chart] 479 input genes in category / 5203 annotations before applied cutoff / 72241 genes in category

	ID	Name	Source	pValue	FDR B&H	FDR B&Y	Bonferroni	Genes from Input	Genes in Annotation
1	hsa-let-7i:mirSVR lowEffct	hsa-let-7i:mirSVR conserved lowEffect-0.1-0.5	MicroRNA.org	2.618E-31	1.362E-27	1.244E-26	1.362E-27	71	1947
2	hsa-let-7e:mirSVR lowEffct	hsa-let-7e:mirSVR conserved lowEffect-0.1-0.5	MicroRNA.org	5.410E-30	1.408E-26	1.286E-25	2.815E-26	70	1985
3	hsa-let-7b:mirSVR lowEffct	hsa-let-7b:mirSVR conserved lowEffect-0.1-0.5	MicroRNA.org	9.875E-30	1.553E-26	1.419E-25	5.138E-26	69	1944
4	hsa-miR-3184:mirSVR lowEffct	hsa-miR-3184:mirSVR nonconserved lowEffect-0.1-0.5	MicroRNA.org	1.241E-29	1.553E-26	1.419E-25	6.457E-26	68	1891
5	hsa-let-7g:mirSVR lowEffct	hsa-let-7g:mirSVR conserved lowEffect-0.1-0.5	MicroRNA.org	1.493E-29	1.553E-26	1.419E-25	7.767E-26	68	1897

Show 45 more annotations

18: Drug [Display Chart] 477 input genes in category / 31314 annotations before applied cutoff / 22832 genes in category

	ID	Name	Source	pValue	FDR B&H	FDR B&Y	Bonferroni	Genes from Input	Genes in Annotation
1	ctd:D010126	Ozone	CTD	4.363E-26	1.366E-21	1.493E-20	1.366E-21	92	1273
2	ctd:C089730	rosiglitazone	CTD	3.691E-24	5.779E-20	6.316E-19	1.156E-19	100	1571
3	CID000006569	methyl ethyl ketone	Stitch	1.716E-21	1.791E-17	1.957E-16	5.372E-17	56	587
4	ctd:D020849	Raloxifene Hydrochloride	CTD	2.824E-18	2.133E-14	2.331E-13	8.844E-14	63	856
5	ctd:D052638	Particulate Matter	CTD	3.405E-18	2.133E-14	2.331E-13	1.066E-13	95	1747

Show 45 more annotations

19: Disease [Display Chart] 425 input genes in category / 5340 annotations before applied cutoff / 16284 genes in category

	ID	Name	Source	pValue	FDR B&H	FDR B&Y	Bonferroni	Genes from Input	Genes in Annotation
1	C0004096	Asthma	DisGeNET Curated	1.599E-16	8.537E-13	7.820E-12	8.537E-13	80	1134
2	C0079731	B-Cell Lymphomas	DisGeNET Curated	1.594E-15	4.256E-12	3.898E-11	8.511E-12	58	684
3	C0024299	Lymphoma	DisGeNET Curated	2.578E-14	4.096E-11	3.752E-10	1.377E-10	80	1242
4	C0023903	Liver neoplasms	DisGeNET Curated	3.068E-14	4.096E-11	3.752E-10	1.638E-10	82	1296
5	C0026769	Multiple Sclerosis	DisGeNET Curated	2.823E-13	2.635E-10	2.414E-9	1.508E-9	65	931

Show 45 more annotations

Table 2.4.2. E2 Unique Upregulated Genes Functional Pathway Analysis by ToppGene.

	Entrez Gene ID	Gene Symbol	Gene Name	Original Symbol
1	151636	DTX3L	deltex E3 ubiquitin ligase 3L	Dtx3l
2	10379	IRF9	interferon regulatory factor 9	Irf9
3	1234	CCR5	C-C motif chemokine receptor 5 (gene/pseudogene)	Ccr5
4	3455	IFNAR2	interferon alpha and beta receptor subunit 2	Ifnar2
5	467	ATF3	activating transcription factor 3	Atf3
6	5610	EIF2AK2	eukaryotic translation initiation factor 2 alpha kinase 2	Eif2ak2
7	3572	IL6ST	interleukin 6 signal transducer	Il6st
8	6714	SRC	SRC proto-oncogene, non-receptor tyrosine kinase	Src
9	3659	IRF1	interferon regulatory factor 1	Irf1
10	6772	STAT1	signal transducer and activator of transcription 1	Stat1
11	6773	STAT2	signal transducer and activator of transcription 2	Stat2
12	6774	STAT3	signal transducer and activator of transcription 3	Stat3
13	3791	KDR	kinase insert domain receptor	Kdr
14	83666	PARP9	poly(ADP-ribose) polymerase family member 9	Parp9
15	50944	SHANK1	SH3 and multiple ankyrin repeat domains 1	Shank1
16	1844	DUSP2	dual specificity phosphatase 2	Dusp2
17	840	CASP7	caspase 7	Casp7
18	9111	NMI	N-myc and STAT interactor	Nmi
19	7132	TNFRSF1A	TNF receptor superfamily member 1A	Tnfrsf1a

Table 2.4.3. STAT1 Pathway Analysis in E1 Unique Upregulated Genes.

	Entrez Gene ID	Gene Symbol	Gene Name	Original Symbol
1	118788	PIK3AP1	phosphoinositide-3-kinase adaptor protein 1	Pik3ap1
2	10318	TNIP1	TNFAIP3 interacting protein 1	Tnip1
3	1154	CISH	cytokine inducible SH2 containing protein	Cish
4	10370	CITED2	Cbp/p300 interacting transactivator with Glu/Asp rich carboxy-terminal domain 2	Cited2
5	3312	HSPA8	heat shock protein family A (Hsp70) member 8	Hspa8
6	3662	IRF4	interferon regulatory factor 4	Irf4
7	3663	IRF5	interferon regulatory factor 5	Irf5
8	596	BCL2	BCL2 apoptosis regulator	Bcl2
9	10013	HDAC6	histone deacetylase 6	Hdac6
10	57154	SMURF1	SMAD specific E3 ubiquitin protein ligase 1	Smurf1
11	54106	TLR9	toll like receptor 9	Tlr9
12	23495	TNFRSF13B	TNF receptor superfamily member 13B	Tnfrsf13b
13	11213	IRAK3	interleukin 1 receptor associated kinase 3	Irak3
14	7128	TNFAIP3	TNF alpha induced protein 3	Tnfaip3

Table 2.4.4. MyD88 Pathway Analysis in E2 Unique Upregulated Genes.

Antibody	Conjugate	Clone
CCR3	FITC	83101
CD101	PE	Moushi101
CD11b	PE	M1/70
CD11c	APC	N418
CD44	PE	IM7
CD62L	PE	MEL-14
CD69	PE	H1.2F3
CD80	APC	16-10A1
F4/80	FITC	BM8
GR-1	PE-Cy7	RB6-8C5
ICAM-1	FITC	YN1/1.7.4
IL-5ra	Alexa488	T21
Ly6C	PE-Cy7	HK1.4
Ly6G	PE-Cy7	1A8
MHCI	APC	AF6-88.5.5.3
PD-L1	PE-Dazzle	10F.9G2
Siglec-F	PE	E50-2440
ST2	FITC	DJ8

Table 2.4.5. Flow Cytometry Antibodies.

Gene	Primer Direction	Primer Sequence
IRF-1	For	CTGTGCGAGTGTACCGGATG
	Rev	ATCCCCACATGACTTCCTCTT
IRF-4	For	GCTGATCGACCAGATCGACAG
	Rev	CGGTTGTAGTCCTGCTTGC
STAT1	For	ATCAGGCTCAGTCGGGGAATA
	Rev	TGGTCTCGTGTTCTCTGTTCT
CCL24	For	CACATCATCCCTACGGGCTCT
	Rev	GGTTGCCAGGATATCTCTGGACAGGG
IL-13	For	CCTCATGGCGCTTTTGTTGAC
	Rev	TCTGGTTCTGGGTGATGTTGA
IL-4	For	CCAACTGCTTCCCCCTCTG
	Rev	TCTGTTACGGTCAACTCGGTG
IL-6	For	ACTCACCTCTTCAGAACGAATTG
	Rev	CCATCTTTGGAAGGTTCAGGTTG
CCL5	For	CCAGCAGTCGTCTTTGTCAC
	Rev	CTCTGGGTTGGCACACACTT
CXCL9	For	CCAGTAGTGAGAAAGGGTCGC
	Rev	AGGGCTTGGGGCAAATTGTT
CXCL10	For	GTGGCATTCAAGGAGTACCTC
	Rev	TGATGGCCTTCGATTCTGGATT
Nos2	For	AGGGACAAGCCTACCCCTC
	Rev	CTCATCTCCCGTCAGTTGGT

Table 2.4.6. Real-Time PCR (RT-PCR) Primers.

2.5 Methods

2.5.1 Mice

All studies were performed with male and female IL-5 NJ.1638 (C57BL/6). Mice were housed under specific pathogen-free conditions and treated according to institutional guidelines and protocols (IACUC protocols A59115-15 and A00004010-18).

2.5.2 Eosinophil isolation from mouse

Eosinophils were isolated from the peripheral blood of IL-5 transgenic NJ.1638 mice as previously described [91]. Buffy coat was separated from erythrocytes by Histopaque

1119 (Sigma-Aldrich, 11191) density centrifugation. Remaining erythrocytes were lysed with distilled water and contaminating cells were removed by magnetic beads against CD45R and CD90.1 (Miltenyi,). Viability was >99% by trypan blue and purity of eosinophils were >98% by Hema 3-stained (Fisher) cytospins and light microscopy.

2.5.3 Mouse Eosinophil Cell Culture and Activation

Eosinophils were cultured at 5 x 10^6 cells/mL in RPMI 1640 (Gibco), GlutaMAX, HEPES (Gibco) supplemented with 10% FBS (HyClone Technologies), 55μM 2-Mercaptoethanol (Thermofisher Scientific), Penicillin-Steptomycin-Glutamine (Thermofisher Scientific), and IL-5 (10ng/mL, Peprotech) for 18hrs at 37°C with 5% CO_2, unless noted otherwise. For activation, type 2 activated eosinophils (E2) were supplemented with IL-33 (30ng/mL; R&D Systems), GM-CSF (10ng/mL; Peprotech) and IL-4 (10ng/mL; Peprotech). Type 1 activated eosinophils (E1) were supplemented with IFNγ (15ng/mL; Peprotech) and TNFα (15ng/mL; Peprotech). Resting eosinophils (E0) were cultured without any additional cytokines.

2.5.4 Human Eosinophil Isolation and Cell Culture Activation

50mL of blood was taken by venous puncture from 4 healthy (non-atopic, non-allergic, non-asthmatic) donors. Eosinophils were isolated from whole blood using MACSxpress Whole Blood Eosinophil Isolation Kit (Miltenyi Biotec) following manufacture protocol. Viability was >99% as measured by trypan blue and purity of eosinophils were >99% by Hema 3-stained (Fisher) cytospins and light microscopy. The study was approved by the Institutional Review Board at Mayo Clinic in Arizona (IRB# 17-007025). Cells were cultured at 2 x 10^6 cells/mL in RPMI 1640 (Gibco), GlutaMAX, HEPES (Gibco)

supplemented with 10% ES FBS (Gibco), 55µM 2-Mercaptoethanol (Thermofisher Scientific), Penicillin-Steptomycin-Glutamine (Thermofisher Scientific), and IL-5 (1ng/mL) for 18hrs at 37°C with 5% CO_2. For activation, type 1 (E1) eosinophils were supplemented with INF-γ and TNF-α (15ng/mL) and type 2 (E2) eosinophils were cultured with IL-33 (50ng/mL) and IL-4 (10ng/mL) and GM-CSF (10ng/mL). All recombinant human cytokines are from R&D Systems.

2.5.5 Morphology

Morphological analysis was performed on cytocentrifuged cultured eosinophils stained with Protocol Hema 3 (Fisher Scientific). Cells were examined and imaged using Axiophat microscope (Zeiss) equipped with EC Plan-Neofluar 40x/0.17 objective (Zeiss) and Axiocam MRc 5 digital camera (Zeiss). For mouse eosinophils, quantification was done blinded manually by cell count module (ImageJ). Vacuole-like structures were defined as an eosinophil containing more than 1 optically clear circle within the cytoplasm. Hypersegemented were defined as an eosinophil containing more than 1 "pinch" in the nucleus. A total of 3 samples from 3 independent experiments were counted for a minimum of 300 cells per cytospin.

2.5.6 Viability

To evaluate viability, eosinophils were cultured with cytokines for the mentioned times and stained with Annexin V FITC and PI flow cytometry kit (Thermofisher Scientific) according to manufacture protocol. Flow cytometry was performed on BD FACSCelesta and/or Fortessa (BD Biosciences) and data were analyzed with FlowJo software v10.6 (Tree Star).

2.5.7 Supernatant Protein Quantification

EPX concentrations were measured in cell-free supernatant using a sandwich ELISA as previously described [280] and cytokines and chemokines were measured by using Multiplexing LASER Bead Assay (Eve Technologies).

2.5.8 Flow Cytometry Surface Markers

Surface staining of single-cell suspensions of cultured eosinophils was performed at 4°C for 30 minutes in FACS buffer (0.5% FBS + 2mM EDTA in PBS). Anti-CD16/32 (clone 2.4G2) was used to block background staining and fixable viability dye eFluor™ 455UV (eBiosciences/Thermofisher) was used to exclude dead cells. All antibodies were used at 1µg/ml per 10^6 cells (full list of antibodies are in Table 2.4.5). Flow cytometry was performed on BD LSRFortessa (BD Biosciences) and data were analyzed with FlowJo software (Tree Star).

2.5.9 RNA Isolation

Total RNA was isolated using Trizol Reagent (Thermofisher), according to the manufacturer's protocol. RNA integrity and purity was analyzed by the Agilent 2100 Bioanalyzer (Agilent Technologies) and NanoDrop spectrophotometer (Thermofisher).

2.5.10 Mouse RNASeq and Analysis

Eosinophil total RNA (>100ng/µL) was amplified using TruSeq RNA Library Prep Kit v2 (Illumina)2and sequencing was performed using HiSeq 2000 PE (Illumina). Samples are sequenced at Mayo sequencing center and processed with our pipeline MAP-RSeq [281]. Where the fastq files are mapped to mouse reference mm10 with STAR [282] and expression is quantified with featureCounts [283]. The expression differential analysis is

performed by edgeR [284]. Volcano plots used R package *EnhancedVolcano* [285] (Blighe K (2019). *EnhancedVolcano: Publication-ready volcano plots with enhanced colouring and labeling. R package version 1.4.0, https://github.com/kevinblighe/EnhancedVolcano).* PCA plots used R package *prcomp and ggfortify*. For generation of the heat map, experimental conditions were normalized to appropriate controls and differential gene expression using R package heatmap.3.

Analysis for functional enrichment and ontology was completed with differential expressed E1 and E2 eosinophil genes (FC≥2, p-value <0.05) for use in the software tools listed. ToppGene program ToppFun [286] (www.toppgene.cchmc.org) uses the following databases ENTREZ Gene, European Molecular Biology Laboratory, Gene Ontology, Human Phenotype Ontology, Mammalian Phenotype (MGI), Gene SigDB, miTarBase, PITA, microRNA.org, GWAS central, Biomolecular Interaction Network Database, The Human Protein Reference Database, General Repository for Interaction Datasets, Comparatrive Toxicogenomics Database, STITCH, Kyoto Encylopedia of Genes and Genome s (KEGG), BioCyc, BioCartaPathways, Small Molecula Patway Database, Panther Pathways, Reactome, Uniprot-Expasy, Pubmed, TargetScan, PicTar, MSigDB, Drug Bank for computational analysis.

2.5.11 Real-Time PCR

For both mouse and human gene expression analysis, cDNA was synthesized from 0.4-1µg total RNA using SuperScript IV VILO with ezDnase kit (Invitrogen) following manufactures protocol. Real-time PCR (RT-PCR) for mouse genes were performed using TaqMan probes and Taqman Universal Master Mix II, with UNG (Applied Biosystems) on a 7900HT Fast Real-Time PCR system (Applied Biosystems) or CFX384 Touch Real-

Time PCR Detection System (Bio-Rad). For human genes, RT-PCR was performed using primers and SsoAdvanced Universal SYBR Green Supermix (Bio-Rad) on a CFX384 Touch Real-Time PCR Detection System (Bio-Rad). List of primers and probes can be found in (Table 2.4.6). Data was analyzed using the comparative Ct (ΔΔCt) method with β-actin as the endogenous control and normalized to E0.

2.5.12 Plasticity

For plasticity experiments, eosinophils were initially activated in E0, E1, or E2 conditions (18hrs) then washed 3 times in MACS buffer (PBS with 0.5% BSA and 2mM EDTA) and placed back into culture with the opposite activation cytokines (i.e., E1 cells into E2 cytokines (E1-E2) and E2 cells into E1 cytokines (E2-E1)) for an additional 24 hrs (i.e., E1-E2 and E2-E1). Controls included cells being placed back into the same cytokine conditions (i.e., E0-E0, E1-E1, and E2-E2). RT-PCR was completed to measure changes in transcription factors and downstream mediators. Flow Cytometry was used to measure changes in cell surface protein expression.

2.5.13 Statistics

Statistical analysis was performed using GraphPad Prism software (Version 8, GraphPad Software, La Jolla, CA.) on figures 2.4.1, 3, 4, and 6. Comparison of 2 samples was performed using unpaired t-test. For comparison of more than 2 groups, ordinary one-way ANOVA followed by Tukey's multiple comparisons test were used.

2.6 References

1. Jacobsen, E.A., et al., *The expanding role(s) of eosinophils in health and disease.* Blood, 2012. 120(19): p. 3882-90.

2. Marichal, T., C. Mesnil, and F. Bureau, *Homeostatic Eosinophils: Characteristics and Functions.* Frontiers in medicine, 2017. 4: p. 101-101.

3. Weller, P.F. and L.A. Spencer, *Functions of tissue-resident eosinophils.* Nature reviews. Immunology, 2017. 17(12): p. 746-760.

4. Onyema, O.O., et al., *Eosinophils promote inducible NOS-mediated lung allograft acceptance.* JCI Insight, 2017. 2(24).

5. Carretero, R., et al., *Eosinophils orchestrate cancer rejection by normalizing tumor vessels and enhancing infiltration of CD8(+) T cells.* Nat Immunol, 2015. 16(6): p. 609-17.

6. Bochner, B.S., *The eosinophil: For better or worse, in sickness and in health.* Ann Allergy Asthma Immunol, 2018. 121(2): p. 150-155.

7. Vu Manh, T.P., et al., *Investigating Evolutionary Conservation of Dendritic Cell Subset Identity and Functions.* Front Immunol, 2015. 6: p. 260.

8. Gabriele, L. and K. Ozato, *The role of the interferon regulatory factor (IRF) family in dendritic cell development and function.* Cytokine Growth Factor Rev, 2007. 18(5-6): p. 503-10.

9. Spits, H., et al., *Innate lymphoid cells--a proposal for uniform nomenclature.* Nat Rev Immunol, 2013. 13(2): p. 145-9.

10. Chistiakov, D.A., et al., *The impact of interferon-regulatory factors to macrophage differentiation and polarization into M1 and M2.* Immunobiology, 2018. 223(1): p. 101-111.

11. Roszer, T., *Understanding the Mysterious M2 Macrophage through Activation Markers and Effector Mechanisms.* Mediators Inflamm, 2015. 2015: p. 816460.

12. Hong, C.W., *Current Understanding in Neutrophil Differentiation and Heterogeneity.* Immune Netw, 2017. 17(5): p. 298-306.

13. Liew, F.Y., *T(H)1 and T(H)2 cells: a historical perspective.* Nat Rev Immunol, 2002. 2(1): p. 55-60.

14. Prin, L., et al., *Heterogeneity of human peripheral blood eosinophils: variability in cell density and cytotoxic ability in relation to the level and the origin of hypereosinophilia.* Int Arch Allergy Appl Immunol, 1983. 72(4): p. 336-46.

15. Prin, L., et al., *Heterogeneity of human eosinophils. II. Variability of respiratory burst activity related to cell density.* Clinical and experimental immunology, 1984. 57(3): p. 735-742.

16. Capron, M., et al., *Functional role of the alpha-chain of complement receptor type 3 in human eosinophil-dependent antibody-mediated cytotoxicity against schistosomes.* J Immunol, 1987. 139(6): p. 2059-65.

17. Rothenberg, M.E., et al., *Human eosinophils have prolonged survival, enhanced functional properties, and become hypodense when exposed to human interleukin 3.* J Clin Invest, 1988. 81(6): p. 1986-92.

18. Caulfield, J.P., et al., *A morphometric study of normodense and hypodense human eosinophils that are derived in vivo and in vitro.* Am J Pathol, 1990. 137(1): p. 27-41.

19. Liu, L.Y., et al., *Generation of Th1 and Th2 chemokines by human eosinophils: evidence for a critical role of TNF-alpha.* J Immunol, 2007. 179(7): p. 4840-8.

20. Spencer, L.A., et al., *Human eosinophils constitutively express multiple Th1, Th2, and immunoregulatory cytokines that are secreted rapidly and differentially.* J Leukoc Biol, 2009. 85(1): p. 117-23.

21. Cherry, W.B., et al., *A novel IL-1 family cytokine, IL-33, potently activates human eosinophils.* J Allergy Clin Immunol, 2008. 121(6): p. 1484-90.

22. Esnault, S. and E.A. Kelly, *Essential Mechanisms of Differential Activation of Eosinophils by IL-3 Compared to GM-CSF and IL-5.* Critical reviews in immunology, 2016. 36(5): p. 429-444.

23. Drake, M.G., et al., *Human and Mouse Eosinophils Have Antiviral Activity against Parainfluenza Virus.* Am J Respir Cell Mol Biol, 2016. 55(3): p. 387-94.

24. Handzel, Z.T., et al., *Eosinophils bind rhinovirus and activate virus-specific T cells.* J Immunol, 1998. 160(3): p. 1279-84.

25. Samarasinghe, A.E., et al., *Eosinophils Promote Antiviral Immunity in Mice Infected with Influenza A Virus.* J Immunol, 2017. 198(8): p. 3214-3226.

26. Arnold, I.C., et al., *Eosinophils suppress Th1 responses and restrict bacterially induced gastrointestinal inflammation.* J Exp Med, 2018.

27. Onyema, O.O., et al., *Eosinophils downregulate lung alloimmunity by decreasing TCR signal transduction.* JCI Insight, 2019. 4(11).

28. Stolarski, B., et al., *IL-33 Exacerbates Eosinophil-Mediated Airway Inflammation.* The Journal of Immunology, 2010. 185(6): p. 3472-3480.

29. Jacobsen, E.A., et al., *Differential activation of airway eosinophils induces IL-13-mediated allergic Th2 pulmonary responses in mice.* Allergy, 2015. 70(9): p. 1148-59.

30. Jacobsen, E.A., et al., *Allergic pulmonary inflammation in mice is dependent on eosinophil-induced recruitment of effector T cells.* Journal of Experimental Medicine, 2008. 205(3): p. 699-710.

31. Jacobsen, E.A., et al., *Eosinophils Regulate Dendritic Cells and Th2 Pulmonary Immune Responses following Allergen Provocation.* The Journal of Immunology, 2011: p. 1102299.

32. Doyle, A.D., et al., *Eosinophil-derived IL-13 promotes emphysema.* Eur Respir J, 2019. 53(5).

33. Khoury, P., et al., *Revisiting the NIH Taskforce on the Research needs of Eosinophil-Associated Diseases (RE-TREAD).* Journal of Leukocyte Biology, 2018. 104(1): p. 69-83.

34. Percopo, C.M., et al., *SiglecF+Gr1hi eosinophils are a distinct subpopulation within the lungs of allergen-challenged mice.* J Leukoc Biol, 2017. 101(1): p. 321-328.

35. Czech, W., et al., *Induction of intercellular adhesion molecule 1 (ICAM-1) expression in normal human eosinophils by inflammatory cytokines.* J Invest Dermatol, 1993. 100(4): p. 417-23.

36. Abdala Valencia, H., et al., *Phenotypic plasticity and targeting of Siglec-F(high) CD11c(low) eosinophils to the airway in a murine model of asthma.* Allergy, 2016. 71(2): p. 267-71.

37. Bochner, B.S., *Siglec-8 on human eosinophils and mast cells, and Siglec-F on murine eosinophils, are functionally related inhibitory receptors.* Clin Exp Allergy, 2009. 39(3): p. 317-24.

38. Johansson, M.W., *Activation states of blood eosinophils in asthma.* Clin Exp Allergy, 2014. 44(4): p. 482-98.

39. Mesnil, C., et al., *Lung-resident eosinophils represent a distinct regulatory eosinophil subset.* J Clin Invest, 2016. 126(9): p. 3279-95.

40. Zhang, M., et al., *Defining the in vivo function of Siglec-F, a CD33-related Siglec expressed on mouse eosinophils.* Blood, 2007. 109(10): p. 4280-4287.

41. Ochkur, S.I., et al., *Coexpression of IL-5 and Eotaxin-2 in Mice Creates an Eosinophil-Dependent Model of Respiratory Inflammation with Characteristics of Severe Asthma.* The Journal of Immunology, 2007. 178(12): p. 7879.

42. Xenakis, J.J., et al., *Resident intestinal eosinophils constitutively express antigen presentation markers and include two phenotypically distinct subsets of eosinophils.* Immunology, 2018. 154(2): p. 298-308.

43. Laumonnier, Y., et al., *Accumulation of pulmonary vacuolated eosinophils in experimental allergic asthma that synergize with dendritic cells to induce Th-17 cells.* Journal of Immunology, 2017. 198(1): p. 53.6.

44. Radonjic-Hoesli, S., et al., *Adhesion-induced eosinophil cytolysis requires the receptor-interacting protein kinase 3 (RIPK3)–mixed lineage kinase-like (MLKL) signaling pathway, which is counterregulated by autophagy.* Journal of Allergy and Clinical Immunology, 2017. 140(6): p. 1632-1642.

45. Muniz-Junqueira, M.I., S.M. Barbosa-Marques, and L.F. Junqueira, Jr., *Morphological changes in eosinophils are reliable markers of the severity of an acute asthma exacerbation in children.* Allergy, 2013. 68(7): p. 911-20.

46. Connell, J.T., *Morphological changes in eosinophils in allergic disease.* Journal of Allergy, 1968. 41(1): p. 1-9.

47. Willebrand, R. and D. Voehringer, *IL-33-Induced Cytokine Secretion and Survival of Mouse Eosinophils Is Promoted by Autocrine GM-CSF.* PLOS ONE, 2016. 11(9): p. e0163751.

48. Melo, R.C.N., et al., *Eosinophil-derived cytokines in health and disease: unraveling novel mechanisms of selective secretion.* Allergy, 2013. 68(3): p. 274-284.

49. Rose, C.E., Jr., et al., *Murine lung eosinophil activation and chemokine production in allergic airway inflammation.* Cell Mol Immunol, 2010. 7(5): p. 361-74.

50. Bouffi, C., et al., *IL-33 markedly activates murine eosinophils by an NF-kappaB-dependent mechanism differentially dependent upon an IL-4-driven autoinflammatory loop.* J Immunol, 2013. 191(8): p. 4317-25.

51. Davoine, F. and P. Lacy, *Eosinophil Cytokines, Chemokines, and Growth Factors: Emerging Roles in Immunity.* Frontiers in Immunology, 2014. 5: p. 570.

52. Dajotoy, T., et al., *Human eosinophils produce the T cell-attracting chemokines MIG and IP-10 upon stimulation with IFN-gamma.* J Leukoc Biol, 2004. 76(3): p. 685-91.

53. Tamura, T., et al., *The IRF family transcription factors in immunity and oncogenesis.* Annu Rev Immunol, 2008. 26: p. 535-84.

54. Ahyi, A.N., et al., *IFN regulatory factor 4 regulates the expression of a subset of Th2 cytokines.* J Immunol, 2009. 183(3): p. 1598-606.

55. Wen, T., et al., *Carbonic anhydrase IV is expressed on IL-5-activated murine eosinophils.* J Immunol, 2014. 192(12): p. 5481-9.

56. Esnault, S., et al., *Identification of genes expressed by human airway eosinophils after an in vivo allergen challenge.* PLoS One, 2013. 8(7): p. e67560.

57. Zhu, J. and W.E. Paul, *Heterogeneity and plasticity of T helper cells.* Cell Res, 2010. 20(1): p. 4-12.

58. Nam, S. and J.S. Lim, *Essential role of interferon regulatory factor 4 (IRF4) in immune cell development.* Arch Pharm Res, 2016. 39(11): p. 1548-1555.

59. Krausgruber, T., et al., *IRF5 promotes inflammatory macrophage polarization and TH1-TH17 responses.* Nat Immunol, 2011. 12(3): p. 231-8.

60. O'Sullivan, J.A. and B.S. Bochner, *Eosinophils and eosinophil-associated diseases: An update.* J Allergy Clin Immunol, 2018. 141(2): p. 505-517.

61. Berek, C., *Eosinophils can more than kill.* J Exp Med, 2018. 215(8): p. 1967-1969.

62. Rosenberg, H.F., K.D. Dyer, and P.S. Foster, *Eosinophils: changing perspectives in health and disease.* Nat Rev Immunol, 2013. 13(1): p. 9-22.

63. Liu, L.Y., et al., *Decreased expression of membrane IL-5 receptor alpha on human eosinophils: I. Loss of membrane IL-5 receptor alpha on airway eosinophils and increased soluble IL-5 receptor alpha in the airway after allergen challenge.* J Immunol, 2002. 169(11): p. 6452-8.

64. Ying, S., et al., *Phenotype of cells expressing mRNA for TH2-type (interleukin 4 and interleukin 5) and TH1-type (interleukin 2 and interferon gamma) cytokines in bronchoalveolar lavage and bronchial biopsies from atopic asthmatic and normal control subjects.* Am J Respir Cell Mol Biol, 1995. 12(5): p. 477-87.

65. Mosher, D.F., et al., *Proteomics of Eosinophil Activation.* Frontiers in medicine, 2017. 4: p. 159-159.

66. Esnault, S., et al., *IL-3 Maintains Activation of the p90S6K/RPS6 Pathway and Increases Translation in Human Eosinophils.* J Immunol, 2015. 195(6): p. 2529-39.

67. Nguyen, W.N.T., et al., *Intravital imaging of eosinophils: Unwrapping the enigma.* J Leukoc Biol, 2020.

68. Lee, J.J., et al., *Eosinophils in health and disease: the LIAR hypothesis.* Clin Exp Allergy, 2010. 40(4): p. 563-75.

69. Abdala-Valencia, H., et al., *Shaping eosinophil identity in the tissue contexts of development, homeostasis, and disease.* J Leukoc Biol, 2018. 104(1): p. 95-108.

70. Klion, A., *Recent advances in understanding eosinophil biology.* F1000Research, 2017. 6: p. 1084-1084.

71. Zheng, C., et al., *Landscape of Infiltrating T Cells in Liver Cancer Revealed by Single-Cell Sequencing.* Cell, 2017. 169(7): p. 1342-1356 e16.

72. Villani, A.-C., et al., *Single-cell RNA-seq reveals new types of human blood dendritic cells, monocytes, and progenitors.* Science, 2017. 356(6335): p. eaah4573.

73. Bjorklund, A.K., et al., *The heterogeneity of human CD127(+) innate lymphoid cells revealed by single-cell RNA sequencing.* Nat Immunol, 2016. 17(4): p. 451-60.

74. Jablonski, K.A., et al., *Novel Markers to Delineate Murine M1 and M2 Macrophages.* PLoS One, 2015. 10(12): p. e0145342.

75. Seder, R.A., et al., *The presence of interleukin 4 during in vitro priming determines the lymphokine-producing potential of CD4+ T cells from T cell receptor transgenic mice.* Journal of Experimental Medicine, 1992. 176(4): p. 1091-1098.

76. Hsieh, C.S., et al., *Differential regulation of T helper phenotype development by interleukins 4 and 10 in an alpha beta T-cell-receptor transgenic system.* Proceedings of the National Academy of Sciences, 1992. 89(13): p. 6065-6069.

77. Murray, P.J. and T.A. Wynn, *Protective and pathogenic functions of macrophage subsets.* Nature Reviews Immunology, 2011. 11(11): p. 723-737.

78. Lacy, P., et al., *Rapid mobilization of intracellularly stored RANTES in response to interferon-gamma in human eosinophils.* Blood, 1999. 94(1): p. 23-32.

79. Grewe, M., et al., *Human eosinophils produce biologically active IL-12: implications for control of T cell responses.* J Immunol, 1998. 161(1): p. 415-20.

80. Johansson, M.W., et al., *Up-regulation and activation of eosinophil integrins in blood and airway after segmental lung antigen challenge.* Journal of immunology (Baltimore, Md. : 1950), 2008. 180(11): p. 7622-7635.

81. Johnston, L.K. and P.J. Bryce, *Understanding Interleukin 33 and Its Roles in Eosinophil Development.* Frontiers in Medicine, 2017. 4: p. 51.

82. Mengelers, H.J., et al., *Down modulation of L-Selectin expression on eosinophils recovered from bronchoalveolar lavage fluid after allergen provocation.* Clin Exp Allergy, 1993. 23(3): p. 196-204.

83. In 't Veen, J., et al., *CD11b and L-selectin expression on eosinophils and neutrophils in blood and induced sputum of patients with asthma compared with normal subjects.* Clinical and experimental allergy : journal of the British Society for Allergy and Clinical Immunology, 1998. 28: p. 606-15.

84. Momose, T., et al., *Interferon-gamma increases CD62L expression on human eosinophils.* Int Arch Allergy Immunol, 1999. 120 Suppl 1: p. 30-3.

85. Tomaki, M., et al., *Eosinophilopoiesis in a murine model of allergic airway eosinophilia: involvement of bone marrow IL-5 and IL-5 receptor alpha.* J Immunol, 2000. 165(7): p. 4040-50.

86. Throsby, M., et al., *CD11c+ Eosinophils in the Murine Thymus: Developmental Regulation and Recruitment upon MHC Class I-Restricted Thymocyte Deletion.* The Journal of Immunology, 2000. 165(4): p. 1965-1975.

87. Chu, D.K., et al., *Indigenous enteric eosinophils control DCs to initiate a primary Th2 immune response in vivo.* The Journal of Experimental Medicine, 2014. 211(8): p. 1657.

88. Carlens, J., et al., *Common γ-Chain-Dependent Signals Confer Selective Survival of Eosinophils in the Murine Small Intestine.* The Journal of Immunology, 2009. 183(9): p. 5600.

89. Wang, H., et al., *CD69 expression on eosinophils is a marker of activation in the lung following allergen provocation.* Journal of Allergy and Clinical Immunology, 2004. 113(2, Supplement): p. S188.

90. Hartnell, A., et al., *CD69 is expressed by human eosinophils activated in vivo in asthma and in vitro by cytokines.* Immunology, 1993. 80(2): p. 281-6.

91. Shubin, A.V., et al., *Cytoplasmic vacuolization in cell death and survival.* Oncotarget, 2016. 7(34): p. 55863-55889.

92. Tai, P.C. and C.J. Spry, *The mechanisms which produce vacuolated and degranulated eosinophils.* Br J Haematol, 1981. 49(2): p. 219-26.

93. Melo, R.C.N. and P.F. Weller, *Unraveling the complexity of lipid body organelles in human eosinophils.* Journal of leukocyte biology, 2014. 96(5): p. 703-712.

94. Mathur, S.K., et al., *Interaction between allergy and innate immunity: model for eosinophil regulation of epithelial cell interferon expression.* Ann Allergy Asthma Immunol, 2013. 111(1): p. 25-31.

95. Phipps, S., et al., *Eosinophils contribute to innate antiviral immunity and promote clearance of respiratory syncytial virus.* Blood, 2007. 110(5): p. 1578-86.

96. Diny, N.L., N.R. Rose, and D. Cihakova, *Eosinophils in Autoimmune Diseases.* Front Immunol, 2017. 8: p. 484.

97. Chu, V.T., et al., *Eosinophils are required for the maintenance of plasma cells in the bone marrow.* Nat Immunol, 2011. 12(2): p. 151-9.

98. Chu, V.T., et al., *Eosinophils promote generation and maintenance of immunoglobulin-A-expressing plasma cells and contribute to gut immune homeostasis.* Immunity, 2014. 40(4): p. 582-93.

99. Chu, V.T. and C. Berek, *Immunization induces activation of bone marrow eosinophils required for plasma cell survival.* Eur J Immunol, 2012. 42(1): p. 130-7.

100. Calcinotto, A., et al., *Microbiota-driven interleukin-17-producing cells and eosinophils synergize to accelerate multiple myeloma progression.* Nat Commun, 2018. 9(1): p. 4832.

101. Wong, T.W., et al., *Eosinophils regulate peripheral B cell numbers in both mice and humans.* J Immunol, 2014. 192(8): p. 3548-58.

102. Tong, Y., et al., *Elevated Plasma Chemokines for Eosinophils in Neuromyelitis Optica Spectrum Disorders during Remission.* Front Neurol, 2018. 9: p. 44.

103. Nguyen, T., et al., *Immunophenotyping of peripheral eosinophils demonstrates activation in eosinophilic esophagitis.* J Pediatr Gastroenterol Nutr, 2011. 53(1): p. 40-7.

104. Nascimento, F.R.F., et al., *Interferon Regulatory Factor (IRF)-1 Is a Master Regulator of the Cross Talk between Macrophages and L929 Fibrosarcoma Cells for Nitric Oxide Dependent Tumoricidal Activity.* PLOS ONE, 2015. 10(2): p. e0117782.

105. Yamamoto, M., et al., *Shared and distinct functions of the transcription factors IRF4 and IRF8 in myeloid cell development.* PLoS One, 2011. 6(10): p. e25812.

106. Honma, K., et al., *Interferon regulatory factor 4 differentially regulates the production of Th2 cytokines in naïve vs. effector/memory CD4⁺ T cells.* Proceedings of the National Academy of Sciences, 2008. 105(41): p. 15890-15895.

107. Mohapatra, A., et al., *Group 2 innate lymphoid cells utilize the IRF4-IL-9 module to coordinate epithelial cell maintenance of lung homeostasis.* Mucosal Immunol, 2016. 9(1): p. 275-86.

108. Lee, M.-C., et al., *GM-CSF– and IRF4-Dependent Signaling Can Regulate Myeloid Cell Numbers and the Macrophage Phenotype during Inflammation.* The Journal of Immunology, 2019: p. ji1801549.

109. Staudt, V., et al., *Interferon-Regulatory Factor 4 Is Essential for the Developmental Program of T Helper 9 Cells.* Immunity, 2010. 33(2): p. 192-202.

110. Ochkur, S.I., et al., *The development of a sensitive and specific ELISA for mouse eosinophil peroxidase: assessment of eosinophil degranulation ex vivo and in models of human disease.* J Immunol Methods, 2012. 375(1-2): p. 138-47.

111. Kalari, K.R., et al., *MAP-RSeq: Mayo Analysis Pipeline for RNA sequencing.* BMC Bioinformatics, 2014. 15(1): p. 224.

112. Dobin, A., et al., *STAR: ultrafast universal RNA-seq aligner.* Bioinformatics (Oxford, England), 2013. 29(1): p. 15-21.

113. Liao, Y., G.K. Smyth, and W. Shi, *featureCounts: an efficient general purpose program for assigning sequence reads to genomic features.* Bioinformatics, 2014. 30(7): p. 923-30.

114. Robinson, M.D., D.J. McCarthy, and G.K. Smyth, *edgeR: a Bioconductor package for differential expression analysis of digital gene expression data.* Bioinformatics (Oxford, England), 2010. 26(1): p. 139-140.

115. Kevin Blighe, S.R., Myles Lewis, *EnhancedVolcano: Publication-ready volcano plots with enhanced colouring and labeling. R package.* 2019, R.

116. Chen, J., et al., *ToppGene Suite for gene list enrichment analysis and candidate gene prioritization.* Nucleic acids research, 2009. 37(Web Server issue): p. W305-W311.

CHAPTER 3

ASSESSMENT OF LUNG EOSINOPHILS IN SITU USING IMMUNOHISTOLOGICAL STAINING

Accepted and soon to be published: Christopher D. Nazaroff, William E. LeSuer, Mia Y. Masuda, Grace Pyon, Paige Lacy, Elizabeth A. Jacobsen, Assessment of Lung Eosinophils *in situ* using Immunohistological Staining, Methods in Molecular Biology, 2020,

3.1 Abstract

Eosinophils are rare white blood cells that are recruited from circulation to accumulate in the lung in mouse models of allergic respiratory inflammation. In hematoxylin-eosin (HE) stained lungs, eosinophils may be difficult to detect despite their bright eosin staining in the secondary granules. For this reason, antibody-mediated detection of eosinophils is preferable for specific and clearer identification of these cells. Moreover, eosinophils may degranulate, releasing their granule proteins into surrounding tissue, and remnants of cytolysed cells cannot be detected by HE staining. The methods here demonstrate the use of eosinophil-specific anti-mouse antibodies to detect eosinophil granule proteins in formalin-fixed cells both *in situ* in paraffin embedded lungs as well as in cytospin preparations from the lung. These antibody staining techniques enable either colorimetric or fluorescence imaging of eosinophils or their granule proteins with the potential for additional antibodies to be added for detection of multiple molecules.

3.2 Introduction

Eosinophils are considered the hallmark cell that mediates destructive [287-289] and immune regulating [76, 84, 97, 222, 290] activities in asthma pathologies [90, 291, 292]. To analyze eosinophils *in situ*, lung sections are often used as a measure of their numbers

and states of activation in allergic respiratory pathology. Allergen models of pulmonary inflammation induce many characteristics of human pathology including increased mucus secretion, smooth muscle thickening, airway inflammation and eosinophilic infiltration [293, 294]. Although evidence of degranulation is controversial in most acute allergen models [83, 295], some chronic models develop significant release of granule proteins in the lungs [296], a feature found in human asthmatic lung biopsies and in lung injury [297]. These pathologic changes are often viewed with use of standard dyes that characterize inflammation (HE), mucus production and goblet cell metaplasia, Periodic-acid Schiff (PAS) or collagen deposition as with Masson's trichrome or Picrosirius Red.

In order to identify eosinophils *in situ*, the lungs of euthanized mice are often formalin-fixed, embedded in paraffin and thinly sliced (5 μm) onto glass slides. These slides are then deparaffinized and stained with dyes meant to highlight eosinophils based on the unique nature of their granule proteins. The most common dyes are acidic and chosen due their tendency to stain cationic eosinophil granule proteins. In short, eosinophils are eosin-*philic* (i.e., eosin--loving), due to the acidic eosin dye accumulating on the highly positively charged and acidophilic granule proteins as discovered by Dr. Paul Ehrlich over a century ago [298]. Additional dyes that are used for identifying eosinophils include Congo red and Luna. With these dyes, however, distinction between neutrophils and eosinophils is challenging, and non-specific staining is present. For these reasons, they tend to produce less specific staining than immunohistochemistry (IHC), which in contrast utilizes antibodies that recognize eosinophil-specific antigens [299]. Although eosinophils can be identified by dyes, they must be differentiated manually

with a trained eye. These dyes are commercially available, have easily accessible instructions on their use, and will not be discussed in this chapter.

Immunostaining assays such as IHC and immunofluorescence (IF) use antibodies that recognize specific proteins of interest [188]. Monoclonal antibodies are superior to polyclonal antibodies due to their specificity for unique epitopes (for reviews [300-302]). Secondary granule proteins in mouse eosinophils include eosinophil peroxidase (EPX), major basic protein (MBP-1) and the divergent homologs mouse ribonucleases (mEARs) that are related to human eosinophil-derived neurotoxin (hEDN) and eosinophil cationic protein (hECP) [26]. mEARS have been found in macrophages, and MBP-1 is a low-abundant protein in basophils. In humans, ECP and EDN are also found in neutrophils [34, 303]. An additional eosinophil-associated molecule that may be targeted with antibodies is Siglec-F [156], although this is found on alveolar macrophage as well as eosinophils [304]. Out of all the granule proteins identified so far in eosinophils, EPX is considered the most specific to this cell type based on mouse knockout studies, and antibodies targeting EPX can be used together with those that recognize MBP-1 for highly sensitive and specific detection of eosinophils in tissues [56, 296, 305]. For this reason, our laboratory has developed monoclonal antibodies that recognize mouse EPX [280] and MBP-1 [82, 306] to specifically target eosinophils for immunostaining of lung tissue and cytospins of bronchoalveolar lavage (BAL).

First, we describe how lungs are isolated and prepared for different immunostaining techniques. Lungs must be carefully inflated and removed to maintain resting lung architecture for proper analysis. Next, we describe 5 staining protocols: MBP IHC, EPX IHC, EPX fluorescent IHC, EPX indirect IF on lung slices and dual EPX/MBP indirect IF

on cytospin-prepped eosinophils. The techniques employed here have advantages depending on the desired end result and equipment available [307, 308]. Colorimetric IHC is highly stable and may be viewed/imaged repeatedly using brightfield microscopy. IF methods allow co-localization/multiplex imaging of antigens at once, yet photobleaching is problematic for repeated viewing/imaging. Conventional IHC utilizes an indirect approach where an enzyme-conjugated secondary antibody recognizes the primary antibody and a signal is developed by chromogen deposition. Using secondary antibodies and enzyme development leads to high amplification of signal. This method is employed in MBP IHC, EPX IHC, and EPX fluorescent IHC. In brief, the most common enzyme protocols are peroxidase-based horseradish peroxidase (HRP)-conjugated secondary antibodies or phosphatase-based alkaline phosphatase (AP)-conjugated secondary antibodies that react with colorimetric dyes to form precipitate at the location of the antibody (i.e., *in situ*). The most common dye used is 3,3'-diaminobenzidine (DAB) that produces a brown/black color, although many alternatives are available that produce a range of blue, red, and purple colorimetric stains. Alternatively, fluorescent IHC can be performed by using tyramide signal amplification (TSA), which highly amplifies the fluorescence signal through HRP activation of the fluorophore-conjugated tyramide molecule [194]. This method allows very high spatial resolution *in situ* compared to colorimetric IHC. Fluorescent IHC or fluorophore-conjugated secondary antibody techniques permit fluorescence imaging up to 3 antigens/markers with most fluorescence microscopes [309]. The fluorescence method chosen may depend on availability of antibodies as well as the auto-fluorescence intensity of the formalin fixed tissue or cell. Additional methods are available for multiplex imaging of >30 antigens *in*

situ in formalin-fixed tissues that often require cyclical staining, multi-spectral microscopes and sophisticated imaging software [310-312]. Fluorescence imaging is superior to conventional chromogenic staining in that it is quantifiable and allows many more stains. This chapter will encompass standard IHC and up to 3-color IF imaging for eosinophils using standard laboratory equipment, microscopes, and imaging software.

3.3 Materials

All reagents should be prepared, stored, and used at room temperature unless otherwise indicated. Follow local waste disposal guidelines. Scale working solution volumes up or down dependent on your experiment.

3.3.1 Lung Collection for Fixation and Embedding

1. 10-mL Luer-lock syringe.
2. Support stand with rod and clamp.
3. 3-way stopcock.
4. Catheters: 20G, 30-mm length.
5. Butterfly needle infusion set: 21GA x 3/4 inch with12 inch tubing.
6. 70% ethanol: To make 200 mL, add 140 mL ethanol to 60 mL distilled water.
7. Surgical scissors.
8. 2 Surgical forceps.
9. 10% formalin
10. 50-mL conical tubes or containers
11. Paper towels
12. 4-0 Non-absorbable silk sutures: Cut into 5-inch lengths per mouse.

13. Euthanasia: Pentobarbital or ketamine-xylazine.

3.3.2 Deparaffinization/Rehydration of Slides

1. Tissue-Tek® Slide Holder (*see* **Note 1**) (Fig. 3.6.1).
2. Tissue-Tek® Staining Dish (*see* **Note 2**).
3. Incubator (55°C).
4. Xylene (*see* **Note 3**).
5. 50:50 Xylene/ethanol solution: To make 200 mL, add 100 mL of xylene to 100 mL of ethanol.
6. 100% Ethanol: 200 Proof (*see* **Note 4**).
7. 95% Ethanol: To make 200 mL, add 190 mL of ethanol to 10 mL of distilled water.
8. 75% Ethanol: To make 200 mL, add 150 mL of ethanol to 50 mL of distilled water.

3.3.3 MBP IHC with a Red Alkaline Phosphatase Substrate as a Chromogen

1. Tissue-Tek® Slide Holder (*see* **Note 1**) (Fig. 3.6.1).
2. Tissue-Tek® Staining Dish (*see* **Note 2**).
3. Shandon™ Sequenza™ Staining Rack and coverplates (*see* **Note 5**) (Fig. 3.6.2).
4. Wash buffer: 0.05 M Tris-HCl, 0.15 M NaCl, 0.05% Tween 20, pH 7.6. Alternatively, a 10x concentrate may be prepared and diluted to a 1:10 ratio before use by adding 10 mL of the concentrate to 90 mL of ultrapure water. Working solution can be stored at room temperature for 1 week.
5. Digest-All™ 3: Ready-to-use pepsin solution. Store at 4 °C (*see* **Note 6**).

6. Antibody Diluent, Background Reducing (Agilent Dako): Ready-to-use. Store at 4 °C
7. Dual Endogenous Enzyme Blocker (Agilent Dako): Ready-to-use. Store at 4 °C (*see* **Note 7**).
8. Blocking buffer: 5% normal goat serum in the wash buffer. Dilute to a 1:20 ratio by adding 10 µL of serum to 190 µL of the wash buffer (*see* **Note 8**).
9. Rat anti-MBP primary antibody: 1 mg/mL, Clone MT-14.7.3 (Mayo Clinic, Arizona). Dilute to a 1:1,000 ratio before use by adding 1 µL of the antibody to 999 µL of the antibody diluent to make a final concentration of 1 µg/mL. Use diluted antibody same day (*see* **Note 9 and 10**).
10. Secondary antibody (ImmPRESS®-AP anti-rat polymer, Vector Labs): Ready-to-use. Store at 4 °C (*see* **Note 11**).
11. Chromogen (ImmPACT® Vector® Red AP Substrate, Vector Labs): To prepare 2.5 mL of Vector Red working solution, add 1 drop of Reagent 1 and 1 drop of Reagent 2 to 2.5 mL of the diluent and mix well before use. Use immediately after preparation (*see* **Note 12**).
12. 0.1% Methyl green: Add 200 mg of methyl green to 200 mL of ultrapure water.
13. Non-aqueous permanent mounting medium.
14. #1.5 Glass coverslip.

3.3.4 EPX IHC with DAB as a Chromogen

1. Items 1-6 from Section 2.3.3
2. Rodent Decloaker Antigen Retrieval, 10x (Biocare Medical): Dilute the concentrate to a 1:10 ratio with ultrapure water before use (*see* **Note 13**).

3. Decloaking chamber™ (*see* **Note 14**) (Fig. 3.6.3).
4. Mouse anti-EPX primary antibody: 1 mg/mL, Clone MM25.82.2.1 (Mayo Clinic, AZ). Dilute to a 1:500 ratio before use by adding 1 µL of the antibody to 499 µL of the antibody diluent to a final concentration of 2 µg/mL. Use diluted antibody same day (*see* **Note 9 and 10**).
5. Rodent Block M (Biocare Medical): Ready-to-use. Store at 4°C (*see* **Note 15**).
6. Goat Anti-mouse IgG (H+L), HRP-conjugated secondary antibody: 0.4 mg/mL. Dilute to a 1:250 ratio before use by adding 1 µL of the antibody to 249 µL of the antibody diluent. Store the antibody at -20 °C. Use diluted antibody same day.
7. SignalStain® DAB Kit (Cell Signaling Technologies): To prepare the DAB working solution, add 1 drop (30 µL) SignalStain® DAB chromogen concentrate to 1 mL of SignalStain® DAB diluent and mix well before use. Working solutions are stable for up to 14 days when stored at 4 °C or up to 5 days when stored at room temperature (*see* **Note 16**).
8. Hematoxylin: Ready-to-use solution is commercially available.
9. Acid rinse solution: To prepare 200 mL, add 4 mL of glacial acetic acid to 196 mL of ultrapure water (*see* **Note 17**).
10. Bluing solution: To prepare 200 mL, add 3 mL of 30% ammonium hydroxide to 197 mL of 70% ethanol (*see* **Note 18**).
11. Non-aqueous permanent mounting medium.
12. #1.5 glass coverslip.

3.3.5 EPX Fluorescent IHC with Tyramide Signal Amplification (TSA)

1. Items 1-6 from Section 2.3.2
2. Rodent Decloaker Antigen Retrieval, 10x (Biocare Medical): Dilute the concentrate to a 1:10 ratio with ultrapure water before use (*see* **Note 13**).
3. Decloaking Chamber™ (*see* **Note 14**) (Fig. 3.6.3).
4. Mouse anti-EPX primary antibody: 1 mg/mL, Clone MM25.82.2.1 (Mayo Clinic, AZ). Dilute to a 1:500 ratio before use by adding 1 µL of the antibody to 499 µL of the antibody diluent to a final concentration of 2 µg/mL (*see* **Note 9** and **10**).
5. Rodent Block M (Biocare Medical): Ready-to-use. Store at 4 °C (*see* **Note 15**).
6. Goat anti-mouse IgG (H+L) secondary antibody: 0.4 mg/mL, HRP-conjugated. Dilute to a 1:250 ratio before use by adding 1 µL of the antibody to 249 µL of the antibody diluent. Store the stock at -20 °C. Use diluted antibody same day.
7. TSA™ Plus Cyanine 3 Kit: Reconstitute TSA Plus stock with DMSO (HPLC-grade) according to manufacture recommendations. Dilute the stock solution to a 1:800 ratio before use by adding 1 µL of TSA dye to 799 µL of 1x Amplification Diluent to make TSA Plus working solution (*see* **Note 19**).
8. Phosphate Buffered Saline (PBS): 1.5mM KH_2PO_4, 155mM NaCl, 2.7mM Na_2HPO_4-$7H_2O$, pH 7.4. To prepare 1 liter, add 210 mg KH_2PO_4, 9 g NaCl, and 726 mg Na_2HPO_4-$7H_2O$ to 900 mL distilled water. Adjust pH to 7.6 and raise volume to 1 L with distilled water.
9. 4',6-Diamidino-2-phenylindole, dilactate (DAPI): 10.9 mM DAPI. Prepare a stock solution by dissolving 5 mg of DAPI in 1 mL ultrapure water. Aliquot and store the stock at -20 °C. To prepare working solution, dilute the stock to 1:5,000 in

phosphate-buffered saline (PBS, pH 7.4) to 1 µg/mL. Store the working solution at 4 °C (*see* **Note 20**).

10. ProLong™ Diamond Antifade Mountant (Invitrogen): Ready-to-use. Store at -20 °C (*see* **Note 21**).
11. #1.5 glass coverslip.

3.3.6 EPX Indirect IF

1. Items 1-6 from Section 2.3.3
2. Rodent Decloaker Antigen Retrieval, 10x (Biocare Medical): Dilute the concentrate to a 1:10 ratio with ultrapure water before use (*see* **Note 13**).
3. Decloaking Chamber™ (*see* **Note 14**) (Fig. 3.6.3).
4. Mouse anti-EPX primary antibody: 1 mg/mL, Clone MM25.82.2.1 (Mayo Clinic, AZ). Dilute to a 1:100 ratio before use by adding 2 µL of the antibody to 198 µL of the antibody diluent to a final concentration of 10 µg/mL. Use diluted antibody same day (*see* **Note 9 and 10**).
5. Rodent Block M (Biocare Medical): Ready-to-use. Store at 4 °C (*see* **Note 15**).
6. Anti-mouse IgG secondary antibody: Alexa 594-conjugated. Dilute to a 1:500 ratio by adding 1 µL of the antibody to 499 µL the antibody diluent. Store stock at 4 °C. Use diluted antibody same day (*see* **Note 22**).
7. Phosphate Buffered Saline (PBS): 1.5mM KH_2PO_4, 155mM NaCl, 2.7mM Na_2HPO_4-$7H_2O$, pH 7.4. To prepare 1 liter, add 210 mg KH_2PO_4, 9 g NaCl, and 726 mg Na_2HPO_4-$7H_2O$ to 900 mL distilled water. Adjust pH to 7.6 and raise volume to 1 L with distilled water.

8. 4',6-Diamidino-2-phenylindole, dilactate (DAPI): 10.9 mM DAPI. Prepare a stock solution by dissolving 5 mg of DAPI in 1 mL of ultrapure water. Aliquot and store the stock at -20 °C. To prepare working solution, dilute stock 1:5,000 in PBS to 1 µg/mL. Store working solution at 4 °C (*see* **Note 20**).
9. ProLong™ Diamond Antifade Mountant (Invitrogen): Ready-to-use. Store at -20 °C (*see* **Note 21**).
10. #1.5 glass coverslip.

3.3.7 MBP and EPX Dual Fluorescent IHC

1. Cells from peripheral blood or bronchoalveolar lavage in 5% BSA in PBS, stored at 4 °C.
2. ThermoScientific Cytospin™ 3 or 4 Cytocentrifuge and components, funnel filter paper, and clip.
3. Phosphate Buffered Saline (PBS): 1.5mM KH_2PO_4, 155mM NaCl, 2.7mM Na_2HPO_4-$7H_2O$, pH 7.4. To prepare 1 liter, add 210 mg KH_2PO_4, 9 g NaCl, and 726 mg Na_2HPO_4-$7H_2O$ to 900 mL distilled water. Adjust pH to 7.6 and raise volume to 1 L with distilled water.
4. 5% (w/v) BSA: To make 100 mL, add 5 g of BSA to 100 mL of PBS. Store at 4 °C and use within one day (*see* **Note 23**).
5. Permeabilization buffer (PBT): PBS containing 0.2% (v/v) Triton™ X-100. First prepare a stock solution of 10% (v/v) Triton™ X-100 by adding 200 µL of Triton™ X-100 to 9.8 mL of PBS. To make working solution, dilute 10% stock to a 1:50 ratio by adding 10 µL of the stock to 490 µL of PBS (*see* **Note 24**).

6. Wash buffer (PBST): PBS containing 0.1% TWEEN® 20. First prepare a stock solution of 10% TWEEN® 20 by adding 100 µL of TWEEN® 20 to 9.9 mL of PBS. To make working solution, dilute 10% stock to 1:100 by adding 5 µL of the stock to 495 µL of PBS (*see* **Note 24**).
7. Antibody diluent: 1% BSA in PBST. To prepare 5 mL, add 1 mL of 5% BSA to 4 mL of PBST. Store at 4 °C.
8. Blocking buffer: 5% Normal donkey serum in antibody diluent. To prepare 1 mL, add 50 µL of normal donkey serum to 950 µL of antibody diluent. Use on the same day (*see* **Note 8**).
9. Primary antibody mix: Mouse anti-EPX [1 mg/mL] (Clone MM25.82.2.2, Mayo Clinic AZ) and rat anti-MBP [1 mg/mL] (Clone MT-14.7.3, Mayo Clinic AZ). To prepare 1 mL, dilute the antibodies to 1:200 by adding 5 µL of anti-EPX and 5 µL of anti-MBP to 990 µL of antibody diluent (*see* **Note 9 and 10**).
10. Secondary antibody mix: Donkey anti-mouse Alexa 594 and donkey anti-rat Alexa 488. To prepare 1 mL, dilute the antibodies to 1:500 by adding 2 µL of anti-mouse Alexa 594 and 2 µL of anti-rat Alexa 488 to 996 µL of the antibody diluent (*see* **Note 19**).
11. 4',6-Diamidino-2-phenylindole, dilactate (DAPI): 10.9 mM DAPI. Prepare a stock solution by dissolving 5 mg DAPI in 1 mL ultrapure water. Aliquot and store stock at -20 °C. To prepare working solution, dilute stock 1:5,000 in PBS to 1 µg/mL. Store working solution at 4 °C (*see* **Note 20**).

12. ProLong™ Diamond Antifade Mountant (Invitrogen): Ready to use. Store at -20 °C (*see* **Note 21**).
13. #1.5 glass coverslip.

3.4 Methods

3.4.1 Lung Collection for Fixation and Embedding

This protocol is optimized for Balb/c or C57BL/6 mice that are >6 weeks of age or 18-40 g in weight. Procedures must be approved by IACUC committee and under the assurances of the Office for Laboratory Animal Welfare. All incubations should be performed at room temperature unless noted otherwise. The mice used in these procedures have undergone a house dust mite allergen sensitization and challenge protocol [57] .

1. Set up a syringe with a stopcock, a butterfly needle, and a catheter on the support stand (*see* **Note 25**) (Fig. 3.6.4).
2. Ensure the stopcock is off (perpendicular to syringe) and fill the syringe with the formalin solution (*see* **Note 26**). With the tip of the catheter placed into a disposable container, open the stopcock to let the formalin fill the length of the catheter and tubing. Make sure there are no air bubbles in the tubing line. Stop the flow by turning the stopcock to the off position.
3. Euthanize a mouse with a lethal dose of sodium pentobarbital or ketamine-xylazine (*see* **Note 27**), and lay the mouse on its back on top of paper towels to absorb excess fluids. Wet the fur around the throat and torso with 70% ethanol.

4. To remove the skin over the chest area, grab the skin under the jaw with forceps, creating a tent, and cut the skin with scissors from the length of the jaw to the bottom of the rib cage.
5. Lift up on the rib cage by grabbing bottom part of the sternum (the xiphoid process) with forceps and make an incision along the edge (beneath) of the rib cage from right to left to expose the diaphragm.
6. Cut the diaphragm away from the ribs (cutting left to right). Be careful not to poke or cut the lung. Any tears will lead to formalin leakage and lung deflation, altering the architecture.
7. While lifting the xiphoid process with forceps up away from the body, use the scissors to cut the rib cage on both sides about 2/3 distance to top of rib cage, approximately right below the clavicles. A final cut is made across the top of the ribcage to remove ribcage and expose the heart and lungs.
8. The clavicles must be cut in order to remove the lungs from the mouse. Cut the clavicle on each side such that the section of bone remaining over the thymus and heart can be carefully removed from the mouse. This allows for total exposure of the trachea, heart, thymus, and lungs.
9. Expose the ventral side of the trachea by moving away the thyroid gland (pull apart, splitting the middle). Carefully cut the muscle layer over the trachea so as to expose the cartilage of the trachea.
10. Carefully loop the 5" suture material underneath the trachea using forceps and then loosely form a knot immediately below the thyroid cartilage/voice box. Do not tighten.

11. Cut the trachea horizontally just enough to allow a 20G catheter insertion at the thyroid cartilage/voice box as this provides a solid and wide location to support this type of cut and provides a reference point (*see* **Note 28**).
12. Put the catheter into the trachea such that it is inserted only a few millimeters, past the loose knot, yet avoid going so far that there is resistance. Holding the catheter in place, tighten the knot until snug.
13. Open the stopcock and allow the lungs to fill. Turn off the stopcock once the lungs are fully inflated.
14. When the lung is fully inflated, at the same time, remove the catheter and tighten the knot completely so no liquid escapes.
15. While holding trachea with forceps at the knot, cut above the forceps to sever trachea and cut any connective tissue holding the lungs in place.
16. Place the whole lung into a 50-mL conical filled with 30 mL formalin and store for 24 h (*see* **Note 29**).
17. Prepare for embedding and sectioning. This is beyond the scope of this chapter but is described elsewhere [313]. Sections stained in this protocol are 5-μm thick coronal slices of formalin-fixed and paraffin-embedded (FFPE) tissue.

3.4.2 Deparaffinization/Rehydration FFPE Slides

1. Place slides in Tissue-Tek® Slide Holder and Tissue-Tek® Staining Dish (Fig. 3.6.1) and incubate the slides at 55 °C for 30 min with lid on the dish (*see* **Note 30**).

2. In a fume hood, set up the indicated number of Tissue-Tek dishes with 200 mL of each solution, and place the slide holder into the staining dishes for the indicated times:
    a. 3 dishes of xylene, 5 min each (*see* **Note 31**).
    b. 1 dish of 50:50 xylene/ethanol, 2 min.
    c. 2 dishes of 100% ethanol, 2 min each.
    d. 1 dish of 95% ethanol, 2 min.
    e. 1 dish of 75% ethanol, 2 min.
3. Rinse the slides in running distilled water for 30 seconds. Store slides in water until next steps to keep hydrated.

3.4.3 MBP IHC with a Red AP Substrate as a Chromogen

1. After deparaffinization/rehydration of slides, load the slides into Shandon™ Sequenza™ Staining Rack with coverplates (*see* **Note 32**) (Fig. 3.6.2).
2. Add 200 µL of Digest-All™ 3 pepsin to the slides and incubate for 10 min.
3. Wash 3 times in wash buffer for 2 min each.
4. Add 200 µL of Dual Endogenous Enzyme Block to the slides and incubate for 10 min.
5. Wash 3 times in wash buffer for 2 min each.
6. Add 200 µL of the blocking buffer to the slides and incubate for 30 min (*see* **Note 33**).
7. Add 200 µL of the diluted anti-MBP antibody (1 µg/mL) to the slides and incubate overnight at 4 °C. For negative control slides, add diluent without the antibody. (*see* **Note 34**).

8. Wash 3 times in wash buffer for 5 min each.
9. Add 200 µL of ImmPRESS Anti-Rat AP polymer to the slides and incubate for 30 min.
10. Wash 3 times in wash buffer for 5 min each.
11. Add 200 µL Vector Red chromogen to slides and incubate for 5 min (*see* **Note 35**).
12. Wash 1 time with distilled water for 2 min then transfer slides to a dish filled with distilled water to keep tissue hydrated..
13. To counterstain with methyl green, place slides in methyl green for 15 sec (*see* **Note 35**), and wash slides in running distilled water until water is clear (about 10 sec).
14. Dehydrate the slides (*see* **Note 36**) by placing them once in 95% ethanol for 1 min and twice in 100% ethanol for 1 min. Air dry the slides.
15. Dip slides in xylene and coverslip with non-aqueous permanent mounting medium (Fig. 3.6.5).

3.4.4 EPX IHC with DAB as a Chromogen

3.4.4.1 Antigen Retrieval

1. Add 500 mL distilled water to the Decloaker or equivalent.
2. Submerge deparaffinized and dehydrated slides into a staining jar with diluted antigen retrieval solution (*see* **Note 37**) and place them in the Decloaker.
3. Incubate the slides in Decloaker at 95 °C for 40 min then 85 °C for 10 min. Remove the staining jar from the Decloaker, keeping the slides in the retrieval buffer, and allow to cool on benchtop for 20 min.

4. Rinse the slides in running distilled water until all the antigen retrieval solution is removed (*see* **Note 38**).

3.4.4.2 Antibody Incubation and Color Development

1. Load slides into Shandon™ Sequenza™ Staining Rack (*see* **Note 32**) (Fig. 3.6.2).
2. Add 200 µL of Digest-All™ 3 pepsin to the slides and incubate for 10 min.
3. Wash 3 times in wash buffer for 2 min each.
4. Add 200 µL Rodent M Block to slides and incubate for 30 min.
5. Wash 3 times in wash buffer for 2 min each.
6. Add 200 µL anti-EPX antibody (2µg/mL) to the slides and incubate overnight at 4 °C. For negative control slides, add diluent without the antibody (*see* **Note 34**).
7. Wash 3 times in wash buffer for 5 min each.
8. Add 200 µL of anti-mouse HRP secondary to slides and incubate for 30 min.
9. Wash 3 times in wash buffer for 5 min each.
10. Add 200 µL of DAB chromogen to slides and incubate for 10 min (*see* **Note 35**).
11. Wash 1 time with distilled water for 2 min then transfer slides to a slide holder submerged in distilled water to keep tissue hydrated.

3.4.4.3 Hematoxylin Counterstaining

1. Incubate slides in hematoxylin for 5 min.
2. Wash slides in running distilled water until water is clear.
3. Immerse slides 10 times into acid rinse solution.
4. Immerse slides 10 times into distilled water.
5. Incubate slides for 1 min in bluing solution.
6. Immerse slides 10 times into distilled water.

3.4.4.4 Dehydration and Coverslipping

1. Incubate slides in 75% ethanol for 1 min.
2. Incubate slides in 1 wash of 95% ethanol for 1 min each.
3. Incubate slides in 2 washes of 100% ethanol for 1 min each.
4. Air dry slides.
5. Dip slides in xylene and coverslip with non-aqueous permanent mounting medium (Fig. 3.6.6).

3.4.5 EPX Fluorescent IHC with TSA

1. Perform antigen retrieval as described in Section 2.4.4.1.
2. Pretreat and block the slides as described by Section 2.4.4.2, Steps 1-5.
3. Add 200 µL of anti-EPX antibody [2 µg/mL] to slides and incubate overnight at 4 °C. For negative control slides, add diluent without the antibody (*see* **Note 34**).
4. Wash 3 times in wash buffer for 5 min each.
5. Add 200 µL of anti-mouse HRP secondary antibody to the slides and incubate for 1 h.
6. Wash 3 times in wash buffer for 5 min each.
7. Add 200 µL of TSA Cy3 dye solution to slides and incubate for 10 min protected from light. All following steps should be protected from light to reduce photobleaching.
8. Wash 3 times in wash buffer for 5 min each and rinse with PBS.
9. Counterstain nuclei by adding 200 µL of DAPI to the slides and incubate for 7 min.
10. Wash 3 times in PBS for 2 min each.

11. Remove one slide at a time from the rack and coverslip using ProLong™ Diamond Antifade mountant. (see **Note 39**).
12. Lay slides flat and allow to dry overnight protected from light before imaging (see **Note 40**) (Fig. 3.6.7).

3.4.6 EPX Indirect IF

This FFPE lung staining method may be adapted for dual IF by adding an additional primary antibody such as a rat or rabbit antibody, combined with an appropriate fluorophore-conjugated secondary antibody (such as goat anti-rat or goat anti-rabbit Alexa 647). Optimization of antigen retrieval and blocking agents will be required for additional primary antibodies.

1. Perform antigen retrieval as described in Section 2.4.4.1.
2. Pretreat and block the slides as described by Section 2.4.4.2, Steps 1-5.
3. Add 200 µL of anti-EPX antibody [10µg/mL] to the slides and incubate overnight at 4 °C. For negative controls, add diluent without the antibody (*see* **Note 34**).
4. Wash 3 times in wash buffer for 5 min each.
5. Add 200 µL of anti-mouse Alexa594 secondary antibody to the slides and incubate for 1h protected from light. All following steps should be protected from light to prevent photobleaching.
6. Rinse, stain with DAPI, and coverslip the slides as described in Section 2.4.5, Steps 8-12.

3.4.7 MBP and EPX Dual Fluorescent IHC

1. Resuspend cells from peripheral blood or bronchoalveolar lavage at 1 x 10^6 cells/mL in cold 5% BSA/PBS (*see* **Note 41**).
2. Set up cytospin cages with microscope slides and funnels. Load into a cytocentrifuge (Fig. 3.6.9).
3. Pre-wet the slides by adding 50 µL of 5% BSA to the funnels, bringing the cytocentrifuge up to 500 RPM (~28 x g) and stopping (*see* **Note 42**).
4. Add 50 µL of the cells to each funnel then add 50 µL of 5% BSA.
5. Spin at 500 RPM (~28 x g), slow acceleration, for 5 min.
6. Remove the slides and immediately immerse in 4% formaldehyde for 15 min.
7. Wash 3 times in PBS for 5 min each.
8. Load the slides into Shandon™ Sequenza™ Staining Rack (*see* **Note 32**) (Fig. 3.6.2).
9. Rinse slides with PBS.
10. Add 200 µL of PBT to slides and incubate for 10 min.
11. Wash 2 times in wash buffer for 2 min each.
12. Add 200 µL of blocking buffer and incubate for 30 min at room temperature (*see* **Note 33**).
13. Add 200 µL of the primary antibody mixture and incubate overnight at 4 °C. For negative control slides, add diluent without the antibody mix (*see* **Note 34**).
14. Wash 3 times in wash buffer for 5 min each.
15. Add 200 µL of the secondary antibody mix and incubate for 1 h protected from light. All following steps should be protected from light to reduce photobleaching.

16. Rinse, stain with DAPI (2 minutes), and coverslip the slides as described in Section 3.5, Steps 8-12.

3.5 Notes

1. Slide holders are not mandatory, but they are convenient for the deparaffinization/rehydration steps when working with multiple slides at once. These come in different sizes to meet your needs. Slide mailers are a cheap alternative that can be used to submerge slides into solutions.
2. Staining dishes are plastic, solvent resistant and can tolerate the high temperature of a pressure cooker. They can handle rapid temperature changes and have a lid to reduce evaporation of solvents. Coplin jars or any solvent resistant container can be used as an alternative. These hold up to 24 slides and we use a volume of 200 mL to submerge slides.
3. Xylene is highly flammable and should be kept under a fume hood in a closed container to avoid evaporation of fumes.
4. Ethanol is flammable and should be stored in a closed container to avoid evaporation.
5. The Shandon™ Sequenza™ Staining Rack requires a minimum 200 µL of solution per slide. The staining rack is convenient as all staining and washing steps are performed in a portable rack. Once the slides are loaded, there is no need to move them until the very end of the protocol. The coverplate/rack system also keeps the slides uniformly hydrated, preventing issues associated with cell or tissue dehydration. Alternatively, staining can be performed using traditional methods (hydrophobic pen/incubation in humidified chamber). However, it is important to

keep the tissue wet throughout staining. Traditional methods require lower reagent volumes to be applied to each slide, which is a benefit over the rack method.

6. This protocol has been optimized using commercially available Digest-All™ 3 pepsin solution. Other pepsin solutions would require further optimization.
7. Dual Endogenous Enzyme Blocker (Agilent Dako) reagent helps to block endogenous peroxidases and phosphatases that may react with the chromogen and develop non-specific background staining [314-316]. It is compatible with both HRP-based and AP-based detection protocols.
8. This step helps to block non-specific binding of the primary antibody as well as the secondary. The species of the serum may match the species in which the secondary antibody was raised, although goat serum is a common serum used for many protocols and sufficient with monoclonal primary rat and mouse antibodies. Normal sera can be stored short term at 4 °C, while long term storage can be done at -20 °C. Centrifuge stock serum at 13,000 x *g* for 5 min before use to remove precipitates.
9. Rat anti-MBP (clone: MT-14.7.3) [82] and mouse anti-EPX (clone: MM25-82.2.1) [280] are only available through Mayo Clinic at this time and can be obtained by contacting the senior author of this chapter and as described here [306]. These antibodies are highly purified by IgG column purification and prepared without sodium azide for storage. Stocks are validated in-house before shipment. Antibodies are aliquoted and shipped as 50 µg lyophilized samples that are stable for many years at -80 °C. Lyophilized antibodies are reconstituted with molecular grade water to generate 1 mg/mL antibody solution. Reconstituted antibodies are stable for greater than 6 months at 4 °C.

10. Antibody dilutions may require adjustment per tissue stained or fixation methods.
11. We have had great success using this specific secondary antibody, but this may be substituted for another AP-polymer secondary antibody system. Alternatively, as the dual enzyme block is used in this protocol, the AP detection system can be swapped for an HRP-based system with an appropriate chromogen (i.e. DAB). Various substrates with different colors and properties are available for both enzymes so one might choose one enzyme over the other based on the substrate of interest [317, 318].
12. This chromogen is also fluorescent and can be viewed using Texas red filter (600-650 λ).
13. This specific retrieval buffer is important in blocking endogenous mouse IgG, which can cross react with the secondary antibody, and be a source of background staining. This buffer also inactivates endogenous peroxidases, serving as an enzyme block and reducing background staining in HRP-based detection systems.
14. During fixation, epitopes are masked and heat induced antigen retrieval helps to unmask these epitopes so the primary antibody can bind the antigen of interest [188, 319, 320]. We prefer to use the Decloaker (Biocare) because of its precise control of temperature and time. This protocol does not call for high temperature/pressure so any incubator that can reach 95 °C may be used.
15. This commercial blocking reagent helps to block endogenous mouse IgG and reduce non-specific background staining in mouse tissues. When performing a mouse-on-mouse protocol, the secondary antibody cannot distinguish between the primary antibody and any endogenous IgG found within the tissue. If this endogenous IgG is not blocked sufficiently, it becomes a cause for high background staining.

16. Alternative DAB kits or HRP substrates can be used in place of this kit, but incubation times may require adjustment. Endogenous phosphatases might not be effectively blocked so we don't recommend using an AP detection system with this protocol.
17. The acid rinse helps to remove non-specific hematoxylin staining.
18. Hematoxylin will stain nuclei a reddish-purple and this reagent changes it to a bluish-purple.
19. Cyanine 3 dye in the TSA kit is light-sensitive and requires protection from light. Working solution can be stored at 4 °C for up to 1 month. The concentration of the dye can be adjusted to increase the staining intensity, but EPX is a very abundant protein and we have found that 1:800 gives a good signal-to-noise ratio. Too high concentrations of the dye can lead to increased background and signal developing outside the cell. Not only does TSA highly amplify the fluorescence signal, it is compatible with highly multiplexed techniques (reviewed here [194]) because the dye is covalently attached to the tissue.
20. DAPI is light-sensitive so protect all solutions from light. DAPI is also a suspected carcinogen so handle with proper personal protection equipment. We have found that DAPI containing mounting media causes background and prefer to do a separate staining step prior to mounting. Stock solution is stable for at least 6 months. The dilactate formulation is more water soluble than the dihydrochloride.
21. ProLong™ Diamond is a hardening reagent whose refractive index is highest once fully cured. Slides can be imaged immediately after coverslipping, but for optimal imaging allow reagent to cure. There is no need to seal the slide edges.

22. Protect fluorophore-conjugated antibodies from light. Centrifuge the antibody solution briefly to pellet aggregates - only use the supernatant. The fluorochrome(s) can be changed depending on the experiment and microscope setup. Alexa-based fluorophores are more stable than original fluorophores, such as FITC or rhodamine, when exposed to ambient light [321]. Autofluorescence in formalin-fixed samples can be seen at all visible wavelengths, but the intensity is the highest around the blue-green region (475-525λ) so we prefer to use red-shifted colors (>525λ) [307]. Various immunostaining methods to reduce FFPE autofluorescence in lung tissues are described elsewhere [322].
23. BSA takes a while to dissolve and it is best to prepare ahead of time. After adding BSA to PBS, incubate at room temperature until fully dissolved (about 45 min for 5 g). To remove BSA stuck to the side of the container, gently swirl the solution but be careful not to over agitate, which will cause it to foam. For long-term storage at 4 °C, filter solution through 0.2 μm flask filter and maintain aseptic techniques.
24. Stock detergent solutions are very viscous. Aspirate and dispense slowly. We have found that swirling the pipette while dispensing into PBS helps to get the detergent into solution faster. 10% solution is not as viscous and is easier to pipette.
25. The syringe holding formalin needs to be 20-25 cm above the table to ensure proper pressure to inflate lungs to 25 cm H_2O. This height results in approximately 70% of the air lung capacity being, providing optimal structural integrity for imaging, rather than complete lung collapse. By the time of embedding and slide preparation, though, the volume of the lung after dehydration and processing is not equivalent to a live viable lung [323, 324].

26. The most commonly used fixative is 10% neutral-buffered formalin (pH 7.0). Depending on the epitope and antibody parameters, many fixatives, such as zinc-formalin or glutaraldehyde-formalin (http://www.ihcworld.com/_protocols/histology/fixatives.htm), provide unique advantages but should be optimized before use as these fixatives may alter the antigenicity of the epitope of interest. Cryo-fixation and sectioning avoid the covalent crosslinking of these fixatives as well as processing-induced removal of lipid-based compounds from tissues. However, these methods are beyond the scope of this chapter. The eosinophil antibody protocols listed here all use phosphate-free neutral-buffered formalin (ThermoFisher), which is the equivalent of a 4% (v/v) formaldehyde solution.
27. Although carbon dioxide (CO_2) exposure is a common method of euthanasia, we recommend either ketamine-xylazine or sodium pentobarbital-based euthanasia method as CO_2 may result in hemorrhaging of the lung [325, 326]. Depending on the physiological kinetics of the molecules being studied, other considerations may be taken into account when selecting euthanasia methods [327]. Please review AVAMA Guidelines for the Euthanasia of Animals (https://www.avma.org/kb/policies/documents/euthanasia.pdf) or appropriate guidelines for animal use at your institution.
28. Before the lung is filled with formalin, the lungs may be manipulated for additional usages. For example, one may perform a bronchoalveolar lavage (BAL) by inserting an 18G catheter with a syringe filled with 1 mL of PBS at a tracheotomy site [328]. However, this may lead to some structural changes in lung architecture due to the

pressure changes to obtain BAL. If perfusion is needed to clear the circulatory system of blood, this may be performed once the heart is exposed soon after euthanasia to avoid clotting. If only one lobe of the lungs is needed for IHC, suture material may be used to tie off the right or left lobe and cut off the main bronchus of that lobe distal to the knot and trachea. The separated lobe may be used for flow cytometry or other measures. The knot creates a closure so that the lobe left behind is still filled with formalin without leakage and may be used for histology.

29. Fixation time and temperature can alter the extent of covalent bonds and therefore the epitope availability for IHC [320, 329, 330]. For long-term storage, formalin-fixed samples may be dehydrated and stored in 100% ethanol (200 proof).
30. This step softens paraffin prior to deparaffinization. Slide should be kept upright and incubated for a minimum of 15 min and up to 1 h. We have found 30 min to be optimal. If problematic, the incubation can be done immersed in xylene so long as ventilation is good, and lid remains sealed on container.
31. Xylene is used to dissolve paraffin wax. During all washes, agitate slides once every minute by lifting them up and down.
32. To avoid trapping air bubbles, load slides onto coverplates submerged in distilled water (Fig. 3.6.2). After loading onto the rack, add water to slides to ensure the flow is slow and consistent. Rapid draining is indicative of an incorrect setup. In this case, try to reload the coverplate and slide and repeat the drain test. Make sure all incubations are done with the lid of the rack on to maintain humidity. This reduces evaporation of reagents on slides. If not using a rack, make sure slides are kept wet in a humid enclosure.

33. Allow at least 30-min incubation to efficiently block the tissue at room temperature. Incubations can be extended without any detrimental effects. Overnight incubations at 4 °C are often acceptable as well. Do not wash off blocking buffer before adding primary antibodies. The staining rack will drain excess blocking buffer when antibodies are added. If not using a staining rack, remove blocking buffer by tapping side of slide on a paper towel before adding antibodies.
34. This is to control for non-specific binding of the secondary antibody. IgG isotype antibody can also be used to control for non-specific binding of the primary antibody. Always run a negative control slide (not containing primary antibody) with experiments and if possible, have the negative control be a serial section of the sample or at minimum the same tissue origin and conditions.
35. Increase or decrease incubation time to optimize staining intensity.
36. While the slides can be air-dried overnight, the dehydration allows the slides to be coverslipped within 10 min.
37. Depending on the number of slides being stained, we use a plastic coplin jar (<5 slides) or staining dish (6-24 slides) to hold our slides during antigen retrieval.
38. Gently run water into the container until all foam/bubbles are gone. Ensure the water stream is not directly on the sections to avoid damaging tissues.
39. Try to remove as much buffer as possible without letting specimen dry by gently tapping the slide on a paper towel. ProLong™ is a viscous reagent. If using a micropipette to dispense the reagent, ensure to pipette slowly to prevent bubbles. We usually load a pipette tip with the mountant before removing slides from the staining rack to prevent excessive drying of the tissue. If bubbles form on specimens, use a

10-µL micropipette tip to pop or aspirate bubbles. If bubbles form in the stock reagent, transfer to a microcentrifuge tube and centrifuge at 10,000 x *g* for 2 min. Protect ProLong™ from light for it is light sensitive.

40. ProLong™ Diamond is a hardening reagent whose refractive index is highest once fully cured. Slides can be imaged immediately after coverslipping, but for the best images, wait for the reagent to cure. There is no need to seal the slide. Caution must be taken when handling/imaging slides that have not been cured as the coverslip can slide around.
41. Techniques for peripheral blood isolation or brochoalveolar isolation are described elsewhere [328, 331]. Make sure the cells stay cold on ice to maintain viability. Cell numbers can be modified to fit experimental needs, but this density of cell suspension yields a nice uncrowded distribution of cells.
42. Pre-wetting the slides with BSA helps the cells stick to the slides. Set up as many cytospin cages as needed for your experiment. Make sure to always have an even number of cages to counterbalance the centrifuge.
43. The lung FFPE EPX IF and TSA protocols can be adapted for multiplex staining by the addition of other primary antibodies and their corresponding secondary antibodies. This will require optimization of antigen retrieval, blocking steps, and antibody dilutions similar to as described above and in literature [332, 333].

3.6 Figures

Figure 3.6.1. Tissue-Tek® Slide Holder and Rack. (**a**) Tissue-Tek® Slide Holder that can hold up to 24 slides (grey) and staining lid and dish. The grey rack fits inside the holder. Slides are fully immersed in liquid when 200 mL of fluid is in the container. (**b**) Tissue-Tek® Rack is a convenient way to organize multiple staining dishes used for deparaffinization and rehydration of tissue sections.

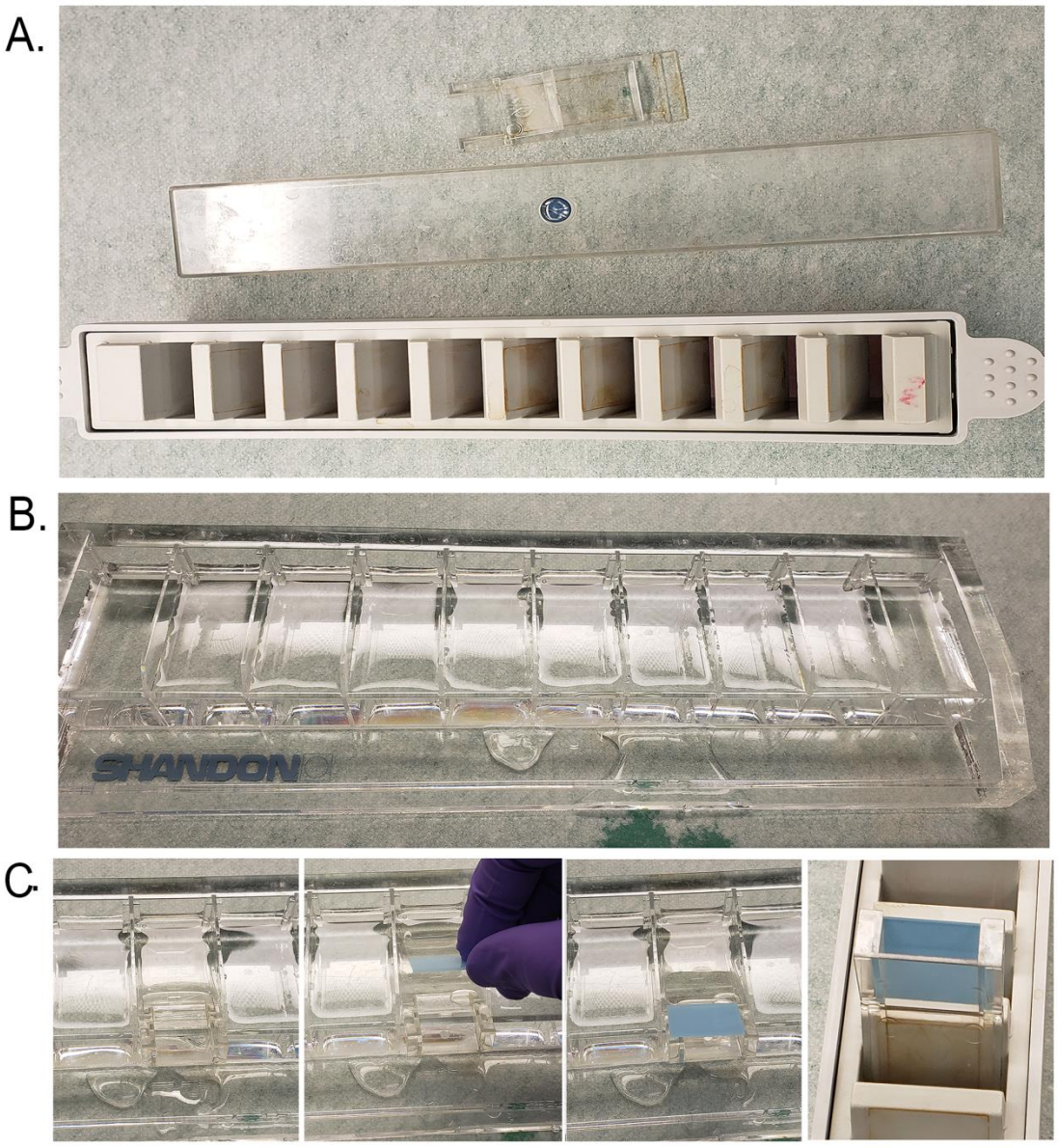

Figure 3.6.2. The use of Shandon™ Sequenza™ Staining Rack and Coverplates Allows for Controlled Flow of 200 µL of Fluid Over Slides and for Several Slides to be Processed at The Same Time. (**a**) Shandon™ Sequenza™ Staining Rack, lid, and coverplate. There is room for 10 slides per rack. (**b**) Slide preparation rack filled with distilled water. (**c**) Instructions of how to load slides onto coverplate: 1) A container is filled with water; 2) Coverplate is submerged under water; 3) A slide is lowered onto the coverplate face-down, creating a small water filled void between the slide and coverplate; 4) Hold in place and then slide into the rack firmly.

Figure 3.6.3. Decloaking Chamber (BioCare) with a Plastic Coplin Jar. Water (500 mL) is placed inside the decloaker to distribute the heat around the coplin jar.

Figure 3.6.4. Syringe and Catheter Setup to Prepare Formalin Inflated Lungs. A 10-mL syringe is held in place by a clamp such that the 10-mL mark on the syringe is 20 cm above the benchtop. The blue stopcock controls the flow of formalin. The catheter is placed into the trachea during instillation of formalin.

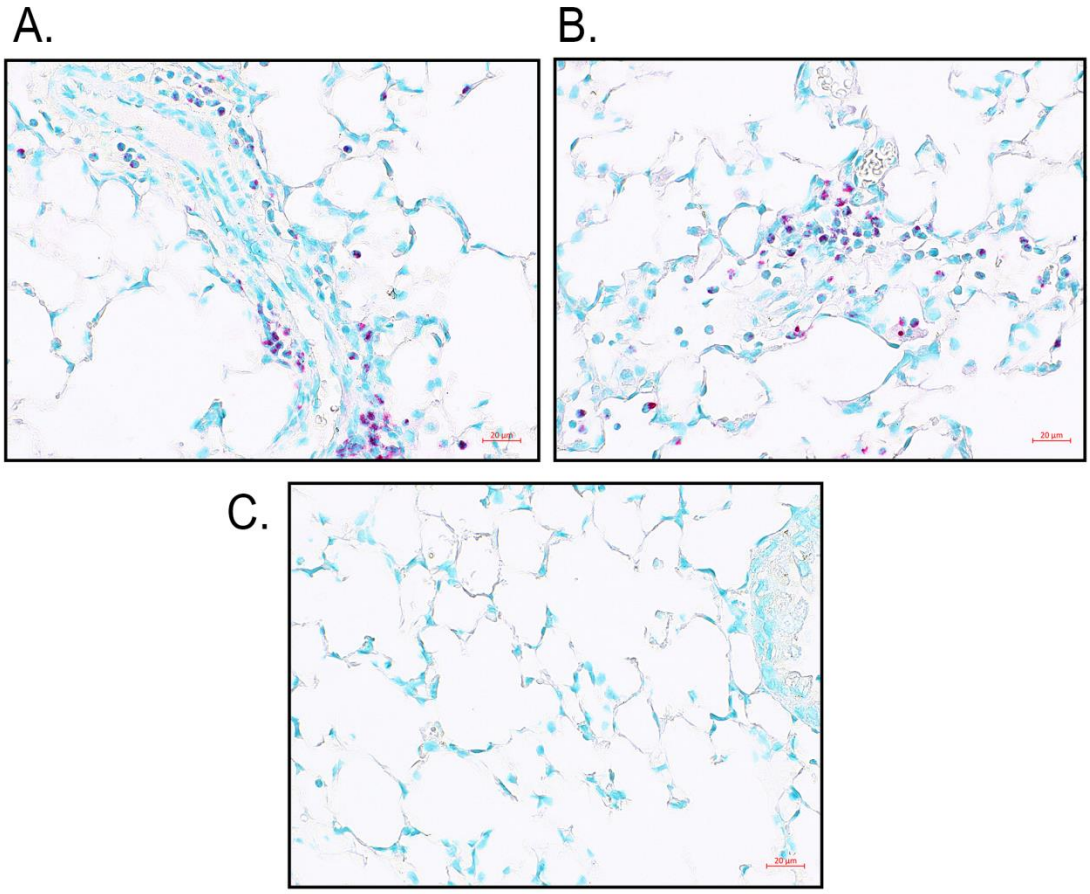

Figure 3.6.5. Allergen-Challenged FFPE Lung Sections with MBP IHC with Red Chromogen. (**a** and **b**) Two examples of MBP IHC in allergen-challenged lung FFPE slices. MBP is stained red showing the location of eosinophils, and methyl green counterstains nuclei green. (**c**) Negative control staining. Images were taken on Zeiss Imager.M2 with a 40x objective.

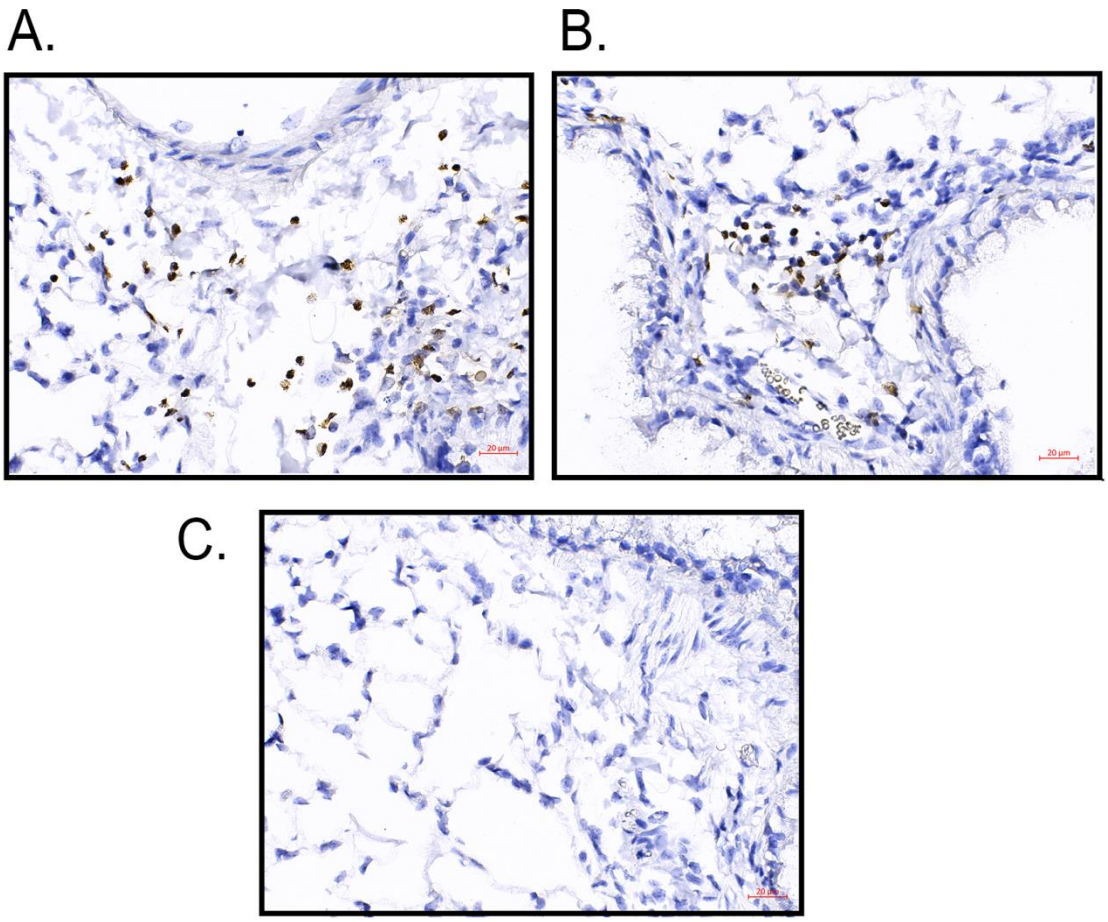

Figure 3.6.6. Allergen-Challenged FFPE Lung Sections with EPX IHC with DAB as The Chromogen. (**a** and **b**) Two examples of EPX IHC in allergen-challenged lung FFPE slices. EPX is stained brown showing the location of eosinophils, and hematoxylin counterstains nuclei blue/purple. (**c**) Negative control staining. Images were taken on Zeiss Imager.M2 with a 40x objective.

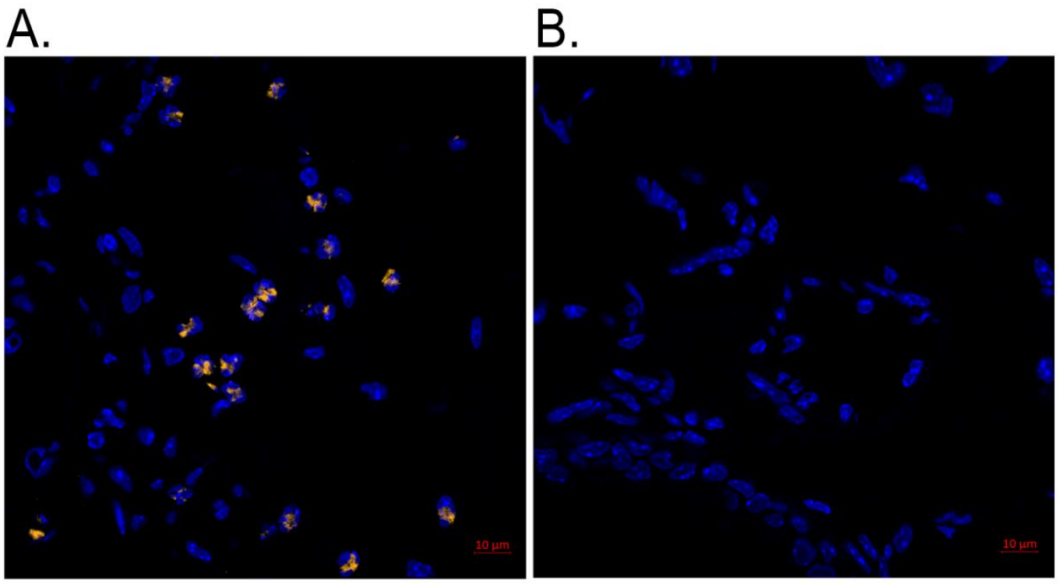

Figure 3.6.7. Allergen-Challenged FFPE Lung Sections with EPX Fluorescent IHC with TSA. (**a**) Eosinophils are stained for EPX with Cy3-conjugated tyramide substrate (orange). Nuclei are counterstained with DAPI (blue). (**b**) Negative control without the primary antibody. Image was acquired with a Plan-Apochromat 63x objective on a Zeiss LSM 800 microscope.

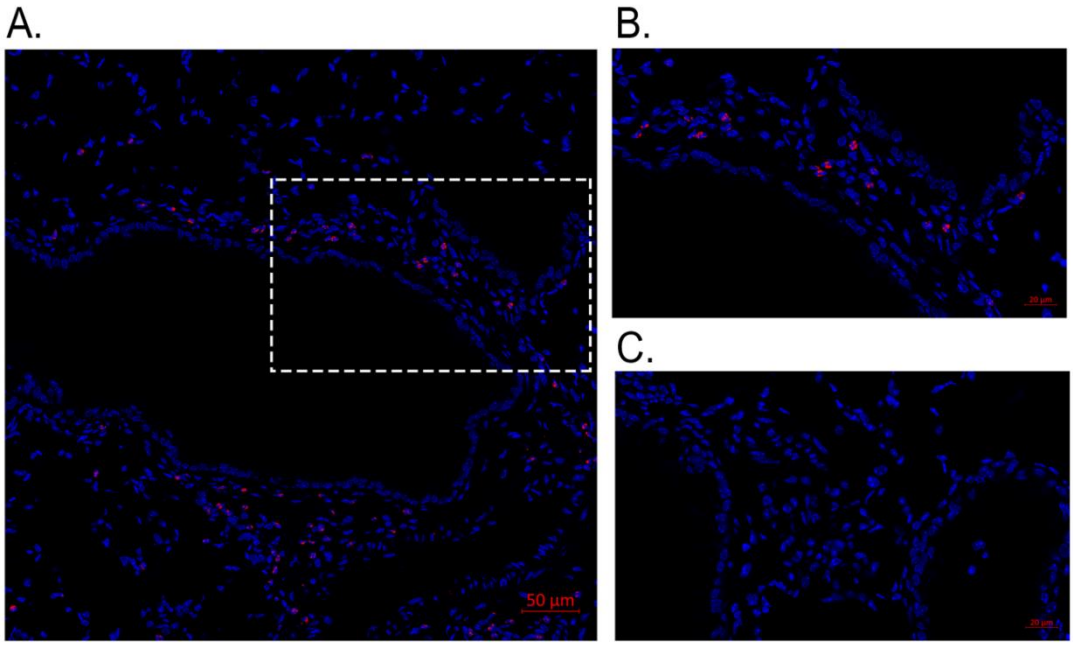

Figure 3.6.8. Allergen-Challenged FFPE Lung Sections with EPX Indirect IF. Eosinophils are stained for EPX (red) and nuclei are counterstained with DAPI (blue). (**a**) Tile (5x5) image was acquired with a Plan-Apochromat 63x objective on a Zeiss LSM 800 microscope. (**b**) Zoomed in image of (a). (**c**) Negative control without the primary antibody.

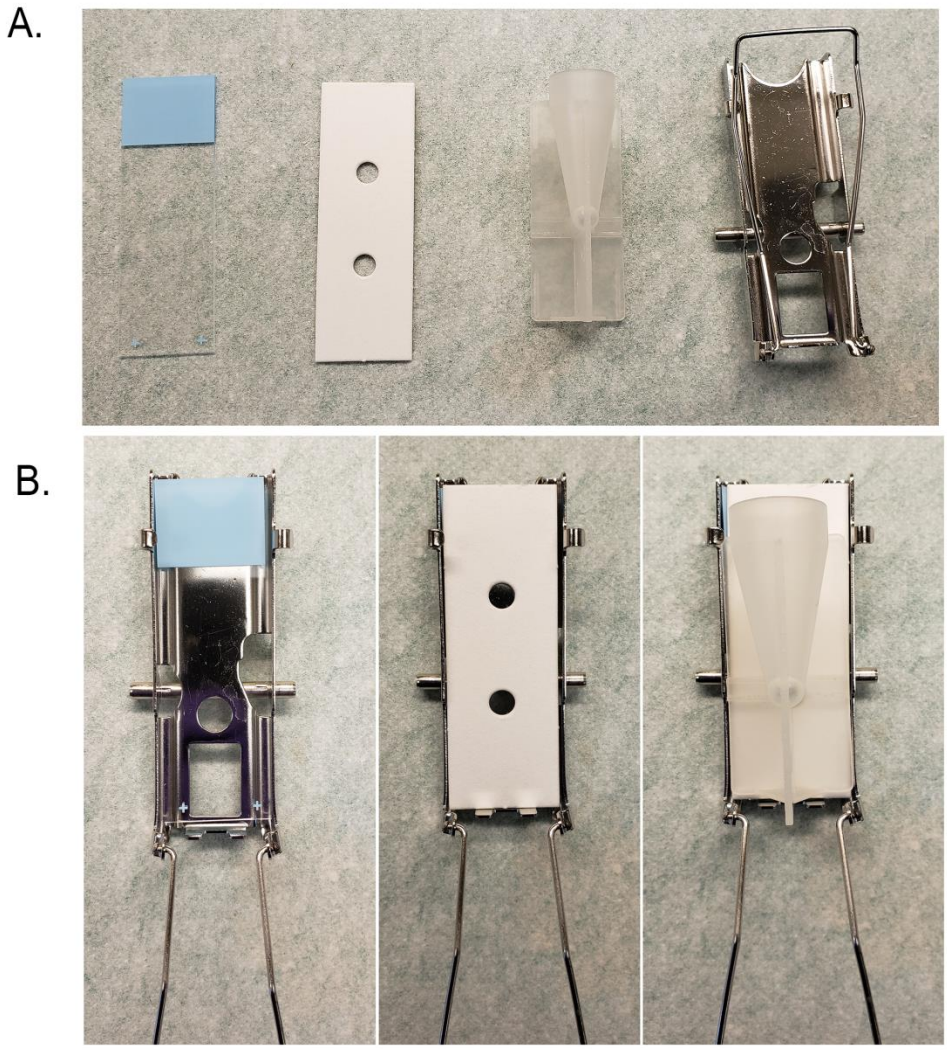

Figure 3.6.9. Cytospin Materials and Slide Preparation. (**a**) Materials include, from left to right, a labelled new clean slide, a filter card, a funnel, and a cage. (**b**) Setup sequence: 1) Place the slide in the cage; 2) Cover the slide with the filter paper, making sure to align its bottom edge flush with the bottom of the cage; 3) Place the funnel over the filter paper and slide, such that the bottom of the funnel is directed toward the hole in the filter paper. Clamp shut and place in cytocentrifuge. The cell suspension is placed into the funnel, and the cells will be distributed onto the slide upon centrifugation.

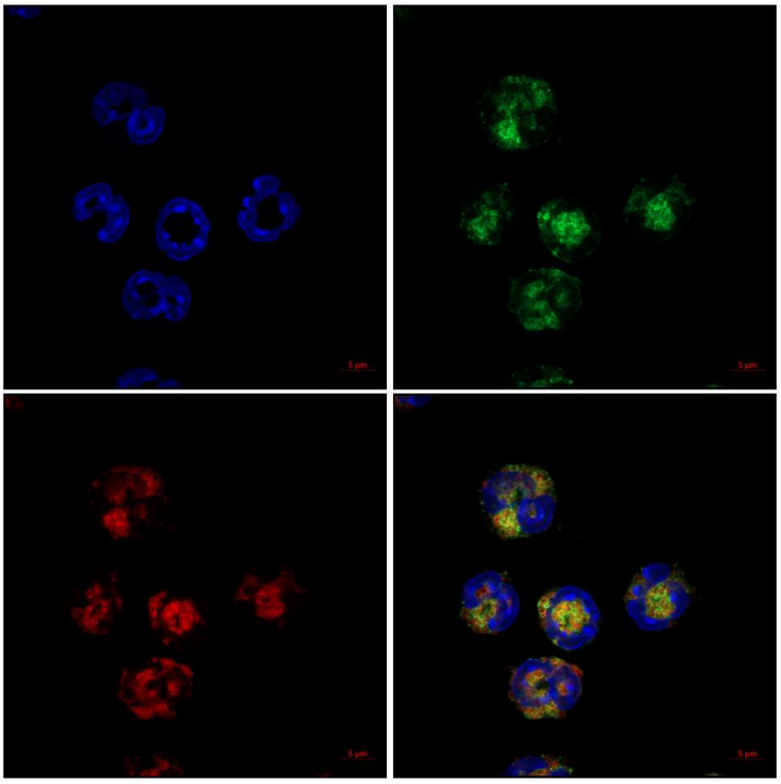

Figure 3.6.10. MBP and EPX Dual Fluorescent IHC. Cells were prepared by cytocentrifugation and then stained for both EPX and MBP. Eosinophils are stained for EPX (red) and MBP (green). Nuclei are counterstained with DAPI (blue). Image was acquired with a Plan-Apochromat 63x objective using Airyscan on a Zeiss LSM 800 microscope.

3.7 References

1. Walsh, G.M., et al., *Control of eosinophil toxicity in the lung.* Curr Drug Targets Inflamm Allergy, 2005. 4(4): p. 481-6.

2. Aleman, F., H.F. Lim, and P. Nair, *Eosinophilic Endotype of Asthma.* Immunol Allergy Clin North Am, 2016. 36(3): p. 559-68.

3. Kariyawasam, H.H. and D.S. Robinson, *The eosinophil: the cell and its weapons, the cytokines, its locations.* Semin Respir Crit Care Med, 2006. 27(2): p. 117-27.

4. Jacobsen, E.A., N.A. Lee, and J.J. Lee, *Re-defining the unique roles for eosinophils in allergic respiratory inflammation.* Clin Exp Allergy, 2014. 44(9): p. 1119-36.

5. Bochner, B.S., *The eosinophil: For better or worse, in sickness and in health.* Ann Allergy Asthma Immunol, 2018. 121(2): p. 150-155.

6. Weller, P.F. and L.A. Spencer, *Functions of tissue-resident eosinophils.* Nat Rev Immunol, 2017. 17(12): p. 746-760.

7. Rosenberg, H.F., K.D. Dyer, and P.S. Foster, *Eosinophils: changing perspectives in health and disease.* Nat Rev Immunol, 2013. 13(1): p. 9-22.

8. Lee, J.J., et al., *Eosinophils in health and disease: the LIAR hypothesis.* Clin Exp Allergy, 2010. 40(4): p. 563-75.

9. Busse, W.W. and R.F. Lemanske, Jr., *Asthma.* N Engl J Med, 2001. 344(5): p. 350-62.

10. Hogan, S.P., et al., *Eosinophils: biological properties and role in health and disease.* Clin Exp Allergy, 2008. 38(5): p. 709-50.

11. Jacobsen, E.A., et al., *The expanding role(s) of eosinophils in health and disease.* Blood, 2012. 120(19): p. 3882-90.

12. Meyer-Martin, H., S. Reuter, and C. Taube, *Mouse models of allergic airway disease.* Methods Mol Biol, 2014. 1193: p. 127-41.

13. Marques-Garcia, F. and E. Marcos-Vadillo, *Review of Mouse Models Applied to the Study of Asthma.* Methods Mol Biol, 2016. 1434: p. 213-22.

14. Denzler, K.L., et al., *Extensive eosinophil degranulation and peroxidase-mediated oxidation of airway proteins do not occur in a mouse ovalbumin-challenge model of pulmonary inflammation.* J Immunol, 2001. 167(3): p. 1672-82.

15. Willetts, L., et al., *Vesicle-associated membrane protein 7-mediated eosinophil degranulation promotes allergic airway inflammation in mice.* Commun Biol, 2018. 1: p. 83.

16. Jacobsen, E.A., et al., *Lung Pathologies in a Chronic Inflammation Mouse Model Are Independent of Eosinophil Degranulation.* Am J Respir Crit Care Med, 2017. 195(10): p. 1321-1332.

17. Willetts, L., et al., *Immunodetection of occult eosinophils in lung tissue biopsies may help predict survival in acute lung injury.* Respir Res, 2011. 12: p. 116.

18. Kay, A.B., *Paul Ehrlich and the Early History of Granulocytes.* Microbiol Spectr, 2016. 4(4).

19. Meyerholz, D.K., et al., *Comparison of histochemical methods for murine eosinophil detection in an RSV vaccine-enhanced inflammation model.* Toxicol Pathol, 2009. 37(2): p. 249-55.

20. Magaki, S., et al., *An Introduction to the Performance of Immunohistochemistry.* Methods Mol Biol, 2019. 1897: p. 289-298.

21. Ivell, R., K. Teerds, and G.E. Hoffman, *Proper application of antibodies for immunohistochemical detection: antibody crimes and how to prevent them.* Endocrinology, 2014. 155(3): p. 676-87.

22. Saper, C.B., *A guide to the perplexed on the specificity of antibodies.* J Histochem Cytochem, 2009. 57(1): p. 1-5.

23. Alkan, S.S., *Monoclonal antibodies: the story of a discovery that revolutionized science and medicine.* Nat Rev Immunol, 2004. 4(2): p. 153-6.

24. Rosenberg, H.F., *Eosinophil-Derived Neurotoxin (EDN/RNase 2) and the Mouse Eosinophil-Associated RNases (mEars): Expanding Roles in Promoting Host Defense.* Int J Mol Sci, 2015. 16(7): p. 15442-55.

25. Acharya, K.R. and S.J. Ackerman, *Eosinophil granule proteins: form and function.* J Biol Chem, 2014. 289(25): p. 17406-15.

26. Ochkur, S.I., et al., *A sensitive high throughput ELISA for human eosinophil peroxidase: a specific assay to quantify eosinophil degranulation from patient-derived sources.* J Immunol Methods, 2012. 384(1-2): p. 10-20.

27. Bochner, B.S., *Siglec-8 on human eosinophils and mast cells, and Siglec-F on murine eosinophils, are functionally related inhibitory receptors.* Clin Exp Allergy, 2009. 39(3): p. 317-24.

28. Feng, Y.H. and H. Mao, *Expression and preliminary functional analysis of Siglec-F on mouse macrophages.* J Zhejiang Univ Sci B, 2012. 13(5): p. 386-94.

29. Lee, J.J., et al., *Defining a link with asthma in mice congenitally deficient in eosinophils.* Science, 2004. 305(5691): p. 1773-6.

30. Ochkur, S.I., et al., *Frontline Science: Eosinophil-deficient MBP-1 and EPX double-knockout mice link pulmonary remodeling and airway dysfunction with type 2 inflammation.* J Leukoc Biol, 2017. 102(3): p. 589-599.

31. Ochkur, S.I., et al., *The development of a sensitive and specific ELISA for mouse eosinophil peroxidase: assessment of eosinophil degranulation ex vivo and in models of human disease.* J Immunol Methods, 2012. 375(1-2): p. 138-47.

32. Khoury, P., et al., *Revisiting the NIH Taskforce on the Research needs of Eosinophil-Associated Diseases (RE-TREAD).* J Leukoc Biol, 2018. 104(1): p. 69-83.

33. Denzler, K.L., et al., *Eosinophil major basic protein-1 does not contribute to allergen-induced airway pathologies in mouse models of asthma.* J Immunol, 2000. 165(10): p. 5509-17.

34. O'Hurley, G., et al., *Garbage in, garbage out: a critical evaluation of strategies used for validation of immunohistochemical biomarkers.* Mol Oncol, 2014. 8(4): p. 783-98.

35. Prost, S., et al., *Choice of Illumination System & Fluorophore for Multiplex Immunofluorescence on FFPE Tissue Sections.* PLoS One, 2016. 11(9): p. e0162419.

36. Stack, E.C., et al., *Multiplexed immunohistochemistry, imaging, and quantitation: a review, with an assessment of Tyramide signal amplification, multispectral imaging and multiplex analysis.* Methods, 2014. 70(1): p. 46-58.

37. Donaldson, J.G., *Immunofluorescence Staining.* Curr Protoc Cell Biol, 2015. 69: p. 4 3 1-7.

38. Dixon, A.R., et al., *Recent developments in multiplexing techniques for immunohistochemistry.* Expert Rev Mol Diagn, 2015. 15(9): p. 1171-86.

39. Koh, J., et al., *High-Throughput Multiplex Immunohistochemical Imaging of the Tumor and Its Microenvironment.* Cancer Res Treat, 2019.

40. Anyaegbu, C.C., et al., *Optimisation of multiplex immunofluorescence for a non-spectral fluorescence scanning system.* J Immunol Methods, 2019. 472: p. 25-34.

41. Jacobsen, E.A., et al., *Eosinophil activities modulate the immune/inflammatory character of allergic respiratory responses in mice.* Allergy, 2014. 69(3): p. 315-27.

42. Morton, J. and T.A. Snider, *Guidelines for collection and processing of lungs from aged mice for histological studies.* Pathobiol Aging Age Relat Dis, 2017. 7(1): p. 1313676.

43. Radulescu, R.T. and T. Boenisch, *Blocking endogenous peroxidases: a cautionary note for immunohistochemistry.* J Cell Mol Med, 2007. 11(6): p. 1419.

44. Garba, M.T. and P.J. Marie, *Alkaline phosphatase inhibition by levamisole prevents 1,25-dihydroxyvitamin D3-stimulated bone mineralization in the mouse.* Calcif Tissue Int, 1986. 38(5): p. 296-302.

45. Kim, S.W., J. Roh, and C.S. Park, *Immunohistochemistry for Pathologists: Protocols, Pitfalls, and Tips.* J Pathol Transl Med, 2016. 50(6): p. 411-418.

46. Petersen, K.H., J. Lohse, and L. Ramsgaard, *Automated sequential chromogenic IHC double staining with two HRP substrates.* PLoS One, 2018. 13(11): p. e0207867.

47. Osman, T.A., et al., *Successful triple immunoenzymatic method employing primary antibodies from same species and same immunoglobulin subclass.* Eur J Histochem, 2013. 57(3): p. e22.

48. Shi, S.R., Y. Shi, and C.R. Taylor, *Antigen retrieval immunohistochemistry: review and future prospects in research and diagnosis over two decades.* J Histochem Cytochem, 2011. 59(1): p. 13-32.

49. Shi, S.R., M.E. Key, and K.L. Kalra, *Antigen retrieval in formalin-fixed, paraffin-embedded tissues: an enhancement method for immunohistochemical staining based on microwave oven heating of tissue sections.* J Histochem Cytochem, 1991. 39(6): p. 741-8.

50. Mahmoudian, J., et al., *Comparison of the Photobleaching and Photostability Traits of Alexa Fluor 568- and Fluorescein Isothiocyanate- conjugated Antibody.* Cell J, 2011. 13(3): p. 169-72.

51. Davis, A.S., et al., *Characterizing and Diminishing Autofluorescence in Formalin-fixed Paraffin-embedded Human Respiratory Tissue.* J Histochem Cytochem, 2014. 62(6): p. 405-423.

52. Lum, H. and W. Mitzner, *Effects of 10% formalin fixation on fixed lung volume and lung tissue shrinkage. A comparison of eleven laboratory species.* Am Rev Respir Dis, 1985. 132(5): p. 1078-83.

53. Limjunyawong, N., J. Mock, and W. Mitzner, *Instillation and Fixation Methods Useful in Mouse Lung Cancer Research.* J Vis Exp, 2015(102): p. e52964.

54. Boivin, G.P., et al., *Review of CO(2) as a Euthanasia Agent for Laboratory Rats and Mice.* J Am Assoc Lab Anim Sci, 2017. 56(5): p. 491-499.

55. Fisher, S., et al., *Interstrain Differences in CO2-Induced Pulmonary Hemorrhage in Mice.* J Am Assoc Lab Anim Sci, 2016. 55(6): p. 811-815.

56. Schoell, A.R., et al., *Euthanasia method for mice in rapid time-course pulmonary pharmacokinetic studies.* J Am Assoc Lab Anim Sci, 2009. 48(5): p. 506-11.

57. Van Hoecke, L., et al., *Bronchoalveolar Lavage of Murine Lungs to Analyze Inflammatory Cell Infiltration.* J Vis Exp, 2017(123).

58. Bass, B.P., et al., *A review of preanalytical factors affecting molecular, protein, and morphological analysis of formalin-fixed, paraffin-embedded (FFPE) tissue: how well do you know your FFPE specimen?* Arch Pathol Lab Med, 2014. 138(11): p. 1520-30.

59. Bogen, S.A., K. Vani, and S.R. Sompuram, *Molecular mechanisms of antigen retrieval: antigen retrieval reverses steric interference caused by formalin-induced cross-links.* Biotech Histochem, 2009. 84(5): p. 207-15.

60. Reichman, H., P. Rozenberg, and A. Munitz, *Mouse Eosinophils: Identification, Isolation, and Functional Analysis.* Curr Protoc Immunol, 2017. 119: p. 14 43 1-14 43 22.

61. Kajimura, J., et al., *Optimization of Single- and Dual-Color Immunofluorescence Protocols for Formalin-Fixed, Paraffin-Embedded Archival Tissues.* J Histochem Cytochem, 2016. 64(2): p. 112-24.

62. Isidro, R.A., et al., *Double immunofluorescent staining of rat macrophages in formalin-fixed paraffin-embedded tissue using two monoclonal mouse antibodies.* Histochem Cell Biol, 2015. 144(6): p. 613-21.

CHAPTER 4

MULTIPLEX IHC WITH CLEAVABLE TYRAMIDE

4.1 Abstract

Eosinophils are found in many different tissues throughout the body during health as well as disease pathologies. It has been indicated that eosinophils in different microenvironments within tissues have differential functions. Here we report a novel multiplex imaging approach to study eosinophils *in situ* to understand their functions in relation to their location and interactions. In this approach, cleavable fluorescent probes were combined with RNA-FISH and IHC techniques to allow multiplex imaging by sequential staining cycles. After staining and imaging, fluorophores were cleaved and washed away, avoiding spectral overlap in the next cycle. We used mouse and human FFPE tissues to optimize and validate this approach. The goal of this approach was to develop a multiplex imaging panel to apply to patient biopsies of eosinophilic disease.

4.2 Introduction

Eosinophils are associated with many different diseases, such as asthma [334] and eosinophilic esophagitis [189], yet their roles have not been well defined. Traditionally eosinophils were thought to be a homogenous, end-stage effector cell population that mediate tissue destruction through cytolytic degranulation [287]. It is now appreciated, particularly in animal studies, that eosinophils have alternative functions under specific conditions [226] and display various activation phenotypes [97, 249]. Even within a single tissue, multiple functionally distinct populations of eosinophils have been identified [111, 335, 336]. Eosinophil activation state and phenotype have mainly been

completed either on homogenized samples or isolated single-cells both of which do not retain any spatial information [73, 239, 337]. While activation states that may have correlation with disease have been identified using these approaches understanding how these states relate to their function within tissues has been overlooked. The relevance of eosinophil subtype locations *in situ* and their interactions with stromal cells and other immune cells are entirely unknown for human eosinophilic diseases.

Many fluorescent based-techniques have been developed to analyze cells *in situ* such as DNA/RNA fluorescence *in situ* hybridization (FISH) [338] and various immunohistochemistry (IHC) based techniques [339]. FISH-based techniques use easily synthesized fluorophore-labeled oligomers to hybridize and label nucleic acid sequences of interest with the ability to quantify transcripts within a single-cell [340]. IHC techniques such as immunofluorescence (IF) are able to visualize antigens by applying either labeled primary (direct IF) or secondary (indirect IF) antibodies. These techniques allow the visualization of multiple markers within a single biopsy, however, they are limited by the number of spectrally distinct fluorophores available [341]. Typically the multiplexing ability of these techniques is limited to 3-5 markers or colors per sample, depending on the microscope set-up.

Many groups have developed techniques to overcome these limitations such as multi-spectral imaging (MSI), mass cytometry and sequential staining [200, 342]. MSI utilizes a special microscope and software to separate the overlapping spectrums between fluorophores increasing multiplexing beyond 5 but limited at 7 [194]. Two mass cytometry-based techniques have been described to date which allows the visualization of up to 32 markers within a single sample in one staining, however imaging is very slow

and available isotope-labelled antibodies are limited [198, 199]. Sequential staining methods involve staining the tissue, imaging it, then removing the signal by chemicals [202, 343], photobleaching [204, 344], or DNA displacement [217, 345]. Up to 60 antibodies [207] or 1001 transcripts [346] have been demonstrated on single sections using these approaches. Although the multiplexing capacity is expanded with these techniques, harsh chemicals can damage epitopes in subsequent cycles [203, 347], photobleaching is time consuming and inefficient [344], and DNA displacement is prone to high background from non-specific binding [216]. Interestingly, many of these techniques involve modified primary antibodies which are expensive and limited in availability, sometimes requiring in-house conjugation which can alter the performance of an already-in-use antibody.

The expense and complex nature of most techniques hinders their widespread use. The ideal technique would be structured around current conventional techniques so minimal training would be necessary and have the ability to be automated to improve throughput and precision of staining. Numerous unmodified primary antibodies have already been validated for biological and clinical applications. Utilizing this is important in rapid implementation of any technique.

Previously we described a method using novel cleavable linkers to analyze single-cells in a highly multiplexed fashion. By this approach, DNA loci, RNA transcripts and proteins were multiplexed and detected in single cells [219, 221]. However, the work thus far has been all done on isolated *in vitro* cells. To successfully stain tissue sections, complications from autofluorescence and off-target background must be overcome. Here, we present two highly multiplexed approaches. The first is a single-molecule RNA-FISH

(smRNA-FISH) technique that is multiplexed through cycles of staining, imaging and cleaving. The second is an IHC approach that utilizes off-the-shelf antibodies combined with our cleavable fluorescent tyramide. This is a highly sensitive technique as a result of the high signal amplification from tyramide reacting with HRP. Through cycles of staining, imaging, cleaving and antibody stripping, this approach has the potential to analyze over 20 markers within a single FFPE sample. To demonstrate the feasibility of this approach we designed a panel of 10 commercially available un-modified antibodies and applied them to standard FFPE human tonsil sections.

4.3 Results

4.3.1 Highly multiplex RNA-FISH approach to identify eosinophils subtypes *in situ*

Previously we described our *in vitro* eosinophil subtype model where eosinophils were activated with either type 1 or type 2 cytokines which we termed E1 and E2 eosinophils respectively (Chapter 1). From these studies we analyzed their gene expression profiles and determined gene panels that were highly upregulated in each subtypes. Utilizing this information we developed a workflow by combining a smRNA-FISH [340] approach with our cleavable linkers to visualize eosinophil subtypes within a FFPE biopsy. Briefly, all eosinophils were to be identified by IF staining using an eosinophil specific antibody, then subtypes would be distinguished by applying RNA-FISH probes designed to recognize subtype specific genes (Figure 4.5.1).

To start optimizing, we tested probes on activated cytospun eosinophils to avoid the complications with FFPE prepped tissues. We started with the standard direct smRNA-FISH approach and applied 20 small fluorophore labeled oligos (Figure 4.5.2a) to the cells but could not detect significant signal. Eosinophils are highly autofluorescent.

To overcome this background, we attempted to amplify the signal by taking an indirect smRNA-FISH approach (Figure 4.5.2b). We designed unlabeled probes that contained a gene recognition site and a tail. After binding, unbound probes are washed and labeled probes that recognize the tails are applied. Probes against the type 2 genes IL13 and CCL24 were applied to E1, E2, and resting unstimulated E0 eosinophils. Both IL13 and CCL24 intensely stained E2 cells compared to E0 and E1 (Figure 4.5.3). To ensure staining was repeatable we completed a second independent trial of this experiment that was unsuccessful. To troubleshoot, we tried new reagents, longer eosinophil activation, overnight probe incubation, snap cooling the probes, proteinase K and pepsin digestions, DNA blocking, permeabilization, antigen retrieval, adding an RNAse inhibitor to storage buffer, different storage conditions as well as designing new probes against the E1 gene CXCL10 and E0 gene STEAP4. In a final attempt we collected bronchoalveolar lavage fluid (BALF) from an allergic mouse model. These samples contain leukocytes, including eosinophils, from a type 2 microenvironment. Again, we were unable to obtain specific staining in eosinophils.

4.3.2 RNA-FISH on isolated eosinophils with alternative technologies

After unsuccessful staining using our in-house smRNA-FISH approach we tried two different commercial techniques. The first technique called hybridization chain reaction (HCR) (Molecular Instruments) uses probes complementary to mRNA transcripts that contain hairpin activating tails [348]. Once fluorophore labeled-hairpins are added, the tails trigger a chain reaction causing the hairpins to assemble into a fluorescent polymer. The second technology called RNAscope®(Bio-Techne) utilizes double Z target mRNA recognition and DNA branching techniques to amplify their signal [349]. Briefly, the

hybridization of 2 probes to an mRNA transcript creates a platform that allows second and tertiary probes to branch out creating a tree effect that contains numerous fluorescent molecules or HRP.

We first tried HCR using probes again IL13, CCL17, CCL24, S1pr3, EDN, and GM-CSF. After multiple attempts, we were unable to detect any successful staining in eosinophils. We additionally tried the housekeeping genes Malat1 and Acta1 but failed to detect these genes as well. We next tried RNAscope on isolated activated eosinophils using control genes UBC, PPIB and the E2 gene IL13. Again, the methods were not successful and additional attempts to optimize these assays by trying different fixation conditions and protease retrieval failed to improve staining.

To determine if this was an eosinophil specific problem or a personnel problem, we stained cytospin prepped innate lymphoid type 2 cells (ILC2s) which are known producers of IL13 [350]. Figure 4.5.4 shows intense specific staining of IL13 mRNA using the HCR technique, indicating the complications were likely due to the cell origin and not personnel.

There are some known differences between mouse and human eosinophils (reviewed here [2]). To see if the difficulty in staining was a mouse eosinophil-specific phenomenon we tested RNAscope probes against the controls genes POLR2A, PPIB, and UBC and the eosinophil marker IL5Rα. Even with different fixation and storage conditions we were unable to detect any expression. Altogether these results indicate eosinophils are uniquely problematic for FISH techniques.

4.3.3 RNA-FISH on mouse FFPE tissue

Eosinophils contain significant amounts of RNAses [351]. With the chance of RNA degradation in isolated eosinophils, we tried RNA-FISH on FFPE tissue sections which is subjected to more extensive fixation and contains other cells types that can be used as a quality control. To obtain tissue that have activated eosinophils present, we put mice through a house dust mite (HDM) allergy challenge protocol [352]. This protocol induces type 2 inflammation and eosinophil infiltration into the lungs. Lungs were harvested, fixed in 4% formaldehyde and incubated at 4^{o}C, 23^{o}C or 37^{o}C for 24 hours to evaluate the best conditions to maintain RNA integrity. The lung mRNA integrity was analyzed by staining for PPIB mRNA using an RNAscope® kit (Figure 4.5.5). RNAscope probes were used because they are highly specific and are the gold standard for FFPE samples. 23^{o}C was determined to be the optimal fixation temperature as it had intense specific staining. With this optimized sample, we started by staining for the control genes UBC (high expression) and PPIB (medium-low expression). As seen in Figure 4.5.6a we obtained specific and bright staining with both genes and the pattern of staining matched as expected. We next stained for IL-13 to demonstrate that a non-housekeeping gene could be detected in our sample (Figure 4.5.6b). This methodology provided a technique with high signal-to-noise that works on lung tissue and used for further study.

4.3.4 Combined RNA-FISH and IF on mouse FFPE tissue

IL13 RNA-FISH alone is insufficient to determine staining specific to eosinophils, thus we required co-staining with an eosinophil-specific marker. To confirm mRNA staining occurs in eosinophils in FFPE lung samples, we performed IF using an eosinophil specific antibody (anti-MBP) to identify all the eosinophils present within the tissue

(Figure 4.5.1). Alone MBP is able to stain eosinophils (Figure 4.5.7a), but when applied after performing RNA-FISH, the antibody staining was not detected (Figure 4.5.7b). The standard MBP IF protocol uses only a mild pepsin digestion for antigen retrieval whereas the RNA-FISH protocol includes protease digestion as well as heat-induced epitope retrieval (HIER). With the chance that the harsher retrieval steps in the RNA-FISH protocol could be damaging the MBP epitope, we used an alternative eosinophil-specific antibody. We tested EPX IF (chapter 2) on the lung section using two approaches, one with an Alexa Fluor 594 conjugated secondary and one with a HRP conjugated secondary with FITC tyramide development (Figure 4.5.8a) before combing IL13 RNA-FISH with EPX (Figure 4.5.8b). Although the RNA staining was very intense in other cells, eosinophils displayed very weak and sporadic staining where only one or two eosinophils had a punctum. Further optimization attempts by varying HIER times, protease incubation times, proteases, and storage conditions were unsuccessful. We also tested another allergy model as well as frozen tissue in case the fixation and embedding process was damaging the RNA in eosinophils. These were unsuccessful, indicating RNA-FISH techniques are uniquely difficult in eosinophils *ex vivo* or *in situ*.

4.3.5 Highly-Multiplexed IHC approach to study eosinophil subtypes *in situ*

With the difficulty of staining eosinophils with RNA-FISH we decided to take an alternative approach and stain for protein rather than RNA as protein is more stable than RNA and proteins have been successfully stained in eosinophils by us and many others [57, 111, 172, 186]. We wanted to develop a novel technique that could be easily implemented in any lab and apply it to patient biopsies with tissue eosinophilia. We took an indirect multiplex IHC approach [194] and combined it with our cleavable tyramide to

enable sequential staining (Figure 4.5.9). Briefly, after standard slide preparation, 2 primary antibodies from different species (for example mouse and rabbit) are applied. Next, an anti-species HRP-conjugated secondary (i.e. anti-mouse) is applied and signal is developed with cleavable FITC-tyramide (cFITC-T). Following detection, the residual HRP activity is blocked and the second primary antibody is detected by the other anti-species secondary (i.e. anti-rabbit) and signal is developed using cCy3-T. After detection of both species, antibodies are stripped in heated buffer so that a third primary of the same species (i.e. mouse) can be applied and detected without cross-reactivity to the first mouse primary antibody. After development of the third primary antibody with cCY5-T, the 3 color slide is imaged and cleaved completing 1 cycle. This process is repeated with the next panel of 3 antibodies, stripping after both mouse and rabbit primaries have been detected and imaged.

4.3.6 Antibody stripping is efficient in mouse FFPE lung tissue

To determine the feasibility of this multiple IHC approach, we tested the capacity of stripping to remove antibodies from the FFPE lung tissue. This enables the ability to stain using primary antibodies from the same species. First, we assessed whether the stripping would alter or damage the presence of fluorescent dye deposited on the tissue. Rabbit anti-CD3ε was applied and detected using anti-rabbit HRP-conjugated secondary and Cy3-T. After collecting a control image, the slide was stripped in citrate pH6 buffer and imaged again to determine the stability of Cy3-T dye after stripping. Figure 4.5.10a demonstrates that the fluorescent signal is still intact after the stripping process.

To evaluate if HRP conjugated secondary antibody was still present after stripping, Cy5-T was added directly to test the presence of HRP conjugated secondary

antibody remaining on the slide. In addition, to test the presence of primary antibody (rabbit anti-CD3ε) after stripping, we added anti-rabbit HRP-conjugated secondary and Cy5-T (Figure 4.5.10b). There was no detectable Cy5 signal from either leftover HRP conjugated secondary antibody or bound primary antibody supporting that stripping was efficient in removing both primary and secondary antibodies. After stripping rabbit anti-CD3ε, we applied mouse anti-EPX followed by anti-mouse HRP-conjugated secondary, and then FITC-T to demonstrate that indirect IHC can be performed on FFPE tissue using two primary antibodies (rabbit anti-CD3ε and mouse anti-EPX) in serial succession after stripping.

4.3.7 Maximum number of cycles on mouse FFPE

In this application, the process of stripping is the same as HIER. HIER is a necessary step in preparing slides for IHC as it reverses the cross-linking induced by formaldehyde fixation to "unmask" or retrieve epitopes so they are accessible by antibodies [319]. Multiple rounds of stripping could lead to damage as the tissue is slowly being "un-fixed". Currently, the highest number of strips reported in the literature is 12 [212]. To check tissue and epitope integrity, CD3ε was detected in lung tissue after multiple rounds of stripping (Figure 4.5.10c). Even after 20 rounds of stripping, the tissue was intact and CD3ε was still detectable. Interestingly, the signal of CD3ε increased with successive rounds of stripping, likely as a result of increase epitope availability.

4.3.8 Developing a panel of antibodies for human FFPE

After determining the feasibility of this approach in mouse FFPE tissue, we developed a panel of antibodies that could be used to study the immune landscape of human biopsies

(Table 4.5.1). The panel contains antibodies to recognize eosinophils, B cells, T cells, mast cells, basophils, monocytes, neutrophils, NK cells, dendritic cells, epithelial cells as well as a type 1 and 2 activation marker. A cell membrane marker was included to assist in cell segmentation for image analysis.

To ensure comparability to clinical IHC standards, protocols needed to be developed to obtain chromogenic IHC controls. The standard protocol included antigen retrieval, blocking, primary incubation, secondary HRP polymer incubation, then detection by 3,3-diaminobenzidine (DAB). Antigen retrieval, blocking conditions and antibody concentrations were optimized to create compatible protocols that reflect intense specific staining (Figure 4.5.11).

4.3.9 Comparing elution performance on individual antibodies

Many different antibody stripping protocols have been published with no optimal universal protocol. In addition, due to antibody affinity for different epitopes, stripping performance is antibody-dependent such that each antibody must be evaluated individually [214]. The stripping efficiency of each antibody was tested with citrate pH6 (Figure 4.5.12). This resulted in only 3 antibodies stripped efficiently, IgA2, EPX and FcER1.

The membrane marker NaK-ATPase had the most intense signal after stripping therefore optimizations of stripping conditions were tested using this antibody. We tested a citrate pH6 buffer for 30 minutes, EDTA pH8 buffer for 15 mins, and citrate pH6 with 0.3% SDS for 15 mins (Figure 4.5.13). Out of all three conditions citrate with SDS had the least amount of residual signal. We then screened the stripping efficiency of citrate

pH6 w/0.3% SDS on the rest of the panel (Figure 4.5.14). In all cases the residual staining decreased, with no detectable signal in majority of the panel.

4.3.10 Epitopes are not damaged after elution

To ensure these conditions would be compatible in our multiplex approach we tested the recognition of each epitope after the equivalent of 10 rounds of stripping in citrate pH 6 w/0.3% SDS. Although, there was some visible tissue damage indicated by edge lift and fainter hematoxylin staining, all epitopes were recognized by our panel of antibodies with similar staining intensity and patterns compared to a non-stripped control (Figure 4.5.15). To minimize damage, IgA2, EPX, and FcER1 were placed at the beginning of the multiplex panel and two markers with the most residual signal, NaK-ATPase and Keratin were placed at the end of the panel.

4.3.11 Fluorescent IHC staining is comparable to brightfield

After establishing IHC protocols and confirming compatibility with our approach, each antibody protocol was converted to a fluorescence tyramide based protocol. The working concentration of the fluorescent tyramide dye was titrated to balance signal versus background. The staining patterns were comparable to conventional indirect IHC with DAB and hematoxylin counterstain (Figure 4.5.16).

4.4 Discussion

How the tissue microenvironment determines eosinophil activities and how they, in turn, contribute or mitigate disease pathology during inflammation is unknown. Using multiplex tissue imaging we aim to spatially map the complex landscape of leukocytes in relation to eosinophil subtypes within inflamed tissues. For the first time, this approach

will allow us to simultaneously visualize cell subtypes, their location, and their interactions *in situ.*

In this study, we have presented a novel fluorescent multiplex imaging technique that builds off our previously published cleavable linkers. We have overcome the limitations of conventional fluorescent imaging by expanding the number of markers that can be simultaneously visualized on a single FFPE section from 5 to over 20. This method is compatible with standard off-the-shelf antibodies and reagents with the exception of our cleavable tyramide fluorescent dye allowing easy implementation into any lab running IHC. Structured after a standard IHC protocol, this technique is adaptable to any IHC validated antibody with minimal optimization. FFPE prepared tissues are the most common format that tissue samples are collected and stored, being compatible with standard samples allows archival samples to be re-evaluated.

Our original approach was to study eosinophils subtypes *in situ* by applying a multiplex RNA-FISH technique but because of technical challenges, we were unsuccessful. Extensive troubleshooting was performed to optimize the assay but reproducibility was never achieved. Within the literature, few papers have shown FISH techniques performed on eosinophils [353-358]. In all cases, no eosinophil-specific IHC was performed to identify the cells and the quality of staining was not ideal with high background. A more recent paper by Ellis *et al*. found that the granule protein ECP in human eosinophils can bind probes more avidly than target mRNA [359] suggesting caution when evaluated eosinophil staining. Alternatively, eosinophils are innate immune cells well equipped to fight various pathogens including RNA viruses as evident by their granule proteins containing different RNAses such as EDN (human) and Ears (mouse)

[26, 45, 351, 360, 361]. We hypothesize that the lack of staining in our experiments is a result of either RNA inaccessibility or RNA integrity. We tried different antigen retrieval techniques and various protease treatments to remove proteins that could potentially be blocking our probes from binding with no avail. Only being successful on other cell types, the data suggests that the mRNA degradation was too extensive to achieve significant signal in eosinophils.

We took an alternative approach and decided to develop a new multiplex imaging assay that would be able to evaluate eosinophil subtypes as well as other cell types *in situ*. Many multiplexing techniques have been developed but are usually slow, expensive, complicated, and not easily implemented in a regular lab [200, 362]. In contrast, the cleavage technology is fast, cost efficient, non-damaging and compatible with multiple *in situ* imaging techniques [219, 221]. For easy integration, our technique was modeled to be as similar to standard IHC protocols as possible. In addition, our method is compatible with basic fluorescent microscope set-ups, commercially available reagents (except for cleavable tyramide), and uses unmodified antibodies. Furthermore, this approach is technologically simple and doesn't require special training beyond normal florescent imaging skills, making it easily adapted to current imaging labs.

This technique like other multiplexing techniques is sequential based which requires multiple rounds of staining and imaging which can be labor intensive. Although not shown here, this technique is compatible with automated IHC staining equipment that would drastically reduce the amount of manual labor. Furthermore, whole-tissue imaging using a basic microscope is also relatively slow. To increase both imaging and throughput, a fluorescent slide scanner can also be used. Taken together, with the proper

equipment this technique can be almost fully automated, requiring minimal hands on time.

This protocol is compatible with both mouse and human FFPE tissue sections which is important for basic research in animal models as well as patient care. We have designed a panel of 11 antibodies and demonstrated their performance in our positive control tonsil tissues.

To enable the use of primary antibodies from the same species, a stripping step was included into our protocol. Our first try of citrate pH6 buffer failed to remove all residual signal from our entire panel however, a few antibodies were efficiently stripped and in all cases the signal was reduced compared to staining without stripping. To efficiently strip the rest of the panel we found citrate pH6 w/0.3% SDS to be a superior buffer but led to some visible tissue damage. Although stripping induced some lifting of the tissue edges and the nuclei to counterstain lighter, there was no significant epitope damage allowing our markers to still be analyzed efficiently. In addition, the light nuclei could potentially be resolved by increasing the incubation in hematoxylin. Of note, when evaluating the epitope damage induced by stripping, the slides went through the equivalent of 10 rounds of stripping with citrate pH6 w/0.3% SDS, enough to complete a panel of 22 antibodies which is double the amount our panel requires.

We succeeded in developing a strategy to identify and study subtypes in cell and tissue biopsies but further work needs to be done before this technique can be applied to patient biopsies. Specifically, the order of the panel needs to be optimized. This entails ordering the antibodies in a way that reduces interferences from residual signal after cleavage. Effort is made to design the panel from low to high expression, reducing spatial

and color overlap in successive rounds, from extra cellular to intracellular, pairing mouse with rabbit primaries each round, and placing the inefficiently stripped antibodies at the end.

After optimization on positive control tissue with cleavable fluorescent dyes this panel will be applied to patient biopsies from Eosinophilic Esophagitis (EoE) and healthy controls to investigate how the immune landscape influences EoE. This novel technique will help to study a disease in a way that has never been done before.

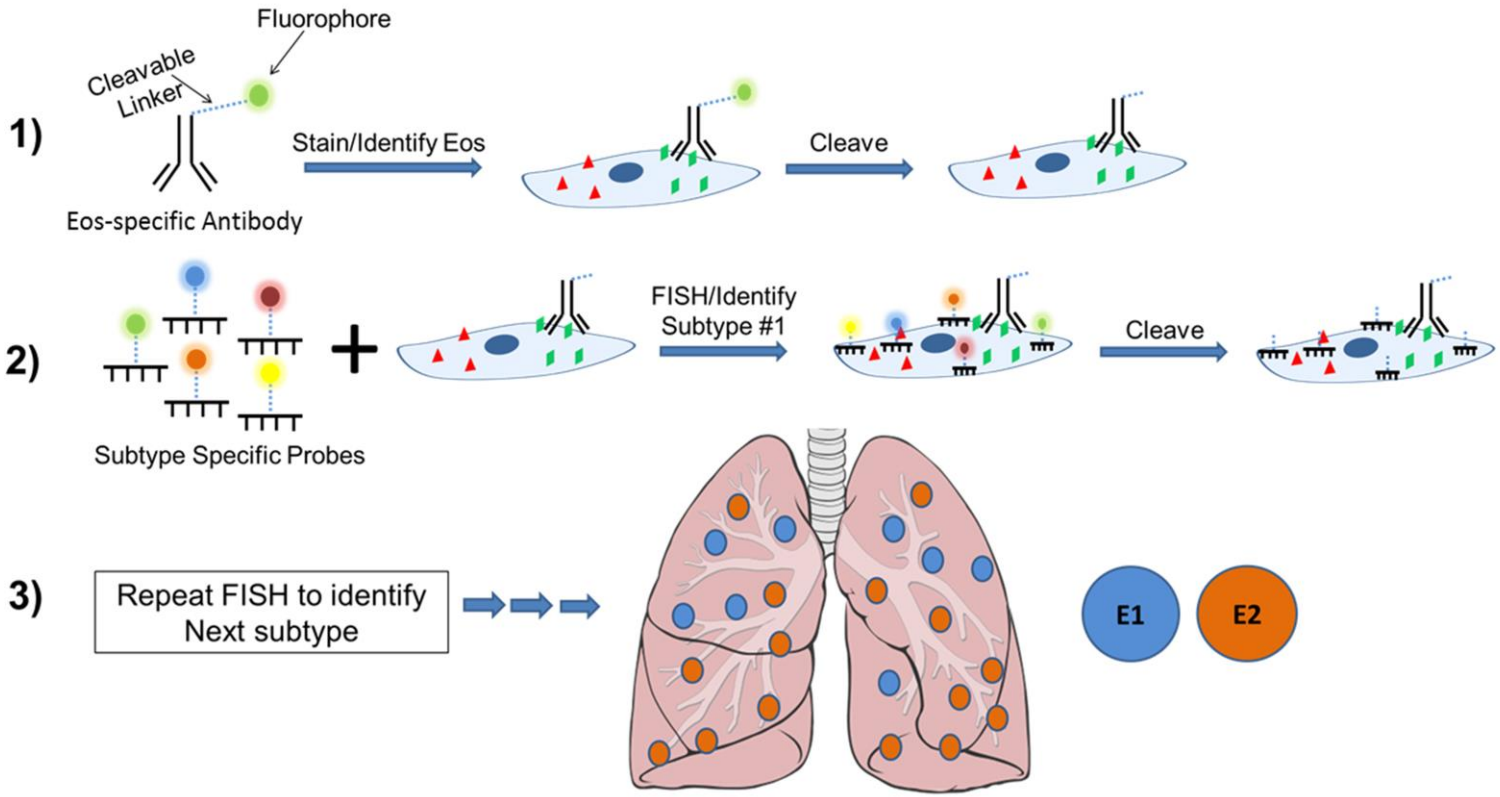

Figure 4.5.1. Multiplex RNA-FISH Imaging Strategy. (1) An eosinophil specific antibody labeled with a cleavable fluorophores is applied to stain and identify all eosinophils present within the tissue section. The fluorophore is then cleaved and washed away. (2) 5 probes, complimentary to subtype specific genes and labeled with cleavable fluorophores, are applied to identify the first eosinophil subtype present. After imaging the fluorophores are cleaved and washed away. (3) This is repeated with the next subtype specific probe set to identify the second eosinophil subtype present within a biopsy such as lung tissue.

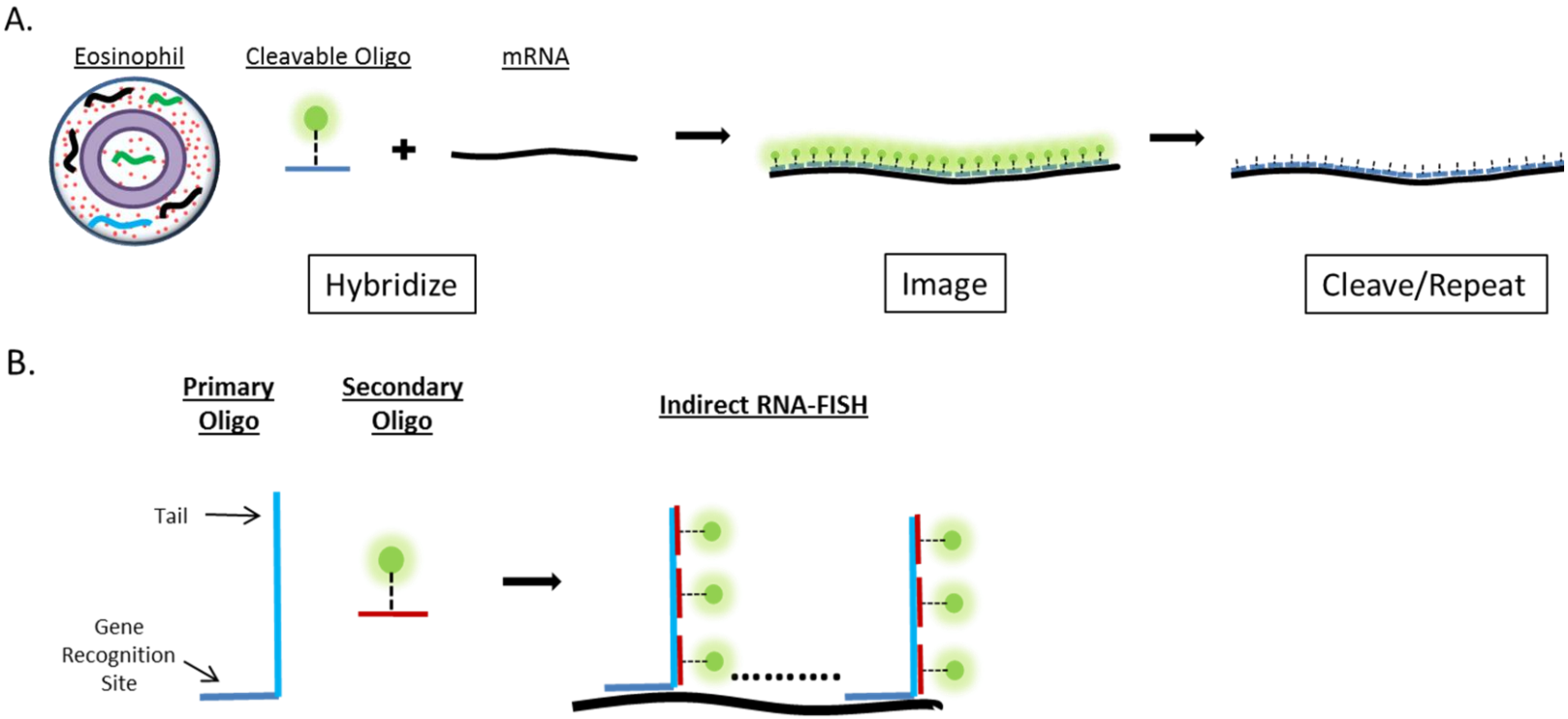

Figure 4.5.2. Multiplex smRNA-FISH Approaches. (A) Direct smRNA-FISH. Multiple small gene-specific cleavable oligo probes are hybridized onto an mRNA transcript of interest, imaged, cleaved, and repeated. (B) Indirect smRNA-FISH. Primary gene-specific oligos containing a tail sequence that is recognized by a fluorophore labeled secondary oligo. After hybridizing multiple primary oligos, multiple secondary oligos bind to the primary tails, amplifying the signal from primary oligos. These techniques are not restricted to 1 color per cycle. Multiple transcripts can be visualized simultaneous using spectrally-distinct fluorophores.

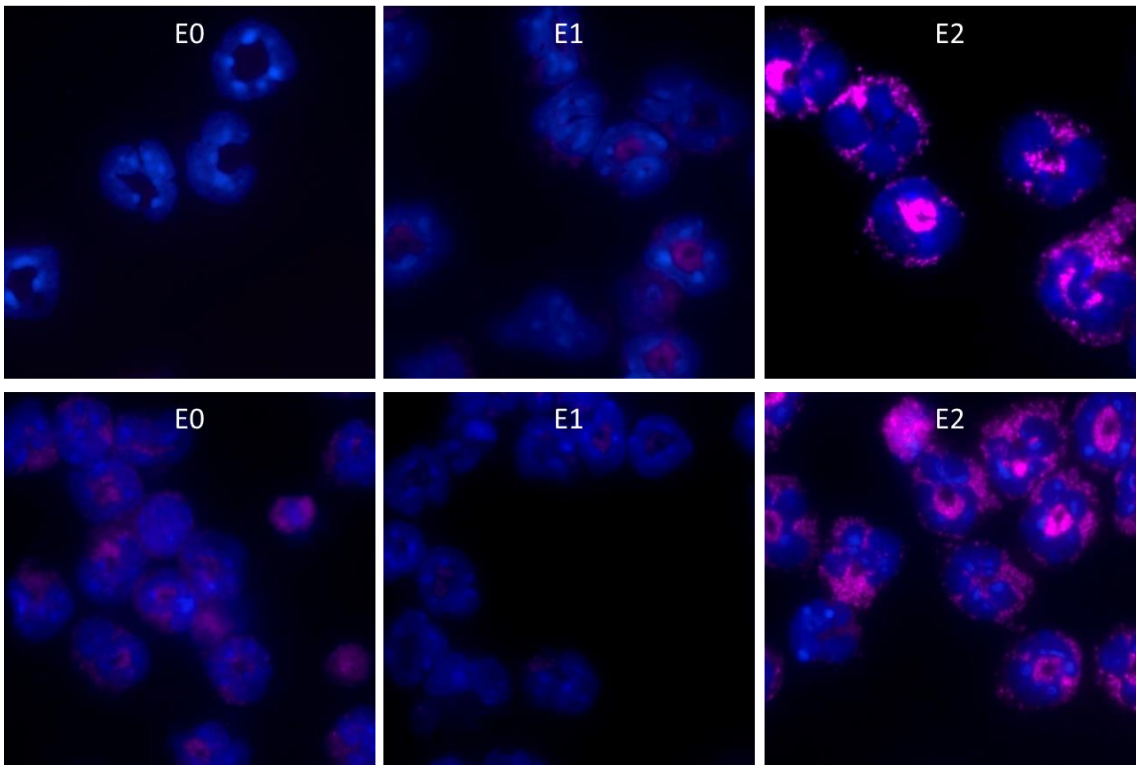

Figure 4.5.3. Cleavable smRNA-FISH on Isolated Eosinophils. *In vitro* activated eosinophils subtypes were cytospun and stained for (A) IL-13 mRNA and (B) CCL24 mRNA. mRNA is labeled with Cy7 (pink) and nuclei are labeled with DAPI (blue).

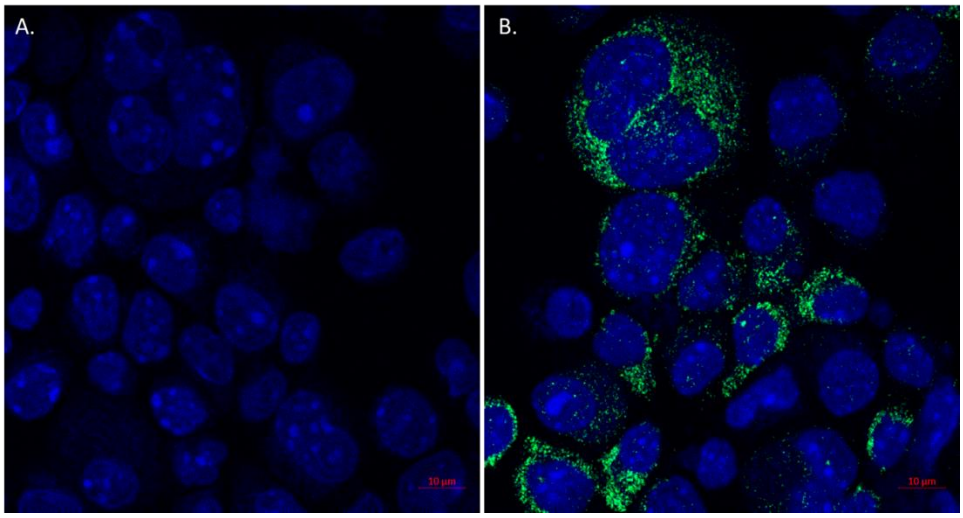

Figure 4.5.4. Innate Lymphoid Type 2 (ILC2) Cells Were Stained for IL-13 mRNA Using HCR (Molecular Instruments). (A) Hairpin negative control. (B) IL-13 mRNA (green). Nuclei are counterstained with DAPI (Blue).

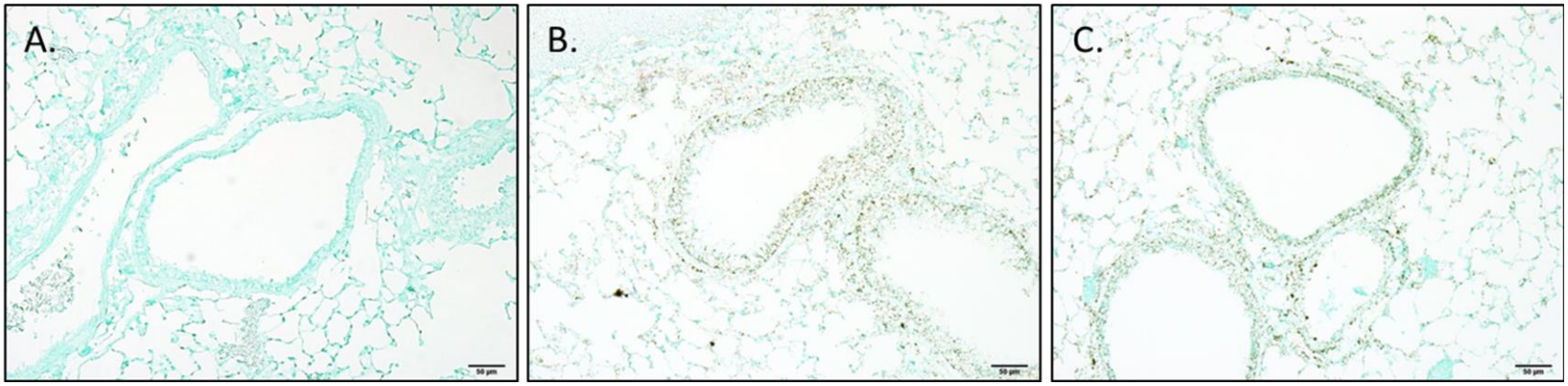

Figure 4.5.5. PPIB RNA-ISH (RNAscope) on Mouse HDM Lung FFPE Tissue Sections Fixed with Different Temperatures. (A) 4ºC. (B) 23ºC. (C) 37ºC.

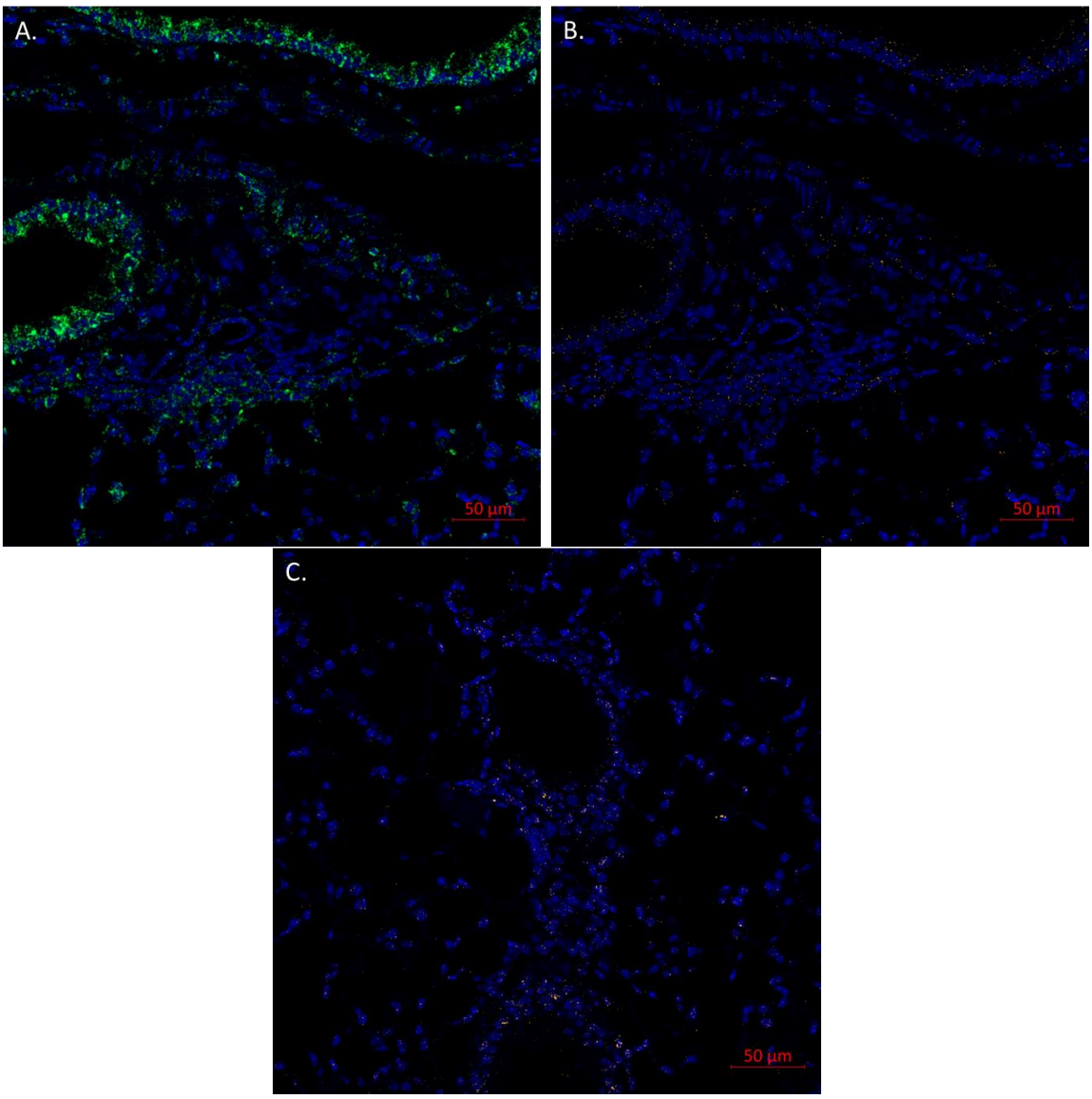

Figure 4.5.6. RNA-FISH (RNAscope) on Mouse HDM Lung FFPE Tissue. (A) High expressing control gene UBC (green). (B) Medium-low expressing control gene PPIB (orange). (C) IL-13 mRNA (orange). Nuclei are counterstained with DAPI (blue).

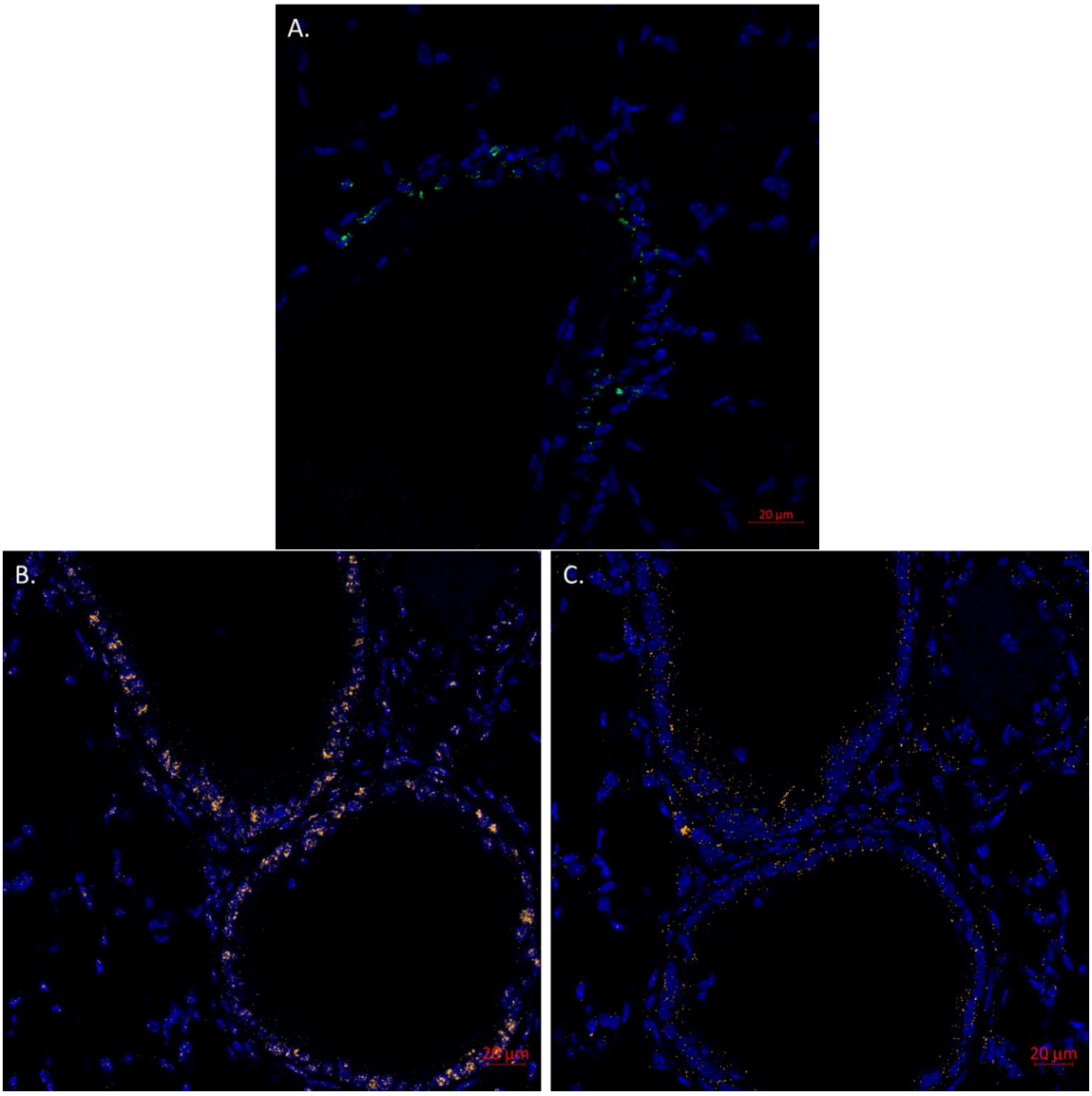

Figure 4.5.7. Anti-MBP Immunofluorescence and RNA-FISH (RNAscope) on Mouse HDM Lung FFPE Tissue. (A) anti-MBP (green). (B) anti-MBP (green) and IL-13 mRNA (orange). (C) anti-MBP (green) and PPIB mRNA (orange). Nuclei are counterstained with DAPI (blue).

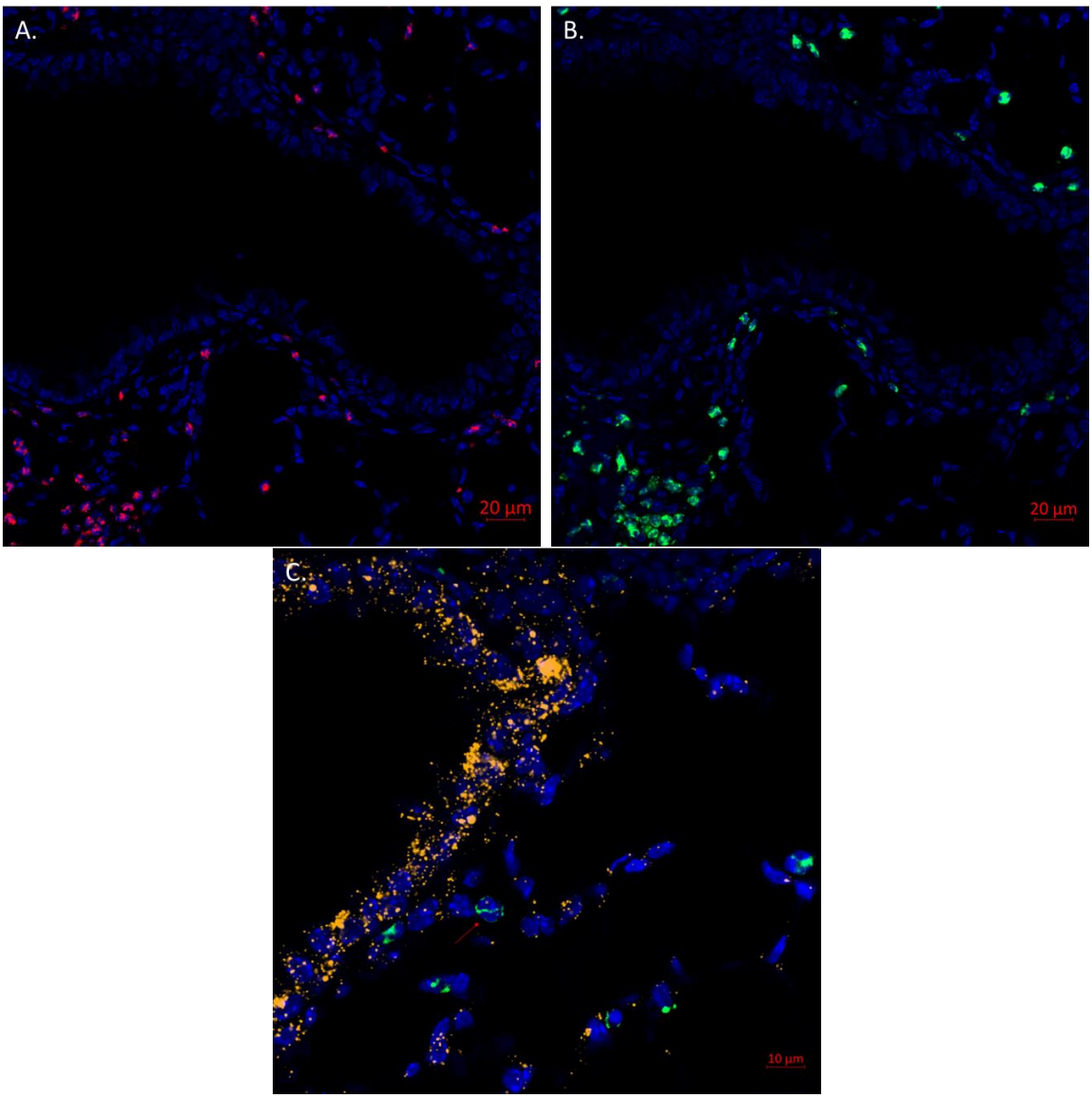

Figure 4.5.8. Anti-EPX Immunofluorescence and RNA-FISH (RNAscope) on Mouse HDM Lung FFPE Tissue. (A). Anti-EPX developed with Alexa 594-secondary (red). (B) Anti-EPX developed with FITC tyramide (green). (C) Anti-EPX (green) and UBC mRNA (orange). Nuclei are counterstained with DAPI (blue).

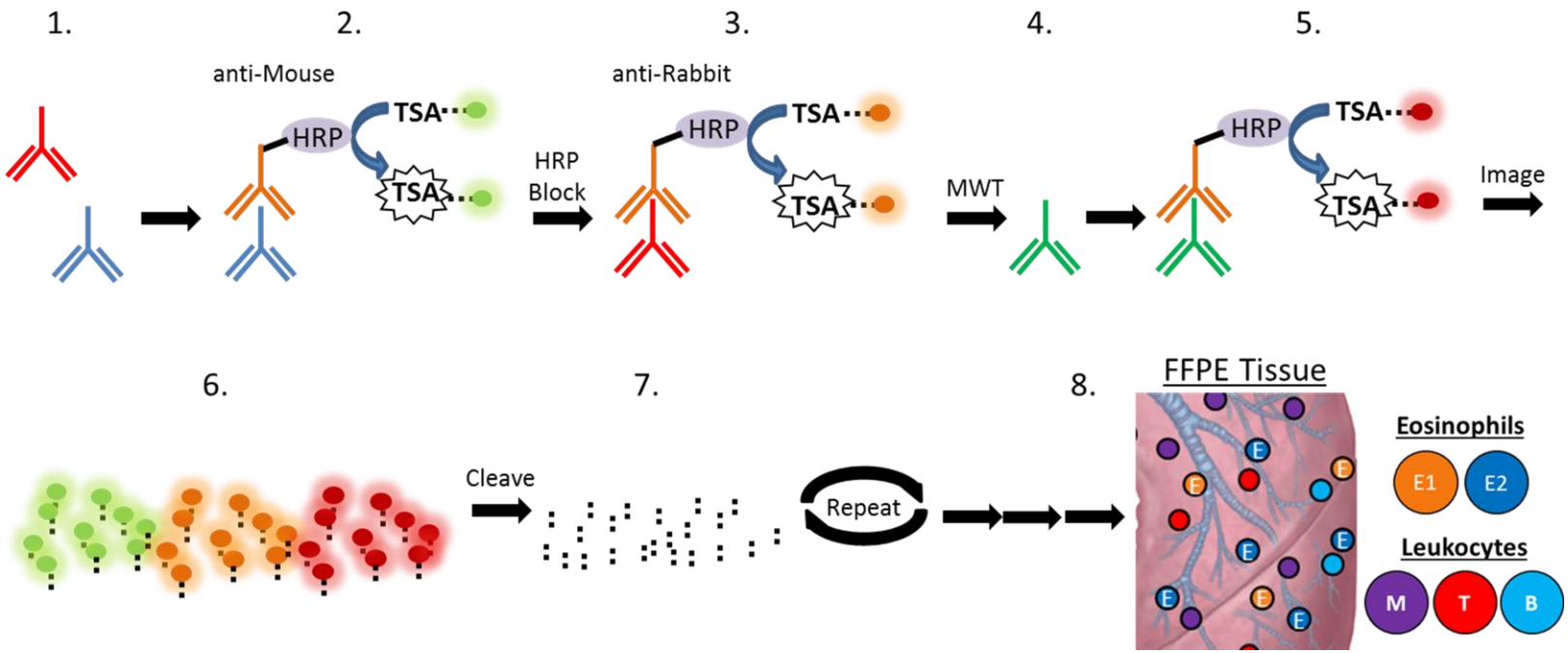

Figure 4.5.9. Multiple IHC Imaging Scheme. (1) Mouse and rabbit primary antibodies are added to tissue. (2) anti-mouse secondary is added and signal is developed with FITC tyramide. (3) HRP is blocked and anti-rabbit is added then developed with Cy3 tyramide. (4) Antibodies are stripped with microwave treatment (MWT) and the third primary antibody is added. (5) The third antibody is developed with Cy5 tyramide. (6) The slide containing three fluorescence colors is imaged. (7) The fluorophores are cleaved and washed away. (8) The process is repeated with the next panel of antibodies until all antibodies have identified eosinophils subtypes as well as other leukocytes.

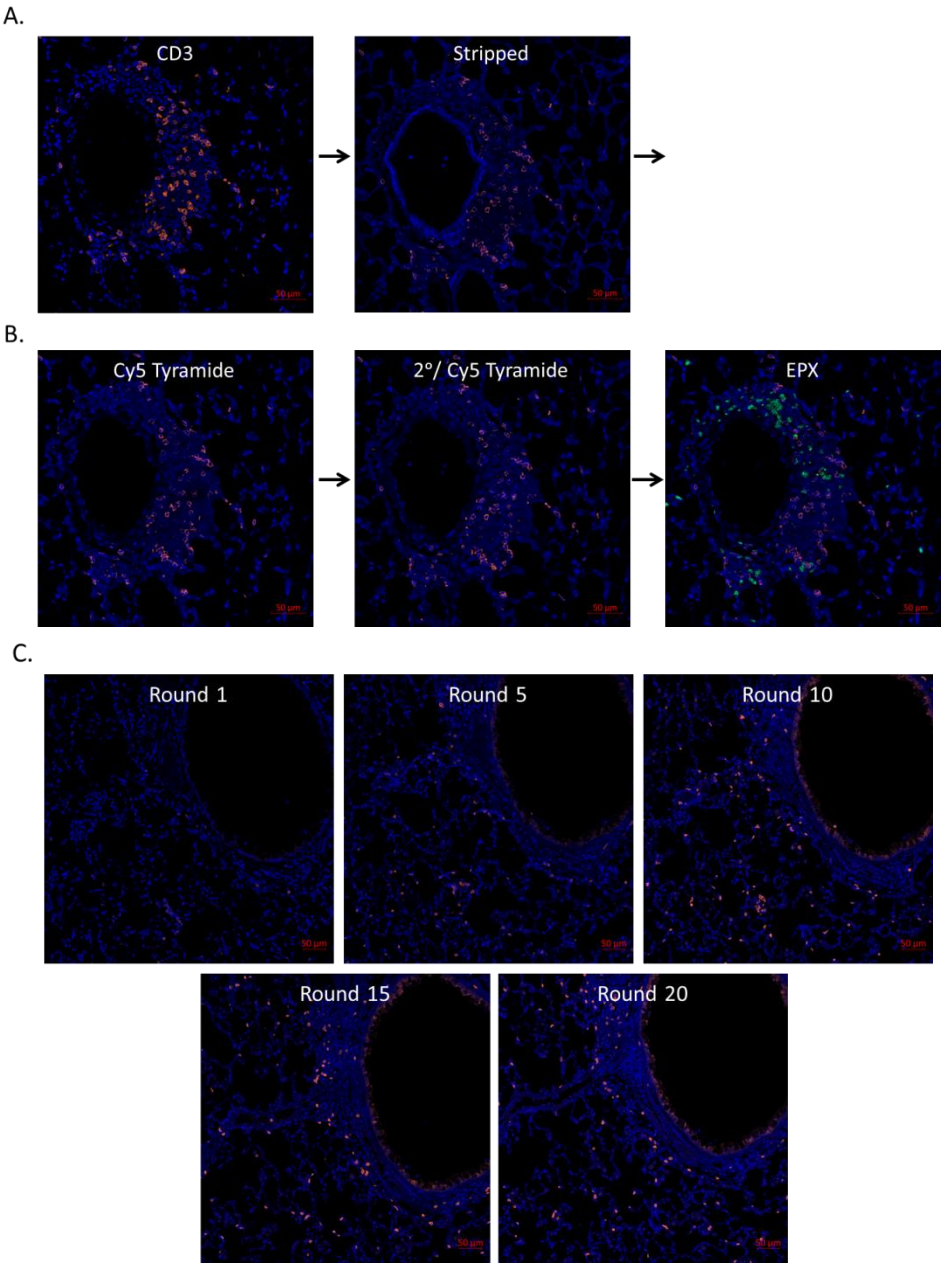

Figure 4.5.10. Fluorescence IHC and Antibody Stripping on Mouse HDM Lung FFPE Tissue. (A,B) A single section was used to evaluate the stripping efficiency. (A) Section stained for CD3 Cy3 (orange) then stripped with citrate pH6 buffer. (B) Cy5 (red) tyramide was added to section to detect residual HRP, secondary (2º) and Cy5 tyramide was added to detect residual primary antibody, finally anti-EPX was added and developed with FITC tyramide (green). (C) Serial sections were put through multiple rounds of stripping prior to staining with CD3. Nuclei are counterstained with DAPI (blue).

Antibody	Clone	Host	Company	Antigen Retreival Buffer	IHC Dilution	Primary Antibody Incubation
CD32b (FcγRIIb)	EP888Y	Rabbit	Abcam	Citrate pH6	4000x	30 mins RT
CD3e	SP7	Rabbit	Thermo	Citrate pH6	300x	overnight
C-kit	D3W6Y	Rabbit	CST	Citrate pH6	100x	30 mins RT
EPX	MM25-82.2.1	Mouse	Lee Lab	Citrate pH6	1000x	30 mins RT
FcεR1	9E1	Mouse	Abcam	Citrate pH6	400x	overnight 4C
IgA2	RM125	Rabbit	Novus	Citrate pH6	8000x	30 mins RT
IgG4	MRQ-44	Mouse	Cell Marque/Sigma	Citrate pH6	pre-diluted	15 mins RT
NaK-ATPase	EP1845Y	Rabbit	Abcam	Citrate pH6	800x	30 mins RT
Pan-keratin	C11	Mouse	CST	Citrate pH6	500x	30 mins RT
pSTAT1	58D6	Rabbit	CST	EDTA pH8	800x	30 mins RT
STAT6	EP325	Rabbit	Cell Marque/Sigma	Citrate pH6	100x	30 mis RT

Table 4.5.1. The 11 Antibody Panel Used to Immune Profile Human FFPE Biopsies.

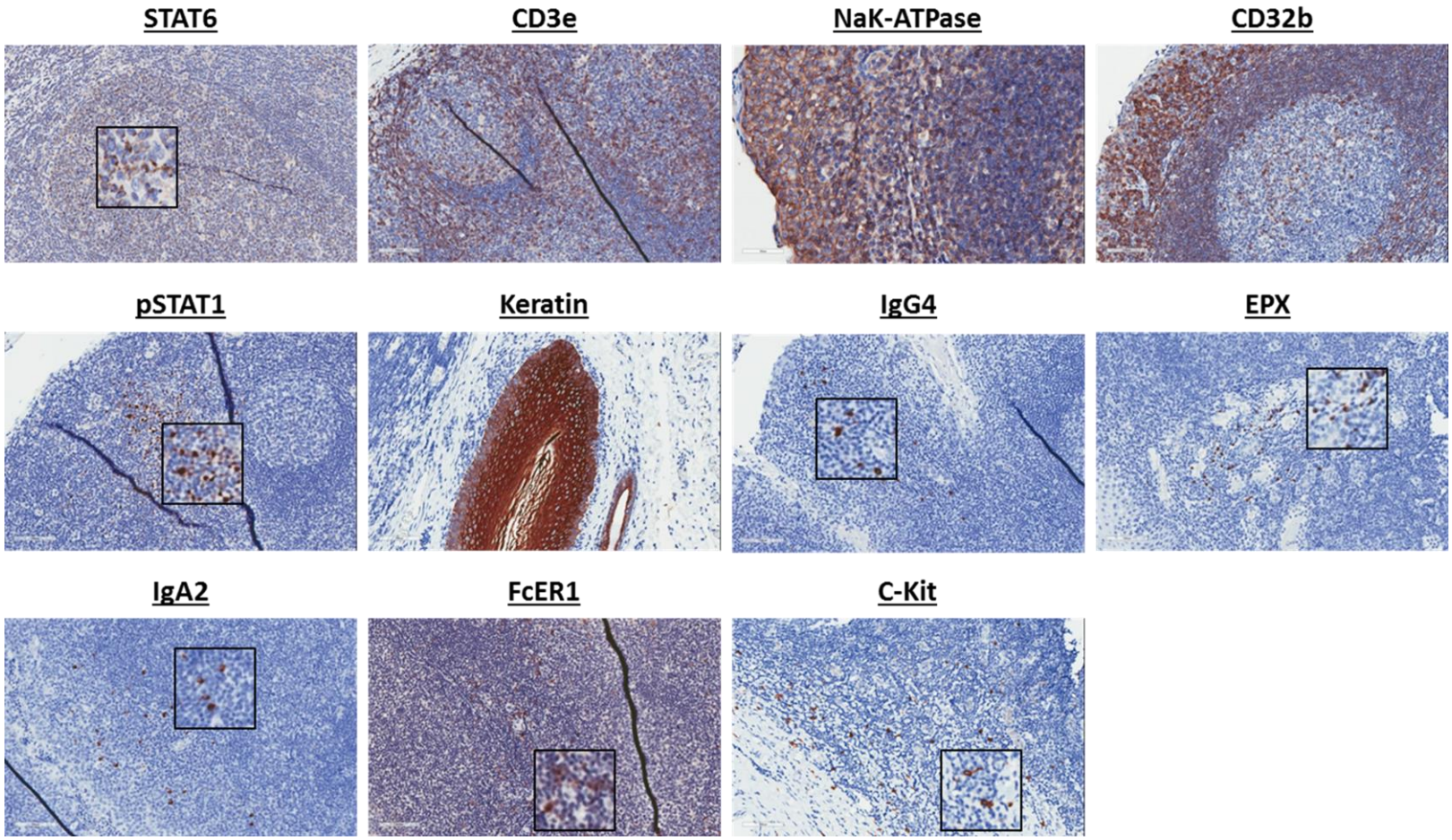

Figure 4.5.11. 11 Uniplex Chromogen IHC on Human Tonsil FFPE. Antigens are stained with DAB (brown) and nuclei are counterstained with hematoxylin (blue).

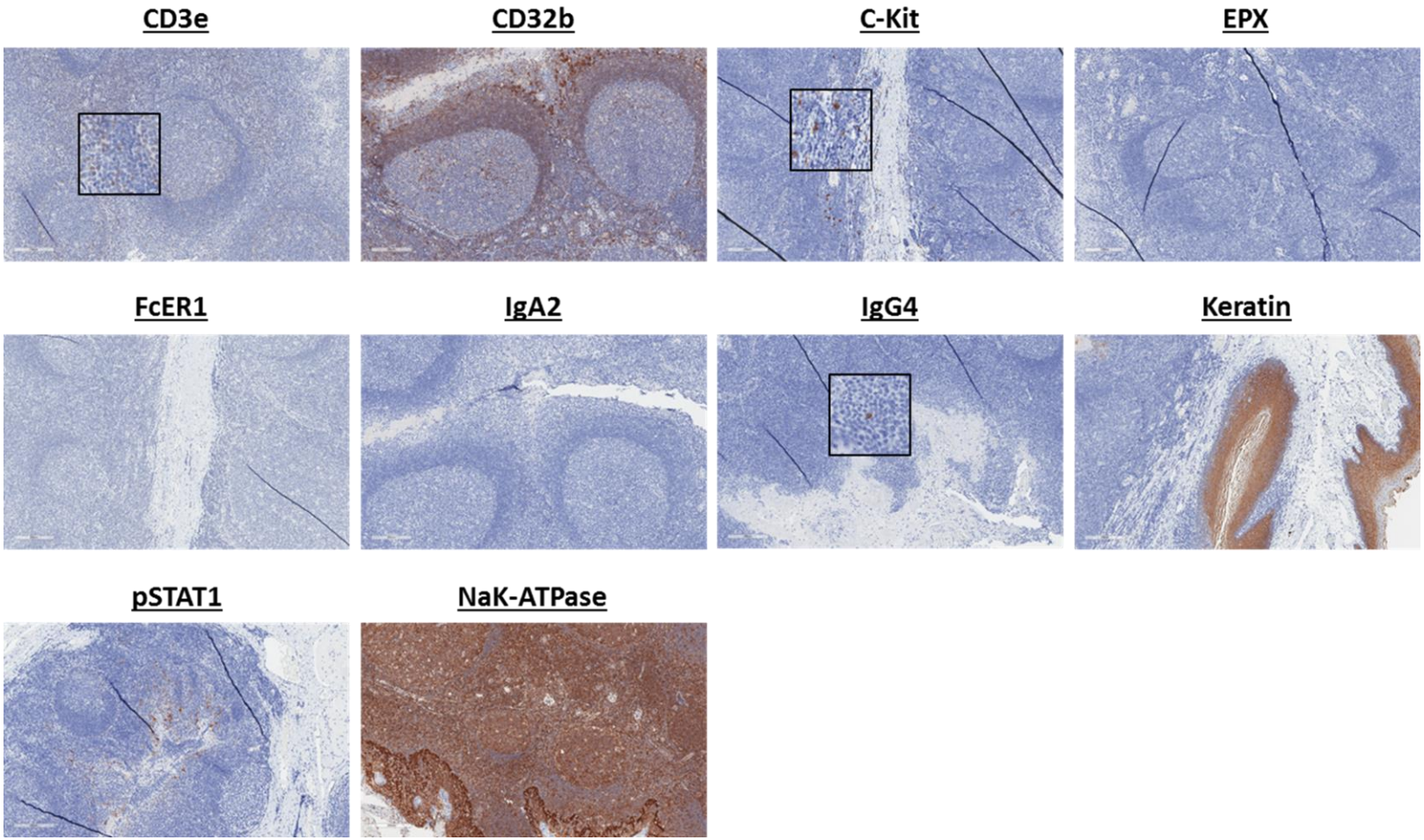

Figure 4.5.12. Stripping Efficiency on Human Tonsil FFPE. 10 slides stained with primary antibodies, stripped in citrate pH6 (15 minutes), and developed with secondary and DAB (brown).

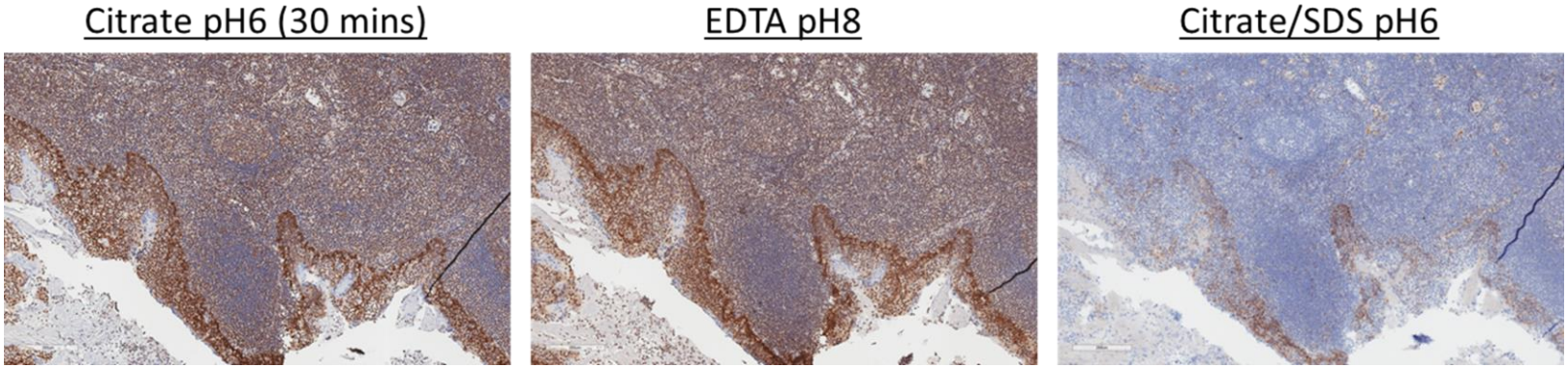

Figure 4.5.13. Stripping Efficiency of NaK-ATPase Under Different Conditions. 3 slides were stained with anti-NaK-ATPase, stripped in either citrate pH6 (30 minutes), EDTA pH8 (15 minutes), or citrate w/0.3% SDS pH6 (15 minutes).

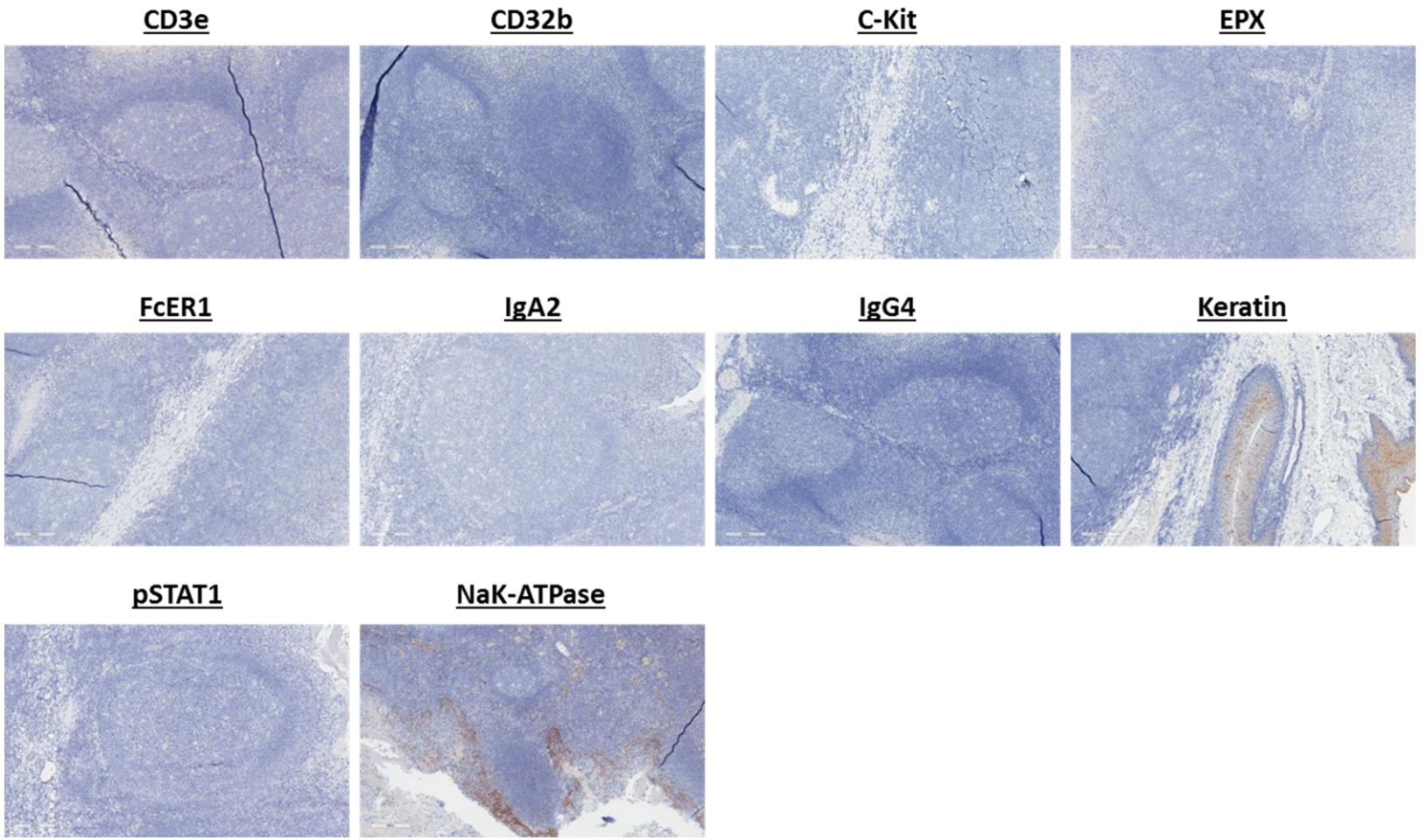

Figure 4.5.14. Stripping Efficiency of Citrate w/0.3% SDS on Human Tonsil FFPE. 10 slides stained with primary antibodies, stripped in citrate pH6 w/0.3% SDS (15 minutes), and developed with secondary and DAB (brown).

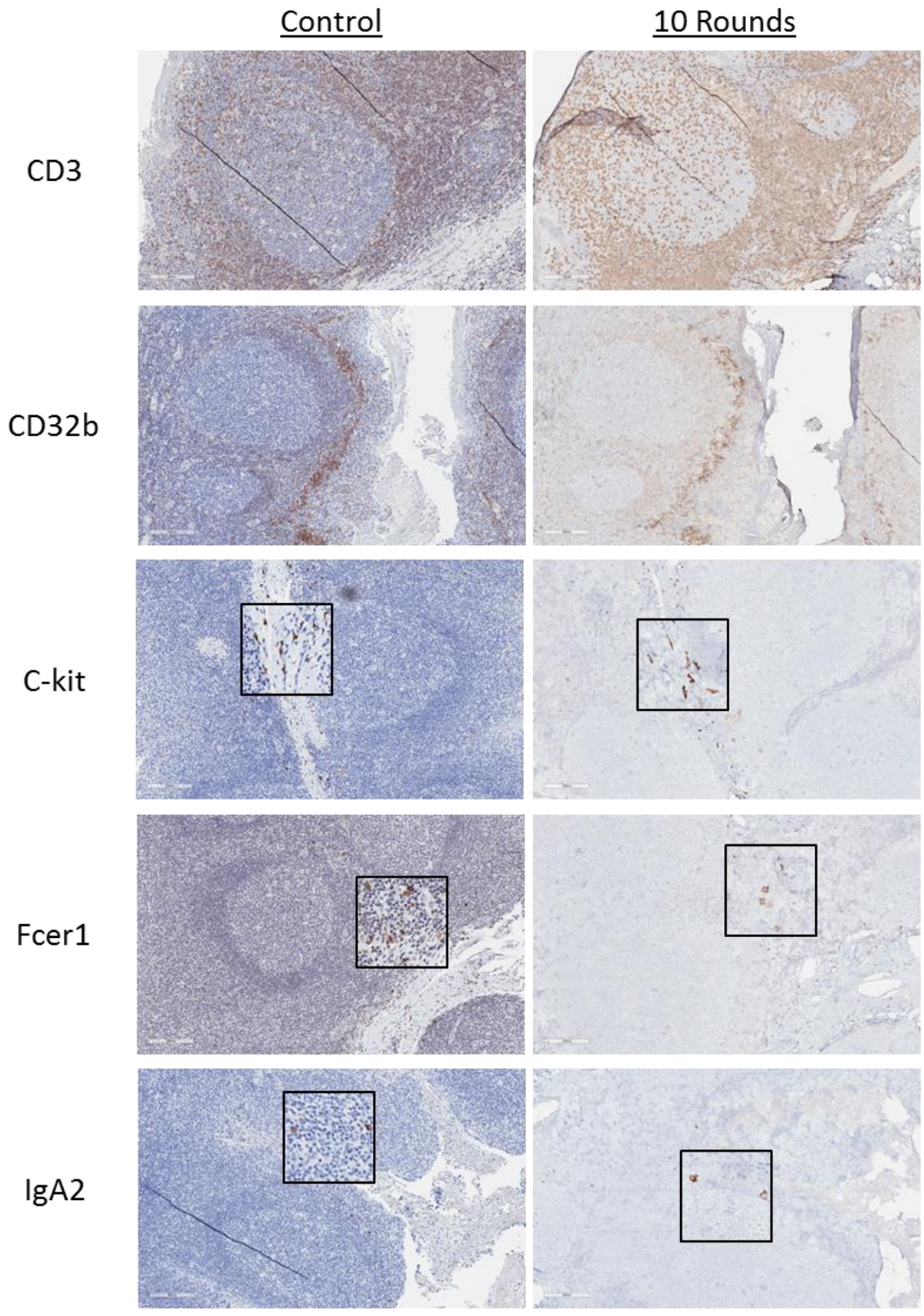
Control
10 Rounds
CD3
CD32b
C-kit
Fcer1
IgA2

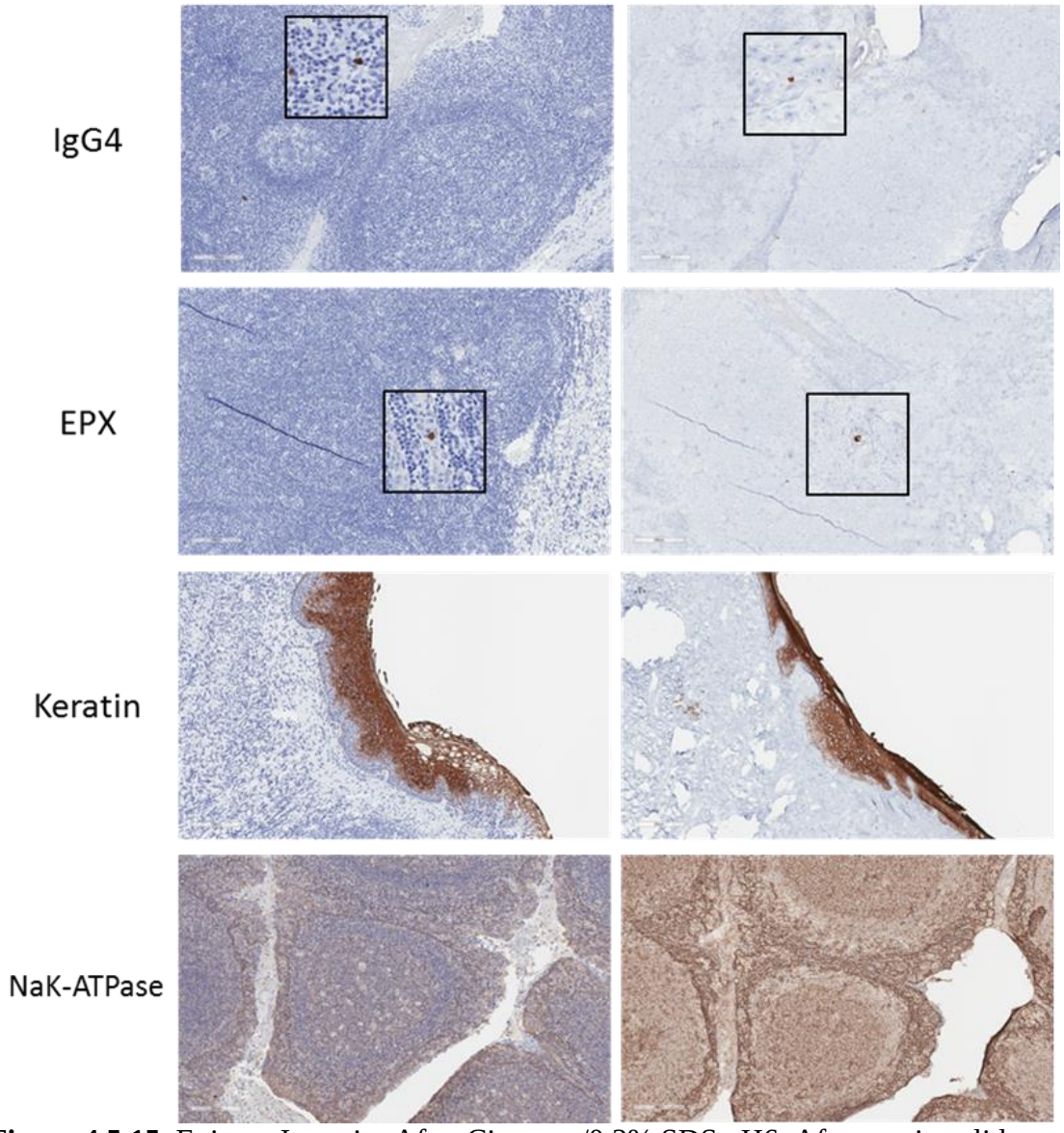

Figure 4.5.15. Epitope Integrity After Citrate w/0.3% SDS pH6. After putting slides through 10 rounds of stripping with citrate w/0.3% SDS pH6, they were stained and compared to a non-stripped control slide.

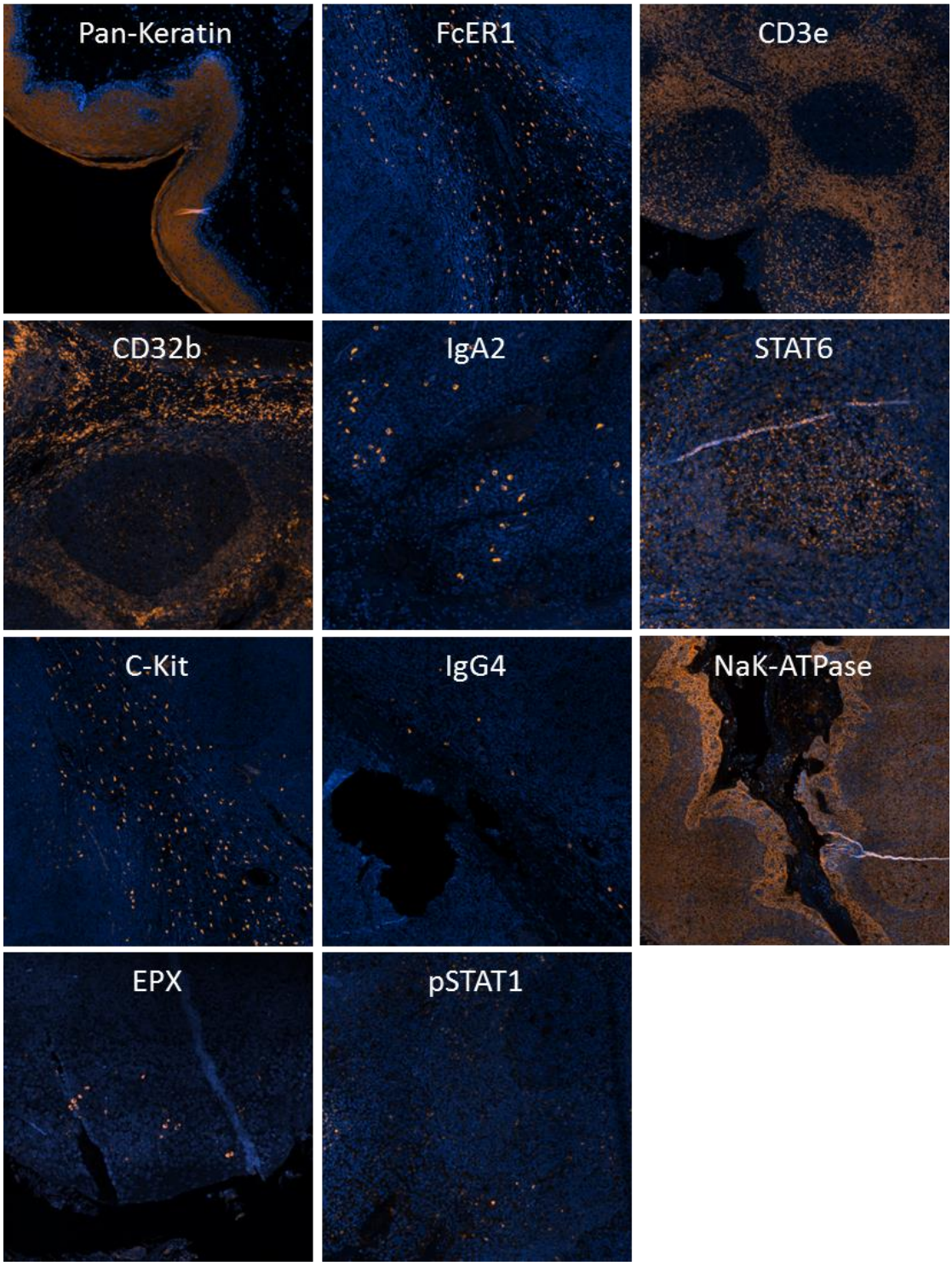

Figure 4.5.16. Uniplex Fluorescence IHC on Human Tonsil FFPE Tissue Sections.

Primary Probes	
Gene	**Probe Sequence**
IL13	TCA TCC GAT ATG GTG ATC CAT TTT TTC ATC CGA TAT GGT GAT CCA TTT TTA GCT GTA GAA CTG TGG GCT G
	TCA TCC GAT ATG GTG ATC CAT TTT TTC ATC CGA TAT GGT GAT CCA TTT TTC AGA GCC AGT GAG AGA ACC A
	TCA TCC GAT ATG GTG ATC CAT TTT TTC ATC CGA TAT GGT GAT CCA TTT TTA CCA CCA AGG CAA GCA AGA G
	TCA TCC GAT ATG GTG ATC CAT TTT TTC ATC CGA TAT GGT GAT CCA TTT TTA GAG ACA CAG ATC TTG GCA C
	TCA TCC GAT ATG GTG ATC CAT TTT TTC ATC CGA TAT GGT GAT CCA TTT TTA TAA GCT CCT TAA GGG TCA G
	TCA TCC GAT ATG GTG ATC CAT TTT TTC ATC CGA TAT GGT GAT CCA TTT TTT CTG GTC TTG TGT GAT GTT G
	TCA TCC GAT ATG GTG ATC CAT TTT TTC ATC CGA TAT GGT GAT CCA TTT TTA ATC CAG GGC TAC ACA GAA C
	TCA TCC GAT ATG GTG ATC CAT TTT TTC ATC CGA TAT GGT GAT CCA TTT TTG CAA TTG GAG ATG TTG GTC A
	TCA TCC GAT ATG GTG ATC CAT TTT TTC ATC CGA TAT GGT GAT CCA TTT TTT ACA GAG GCC ATG CAA TAT C
	TCA TCC GAT ATG GTG ATC CAT TTT TTC ATC CGA TAT GGT GAT CCA TTT TTA CTT CGA TTT TGG TAT CGG G
	TCA TCC GAT ATG GTG ATC CAT TTT TTC ATC CGA TAT GGT GAT CCA TTT TTA GCT GAG CAG TTT TGT TAT A
	TCA TCC GAT ATG GTG ATC CAT TTT TTC ATC CGA TAT GGT GAT CCA TTT TTG TGG CGA AAC AGT TGC TTT G
	TCA TCC GAT ATG GTG ATC CAT TTT TTC ATC CGA TAT GGT GAT CCA TTT TTA TGG TCT CTC CTC ATT AGA A
	TCA TCC GAT ATG GTG ATC CAT TTT TTC ATC CGA TAT GGT GAT CCA TTT TTA ATG AGT CCA CAG CTG AGA T
	TCA TCC GAT ATG GTG ATC CAT TTT TTC ATC CGA TAT GGT GAT CCA TTT TTC CAG CAA AGT CTG ATG TGA G
	TCA TCC GAT ATG GTG ATC CAT TTT TTC ATC CGA TAT GGT GAT CCA TTT TTT GAG GCC AAA GCT GAG GCA T
	TCA TCC GAT ATG GTG ATC CAT TTT TTC ATC CGA TAT GGT GAT CCA TTT TTT GCA GTT TTC TGT AGG GAT G
	TCA TCC GAT ATG GTG ATC CAT TTT TTC ATC CGA TAT GGT GAT CCA TTT TTG AAA TGT GCT CAA GCT GCT G
	TCA TCC GAT ATG GTG ATC CAT TTT TTC ATC CGA TAT GGT GAT CCA TTT TTC GGG ATA CTG ACA GAC TCA T
	TCA TCC GAT ATG GTG ATC CAT TTT TTC ATC CGA TAT GGT GAT CCA TTT TTC ATA GGC AGC AAA CCA TGT C
	TCA TCC GAT ATG GTG ATC CAT TTT TTC ATC CGA TAT GGT GAT CCA TTT TTC ACT GCT TCA ATG CTG GAG C
	TCA TCC GAT ATG GTG ATC CAT TTT TTC ATC CGA TAT GGT GAT CCA TTT TTA CAG TAA TAT TGC CAG GGA C
	TCA TCC GAT ATG GTG ATC CAT TTT TTC ATC CGA TAT GGT GAT CCA TTT TTA CAG TGA GGT AGC AGA GTT A
	TCA TCC GAT ATG GTG ATC CAT TTT TTC ATC CGA TAT GGT GAT CCA TTT TTC AGA CAG GAG TGT TGC TCT G
	TCA TCC GAT ATG GTG ATC CAT TTT TTC ATC CGA TAT GGT GAT CCA TTT TTA GTT ATT TCA TGG CTG AGG G
	TCA TCC GAT ATG GTG ATC CAT TTT TTC ATC CGA TAT GGT GAT CCA TTT TTA CTC TTT GCT AAG CTA TTT A
	TCA TCC GAT ATG GTG ATC CAT TTT TTC ATC CGA TAT GGT GAT CCA TTT TTG GCC ATT CTT CCA TAT ATT A
	TCA TCC GAT ATG GTG ATC CAT TTT TTC ATC CGA TAT GGT GAT CCA TTT TTC ATT CAC TAC ACA TCA CCT T
	TCA TCC GAT ATG GTG ATC CAT TTT TTC ATC CGA TAT GGT GAT CCA TTT TTT TGT TCA GTG ACA AAC CCA C
	TCA TCC GAT ATG GTG ATC CAT TTT TTC ATC CGA TAT GGT GAT CCA TTT TTC GGT TTC TAG TTT GAC AGT C
	TCA TCC GAT ATG GTG ATC CAT TTT TTC ATC CGA TAT GGT GAT CCA TTT TTT TTT TAT CTG TCA CCA TCT T
CCL24	GTCTTTACAGATGTCTGCGGTTTTTGTCTTTACAGATGTCTGCGGTTTTTGATCCTGGAGATATGAGGAC
	GTCTTTACAGATGTCTGCGGTTTTTGTCTTTACAGATGTCTGCGGTTTTTTCAAAGCTGGGGTGCAGAAA
	GTCTTTACAGATGTCTGCGGTTTTTGTCTTTACAGATGTCTGCGGTTTTTATGTTCTGGAGGTCAGGCAC
	GTCTTTACAGATGTCTGCGGTTTTTGTCTTTACAGATGTCTGCGGTTTTTCGGCAACGATCGTAGCAGAG
	GTCTTTACAGATGTCTGCGGTTTTTGTCTTTACAGATGTCTGCGGTTTTTATGGGGAAGATGCAACACGC
	GTCTTTACAGATGTCTGCGGTTTTTGTCTTTACAGATGTCTGCGGTTTTTTGAGGGGATGGTCACAGAAT
	GTCTTTACAGATGTCTGCGGTTTTTGTCTTTACAGATGTCTGCGGTTTTTTGGAAATAAAGGACGTGCAGC
	GTCTTTACAGATGTCTGCGGTTTTTGTCTTTACAGATGTCTGCGGTTTTTCTCGGTTTTCTGGAATTTTC
	GTCTTTACAGATGTCTGCGGTTTTTGTCTTTACAGATGTCTGCGGTTTTTTTGGCCAACTGGTAGCTAAC
	GTCTTTACAGATGTCTGCGGTTTTTGTCTTTACAGATGTCTGCGGTTTTTCTTGGTGATGAAGATGACCC
	GTCTTTACAGATGTCTGCGGTTTTTGTCTTTACAGATGTCTGCGGTTTTTGTCAGTACAGATCTTATGGC
	GTCTTTACAGATGTCTGCGGTTTTTGTCTTTACAGATGTCTGCGGTTTTTGCATCCAGTTTTTGTATGTG
	GTCTTTACAGATGTCTGCGGTTTTTGTCTTTACAGATGTCTGCGGTTTTTCCTTTAGAAGGCTGGTTTTT
	GTCTTTACAGATGTCTGCGGTTTTTGTCTTTACAGATGTCTGCGGTTTTTCAGCAAACTTGGTTCTCACT
	GTCTTTACAGATGTCTGCGGTTTTTGTCTTTACAGATGTCTGCGGTTTTTCTAAACCTCGGTGCTATTGC
	GTCTTTACAGATGTCTGCGGTTTTTGTCTTTACAGATGTCTGCGGTTTTTTAGTTCAGGGACAGAGGAGAG
	GTCTTTACAGATGTCTGCGGTTTTTGTCTTTACAGATGTCTGCGGTTTTTCTGGTAAAGCGTCAATACCT
	GTCTTTACAGATGTCTGCGGTTTTTGTCTTTACAGATGTCTGCGGTTTTTTGGTCTGTCAAACCCCAAAG
	GTCTTTACAGATGTCTGCGGTTTTTGTCTTTACAGATGTCTGCGGTTTTTATGAACTTAGACCTCATCCC
	GTCTTTACAGATGTCTGCGGTTTTTGTCTTTACAGATGTCTGCGGTTTTTTCACTCAGGTTCTCACAGAA
	GTCTTTACAGATGTCTGCGGTTTTTGTCTTTACAGATGTCTGCGGTTTTTTTTTCACTCAGCACAGGAGA
	GTCTTTACAGATGTCTGCGGTTTTTGTCTTTACAGATGTCTGCGGTTTTTGCCACACAAGAGATAACACA
	GTCTTTACAGATGTCTGCGGTTTTTGTCTTTACAGATGTCTGCGGTTTTTTGGGCTCTGATGAAGCCTTT
	GTCTTTACAGATGTCTGCGGTTTTTGTCTTTACAGATGTCTGCGGTTTTTGAAGCCAGCTGCAAGCAAGG
	GTCTTTACAGATGTCTGCGGTTTTTGTCTTTACAGATGTCTGCGGTTTTTACCCTAAGACAAGAACCCTA
	GTCTTTACAGATGTCTGCGGTTTTTGTCTTTACAGATGTCTGCGGTTTTTTGCTGTTGACAGATCTTCAC
	GTCTTTACAGATGTCTGCGGTTTTTGTCTTTACAGATGTCTGCGGTTTTTTCATCAGCATGTTTGGGAGTT
	GTCTTTACAGATGTCTGCGGTTTTTGTCTTTACAGATGTCTGCGGTTTTTTGTTCCAAGTTCTGGGGATG
	GTCTTTACAGATGTCTGCGGTTTTTGTCTTTACAGATGTCTGCGGTTTTTTAATGCTGCTGTTGAAATCCT
	GTCTTTACAGATGTCTGCGGTTTTTGTCTTTACAGATGTCTGCGGTTTTTTCATCCTGGCAGCAAGAGGAG

Steap4	CCAGGCAATATGGTGGTACATTTTTCCAGGCAATATGGTGGTACATTTTTGAAACTCATCTGCATGTGCT
	CCAGGCAATATGGTGGTACATTTTTCCAGGCAATATGGTGGTACATTTTTGAAAATGCAGACAACCCCTT
	CCAGGCAATATGGTGGTACATTTTTCCAGGCAATATGGTGGTACATTTTTGGTTTCGACTCCCAAAAACG
	CCAGGCAATATGGTGGTACATTTTTCCAGGCAATATGGTGGTACATTTTTTGTGCATGGCTAGGATTATG
	CCAGGCAATATGGTGGTACATTTTTCCAGGCAATATGGTGGTACATTTTTGTGAGGGAATCATAGTGCTC
	CCAGGCAATATGGTGGTACATTTTTCCAGGCAATATGGTGGTACATTTTTTTTTGCGGTTGTTACTGACG
	CCAGGCAATATGGTGGTACATTTTTCCAGGCAATATGGTGGTACATTTTTAAGGTATTCCGCATTTGACT
	CCAGGCAATATGGTGGTACATTTTTCCAGGCAATATGGTGGTACATTTTTGAGCAATGTCCATTACTCTT
	CCAGGCAATATGGTGGTACATTTTTCCAGGCAATATGGTGGTACATTTTTTTTTCAATTTCACTGGCTGC
	CCAGGCAATATGGTGGTACATTTTTCCAGGCAATATGGTGGTACATTTTTAGGAAACCTCCACATTGGAA
	CCAGGCAATATGGTGGTACATTTTTCCAGGCAATATGGTGGTACATTTTTAGAAGACGCACAGCACAGAG
	CCAGGCAATATGGTGGTACATTTTTCCAGGCAATATGGTGGTACATTTTTCTCGTATTGCACAGTACACA
	CCAGGCAATATGGTGGTACATTTTTCCAGGCAATATGGTGGTACATTTTTTTCACGTAGGGGTATATCAC
	CCAGGCAATATGGTGGTACATTTTTCCAGGCAATATGGTGGTACATTTTTCGATTCGGGATGGAAATGGC
	CCAGGCAATATGGTGGTACATTTTTCCAGGCAATATGGTGGTACATTTTTGGATCAGTGCTGTTATAGGA
	CCAGGCAATATGGTGGTACATTTTTCCAGGCAATATGGTGGTACATTTTTGAGAATACCAGGGAGGTACA
	CCAGGCAATATGGTGGTACATTTTTCCAGGCAATATGGTGGTACATTTTTTACTTTGTGCCTCGATAGAG
	CCAGGCAATATGGTGGTACATTTTTCCAGGCAATATGGTGGTACATTTTTGAAGGAAGGCAAATCCCAGA
	CCAGGCAATATGGTGGTACATTTTTCCAGGCAATATGGTGGTACATTTTTCCTGAGTAATGGTTGCATTT
	CCAGGCAATATGGTGGTACATTTTTCCAGGCAATATGGTGGTACATTTTTTGACCATGTTGCTTACTGAT
	CCAGGCAATATGGTGGTACATTTTTCCAGGCAATATGGTGGTACATTTTTAACAAACCGGAACTCTCTCC
	CCAGGCAATATGGTGGTACATTTTTCCAGGCAATATGGTGGTACATTTTTTCAGATAACCCAGTTTGGAC
	CCAGGCAATATGGTGGTACATTTTTCCAGGCAATATGGTGGTACATTTTTACCTTAGAATCGAAGGGCTG
	CCAGGCAATATGGTGGTACATTTTTCCAGGCAATATGGTGGTACATTTTTGGGATGACGAGTGCCAAAAT
	CCAGGCAATATGGTGGTACATTTTTCCAGGCAATATGGTGGTACATTTTTTGTCTATGCATGGCATGATG
	CCAGGCAATATGGTGGTACATTTTTCCAGGCAATATGGTGGTACATTTTTTTCAGTGCTGATTGTGTGTA
	CCAGGCAATATGGTGGTACATTTTTCCAGGCAATATGGTGGTACATTTTTCCACAATGAGTCATCACGTG
	CCAGGCAATATGGTGGTACATTTTTCCAGGCAATATGGTGGTACATTTTTATCAAGAAGCTTCGCTGTGT
	CCAGGCAATATGGTGGTACATTTTTCCAGGCAATATGGTGGTACATTTTTCATTGCGTCATTCAACTTGC
	CCAGGCAATATGGTGGTACATTTTTCCAGGCAATATGGTGGTACATTTTTACACTCTTCCAGAACTCTAC
	CCAGGCAATATGGTGGTACATTTTTCCAGGCAATATGGTGGTACATTTTTGCTGCTTTTTCACTTACATC
	CCAGGCAATATGGTGGTACATTTTTCCAGGCAATATGGTGGTACATTTTTAGCAAAACCTGTAGTATGCC
	CCAGGCAATATGGTGGTACATTTTTCCAGGCAATATGGTGGTACATTTTTCCACTTCTTCCAGGAAACAA
	CCAGGCAATATGGTGGTACATTTTTCCAGGCAATATGGTGGTACATTTTTAGGGGGTACATATGACTACA
	CCAGGCAATATGGTGGTACATTTTTCCAGGCAATATGGTGGTACATTTTTCCCCATAGTAAGAATCCATA
	CCAGGCAATATGGTGGTACATTTTTCCAGGCAATATGGTGGTACATTTTTAGCTTTCCATATATCCAAGG
	CCAGGCAATATGGTGGTACATTTTTCCAGGCAATATGGTGGTACATTTTTGTCCTTTGTGGAGGAAGAAT
	CCAGGCAATATGGTGGTACATTTTTCCAGGCAATATGGTGGTACATTTTTAACTTAGGATCGCTGCTCAA
	CCAGGCAATATGGTGGTACATTTTTCCAGGCAATATGGTGGTACATTTTTGCGGCACTTGAAAAACCCAA
	CCAGGCAATATGGTGGTACATTTTTCCAGGCAATATGGTGGTACATTTTTTTGCGTAGCTTACTAGCTAA
	CCAGGCAATATGGTGGTACATTTTTCCAGGCAATATGGTGGTACATTTTTACTGCACCACTTACATTGAT
	CCAGGCAATATGGTGGTACATTTTTCCAGGCAATATGGTGGTACATTTTTCGACGAGTTCAGATGATTCC
	CCAGGCAATATGGTGGTACATTTTTCCAGGCAATATGGTGGTACATTTTTCTGAAGGTCACCTTGGGAAA
	CCAGGCAATATGGTGGTACATTTTTCCAGGCAATATGGTGGTACATTTTTGCTAGAGCTAAGGATTCTCA
	CCAGGCAATATGGTGGTACATTTTTCCAGGCAATATGGTGGTACATTTTTAAAGATCTCCTTTTAGCTCC
	CCAGGCAATATGGTGGTACATTTTTCCAGGCAATATGGTGGTACATTTTTAGTGACACGCGGGAAGATTG
CXCL10	ATCTCCAGTGGCATCCTTCTTTTTTATCTCCAGTGGCATCCTTCTTTTTTGATGAAGCGCTTCTCGAGTG
	ATCTCCAGTGGCATCCTTCTTTTTTATCTCCAGTGGCATCCTTCTTTTTTTTGGGTTCATGGTGCTGATG
	ATCTCCAGTGGCATCCTTCTTTTTTATCTCCAGTGGCATCCTTCTTTTTTTAGGCAGAAAATGACGGCAGC
	ATCTCCAGTGGCATCCTTCTTTTTTATCTCCAGTGGCATCCTTCTTTTTTCGATATGGATGCAGTTGCAG
	ATCTCCAGTGGCATCCTTCTTTTTTATCTCCAGTGGCATCCTTCTTTTTTTCAACACGTGGGCAGGATAG
	ATCTCCAGTGGCATCCTTCTTTTTTATCTCCAGTGGCATCCTTCTTTTTTCTTTTTCATCGTGGCAATGA
	ATCTCCAGTGGCATCCTTCTTTTTTATCTCCAGTGGCATCCTTCTTTTTTATTCAGACATCTCTGCTCAT
	ATCTCCAGTGGCATCCTTCTTTTTTATCTCCAGTGGCATCCTTCTTTTTTCTTGATGGTCTTAGATTCC
	ATCTCCAGTGGCATCCTTCTTTTTTATCTCCAGTGGCATCCTTCTTTTTTGCTTCACTCCAGTTAAGGAG
	ATCTCCAGTGGCATCCTTCTTTTTTATCTCCAGTGGCATCCTTCTTTTTTGGTAAAGGGGAGTGATGGAG
	ATCTCCAGTGGCATCCTTCTTTTTTATCTCCAGTGGCATCCTTCTTTTTTAATTAGGACTAGCCATCCAC
	ATCTCCAGTGGCATCCTTCTTTTTTATCTCCAGTGGCATCCTTCTTTTTTCACCTTTCAGAAGACCAAGG
	ATCTCCAGTGGCATCCTTCTTTTTTATCTCCAGTGGCATCCTTCTTTTTTAGGAGTAGCAGCTGATGTGA
	ATCTCCAGTGGCATCCTTCTTTTTTATCTCCAGTGGCATCCTTCTTTTTTATGGCTTGACCATCATCCTG
	ATCTCCAGTGGCATCCTTCTTTTTTATCTCCAGTGGCATCCTTCTTTTTTCAGTTACTTTTGTCTCAGGA
	ATCTCCAGTGGCATCCTTCTTTTTTATCTCCAGTGGCATCCTTCTTTTTTGCCCTTAAAGAATTCTTGCT
	ATCTCCAGTGGCATCCTTCTTTTTTATCTCCAGTGGCATCCTTCTTTTTTACTTGAGCGAGGACTCAGAC
	ATCTCCAGTGGCATCCTTCTTTTTTATCTCCAGTGGCATCCTTCTTTTTTCTCCACATAGCTTACAGTAC
	ATCTCCAGTGGCATCCTTCTTTTTTATCTCCAGTGGCATCCTTCTTTTTTCATGGCACATGGTGAAGGGC
	ATCTCCAGTGGCATCCTTCTTTTTTATCTCCAGTGGCATCCTTCTTTTTTTAGGGAGGACAAGGAGGGTG
	ATCTCCAGTGGCATCCTTCTTTTTTATCTCCAGTGGCATCCTTCTTTTTTACTTAGAACTGACGAGCCTG
	ATCTCCAGTGGCATCCTTCTTTTTTATCTCCAGTGGCATCCTTCTTTTTTTGGTTAAGTTCGTCCTTACA
	ATCTCCAGTGGCATCCTTCTTTTTTATCTCCAGTGGCATCCTTCTTTTTTTAGTATCTTGATAACCCCTTG
	ATCTCCAGTGGCATCCTTCTTTTTTATCTCCAGTGGCATCCTTCTTTTTTTCATACATTTTCAGGTTCCTC
	ATCTCCAGTGGCATCCTTCTTTTTTATCTCCAGTGGCATCCTTCTTTTTTTCTACTTTGTACAGTCGTTCA
	ATCTCCAGTGGCATCCTTCTTTTTTATCTCCAGTGGCATCCTTCTTTTTTACAAAAGGTATTGGACGGTT

Secondary Probes	
Gene	**Probe Sequence**
IL13 Secondary	TGG ATC ACC ATA TCG GAT GA TTTTT GCC AAT CAT TAT GAC TGG TG TTTTT GCC AAT CAT TAT GAC TGG TG
CCL24 secondary	CCG CAG ACA TCT GTA AAG AC TTTTT CCG ATG TTG ACG GAC TAA TC TTTTT CCG ATG TTG ACG GAC TAA TC
CXCL10 secondary	AGA AGG ATG CCA CTG GAG AT TTTTT GGT AAC TGC GCA TAG TTG GC TTTTT GGT AAC TGC GCA TAG TTG GC
STEAP4 secondary	TGT ACC ACC ATA TTG CCT GG TTTTT CGT GAA GCT TGA GTG GAA TC TTTTT CGT GAA GCT TGA GTG GAA TC

Table 4.5.2. smRNA-FISH Probe Sequences for Mouse Eosinophil Genes.

4.6 Methods

4.6.1 Mice

All studies were performed with 8- to 28-week-old male and female mice on C57BL/6 background. IL-5 transgenic NJ.1638 mice were generated from established institutional colonies. Mice were housed under specific pathogen-free conditions and treated according to institutional guidelines and protocols.

4.6.2 Eosinophil isolation from mouse

Eosinophils were isolated from the blood of IL-5 transgenic NJ.1638 mice as previously described [18]. Buffy coat was separated from erythrocytes by Histopaque 1119 (Sigma-Aldrich, 11191-100ML) density centrifugation. Remaining erythrocytes were lysed with distilled water and contaminating cells were removed by magnetic beads against CD45R and CD90.1 (Miltenyi,). Purity of eosinophils were >97% by Hema 3-stained cytospins and light microscopy (Fisher).

4.6.3 Eosinophil isolation from human

Blood was taken by venous puncture from healthy donors. Eosinophils were isolated from whole blood using MACSxpress Whole Blood Eosinophil Isolation Kit (Miltenyi Biotec) following manufacture protocol. Purity of eosinophils were >98% by Hema 3-

stained (Fisher) cytospins and light microscopy. The study was approved by the Institutional Review Board at Mayo Clinic in Arizona.

4.6.4 Eosinophil cell culture and activation

Eosinophils were cultured at 5 x 10^6 cells/mL in RPMI 1640, GlutaMAX, HEPES (GIBCO) supplemented with 10% FBS (HyClone Technologies), 55µM 2-Mercaptoethanol (Thermofisher Scientific), Penicillin-Steptomycin-Glutamine (Thermofisher Scientific) and IL-5 [10 ng/mL] (Peprotech) for 16-18hrs at 37°C with 5% CO2. For activation, Th2 activated eosinophils ("E2") were supplemented with IL-33 (30ng/µL; R&D Systems), GM-CSF (10ng/µL; Peprotech) and IL-4 (10ng/µL; Peprotech). Th1 activated eosinophils ("E1") were supplemented with IFNγ (15ng/µL; Peprotech) and TNFα (15ng/µL; Peprotech). Resting eosinophils ("E0") were cultured without any additional cytokines. The viability was assessed by Trypan blue exclusion and was >85%.

4.6.5 RNA-FISH

smRNA-FISH Cytospin. Direct RNA-FISH was performed on cells as previously reported [221]. Briefly, cells were collected, washed with PBS and put on slides using a Cytospin (Thermofisher). Once adhered to slides, cells were fixed with 4% formaldehyde at 37°C for 15 minutes unless otherwise noted. Cells were washed with wash buffer (10% formamide in 2× SSC, 2 mM vanadyl ribonucleoside complex) for 5 mins before adding probes (4µL probe stock, 100 mg/mL dextran sulfate, 1 mg/mL Escherichia Coli tRNA, 2 mM vanadyl ribonucleoside complex, 20 µg/mL bovine serum albumin and 10% formamide in 2× saline-sodium citrate (SSC)) and incubating overnight at 37°C. After

staining, cells were washed 2 x 30 min at 37°C then coverslipped with Prolong Diamond (Thermofisher) before imaging. Gene specific probes are designed using BioSearch Technologies Stellaris Probe designer Version 4.2.

smRNA-FISH FFPE. Indirect RNA-FISH was performed on cells as previously reported [221]. Cells were prepared as mentioned above. Briefly, Cells were washed in 2x SSC for 5 min before unlabeled probes (50µM) in hybridization buffer were added. Slides were incubated at 37C for 4 hours then washed 3 x 30 min with wash buffer at 37C. Secondary probes (1µm) were added to cells and incubated at 37C for 30 min. Slides were washed with 2x SSC and mounted in ProLong Diamond (Thermofisher) before imaging. Gene specific probes are designed using BioSearch Technologies Stellaris Probe designer Version 4.2 (Table 4.5.2).

HCR on Cytospin. Cells were prepared on slides as stated above, but fixed at 23°C for 15 minutes. Cells were washed 3 x 5 min with PBS prior to permeabilization with 70% ethanol overnight at 4C. Samples were pre-hybridized in probe hybridization buffer (50% formamide, 5x sodium chloride sodium citrate (SSC), 9nM citric acid pH6.0, 0.1% Tween 20, 50µg/mL heparin, 1x Denhardt's solution, 10% dextran sulfate) for 30 min at 45°C. Probes (Molecular Instruments) (Table 4.5.3) were prepared (2nM) in probe hybridization buffer and prewarmed to 45°C. Probes were added to cells and incubated overnight at 45°C. Excess probes were washed at 45°C in decreasing amounts of probe wash buffer (50% formamide, 5x SSC, 9nM citric acid pH6.0, 0.1% Tween 20, 50µg/mL heparin) and 5x SSCT (2x SSC, 0.1% Tween 20): 75% probe wash buffer / 25% 5 x SSCT for 10 min, 50% probe wash buffer / 50% 5 x SSCT for 10 min, 25% probe wash buffer / 75% 5 x SSCT for 10 min, 100% 5 x SSCT for 10 min. Samples were then

incubated in amplification buffer (5x SSC, 9nM citric acid pH6.0, 0.1% Tween 20, 50µg/mL heparin, 1x Denhardt's solution, 10% dextran sulfate) for 30 minutes at room temperature. Hairpins were prepared by first snap cooling (heat at 95°C for 90 secs and cooling to room temperature for 30 mins) then mixing two hairpins together in amplification buffer at a final concentration of 60nM. Pre-amplification buffer was removed from slides and hairpin mixture was added. Slides were incubated overnight at room temperature. Finally slides were washed with 5x SSCT to removed excess hairpins (2 x 5 min, 2 x 10 min, 1 x 5 min) and mounted with ProLong Diamond antifade (Thermofisher).

RNAscope. Fluorescence in situ hybridization was performed using RNAscope® Multiple Fluorescent Reagent Kit v2 (Advanced Cell Diagnostics) according to manufacturer's protocol. Signal was developed with FITC, Cy3, or Cy5 TSA kits (Perkin Elmer). Slides were mounted with ProLong Diamond antifade (Thermofisher).

RNAscope/IF. After completing the RNA-FISH protocol slides were washed 3 x 5 mins in Dako wash buffer (Agilent) and blocked with 5% normal goat serum diluted in wash buffer. Anti-EPX antibody (clone M25.82.2.1, Mayo Clinic) was added to slides and incubated overnight at 4C. Slides were then washed 3 x 5 mins and incubated for 1 hr at room temperature with anti-mouse HRP-conjugated secondary. After washing 3 x 5 mins, FITC tyramide (Perkin Elmer) was allowed to develop for 10 mins at room temperature. After a final wash 3 x 5 min, nuclei were counterstained with DAPI and slides mounted with ProLong Diamond antifade (Thermofisher).

4.6.6 FFPE Tissue

5-µm thick human tonsil FFPE tissues were obtained from the Pathology Research Core (PRC) at Mayo Clinic Arizona (Scottsdale, AZ). The samples are anonymous and all patient-related data and unique identifiers were removed.

4.6.7 Immunohistochemistry (IHC)

All antibodies used in this study are listed in Table 4.5.1.

Slides were incubated at 55°C for 30 minutes to soften the paraffin wax before deparaffinization in 100% xylene (3 x 5 minutes) and xylene/ethanol 50%/50% (1 x 2 minutes). Slides were rehydrated through decreasing concentrations of ethanol (100%-70%) before being rinsed with distilled water. After deparaffinization, slides were placed in a microwave safe plastic container filled with either EDTA pH8 buffer (Abcam) or citrate pH6 buffer (Abcam) and placed into a microwave. Slides were microwaved treated (MWT) on high power to initiate boiling, then switched to low power to keep a sub-boil (~99C) for 15 minutes. Slides were allowed to cool in buffer for 30 minutes on benchtop. Endogenous peroxidase activity was blocked using 3% H_2O_2 for 10 minutes at room temperature (RT). Protein blocking was performed in DAKO wash buffer (Agilent) with 5% normal goat for 30 min at RT before primary antibody was applied on the slides. Primary antibodies were detected by either goat anti-mouse or anti-rabbit HRP polymer secondary antibodies (Vector labs). Signal was developed using SignalStain™ DAB (Cell Signaling Technologies) according to manufacturer's instructions for 10 min at RT. Slides were counterstained in hematoxylin (Cell Signaling Technology) for 5 minutes following manufacturer's instructions. Slides were dehydrated with increasing concentrations of ethanol and mounted with ClearMount™, mounting media

(ThermoFisher). Images were taken on Aperio Slide Scanner (Leica) with a 40x objective.

4.6.8 Fluorescence IHC

Slides were processed as above up to secondary antibody incubation. After application of secondary HRP polymer antibodies, slides were incubated at RT for 10 minutes with TSA Cyanine 3 Kit (Perkin-Elmer) following manufacturer's instructions. Nuclei were counterstained with DAPI for 7 minutes before being coverslipped with ProLong Diamond™ (ThermoFisher). Images were taken using 63x N/A 1.4 objective (Zeiss) on LSM 800 confocal microscope (Zeiss).

4.6.9 Elution Performance

To evaluate the stripping efficiency of each antibody, FFPE slides were prepped for IHC as mentioned earlier up to primary antibody incubation. Following antibody incubation, slides were placed in citrate pH6, ETDA pH8, or citrate/0.3% SDS pH6 and MWT for 15 mins. After stripping, slides were protein blocked again and signal was developed by HRP polymer secondary antibodies and DAB. Slides were compared to standard IHC controls.

4.6.10 Epitope Integrity

To evaluate the damage from multiple rounds of stripping on epitope integrity, FFPE slides were first deparaffinized and rehydrated as mention earlier then they were submerged in buffer (citrate pH6 or citrate/0.3% SDS pH6) and placed into IHC pressure cooker (Decloaker, BioCare). Slides were incubated at 99^{o}C for 150 minutes (equivalent to 10 rounds) then allowed to cool on benchtop for 30 mins. After cooling slides were

rinsed in distilled water then put through the standard IHC protocol starting with protein blocking. Slides were compared to standard IHC controls.

4.7 References

1. Ray, A., T.B. Oriss, and S.E. Wenzel, *Emerging molecular phenotypes of asthma.* Am J Physiol Lung Cell Mol Physiol, 2015. 308(2): p. L130-40.

2. Protheroe, C., et al., *A novel histologic scoring system to evaluate mucosal biopsies from patients with eosinophilic esophagitis.* Clin Gastroenterol Hepatol, 2009. 7(7): p. 749-755.e11.

3. Walsh, G.M., et al., *Control of eosinophil toxicity in the lung.* Curr Drug Targets Inflamm Allergy, 2005. 4(4): p. 481-6.

4. Khoury, P., et al., *Revisiting the NIH Taskforce on the Research needs of Eosinophil-Associated Diseases (RE-TREAD).* Journal of Leukocyte Biology, 2018. 104(1): p. 69-83.

5. Abdala-Valencia, H., et al., *Shaping eosinophil identity in the tissue contexts of development, homeostasis, and disease.* J Leukoc Biol, 2018. 104(1): p. 95-108.

6. Lee, J.J., et al., *Eosinophils in health and disease: the LIAR hypothesis.* Clin Exp Allergy, 2010. 40(4): p. 563-75.

7. Mesnil, C., et al., *Lung-resident eosinophils represent a distinct regulatory eosinophil subset.* J Clin Invest, 2016. 126(9): p. 3279-95.

8. Reichman, H., et al., *Activated Eosinophils Exert Antitumorigenic Activities in Colorectal Cancer.* Cancer Immunol Res, 2019. 7(3): p. 388-400.

9. Chojnacki, A., et al., *Intravital imaging allows real-time characterization of tissue resident eosinophils.* Commun Biol, 2019. 2: p. 181.

10. Barnig, C., et al., *Circulating Human Eosinophils Share a Similar Transcriptional Profile in Asthma and Other Hypereosinophilic Disorders.* PLoS One, 2015. 10(11): p. e0141740.

11. Esnault, S., et al., *Identification of genes expressed by human airway eosinophils after an in vivo allergen challenge.* PLoS One, 2013. 8(7): p. e67560.

12. Johansson, M.W., *Activation states of blood eosinophils in asthma.* Clin Exp Allergy, 2014. 44(4): p. 482-98.

13. Levsky, J.M. and R.H. Singer, *Fluorescence in situ hybridization: past, present and future.* J Cell Sci, 2003. 116(Pt 14): p. 2833-8.

14. Ramos-Vara, J.A., *Principles and methods of immunohistochemistry.* Methods Mol Biol, 2011. 691: p. 83-96.

15. Raj, A., et al., *Imaging individual mRNA molecules using multiple singly labeled probes.* Nat Methods, 2008. 5(10): p. 877-9.

16. Levenson, R.M., A.D. Borowsky, and M. Angelo, *Immunohistochemistry and mass spectrometry for highly multiplexed cellular molecular imaging.* Laboratory Investigation, 2015. 95(4): p. 397-405.

17. Bodenmiller, B., *Multiplexed Epitope-Based Tissue Imaging for Discovery and Healthcare Applications.* Cell Syst, 2016. 2(4): p. 225-38.

18. Mondal, M., R. Liao, and J. Guo, *Highly Multiplexed Single-Cell Protein Analysis.* Chemistry, 2018. 24(28): p. 7083-7091.

19. Stack, E.C., et al., *Multiplexed immunohistochemistry, imaging, and quantitation: a review, with an assessment of Tyramide signal amplification, multispectral imaging and multiplex analysis.* Methods, 2014. 70(1): p. 46-58.

20. Angelo, M., et al., *Multiplexed ion beam imaging of human breast tumors.* Nat Med, 2014. 20(4): p. 436-42.

21. Giesen, C., et al., *Highly multiplexed imaging of tumor tissues with subcellular resolution by mass cytometry.* Nat Methods, 2014. 11(4): p. 417-22.

22. Lin, J.R., et al., *Cyclic Immunofluorescence (CycIF), A Highly Multiplexed Method for Single-cell Imaging.* Curr Protoc Chem Biol, 2016. 8(4): p. 251-264.

23. Pirici, D., et al., *Antibody elution method for multiple immunohistochemistry on primary antibodies raised in the same species and of the same subtype.* J Histochem Cytochem, 2009. 57(6): p. 567-75.

24. Schubert, W., et al., *Analyzing proteome topology and function by automated multidimensional fluorescence microscopy.* Nat Biotechnol, 2006. 24(10): p. 1270-8.

25. Xiao, L. and J. Guo, *Multiplexed single-cell in situ RNA analysis by reiterative hybridization.* Analytical Methods, 2015. 7(17): p. 7290-7295.

26. Schweller, R.M., et al., *Multiplexed in situ immunofluorescence using dynamic DNA complexes.* Angew Chem Int Ed Engl, 2012. 51(37): p. 9292-6.

27. Lubeck, E., et al., *Single-cell in situ RNA profiling by sequential hybridization.* Nat Methods, 2014. 11(4): p. 360-1.

28. Lin, J.R., et al., *Highly multiplexed immunofluorescence imaging of human tissues and tumors using t-CyCIF and conventional optical microscopes.* Elife, 2018. 7.

29. Chen, K.H., et al., *RNA imaging. Spatially resolved, highly multiplexed RNA profiling in single cells.* Science, 2015. 348(6233): p. aaa6090.

30. Remark, R., et al., *In-depth tissue profiling using multiplexed immunohistochemical consecutive staining on single slide.* Science Immunology, 2016. 1(1).

31. Gerdes, M.J., et al., *Highly multiplexed single-cell analysis of formalin-fixed, paraffin-embedded cancer tissue.* Proc Natl Acad Sci U S A, 2013. 110(29): p. 11982-7.

32. Wang, Y., et al., *Rapid Sequential in Situ Multiplexing with DNA Exchange Imaging in Neuronal Cells and Tissues.* Nano Lett, 2017. 17(10): p. 6131-6139.

33. Mondal, M., et al., *Highly Multiplexed Single-Cell In Situ Protein Analysis with Cleavable Fluorescent Antibodies.* Angew Chem Int Ed Engl, 2017. 56(10): p. 2636-2639.

34. Mondal, M., et al., *Highly multiplexed single-cell in situ RNA and DNA analysis with bioorthogonal cleavable fluorescent oligonucleotides.* Chem Sci, 2018. 9(11): p. 2909-2917.

35. Choi, H.M., V.A. Beck, and N.A. Pierce, *Next-generation in situ hybridization chain reaction: higher gain, lower cost, greater durability.* ACS Nano, 2014. 8(5): p. 4284-94.

36. Wang, F., et al., *RNAscope: a novel in situ RNA analysis platform for formalin-fixed, paraffin-embedded tissues.* J Mol Diagn, 2012. 14(1): p. 22-9.

37. Zhu, P., et al., *IL-13 secreted by ILC2s promotes the self-renewal of intestinal stem cells through circular RNA circPan3.* Nat Immunol, 2019. 20(2): p. 183-194.

38. Lee, J.J., et al., *Human versus mouse eosinophils: "that which we call an eosinophil, by any other name would stain as red".* J Allergy Clin Immunol, 2012. 130(3): p. 572-84.

39. Rosenberg, H.F., *Eosinophil-derived neurotoxin / RNase 2: connecting the past, the present and the future.* Current pharmaceutical biotechnology, 2008. 9(3): p. 135-140.

40. Cates, E.C., et al., *Intranasal Exposure of Mice to House Dust Mite Elicits Allergic Airway Inflammation via a GM-CSF-Mediated Mechanism.* The Journal of Immunology, 2004. 173(10): p. 6384.

41. Le-Carlson, M., et al., *Markers of antigen presentation and activation on eosinophils and T cells in the esophageal tissue of patients with eosinophilic esophagitis.* J Pediatr Gastroenterol Nutr, 2013. 56(3): p. 257-62.

42. Jacobsen, E.A., et al., *Eosinophil activities modulate the immune/inflammatory character of allergic respiratory responses in mice.* Allergy, 2014. 69(3): p. 315-27.

43. Wright, B.L., et al., *Normalized serum eosinophil peroxidase levels are inversely correlated with esophageal eosinophilia in eosinophilic esophagitis.* Diseases of the Esophagus, 2017. 31(2).

44. Shi, S.R., Y. Shi, and C.R. Taylor, *Antigen retrieval immunohistochemistry: review and future prospects in research and diagnosis over two decades.* J Histochem Cytochem, 2011. 59(1): p. 13-32.

45. Tsujikawa, T., et al., *Quantitative multiplex immunohistochemistry reveals myeloid-inflamed tumor-immune complexity associated with poor prognosis.* Cell reports, 2017. 19(1): p. 203-217.

46. Gendusa, R., et al., *Elution of High-affinity (>10(-9) K(D)) Antibodies from Tissue Sections: Clues to the Molecular Mechanism and Use in Sequential Immunostaining.* Journal of Histochemistry and Cytochemistry, 2014. 62(7): p. 519-531.

47. Wong, D.T., et al., *Human eosinophils express transforming growth factor alpha.* J Exp Med, 1990. 172(3): p. 673-81.

48. Ohno, I., et al., *Granulocyte/macrophage colony-stimulating factor (GM-CSF) gene expression by eosinophils in nasal polyposis.* Am J Respir Cell Mol Biol, 1991. 5(6): p. 505-10.

49. Desreumaux, P., et al., *Interleukin 5 messenger RNA expression by eosinophils in the intestinal mucosa of patients with coeliac disease.* J Exp Med, 1992. 175(1): p. 293-6.

50. Finotto, S., et al., *TNF-alpha production by eosinophils in upper airways inflammation (nasal polyposis).* J Immunol, 1994. 153(5): p. 2278-89.

51. Bosse, M., et al., *Gene expression of interleukin-2 in purified human peripheral blood eosinophils.* Immunology, 1996. 87(1): p. 149-54.

52. Ying, S., et al., *Associations between IL-13 and IL-4 (mRNA and protein), vascular cell adhesion molecule-1 expression, and the infiltration of eosinophils, macrophages, and T cells in allergen-induced late-phase cutaneous reactions in atopic subjects.* Journal of Immunology, 1997. 158(10): p. 5050-5057.

53. Ellis, R.D., et al., *Selective binding of nucleotide probes by eosinophilic cationic protein during in situ hybridisation.* Histochem J, 2002. 34(3-4): p. 153-60.

54. Nitto, T., et al., *Characterization of the divergent eosinophil ribonuclease, mEar 6, and its expression in response to Schistosoma mansoni infection in vivo.* Genes & Immunity, 2004. 5(8): p. 668-674.

55. Domachowske, J.B., et al., *Eosinophil cationic protein/RNase 3 is another RNase A-family ribonuclease with direct antiviral activity.* Nucleic Acids Res, 1998. 26(14): p. 3358-63.

56. Yamada, K.J., et al., *Eosinophil-associated ribonuclease 11 is a macrophage chemoattractant.* J Biol Chem, 2015. 290(14): p. 8863-75.

57. Rosenberg, H.F., *Eosinophil-Derived Neurotoxin (EDN/RNase 2) and the Mouse Eosinophil-Associated RNases (mEars): Expanding Roles in Promoting Host Defense.* Int J Mol Sci, 2015. 16(7): p. 15442-55.

58. Hofman, P., et al., *Multiplexed Immunohistochemistry for Molecular and Immune Profiling in Lung Cancer-Just About Ready for Prime-Time?* Cancers, 2019. 11(3): p. 283.

CHAPTER 5

CONCLUSION

In conclusion, it is now appreciated that eosinophils are more than an end stage destructive cell solely in type 2 immune responses. They display different functions in various immune responses such as type 1 and type 2. These differing functions could be explained by different subtypes of eosinophils. To better understand their roles in health and disease this thesis tries to identify and characterize these eosinophils subtypes to answer these questions.

In chapter 2, I take a reductionist approach and developed an *in vitro* cytokine induced eosinophil model to simplify characterizing their unique features. This was done with the intent to identify unique biomolecules that could be used to identify and modulate subtypes *in vivo*. This approach avoids the difficulties of directly characterizing cell phenotypes *in vivo* where other cells have been shown to display a spectrum of phenotypes [253, 363]. We demonstrated that these *in vitro* subtypes displayed subtype specific characteristics that reflected features of eosinophils found *in vivo* such as morphology, cell surface marker expression, and protein mediator secretion; supporting the relevance to *in vivo* conditions. The results show that E1 eosinophils had reduced viability, expressed PDL1, MHC-I, ICAM-1 and the GR-1 antigen Ly6C, and released the type 1 mediators CXC9, CXCL10, and CCL5. These are all important for their functions interacting with CD8 T cells and functions in infection, cancer, and transplant [49, 164, 183]. E2 eosinophils on the other hand, displayed hypersegmented nuclei and cytoplasmic vacuoles, increased CD11b, ST2, F4/80 and Siglec-F expression, and secreted the type 2 mediators IL-6, IL-9, IL-13, CCL2, CCL3, CCL22, and CCL17.

These reflected the eosinophil characteristics typically found in allergic disease such as asthma [111, 170, 234]. Interestingly, E2 eosinophils and not E1 eosinophils degranulate, further suggesting that this subtype is more representative of the traditional eosinophil associated with type 2 diseases.

Sequencing their transcriptome was insightful in understanding the pathways that each subtype utilizes. Pathway analysis revealed the interferon pathways with STAT1 were activated in E1 eosinophils whereas in E2 eosinophils, MyD88, FYN, IRAK1, and MAPK interactions were dominant. Interestingly, evaluation into these pathways found the interferon regulator factors, IRF1 and IRF4, to be uniquely elevated in E1 and E2 eosinophils, respectively. These transcription factors are important regulators in other myeloid cells but have not been studied in eosinophils. These IRFs could also be stimulated in human eosinophils suggesting similar pathways might be conserved between species, suggesting the translational ability of this research.

These transcription factors are plastic in nature as cytokine stimulation can modulate and switch their expression in each subtype. This suggests that *in vivo*, eosinophils subtypes are potentially fluid, namely they can adapt to the changes in the microenvironment. For example, macrophage subtype switching is important for the healthy cycle of initiation and repression of inflammation [364]. Furthermore, these transcription factors can be utilized to modulate eosinophil responses *in vivo*. Eosinophil specific knockouts through cre recombinase would be useful in understanding the impact each subtype has in type 1 and type 2 models. Future studies will help to define if these IRFs are master regulators of type 1 and type 2 eosinophil subtypes.

In chapter 3, I introduced five eosinophil specific immunoassay staining protocols that allow the identification of eosinophils within tissue preps as well as single-cell suspensions. This is an improvement over older techniques that relied on dyes binding to their cationic granule proteins that were less specific in their staining for eosinophils. Moreover, certain eosinophil-associated diseases contain degranulated or lysed eosinophils whereby detection of the cells by dyes would be difficult and the free granule components would be difficult to identify [187]. As such pathological scoring of eosinophil infiltration would not accurately represent the total number of eosinophils influencing pathology. It was not until eosinophil specific antibodies were developed that the remnants (i.e., free granules) were able to be detected and visualized in tissues [186, 189]. Although this was an improvement for identifying eosinophil presence *in situ,* their functional roles remained to be defined. To include information on effector functions in the assessment of eosinophil in health and disease additional markers need to be included.

In Chapter 4, I developed staining techniques with the intent of identifying eosinophil subtypes and other immune cells simultaneously, to study eosinophil effector functions and interactions in tissues. In order to do this, I introduced a novel multiplex protocol that utilizes indirect IHC combined with cleavable tyramide dye. This allows multiplexing through cycles of staining, imaging and cleaving the fluorophores. Many different multiplex imaging techniques have been proposed, yet many of them are slow, complicated, expensive, and/or inefficient [192, 198, 203, 207]. The cleavable dye technique is quick and simple, only requiring 30-minute incubation with the reducing agent TCEP. The structure of my method allows quick adaptation to any lab already performing IHC. The protocol uses commercially available reagents and unlabeled

primary antibodies with only the cleavable dye not commercially available. With this approach, I combined the EPX IHC protocol from chapter 3 with 10 other antibodies to map the immune landscape of human biopsies. While I propose a panel of 11 antibodies, these antibodies can be swapped with others but will require some optimization such as testing stripping efficiency. Stripping efficiency is antibody dependent and variable due to antibody binding affinity. Improvements in stripping conditions, such as reducing tissue damage, will ultimately increase the maximum number of antibodies that can be combined onto a single tissue section. Future work will apply this panel to study the influences eosinophils subtypes and the immune landscape has on esophagus biopsies from Eosinophilic esophagitis (EoE). Furthermore, this is not limited to EoE, this panel can be applied to study eosinophil subtypes in all other eosinophil containing tissues.

5.1 References

1. Mosser, D.M. and J.P. Edwards, *Exploring the full spectrum of macrophage activation.* Nature Reviews Immunology, 2008. 8(12): p. 958-969.

2. Jablonski, K.A., et al., *Novel Markers to Delineate Murine M1 and M2 Macrophages.* PLoS One, 2015. 10(12): p. e0145342.

3. Carretero, R., et al., *Eosinophils orchestrate cancer rejection by normalizing tumor vessels and enhancing infiltration of CD8(+) T cells.* Nat Immunol, 2015. 16(6): p. 609-17.

4. Arnold, I.C., et al., *Eosinophils suppress Th1 responses and restrict bacterially induced gastrointestinal inflammation.* J Exp Med, 2018.

5. Onyema, O.O., et al., *Eosinophils promote inducible NOS-mediated lung allograft acceptance.* JCI Insight, 2017. 2(24).

6. Abdala Valencia, H., et al., *Phenotypic plasticity and targeting of Siglec-F(high) CD11c(low) eosinophils to the airway in a murine model of asthma.* Allergy, 2016. 71(2): p. 267-71.

7. Mesnil, C., et al., *Lung-resident eosinophils represent a distinct regulatory eosinophil subset.* J Clin Invest, 2016. 126(9): p. 3279-95.

8. Rose, C.E., Jr., et al., *Murine lung eosinophil activation and chemokine production in allergic airway inflammation.* Cell Mol Immunol, 2010. 7(5): p. 361-74.

9. Ortega-Gomez, A., M. Perretti, and O. Soehnlein, *Resolution of inflammation: an integrated view.* EMBO Mol Med, 2013. 5(5): p. 661-74.

10. Martin, L.J., et al., *Pediatric Eosinophilic Esophagitis Symptom Scores (PEESS v2.0) identify histologic and molecular correlates of the key clinical features of disease.* J Allergy Clin Immunol, 2015. 135(6): p. 1519-28.e8.

11. Wright, B.L., et al., *Normalized serum eosinophil peroxidase levels are inversely correlated with esophageal eosinophilia in eosinophilic esophagitis.* Diseases of the Esophagus, 2017. 31(2).

12. Protheroe, C., et al., *A novel histologic scoring system to evaluate mucosal biopsies from patients with eosinophilic esophagitis.* Clin Gastroenterol Hepatol, 2009. 7(7): p. 749-755.e11.

13. Angelo, M., et al., *Multiplexed ion beam imaging of human breast tumors.* Nat Med, 2014. 20(4): p. 436-42.

14. Gerdes, M.J., et al., *Highly multiplexed single-cell analysis of formalin-fixed, paraffin-embedded cancer tissue.* Proc Natl Acad Sci U S A, 2013. 110(29): p. 11982-7.

15. Lin, J.R., et al., *Highly multiplexed immunofluorescence imaging of human tissues and tumors using t-CyCIF and conventional optical microscopes.* Elife, 2018. 7.

16. Goltsev, Y., et al., *Deep Profiling of Mouse Splenic Architecture with CODEX Multiplexed Imaging.* Cell, 2018.

REFERENCES

1. Kay, A.B., *The early history of the eosinophil.* Clin Exp Allergy, 2015. 45(3): p. 575-82.

2. Lee, J.J., et al., *Human versus mouse eosinophils: "that which we call an eosinophil, by any other name would stain as red".* J Allergy Clin Immunol, 2012. 130(3): p. 572-84.

3. Park, Y.M. and B.S. Bochner, *Eosinophil survival and apoptosis in health and disease.* Allergy Asthma Immunol Res, 2010. 2(2): p. 87-101.

4. Fulkerson, P.C., *Transcription Factors in Eosinophil Development and As Therapeutic Targets.* Frontiers in Medicine, 2017. 4(115).

5. Zhang, D.-E., et al., *Absence of granulocyte colony-stimulating factor signaling and neutrophil development in CCAAT enhancer binding protein α-deficient mice.* Proceedings of the National Academy of Sciences, 1997. 94(2): p. 569-574.

6. Yamanaka, R., et al., *Impaired granulopoiesis, myelodysplasia, and early lethality in CCAAT/enhancer binding protein epsilon-deficient mice.* Proc Natl Acad Sci U S A, 1997. 94(24): p. 13187-92.

7. Tanaka, T., et al., *Targeted disruption of the NF-IL6 gene discloses its essential role in bacteria killing and tumor cytotoxicity by macrophages.* Cell, 1995. 80(2): p. 353-361.

8. Hirasawa, R., et al., *Essential and instructive roles of GATA factors in eosinophil development.* J Exp Med, 2002. 195(11): p. 1379-86.

9. Yu, C., et al., *Targeted deletion of a high-affinity GATA-binding site in the GATA-1 promoter leads to selective loss of the eosinophil lineage in vivo.* J Exp Med, 2002. 195(11): p. 1387-95.

10. Bettigole, S.E., et al., *The transcription factor XBP1 is selectively required for eosinophil differentiation.* Nature Immunology, 2015. 16(8): p. 829-837.

11. Rothenberg, M.E. and S.P. Hogan, *The eosinophil.* Annu Rev Immunol, 2006. 24: p. 147-74.

12. Sanderson, C.J., *Interleukin-5, eosinophils, and disease.* Blood, 1992. 79(12): p. 3101-9.

13. Geijsen, N., L. Koenderman, and P.J. Coffer, *Specificity in cytokine signal transduction: lessons learned from the IL-3/IL-5/GM-CSF receptor family.* Cytokine & Growth Factor Reviews, 2001. 12(1): p. 19-25.

14. Dent, L.A., et al., *Eosinophilia in transgenic mice expressing interleukin 5.* J Exp Med, 1990. 172(5): p. 1425-31.

15. Lee, N.A., et al., *Expression of IL-5 in thymocytes/T cells leads to the development of a massive eosinophilia, extramedullary eosinophilopoiesis, and unique histopathologies.* J Immunol, 1997. 158(3): p. 1332-44.

16. Yoshida, T., et al., *Defective B-1 cell development and impaired immunity against Angiostrongylus cantonensis in IL-5R alpha-deficient mice.* Immunity, 1996. 4(5): p. 483-94.

17. Kopf, M., et al., *IL-5-deficient mice have a developmental defect in CD5+ B-1 cells and lack eosinophilia but have normal antibody and cytotoxic T cell responses.* Immunity, 1996. 4(1): p. 15-24.

18. McGregor, M.C., et al., *Role of Biologics in Asthma.* American journal of respiratory and critical care medicine, 2019. 199(4): p. 433-445.

19. Yamaguchi, Y., et al., *Highly purified murine interleukin 5 (IL-5) stimulates eosinophil function and prolongs in vitro survival. IL-5 as an eosinophil chemotactic factor.* J Exp Med, 1988. 167(5): p. 1737-42.

20. Coeffier, E., D. Joseph, and B.B. Vargaftig, *Role of interleukin-5 in enhanced migration of eosinophils from airways of immunized guinea-pigs.* Br J Pharmacol, 1994. 113(3): p. 749-56.

21. Herndon, F.J. and S.G. Kayes, *Depletion of eosinophils by anti-IL-5 monoclonal antibody treatment of mice infected with Trichinella spiralis does not alter parasite burden or immunologic resistance to reinfection.* The Journal of Immunology, 1992. 149(11): p. 3642.

22. Johnston, L.K. and P.J. Bryce, *Understanding Interleukin 33 and Its Roles in Eosinophil Development.* Frontiers in Medicine, 2017. 4: p. 51.

23. Stolarski, B., et al., *IL-33 Exacerbates Eosinophil-Mediated Airway Inflammation.* The Journal of Immunology, 2010. 185(6): p. 3472-3480.

24. Dubucquoi, S., et al., *Interleukin 5 synthesis by eosinophils: association with granules and immunoglobulin-dependent secretion.* J Exp Med, 1994. 179(2): p. 703-8.

25. Shen, Z.J. and J.S. Malter, *Determinants of eosinophil survival and apoptotic cell death.* Apoptosis, 2015. 20(2): p. 224-34.

26. Rosenberg, H.F., *Eosinophil-Derived Neurotoxin (EDN/RNase 2) and the Mouse Eosinophil-Associated RNases (mEars): Expanding Roles in Promoting Host Defense.* Int J Mol Sci, 2015. 16(7): p. 15442-55.

27. Weller, P.F. and L.A. Spencer, *Functions of tissue-resident eosinophils.* Nature reviews. Immunology, 2017. 17(12): p. 746-760.

28. Schmitz, J., et al., *IL-33, an interleukin-1-like cytokine that signals via the IL-1 receptor-related protein ST2 and induces T helper type 2-associated cytokines.* Immunity, 2005. 23(5): p. 479-90.

29. Davoine, F. and P. Lacy, *Eosinophil Cytokines, Chemokines, and Growth Factors: Emerging Roles in Immunity.* Frontiers in Immunology, 2014. 5: p. 570.

30. Spencer, L.A., et al., *Eosinophil secretion of granule-derived cytokines.* Front Immunol, 2014. 5: p. 496.

31. Hamann, K.J., et al., *The molecular biology of eosinophil granule proteins.* Int Arch Allergy Appl Immunol, 1991. 94(1-4): p. 202-9.

32. Macias, M.P., et al., *Identification of a new murine eosinophil major basic protein (mMBP) gene: cloning and characterization of mMBP-2.* J Leukoc Biol, 2000. 67(4): p. 567-76.

33. Plager, D.A., et al., *A novel and highly divergent homolog of human eosinophil granule major basic protein.* J Biol Chem, 1999. 274(20): p. 14464-73.

34. Acharya, K.R. and S.J. Ackerman, *Eosinophil granule proteins: form and function.* J Biol Chem, 2014. 289(25): p. 17406-15.

35. G J Gleich, a. C R Adolphson, and K.M. Leiferman, *The Biology of the Eosinophilic Leukocyte.* Annual Review of Medicine, 1993. 44(1): p. 85-101.

36. Wasmoen, T.L., et al., *Biochemical and amino acid sequence analysis of human eosinophil granule major basic protein.* J Biol Chem, 1988. 263(25): p. 12559-63.

37. Gundel, R.H., L.G. Letts, and G.J. Gleich, *Human eosinophil major basic protein induces airway constriction and airway hyperresponsiveness in primates.* The Journal of Clinical Investigation, 1991. 87(4): p. 1470-1473.

38. Pégorier, S., et al., *Eosinophil-Derived Cationic Proteins Activate the Synthesis of Remodeling Factors by Airway Epithelial Cells.* The Journal of Immunology, 2006. 177(7): p. 4861-4869.

39. Jacoby, D.B., R.M. Costello, and A.D. Fryer, *Eosinophil recruitment to the airway nerves.* Journal of Allergy and Clinical Immunology, 2001. 107(2): p. 211-218.

40. Auriault, C., M. Capron, and A. Capron, *Activation of rat and human eosinophils by soluble factor(s) released by Schistosoma mansoni schistosomula.* Cellular Immunology, 1982. 66(1): p. 59-69.

41. Locksley, R.M., C.B. Wilson, and S.J. Klebanoff, *Role for Endogenous and Acquired Peroxidase in the Toxoplasmacidal Activity of Murine and Human Mononuclear Phagocytes.* The Journal of Clinical Investigation, 1982. 69(5): p. 1099-1111.

42. Colon, S., et al., *Peroxidasin and eosinophil peroxidase, but not myeloperoxidase, contribute to renal fibrosis in the murine unilateral ureteral obstruction model.* Am J Physiol Renal Physiol, 2019. 316(2): p. F360-f371.

43. Jacobsen, E.A., et al., *Lung Pathologies in a Chronic Inflammation Mouse Model Are Independent of Eosinophil Degranulation.* American Journal of Respiratory and Critical Care Medicine, 2017. 195(10): p. 1321-1332.

44. Zhang, J., K.D. Dyer, and H.F. Rosenberg, *Evolution of the rodent eosinophil-associated RNase gene family by rapid gene sorting and positive selection.* Proc Natl Acad Sci U S A, 2000. 97(9): p. 4701-6.

45. Yamada, K.J., et al., *Eosinophil-associated ribonuclease 11 is a macrophage chemoattractant.* J Biol Chem, 2015. 290(14): p. 8863-75.

46. Spencer, L.A., et al., *Human eosinophils constitutively express multiple Th1, Th2, and immunoregulatory cytokines that are secreted rapidly and differentially.* J Leukoc Biol, 2009. 85(1): p. 117-23.

47. Bandeira-Melo, C. and P.F. Weller, *Mechanisms of eosinophil cytokine release.* Mem Inst Oswaldo Cruz, 2005. 100 Suppl 1: p. 73-81.

48. Annunziato, F., C. Romagnani, and S. Romagnani, *The 3 major types of innate and adaptive cell-mediated effector immunity.* Journal of Allergy and Clinical Immunology, 2015. 135(3): p. 626-635.

49. Carretero, R., et al., *Eosinophils orchestrate cancer rejection by normalizing tumor vessels and enhancing infiltration of CD8(+) T cells.* Nat Immunol, 2015. 16(6): p. 609-17.

50. Willebrand, R. and D. Voehringer, *IL-33-Induced Cytokine Secretion and Survival of Mouse Eosinophils Is Promoted by Autocrine GM-CSF.* PLOS ONE, 2016. 11(9): p. e0163751.

51. Huang, L., et al., *Eosinophil-Derived IL-10 Supports Chronic Nematode Infection.* The Journal of Immunology, 2014. 193(8): p. 4178-4187.

52. Guerra, E.S., et al., *Central Role of IL-23 and IL-17 Producing Eosinophils as Immunomodulatory Effector Cells in Acute Pulmonary Aspergillosis and Allergic Asthma.* PLoS Pathog, 2017. 13(1): p. e1006175.

53. Oyoshi, M.K., et al., *Eosinophil-derived leukotriene C4 signals via type 2 cysteinyl leukotriene receptor to promote skin fibrosis in a mouse model of atopic dermatitis.* Proceedings of the National Academy of Sciences of the United States of America, 2012. 109(13): p. 4992-4997.

54. Isobe, Y., T. Kato, and M. Arita, *Emerging roles of eosinophils and eosinophil-derived lipid mediators in the resolution of inflammation.* Frontiers in immunology, 2012. 3: p. 270-270.

55. Ohno, I., et al., *Eosinophils as a source of matrix metalloproteinase-9 in asthmatic airway inflammation.* Am J Respir Cell Mol Biol, 1997. 16(3): p. 212-9.

56. Lee, J.J., et al., *Defining a link with asthma in mice congenitally deficient in eosinophils.* Science, 2004. 305(5691): p. 1773-6.

57. Jacobsen, E.A., et al., *Eosinophil activities modulate the immune/inflammatory character of allergic respiratory responses in mice.* Allergy, 2014. 69(3): p. 315-27.

58. Doyle, A.D., et al., *Homologous recombination into the eosinophil peroxidase locus generates a strain of mice expressing Cre recombinase exclusively in eosinophils.* Journal of leukocyte biology, 2013. 94(1): p. 17-24.

59. Ortaldo, J.R., et al., *Modulation of lymphocyte function with inhibitory CD2: Loss of NK and NKT cells.* Cellular Immunology, 2007. 249(1): p. 8-19.

60. Rosenthal, N. and S. Brown, *The mouse ascending: perspectives for human-disease models.* Nat Cell Biol, 2007. 9(9): p. 993-9.

61. McGarry, M.P., C.A. Protheroe, and J.J. Lee, *Mouse Hematology: A Laboratory Manual*. 2010: Cold Spring Harbor Laboratory Press.

62. Borchers, M.T., et al., *In vitro assessment of chemokine receptor-ligand interactions mediating mouse eosinophil migration.* J Leukoc Biol, 2002. 71(6): p. 1033-41.

63. Rot, A., et al., *RANTES and macrophage inflammatory protein 1 alpha induce the migration and activation of normal human eosinophil granulocytes.* The Journal of experimental medicine, 1992. 176(6): p. 1489-1495.

64. Das, A.M., et al., *Contrasting roles for RANTES and macrophage inflammatory protein-1 alpha (MIP-1 alpha) in a murine model of allergic peritonitis.* Clinical and experimental immunology, 1999. 117(2): p. 223-229.

65. Gonzalo, J.A., et al., *The coordinated action of CC chemokines in the lung orchestrates allergic inflammation and airway hyperresponsiveness.* The Journal of experimental medicine, 1998. 188(1): p. 157-167.

66. Lee, J.B., et al., *The role of RANTES in a murine model of food allergy.* Immunol Invest, 2004. 33(1): p. 27-38.

67. Schall, T.J., N.J. Simpson, and J.Y. Mak, *Molecular cloning and expression of the murine RANTES cytokine: structural and functional conservation between mouse and man.* Eur J Immunol, 1992. 22(6): p. 1477-81.

68. Coelho, A.L., et al., *The Chemokine CCL6 Promotes Innate Immunity via Immune Cell Activation and Recruitment.* The Journal of Immunology, 2007. 179(8): p. 5474-5482.

69. Lukawska, J.J., et al., *Real-time differential tracking of human neutrophil and eosinophil migration in vivo.* The Journal of allergy and clinical immunology, 2014. 133(1): p. 233-9.e1.

70. Liu, L.Y., et al., *Generation of Th1 and Th2 chemokines by human eosinophils: evidence for a critical role of TNF-alpha.* J Immunol, 2007. 179(7): p. 4840-8.

71. Esnault, S. and E.A. Kelly, *Essential Mechanisms of Differential Activation of Eosinophils by IL-3 Compared to GM-CSF and IL-5.* Critical reviews in immunology, 2016. 36(5): p. 429-444.

72. Bouffi, C., et al., *IL-33 markedly activates murine eosinophils by an NF-kappaB-dependent mechanism differentially dependent upon an IL-4-driven autoinflammatory loop.* J Immunol, 2013. 191(8): p. 4317-25.

73. Johansson, M.W., *Activation states of blood eosinophils in asthma.* Clin Exp Allergy, 2014. 44(4): p. 482-98.

74. Huang, L. and J.A. Appleton, *Eosinophils in Helminth Infection: Defenders and Dupes.* Trends in parasitology, 2016. 32(10): p. 798-807.

75. Lambrecht, B.N. and H. Hammad, *The immunology of asthma.* Nat Immunol, 2015. 16(1): p. 45-56.

76. Rosenberg, H.F., K.D. Dyer, and P.S. Foster, *Eosinophils: changing perspectives in health and disease.* Nat Rev Immunol, 2013. 13(1): p. 9-22.

77. McBrien, C.N. and A. Menzies-Gow, *The Biology of Eosinophils and Their Role in Asthma.* Frontiers in Medicine, 2017. 4(93).

78. Wardlaw, A.J., et al., *Eosinophils and Mast Cells in Bronchoalveolar Lavage in Subjects with Mild Asthma: Relationship to Bronchial Hyperreactivity.* American Review of Respiratory Disease, 1988. 137(1): p. 62-69.

79. Nair, P., et al., *Eosinophil peroxidase in sputum represents a unique biomarker of airway eosinophilia.* Allergy, 2013. 68(9): p. 1177-1184.

80. Blanchet, M.R., M.J. Gold, and K.M. McNagny, *Mouse models to evaluate the function of genes associated with allergic airway disease.* Curr Opin Allergy Clin Immunol, 2012. 12(5): p. 467-74.

81. Kumar, R.K., C. Herbert, and P.S. Foster, *Mouse models of acute exacerbations of allergic asthma.* Respirology, 2016. 21(5): p. 842-9.

82. Denzler, K.L., et al., *Eosinophil major basic protein-1 does not contribute to allergen-induced airway pathologies in mouse models of asthma.* J Immunol, 2000. 165(10): p. 5509-17.

83. Denzler, K.L., et al., *Extensive eosinophil degranulation and peroxidase-mediated oxidation of airway proteins do not occur in a mouse ovalbumin-challenge model of pulmonary inflammation.* J Immunol, 2001. 167(3): p. 1672-82.

84. Jacobsen, E.A., N.A. Lee, and J.J. Lee, *Re-defining the unique roles for eosinophils in allergic respiratory inflammation.* Clin Exp Allergy, 2014. 44(9): p. 1119-36.

85. Jacobsen, E.A., et al., *Allergic pulmonary inflammation in mice is dependent on eosinophil-induced recruitment of effector T cells.* Journal of Experimental Medicine, 2008. 205(3): p. 699-710.

86. Walsh, E.R., et al., *Strain-specific requirement for eosinophils in the recruitment of T cells to the lung during the development of allergic asthma.* J Exp Med, 2008. 205(6): p. 1285-92.

87. Akuthota, P., H.B. Wang, and P.F. Weller, *Eosinophils as antigen-presenting cells in allergic upper airway disease.* Current Opinion in Allergy and Clinical Immunology, 2010. 10(1): p. 14-19.

88. Shi, H.-Z., et al., *Lymph node trafficking and antigen presentation by endobronchial eosinophils.* The Journal of Clinical Investigation, 2000. 105(7): p. 945-953.

89. Jacobsen, E.A., et al., *Eosinophils Regulate Dendritic Cells and Th2 Pulmonary Immune Responses following Allergen Provocation.* The Journal of Immunology, 2011: p. 1102299.

90. Jacobsen, E.A., et al., *The expanding role(s) of eosinophils in health and disease.* Blood, 2012. 120(19): p. 3882-90.

91. Jacobsen, E.A., et al., *Differential activation of airway eosinophils induces IL-13-mediated allergic Th2 pulmonary responses in mice.* Allergy, 2015. 70(9): p. 1148-59.

92. Rothenberg, M.E., *Eosinophilic gastrointestinal disorders (EGID).* Journal of Allergy and Clinical Immunology, 2004. 113(1): p. 11-28.

93. Blanchard, C., et al., *Eotaxin-3 and a uniquely conserved gene-expression profile in eosinophilic esophagitis.* J Clin Invest, 2006. 116(2): p. 536-47.

94. Straumann, A., et al., *Anti-interleukin-5 antibody treatment (mepolizumab) in active eosinophilic oesophagitis: a randomised, placebo-controlled, double-blind trial.* Gut, 2010. 59(1): p. 21-30.

95. Takedatsu, H., et al., *Interleukin-5 participates in the pathogenesis of ileitis in SAMP1/Yit mice.* European journal of immunology, 2004. 34: p. 1561-9.

96. Lampinen, M., et al., *Different regulation of eosinophil activity in Crohn's disease compared with ulcerative colitis.* J Leukoc Biol, 2008. 84(6): p. 1392-9.

97. Lee, J.J., et al., *Eosinophils in health and disease: the LIAR hypothesis.* Clin Exp Allergy, 2010. 40(4): p. 563-75.

98. Marichal, T., C. Mesnil, and F. Bureau, *Homeostatic Eosinophils: Characteristics and Functions.* Frontiers in medicine, 2017. 4: p. 101-101.

99. Throsby, M., et al., *CD11c+ Eosinophils in the Murine Thymus: Developmental Regulation and Recruitment upon MHC Class I-Restricted Thymocyte Deletion.* The Journal of Immunology, 2000. 165(4): p. 1965-1975.

100. Ross , R. and S.J. Klebanoff *THE EOSINOPHILIC LEUKOCYTE : FINE STRUCTURE STUDIES OF CHANGES IN THE UTERUS DURING THE ESTROUS CYCLE.* Journal of Experimental Medicine, 1966. 124(4): p. 653-660.

101. Wang, D., et al., *Eosinophils are cellular targets of the novel uteroplacental heparin-binding cytokine decidual/trophoblast prolactin-related protein.* Journal of Endocrinology, 2000. 167(1): p. 15-28.

102. Timmons, B.C., A.-M. Fairhurst, and M.S. Mahendroo, *Temporal Changes in Myeloid Cells in the Cervix during Pregnancy and Parturition.* The Journal of Immunology, 2009. 182(5): p. 2700-2707.

103. Wu, D., et al., *Eosinophils Sustain Adipose Alternatively Activated Macrophages Associated with Glucose Homeostasis.* Science, 2011. 332(6026): p. 243-247.

104. Qiu, Y., et al., *Eosinophils and type 2 cytokine signaling in macrophages orchestrate development of functional beige fat.* Cell, 2014. 157(6): p. 1292-308.

105. Molofsky, A.B., et al., *Innate lymphoid type 2 cells sustain visceral adipose tissue eosinophils and alternatively activated macrophages.* J Exp Med, 2013. 210(3): p. 535-49.

106. Chu, V.T., et al., *Eosinophils promote generation and maintenance of immunoglobulin-A-expressing plasma cells and contribute to gut immune homeostasis.* Immunity, 2014. 40(4): p. 582-93.

107. Jung, Y., et al., *IL-1beta in eosinophil-mediated small intestinal homeostasis and IgA production.* Mucosal Immunol, 2015. 8(4): p. 930-42.

108. Sugawara, R., et al., *Small intestinal eosinophils regulate Th17 cells by producing IL-1 receptor antagonist.* Journal of Experimental Medicine, 2016. 213(4): p. 555-567.

109. Chen, H.H., et al., *Eosinophils from Murine Lamina Propria Induce Differentiation of Naive T Cells into Regulatory T Cells via TGF-beta1 and Retinoic Acid.* PLoS One, 2015. 10(11): p. e0142881.

110. Gouon-Evans, V., M.E. Rothenberg, and J.W. Pollard, *Postnatal mammary gland development requires macrophages and eosinophils.* Development, 2000. 127(11): p. 2269-82.

111. Mesnil, C., et al., *Lung-resident eosinophils represent a distinct regulatory eosinophil subset.* J Clin Invest, 2016. 126(9): p. 3279-95.

112. Fang, P., et al., *Immune cell subset differentiation and tissue inflammation.* J Hematol Oncol, 2018. 11(1): p. 97.

113. Cantor, H. and E.A. Boyse, *Functional subclasses of T-lymphocytes bearing different Ly antigens. I. The generation of functionally distinct T-cell subclasses is a differentiative process independent of antigen.* Journal of Experimental Medicine, 1975. 141(6): p. 1376-1389.

114. Marrack, P.C. and J.W. Kappler, *Antigen-specific and nonspecific mediators of T cell/B cell cooperation. I. Evidence for their production by different T cells.* J Immunol, 1975. 114(3): p. 1116-25.

115. Liew, F.Y. and C.R. Parish, *Lack of a correlation between cell-mediated immunity to the carrier and the carrier-hapten helper effect.* J Exp Med, 1974. 139(3): p. 779-84.

116. Janeway, C.A., Jr., *Cellular cooperation during in vivo anti-hapten antibody responses. I. The effect of cell number on the response.* J Immunol, 1975. 114(4): p. 1394-401.

117. Mosmann, T.R., et al., *Two types of murine helper T cell clone. I. Definition according to profiles of lymphokine activities and secreted proteins.* J Immunol, 1986. 136(7): p. 2348-57.

118. Seder, R.A., et al., *The presence of interleukin 4 during in vitro priming determines the lymphokine-producing potential of CD4+ T cells from T cell receptor transgenic mice.* Journal of Experimental Medicine, 1992. 176(4): p. 1091-1098.

119. Hsieh, C.S., et al., *Differential regulation of T helper phenotype development by interleukins 4 and 10 in an alpha beta T-cell-receptor transgenic system.* Proceedings of the National Academy of Sciences, 1992. 89(13): p. 6065-6069.

120. Hsieh, C., et al., *Development of TH1 CD4+ T cells through IL-12 produced by Listeria-induced macrophages.* Science, 1993. 260(5107): p. 547-549.

121. Seder, R.A., et al., *Interleukin 12 acts directly on CD4+ T cells to enhance priming for interferon gamma production and diminishes interleukin 4 inhibition of such priming.* Proceedings of the National Academy of Sciences, 1993. 90(21): p. 10188-10192.

122. Jacobson, N.G., et al., *Interleukin 12 signaling in T helper type 1 (Th1) cells involves tyrosine phosphorylation of signal transducer and activator of transcription (Stat)3 and Stat4.* Journal of Experimental Medicine, 1995. 181(5): p. 1755-1762.

123. Szabo, S.J., et al., *A Novel Transcription Factor, T-bet, Directs Th1 Lineage Commitment.* Cell, 2000. 100(6): p. 655-669.

124. Liew, F.Y., *T(H)1 and T(H)2 cells: a historical perspective.* Nat Rev Immunol, 2002. 2(1): p. 55-60.

125. Gajewski, T.F. and F.W. Fitch, *Anti-proliferative effect of IFN-gamma in immune regulation. I. IFN-gamma inhibits the proliferation of Th2 but not Th1 murine helper T lymphocyte clones.* J Immunol, 1988. 140(12): p. 4245-52.

126. Fernandez-Botran, R., et al., *Lymphokine-mediated regulation of the proliferative response of clones of T helper 1 and T helper 2 cells.* Journal of Experimental Medicine, 1988. 168(2): p. 543-558.

127. Golubovskaya, V. and L. Wu, *Different Subsets of T Cells, Memory, Effector Functions, and CAR-T Immunotherapy.* Cancers, 2016. 8(3): p. 36.

128. Vivier, E., et al., *Innate Lymphoid Cells: 10 Years On.* Cell, 2018. 174(5): p. 1054-1066.

129. Spits, H., et al., *Innate lymphoid cells--a proposal for uniform nomenclature.* Nat Rev Immunol, 2013. 13(2): p. 145-9.

130. Robinette, M.L., et al., *Transcriptional programs define molecular characteristics of innate lymphoid cell classes and subsets.* Nat Immunol, 2015. 16(3): p. 306-17.

131. Fang, P., et al., *Immune cell subset differentiation and tissue inflammation.* Journal of hematology & oncology, 2018. 11(1): p. 97-97.

132. Mills, C.D., et al., *M-1/M-2 Macrophages and the Th1/Th2 Paradigm.* The Journal of Immunology, 2000. 164(12): p. 6166-6173.

133. Murray, P.J. and T.A. Wynn, *Protective and pathogenic functions of macrophage subsets.* Nature Reviews Immunology, 2011. 11(11): p. 723-737.

134. Qian, B.Z. and J.W. Pollard, *Macrophage diversity enhances tumor progression and metastasis.* Cell, 2010. 141(1): p. 39-51.

135. Mantovani, A., et al., *The chemokine system in diverse forms of macrophage activation and polarization.* Trends Immunol, 2004. 25(12): p. 677-86.

136. Roszer, T., *Understanding the Mysterious M2 Macrophage through Activation Markers and Effector Mechanisms.* Mediators Inflamm, 2015. 2015: p. 816460.

137. Vu Manh, T.P., et al., *Investigating Evolutionary Conservation of Dendritic Cell Subset Identity and Functions.* Front Immunol, 2015. 6: p. 260.

138. Galli, S.J., N. Borregaard, and T.A. Wynn, *Phenotypic and functional plasticity of cells of innate immunity: macrophages, mast cells and neutrophils.* Nat Immunol, 2011. 12(11): p. 1035-44.

139. Villani, A.-C., et al., *Single-cell RNA-seq reveals new types of human blood dendritic cells, monocytes, and progenitors.* Science, 2017. 356(6335): p. eaah4573.

140. Gabriele, L. and K. Ozato, *The role of the interferon regulatory factor (IRF) family in dendritic cell development and function.* Cytokine Growth Factor Rev, 2007. 18(5-6): p. 503-10.

141. Chistiakov, D.A., et al., *The impact of interferon-regulatory factors to macrophage differentiation and polarization into M1 and M2.* Immunobiology, 2018. 223(1): p. 101-111.

142. Prin, L., et al., *Heterogeneity of human eosinophils. II. Variability of respiratory burst activity related to cell density.* Clinical and experimental immunology, 1984. 57(3): p. 735-742.

143. Prin, L., et al., *Heterogeneity of human peripheral blood eosinophils: variability in cell density and cytotoxic ability in relation to the level and the origin of hypereosinophilia.* Int Arch Allergy Appl Immunol, 1983. 72(4): p. 336-46.

144. Capron, M., et al., *Functional role of the alpha-chain of complement receptor type 3 in human eosinophil-dependent antibody-mediated cytotoxicity against schistosomes.* J Immunol, 1987. 139(6): p. 2059-65.

145. Rothenberg, M.E., et al., *Human eosinophils have prolonged survival, enhanced functional properties, and become hypodense when exposed to human interleukin 3.* J Clin Invest, 1988. 81(6): p. 1986-92.

146. Caulfield, J.P., et al., *A morphometric study of normodense and hypodense human eosinophils that are derived in vivo and in vitro.* Am J Pathol, 1990. 137(1): p. 27-41.

147. Ruhle, P.F., et al., *Development of a Modular Assay for Detailed Immunophenotyping of Peripheral Human Whole Blood Samples by Multicolor Flow Cytometry.* Int J Mol Sci, 2016. 17(8).

148. Ethier, C., P. Lacy, and F. Davoine, *Identification of human eosinophils in whole blood by flow cytometry.* Methods Mol Biol, 2014. 1178: p. 81-92.

149. Geslewitz, W.E., C.M. Percopo, and H.F. Rosenberg, *FACS isolation of live mouse eosinophils at high purity via a protocol that does not target Siglec F.* J Immunol Methods, 2018. 454: p. 27-31.

150. Dyer, K.D., et al., *Functionally competent eosinophils differentiated ex vivo in high purity from normal mouse bone marrow.* J Immunol, 2008. 181(6): p. 4004-9.

151. Liu, L.Y., et al., *Decreased expression of membrane IL-5 receptor alpha on human eosinophils: I. Loss of membrane IL-5 receptor alpha on airway eosinophils and increased soluble IL-5 receptor alpha in the airway after allergen challenge.* J Immunol, 2002. 169(11): p. 6452-8.

152. Wang, P., et al., *Selective inhibition of IL-5 receptor alpha-chain gene transcription by IL-5, IL-3, and granulocyte-macrophage colony-stimulating factor in human blood eosinophils.* J Immunol, 1998. 160(9): p. 4427-32.

153. Tomaki, M., et al., *Eosinophilopoiesis in a murine model of allergic airway eosinophilia: involvement of bone marrow IL-5 and IL-5 receptor alpha.* J Immunol, 2000. 165(7): p. 4040-50.

154. Gorski, S.A., et al., *Expression of IL-5 receptor alpha by murine and human lung neutrophils.* PLoS One, 2019. 14(8): p. e0221113.

155. Tateyama, H., et al., *Siglec-F is induced by granulocyte-macrophage colony-stimulating factor and enhances interleukin-4-induced expression of arginase-1 in mouse macrophages.* Immunology, 2019. 158(4): p. 340-352.

156. Bochner, B.S., *Siglec-8 on human eosinophils and mast cells, and Siglec-F on murine eosinophils, are functionally related inhibitory receptors.* Clin Exp Allergy, 2009. 39(3): p. 317-24.

157. Tateno, H., P.R. Crocker, and J.C. Paulson, *Mouse Siglec-F and human Siglec-8 are functionally convergent paralogs that are selectively expressed on eosinophils and recognize 6'-sulfo-sialyl Lewis X as a preferred glycan ligand.* Glycobiology, 2005. 15(11): p. 1125-35.

158. McGarry, M.P. and C.C. Stewart, *Murine eosinophil granulocytes bind the murine macrophage-monocyte specific monoclonal antibody F4/80.* J Leukoc Biol, 1991. 50(5): p. 471-8.

159. Hamann, J., et al., *EMR1, the human homolog of F4/80, is an eosinophil-specific receptor.* Eur J Immunol, 2007. 37(10): p. 2797-802.

160. Percopo, C.M., et al., *SiglecF+Gr1hi eosinophils are a distinct subpopulation within the lungs of allergen-challenged mice.* J Leukoc Biol, 2017. 101(1): p. 321-328.

161. Johansson, M.W., et al., *Characterization of Siglec-8 Expression on Lavage Cells after Segmental Lung Allergen Challenge.* Int Arch Allergy Immunol, 2018. 177(1): p. 16-28.

162. Diener, K.R., et al., *Multi-parameter flow cytometric analysis of uterine immune cell fluctuations over the murine estrous cycle.* Journal of Reproductive Immunology, 2016. 113: p. 61-67.

163. Xenakis, J.J., et al., *Resident intestinal eosinophils constitutively express antigen presentation markers and include two phenotypically distinct subsets of eosinophils.* Immunology, 2018. 154(2): p. 298-308.

164. Arnold, I.C., et al., *Eosinophils suppress Th1 responses and restrict bacterially induced gastrointestinal inflammation.* J Exp Med, 2018.

165. Boonpiyathad, T., et al., *Immunologic mechanisms in asthma.* Semin Immunol, 2019. 46: p. 101333.

166. Lambrecht, B.N., H. Hammad, and J.V. Fahy, *The Cytokines of Asthma.* Immunity, 2019. 50(4): p. 975-991.

167. Metcalfe, D.D., et al., *Biomarkers of the involvement of mast cells, basophils and eosinophils in asthma and allergic diseases.* World Allergy Organization Journal, 2016. 9(1): p. 7.

168. Johansson, M.W., *Eosinophil Activation Status in Separate Compartments and Association with Asthma.* Frontiers in Medicine, 2017. 4: p. 75.

169. Tak, T., et al., *Similar activation state of neutrophils in sputum of asthma patients irrespective of sputum eosinophilia.* Clin Exp Immunol, 2015. 182(2): p. 204-12.

170. Abdala Valencia, H., et al., *Phenotypic plasticity and targeting of Siglec-F(high) CD11c(low) eosinophils to the airway in a murine model of asthma.* Allergy, 2016. 71(2): p. 267-71.

171. Ochkur, S.I., et al., *Coexpression of IL-5 and Eotaxin-2 in Mice Creates an Eosinophil-Dependent Model of Respiratory Inflammation with Characteristics of Severe Asthma.* The Journal of Immunology, 2007. 178(12): p. 7879.

172. Le-Carlson, M., et al., *Markers of antigen presentation and activation on eosinophils and T cells in the esophageal tissue of patients with eosinophilic esophagitis.* J Pediatr Gastroenterol Nutr, 2013. 56(3): p. 257-62.

173. Venkateshaiah, S.U., et al., *Possible Noninvasive Biomarker of Eosinophilic Esophagitis: Clinical and Experimental Evidence.* Case reports in gastroenterology, 2016. 10(3): p. 685-692.

174. Nguyen, T., et al., *Immunophenotyping of peripheral eosinophils demonstrates activation in eosinophilic esophagitis.* J Pediatr Gastroenterol Nutr, 2011. 53(1): p. 40-7.

175. N., R., et al., *Distinct eosinophil cytokine expression patterns in skin diseases – the possible existence of functionally different eosinophil subpopulations.* Allergy, 2011. 66(11): p. 1477-1486.

176. Ryffel, B., *Introduction*, in *International Review of Experimental Pathology*, G.W. Richter and K. Solez, Editors. 1993, Academic Press. p. 3-6.

177. Velazquez, J.R., et al., *Effects of interferon-gamma on mobilization and release of eosinophil-derived RANTES.* Int Arch Allergy Immunol, 1999. 118(2-4): p. 447-9.

178. Handzel, Z.T., et al., *Eosinophils bind rhinovirus and activate virus-specific T cells.* J Immunol, 1998. 160(3): p. 1279-84.

179. Phipps, S., et al., *Eosinophils contribute to innate antiviral immunity and promote clearance of respiratory syncytial virus.* Blood, 2007. 110(5): p. 1578-86.

180. Samarasinghe, A.E., et al., *Eosinophils Promote Antiviral Immunity in Mice Infected with Influenza A Virus.* J Immunol, 2017. 198(8): p. 3214-3226.

181. Drake, M.G., et al., *Human and Mouse Eosinophils Have Antiviral Activity against Parainfluenza Virus.* Am J Respir Cell Mol Biol, 2016. 55(3): p. 387-94.

182. Dyer, K.D., et al., *Pneumoviruses infect eosinophils and elicit MyD88-dependent release of chemoattractant cytokines and interleukin-6.* Blood, 2009. 114(13): p. 2649-56.

183. Onyema, O.O., et al., *Eosinophils promote inducible NOS-mediated lung allograft acceptance.* JCI Insight, 2017. 2(24).

184. Onyema, O.O., et al., *Eosinophils downregulate lung alloimmunity by decreasing TCR signal transduction.* JCI Insight, 2019. 4(11).

185. Fischer, A.H., et al., *Hematoxylin and eosin staining of tissue and cell sections.* CSH Protoc, 2008. 2008: p. pdb.prot4986.

186. Wright, B.L., et al., *Normalized serum eosinophil peroxidase levels are inversely correlated with esophageal eosinophilia in eosinophilic esophagitis.* Diseases of the Esophagus, 2017. 31(2).

187. Martin, L.J., et al., *Pediatric Eosinophilic Esophagitis Symptom Scores (PEESS v2.0) identify histologic and molecular correlates of the key clinical features of disease.* J Allergy Clin Immunol, 2015. 135(6): p. 1519-28.e8.

188. Magaki, S., et al., *An Introduction to the Performance of Immunohistochemistry.* Methods Mol Biol, 2019. 1897: p. 289-298.

189. Protheroe, C., et al., *A novel histologic scoring system to evaluate mucosal biopsies from patients with eosinophilic esophagitis.* Clin Gastroenterol Hepatol, 2009. 7(7): p. 749-755.e11.

190. Wright, B.L., et al., *Baseline Gastrointestinal Eosinophilia Is Common in Oral Immunotherapy Subjects With IgE-Mediated Peanut Allergy.* Frontiers in Immunology, 2018. 9(2624).

191. Sonnenberg, G.F. and M.R. Hepworth, *Functional interactions between innate lymphoid cells and adaptive immunity.* Nature Reviews Immunology, 2019. 19(10): p. 599-613.

192. Goltsev, Y., et al., *Deep Profiling of Mouse Splenic Architecture with CODEX Multiplexed Imaging.* Cell, 2018.

193. Galon, J., et al., *Type, density, and location of immune cells within human colorectal tumors predict clinical outcome.* Science, 2006. 313(5795): p. 1960-4.

194. Stack, E.C., et al., *Multiplexed immunohistochemistry, imaging, and quantitation: a review, with an assessment of Tyramide signal amplification, multispectral imaging and multiplex analysis.* Methods, 2014. 70(1): p. 46-58.

195. Dickinson, M.E., et al., *Multi-spectral imaging and linear unmixing add a whole new dimension to laser scanning fluorescence microscopy.* Biotechniques, 2001. 31(6): p. 1272, 1274-6, 1278.

196. Mansfield, J.R., *Multispectral Imaging: A Review of Its Technical Aspects and Applications in Anatomic Pathology.* Veterinary Pathology, 2013. 51(1): p. 185-210.

197. Bandura, D.R., et al., *Mass cytometry: technique for real time single cell multitarget immunoassay based on inductively coupled plasma time-of-flight mass spectrometry.* Anal Chem, 2009. 81(16): p. 6813-22.

198. Angelo, M., et al., *Multiplexed ion beam imaging of human breast tumors.* Nat Med, 2014. 20(4): p. 436-42.

199. Giesen, C., et al., *Highly multiplexed imaging of tumor tissues with subcellular resolution by mass cytometry.* Nat Methods, 2014. 11(4): p. 417-22.

200. Bodenmiller, B., *Multiplexed Epitope-Based Tissue Imaging for Discovery and Healthcare Applications.* Cell Syst, 2016. 2(4): p. 225-38.

201. Glass, G., J.A. Papin, and J.W. Mandell, *SIMPLE: a sequential immunoperoxidase labeling and erasing method.* J Histochem Cytochem, 2009. 57(10): p. 899-905.

202. Pirici, D., et al., *Antibody elution method for multiple immunohistochemistry on primary antibodies raised in the same species and of the same subtype.* J Histochem Cytochem, 2009. 57(6): p. 567-75.

203. Gerdes, M.J., et al., *Highly multiplexed single-cell analysis of formalin-fixed, paraffin-embedded cancer tissue.* Proc Natl Acad Sci U S A, 2013. 110(29): p. 11982-7.

204. Schubert, W., et al., *Analyzing proteome topology and function by automated multidimensional fluorescence microscopy.* Nat Biotechnol, 2006. 24(10): p. 1270-8.

205. Wahlby, C., et al., *Sequential immunofluorescence staining and image analysis for detection of large numbers of antigens in individual cell nuclei.* Cytometry, 2002. 47(1): p. 32-41.

206. Adams, D.L., et al., *Multi-Phenotypic subtyping of circulating tumor cells using sequential fluorescent quenching and restaining.* Scientific Reports, 2016. 6: p. 33488.

207. Lin, J.R., et al., *Highly multiplexed immunofluorescence imaging of human tissues and tumors using t-CyCIF and conventional optical microscopes.* Elife, 2018. 7.

208. Bolognesi, M.M., et al., *Multiplex Staining by Sequential Immunostaining and Antibody Removal on Routine Tissue Sections.* Journal of Histochemistry & Cytochemistry, 2017. 65(8): p. 431-444.

209. Toth, Z.E. and E. Mezey, *Simultaneous visualization of multiple antigens with tyramide signal amplification using antibodies from the same species.* J Histochem Cytochem, 2007. 55(6): p. 545-54.

210. Carstens, J.L., et al., *Spatial computation of intratumoral T cells correlates with survival of patients with pancreatic cancer.* Nat Commun, 2017. 8: p. 15095.

211. Parra, E.R., et al., *Validation of multiplex immunofluorescence panels using multispectral microscopy for immune-profiling of formalin-fixed and paraffin-embedded human tumor tissues.* Scientific Reports, 2017. 7: p. 13380.

212. Tsujikawa, T., et al., *Quantitative multiplex immunohistochemistry reveals myeloid-inflamed tumor-immune complexity associated with poor prognosis.* Cell reports, 2017. 19(1): p. 203-217.

213. Lan, H.Y., et al., *A novel, simple, reliable, and sensitive method for multiple immunoenzyme staining: use of microwave oven heating to block antibody crossreactivity and retrieve antigens.* Journal of Histochemistry & Cytochemistry, 1995. 43(1): p. 97-102.

214. Gendusa, R., et al., *Elution of High-affinity (>10(-9) K(D)) Antibodies from Tissue Sections: Clues to the Molecular Mechanism and Use in Sequential Immunostaining.* Journal of Histochemistry and Cytochemistry, 2014. 62(7): p. 519-531.

215. Lin, J.R., M. Fallahi-Sichani, and P.K. Sorger, *Highly multiplexed imaging of single cells using a high-throughput cyclic immunofluorescence method.* Nat Commun, 2015. 6: p. 8390.

216. Wang, Y., et al., *Rapid Sequential in Situ Multiplexing with DNA Exchange Imaging in Neuronal Cells and Tissues.* Nano Lett, 2017. 17(10): p. 6131-6139.

217. Schweller, R.M., et al., *Multiplexed in situ immunofluorescence using dynamic DNA complexes.* Angew Chem Int Ed Engl, 2012. 51(37): p. 9292-6.

218. Vira, S., et al., *Fluorescent-labeled antibodies: Balancing functionality and degree of labeling.* Analytical Biochemistry, 2010. 402(2): p. 146-150.

219. Mondal, M., et al., *Highly Multiplexed Single-Cell In Situ Protein Analysis with Cleavable Fluorescent Antibodies.* Angew Chem Int Ed Engl, 2017. 56(10): p. 2636-2639.

220. Guo, J., *System and method for iterative detection of biological molecules*. 2018, Google Patents.

221. Mondal, M., et al., *Highly multiplexed single-cell in situ RNA and DNA analysis with bioorthogonal cleavable fluorescent oligonucleotides.* Chem Sci, 2018. 9(11): p. 2909-2917.

222. Bochner, B.S., *The eosinophil: For better or worse, in sickness and in health.* Ann Allergy Asthma Immunol, 2018. 121(2): p. 150-155.

223. Hong, C.W., *Current Understanding in Neutrophil Differentiation and Heterogeneity.* Immune Netw, 2017. 17(5): p. 298-306.

224. Cherry, W.B., et al., *A novel IL-1 family cytokine, IL-33, potently activates human eosinophils.* J Allergy Clin Immunol, 2008. 121(6): p. 1484-90.

225. Doyle, A.D., et al., *Eosinophil-derived IL-13 promotes emphysema.* Eur Respir J, 2019. 53(5).

226. Khoury, P., et al., *Revisiting the NIH Taskforce on the Research needs of Eosinophil-Associated Diseases (RE-TREAD).* Journal of Leukocyte Biology, 2018. 104(1): p. 69-83.

227. Czech, W., et al., *Induction of intercellular adhesion molecule 1 (ICAM-1) expression in normal human eosinophils by inflammatory cytokines.* J Invest Dermatol, 1993. 100(4): p. 417-23.

228. Zhang, M., et al., *Defining the in vivo function of Siglec-F, a CD33-related Siglec expressed on mouse eosinophils.* Blood, 2007. 109(10): p. 4280-4287.

229. Laumonnier, Y., et al., *Accumulation of pulmonary vacuolated eosinophils in experimental allergic asthma that synergize with dendritic cells to induce Th-17 cells.* Journal of Immunology, 2017. 198(1): p. 53.6.

230. Radonjic-Hoesli, S., et al., *Adhesion-induced eosinophil cytolysis requires the receptor-interacting protein kinase 3 (RIPK3)–mixed lineage kinase-like (MLKL) signaling pathway, which is counterregulated by autophagy.* Journal of Allergy and Clinical Immunology, 2017. 140(6): p. 1632-1642.

231. Muniz-Junqueira, M.I., S.M. Barbosa-Marques, and L.F. Junqueira, Jr., *Morphological changes in eosinophils are reliable markers of the severity of an acute asthma exacerbation in children.* Allergy, 2013. 68(7): p. 911-20.

232. Connell, J.T., *Morphological changes in eosinophils in allergic disease.* Journal of Allergy, 1968. 41(1): p. 1-9.

233. Melo, R.C.N., et al., *Eosinophil-derived cytokines in health and disease: unraveling novel mechanisms of selective secretion.* Allergy, 2013. 68(3): p. 274-284.

234. Rose, C.E., Jr., et al., *Murine lung eosinophil activation and chemokine production in allergic airway inflammation.* Cell Mol Immunol, 2010. 7(5): p. 361-74.

235. Dajotoy, T., et al., *Human eosinophils produce the T cell-attracting chemokines MIG and IP-10 upon stimulation with IFN-gamma.* J Leukoc Biol, 2004. 76(3): p. 685-91.

236. Tamura, T., et al., *The IRF family transcription factors in immunity and oncogenesis.* Annu Rev Immunol, 2008. 26: p. 535-84.

237. Ahyi, A.N., et al., *IFN regulatory factor 4 regulates the expression of a subset of Th2 cytokines.* J Immunol, 2009. 183(3): p. 1598-606.

238. Wen, T., et al., *Carbonic anhydrase IV is expressed on IL-5-activated murine eosinophils.* J Immunol, 2014. 192(12): p. 5481-9.

239. Esnault, S., et al., *Identification of genes expressed by human airway eosinophils after an in vivo allergen challenge.* PLoS One, 2013. 8(7): p. e67560.

240. Zhu, J. and W.E. Paul, *Heterogeneity and plasticity of T helper cells.* Cell Res, 2010. 20(1): p. 4-12.

241. Nam, S. and J.S. Lim, *Essential role of interferon regulatory factor 4 (IRF4) in immune cell development.* Arch Pharm Res, 2016. 39(11): p. 1548-1555.

242. Krausgruber, T., et al., *IRF5 promotes inflammatory macrophage polarization and TH1-TH17 responses.* Nat Immunol, 2011. 12(3): p. 231-8.

243. O'Sullivan, J.A. and B.S. Bochner, *Eosinophils and eosinophil-associated diseases: An update.* J Allergy Clin Immunol, 2018. 141(2): p. 505-517.

244. Berek, C., *Eosinophils can more than kill.* J Exp Med, 2018. 215(8): p. 1967-1969.

245. Ying, S., et al., *Phenotype of cells expressing mRNA for TH2-type (interleukin 4 and interleukin 5) and TH1-type (interleukin 2 and interferon gamma) cytokines in bronchoalveolar lavage and bronchial biopsies from atopic asthmatic and normal control subjects.* Am J Respir Cell Mol Biol, 1995. 12(5): p. 477-87.

246. Mosher, D.F., et al., *Proteomics of Eosinophil Activation.* Frontiers in medicine, 2017. 4: p. 159-159.

247. Esnault, S., et al., *IL-3 Maintains Activation of the p90S6K/RPS6 Pathway and Increases Translation in Human Eosinophils.* J Immunol, 2015. 195(6): p. 2529-39.

248. Nguyen, W.N.T., et al., *Intravital imaging of eosinophils: Unwrapping the enigma.* J Leukoc Biol, 2020.

249. Abdala-Valencia, H., et al., *Shaping eosinophil identity in the tissue contexts of development, homeostasis, and disease.* J Leukoc Biol, 2018. 104(1): p. 95-108.

250. Klion, A., *Recent advances in understanding eosinophil biology.* F1000Research, 2017. 6: p. 1084-1084.

251. Zheng, C., et al., *Landscape of Infiltrating T Cells in Liver Cancer Revealed by Single-Cell Sequencing.* Cell, 2017. 169(7): p. 1342-1356 e16.

252. Bjorklund, A.K., et al., *The heterogeneity of human CD127(+) innate lymphoid cells revealed by single-cell RNA sequencing.* Nat Immunol, 2016. 17(4): p. 451-60.

253. Jablonski, K.A., et al., *Novel Markers to Delineate Murine M1 and M2 Macrophages.* PLoS One, 2015. 10(12): p. e0145342.

254. Lacy, P., et al., *Rapid mobilization of intracellularly stored RANTES in response to interferon-gamma in human eosinophils.* Blood, 1999. 94(1): p. 23-32.

255. Grewe, M., et al., *Human eosinophils produce biologically active IL-12: implications for control of T cell responses.* J Immunol, 1998. 161(1): p. 415-20.

256. Johansson, M.W., et al., *Up-regulation and activation of eosinophil integrins in blood and airway after segmental lung antigen challenge.* Journal of immunology (Baltimore, Md. : 1950), 2008. 180(11): p. 7622-7635.

257. Mengelers, H.J., et al., *Down modulation of L-Selectin expression on eosinophils recovered from bronchoalveolar lavage fluid after allergen provocation.* Clin Exp Allergy, 1993. 23(3): p. 196-204.

258. In 't Veen, J., et al., *CD11b and L-selectin expression on eosinophils and neutrophils in blood and induced sputum of patients with asthma compared with normal subjects.* Clinical and experimental allergy : journal of the British Society for Allergy and Clinical Immunology, 1998. 28: p. 606-15.

259. Momose, T., et al., *Interferon-gamma increases CD62L expression on human eosinophils.* Int Arch Allergy Immunol, 1999. 120 Suppl 1: p. 30-3.

260. Chu, D.K., et al., *Indigenous enteric eosinophils control DCs to initiate a primary Th2 immune response in vivo.* The Journal of Experimental Medicine, 2014. 211(8): p. 1657.

261. Carlens, J., et al., *Common γ-Chain-Dependent Signals Confer Selective Survival of Eosinophils in the Murine Small Intestine.* The Journal of Immunology, 2009. 183(9): p. 5600.

262. Wang, H., et al., *CD69 expression on eosinophils is a marker of activation in the lung following allergen provocation.* Journal of Allergy and Clinical Immunology, 2004. 113(2, Supplement): p. S188.

263. Hartnell, A., et al., *CD69 is expressed by human eosinophils activated in vivo in asthma and in vitro by cytokines.* Immunology, 1993. 80(2): p. 281-6.

264. Shubin, A.V., et al., *Cytoplasmic vacuolization in cell death and survival.* Oncotarget, 2016. 7(34): p. 55863-55889.

265. Tai, P.C. and C.J. Spry, *The mechanisms which produce vacuolated and degranulated eosinophils.* Br J Haematol, 1981. 49(2): p. 219-26.

266. Melo, R.C.N. and P.F. Weller, *Unraveling the complexity of lipid body organelles in human eosinophils.* Journal of leukocyte biology, 2014. 96(5): p. 703-712.

267. Mathur, S.K., et al., *Interaction between allergy and innate immunity: model for eosinophil regulation of epithelial cell interferon expression.* Ann Allergy Asthma Immunol, 2013. 111(1): p. 25-31.

268. Diny, N.L., N.R. Rose, and D. Cihakova, *Eosinophils in Autoimmune Diseases.* Front Immunol, 2017. 8: p. 484.

269. Chu, V.T., et al., *Eosinophils are required for the maintenance of plasma cells in the bone marrow.* Nat Immunol, 2011. 12(2): p. 151-9.

270. Chu, V.T. and C. Berek, *Immunization induces activation of bone marrow eosinophils required for plasma cell survival.* Eur J Immunol, 2012. 42(1): p. 130-7.

271. Calcinotto, A., et al., *Microbiota-driven interleukin-17-producing cells and eosinophils synergize to accelerate multiple myeloma progression.* Nat Commun, 2018. 9(1): p. 4832.

272. Wong, T.W., et al., *Eosinophils regulate peripheral B cell numbers in both mice and humans.* J Immunol, 2014. 192(8): p. 3548-58.

273. Tong, Y., et al., *Elevated Plasma Chemokines for Eosinophils in Neuromyelitis Optica Spectrum Disorders during Remission.* Front Neurol, 2018. 9: p. 44.

274. Nascimento, F.R.F., et al., *Interferon Regulatory Factor (IRF)-1 Is a Master Regulator of the Cross Talk between Macrophages and L929 Fibrosarcoma Cells for Nitric Oxide Dependent Tumoricidal Activity.* PLOS ONE, 2015. 10(2): p. e0117782.

275. Lee, M.-C., et al., *GM-CSF– and IRF4-Dependent Signaling Can Regulate Myeloid Cell Numbers and the Macrophage Phenotype during Inflammation.* The Journal of Immunology, 2019: p. ji1801549.

276. Staudt, V., et al., *Interferon-Regulatory Factor 4 Is Essential for the Developmental Program of T Helper 9 Cells.* Immunity, 2010. 33(2): p. 192-202.

277. Yamamoto, M., et al., *Shared and distinct functions of the transcription factors IRF4 and IRF8 in myeloid cell development.* PLoS One, 2011. 6(10): p. e25812.

278. Honma, K., et al., *Interferon regulatory factor 4 differentially regulates the production of Th2 cytokines in naïve vs. effector/memory CD4⁺ T cells.* Proceedings of the National Academy of Sciences, 2008. 105(41): p. 15890-15895.

279. Mohapatra, A., et al., *Group 2 innate lymphoid cells utilize the IRF4-IL-9 module to coordinate epithelial cell maintenance of lung homeostasis.* Mucosal Immunol, 2016. 9(1): p. 275-86.

280. Ochkur, S.I., et al., *The development of a sensitive and specific ELISA for mouse eosinophil peroxidase: assessment of eosinophil degranulation ex vivo and in models of human disease.* J Immunol Methods, 2012. 375(1-2): p. 138-47.

281. Kalari, K.R., et al., *MAP-RSeq: Mayo Analysis Pipeline for RNA sequencing.* BMC Bioinformatics, 2014. 15(1): p. 224.

282. Dobin, A., et al., *STAR: ultrafast universal RNA-seq aligner.* Bioinformatics (Oxford, England), 2013. 29(1): p. 15-21.

283. Liao, Y., G.K. Smyth, and W. Shi, *featureCounts: an efficient general purpose program for assigning sequence reads to genomic features.* Bioinformatics, 2014. 30(7): p. 923-30.

284. Robinson, M.D., D.J. McCarthy, and G.K. Smyth, *edgeR: a Bioconductor package for differential expression analysis of digital gene expression data.* Bioinformatics (Oxford, England), 2010. 26(1): p. 139-140.

285. Kevin Blighe, S.R., Myles Lewis, *EnhancedVolcano: Publication-ready volcano plots with enhanced colouring and labeling. R package.* 2019, R.

286. Chen, J., et al., *ToppGene Suite for gene list enrichment analysis and candidate gene prioritization.* Nucleic acids research, 2009. 37(Web Server issue): p. W305-W311.

287. Walsh, G.M., et al., *Control of eosinophil toxicity in the lung.* Curr Drug Targets Inflamm Allergy, 2005. 4(4): p. 481-6.

288. Aleman, F., H.F. Lim, and P. Nair, *Eosinophilic Endotype of Asthma.* Immunol Allergy Clin North Am, 2016. 36(3): p. 559-68.

289. Kariyawasam, H.H. and D.S. Robinson, *The eosinophil: the cell and its weapons, the cytokines, its locations.* Semin Respir Crit Care Med, 2006. 27(2): p. 117-27.

290. Weller, P.F. and L.A. Spencer, *Functions of tissue-resident eosinophils.* Nat Rev Immunol, 2017. 17(12): p. 746-760.

291. Busse, W.W. and R.F. Lemanske, Jr., *Asthma.* N Engl J Med, 2001. 344(5): p. 350-62.

292. Hogan, S.P., et al., *Eosinophils: biological properties and role in health and disease.* Clin Exp Allergy, 2008. 38(5): p. 709-50.

293. Meyer-Martin, H., S. Reuter, and C. Taube, *Mouse models of allergic airway disease.* Methods Mol Biol, 2014. 1193: p. 127-41.

294. Marques-Garcia, F. and E. Marcos-Vadillo, *Review of Mouse Models Applied to the Study of Asthma.* Methods Mol Biol, 2016. 1434: p. 213-22.

295. Willetts, L., et al., *Vesicle-associated membrane protein 7-mediated eosinophil degranulation promotes allergic airway inflammation in mice.* Commun Biol, 2018. 1: p. 83.

296. Jacobsen, E.A., et al., *Lung Pathologies in a Chronic Inflammation Mouse Model Are Independent of Eosinophil Degranulation.* Am J Respir Crit Care Med, 2017. 195(10): p. 1321-1332.

297. Willetts, L., et al., *Immunodetection of occult eosinophils in lung tissue biopsies may help predict survival in acute lung injury.* Respir Res, 2011. 12: p. 116.

298. Kay, A.B., *Paul Ehrlich and the Early History of Granulocytes.* Microbiol Spectr, 2016. 4(4).

299. Meyerholz, D.K., et al., *Comparison of histochemical methods for murine eosinophil detection in an RSV vaccine-enhanced inflammation model.* Toxicol Pathol, 2009. 37(2): p. 249-55.

300. Ivell, R., K. Teerds, and G.E. Hoffman, *Proper application of antibodies for immunohistochemical detection: antibody crimes and how to prevent them.* Endocrinology, 2014. 155(3): p. 676-87.

301. Saper, C.B., *A guide to the perplexed on the specificity of antibodies.* J Histochem Cytochem, 2009. 57(1): p. 1-5.

302. Alkan, S.S., *Monoclonal antibodies: the story of a discovery that revolutionized science and medicine.* Nat Rev Immunol, 2004. 4(2): p. 153-6.

303. Ochkur, S.I., et al., *A sensitive high throughput ELISA for human eosinophil peroxidase: a specific assay to quantify eosinophil degranulation from patient-derived sources.* J Immunol Methods, 2012. 384(1-2): p. 10-20.

304. Feng, Y.H. and H. Mao, *Expression and preliminary functional analysis of Siglec-F on mouse macrophages.* J Zhejiang Univ Sci B, 2012. 13(5): p. 386-94.

305. Ochkur, S.I., et al., *Frontline Science: Eosinophil-deficient MBP-1 and EPX double-knockout mice link pulmonary remodeling and airway dysfunction with type 2 inflammation.* J Leukoc Biol, 2017. 102(3): p. 589-599.

306. Khoury, P., et al., *Revisiting the NIH Taskforce on the Research needs of Eosinophil-Associated Diseases (RE-TREAD).* J Leukoc Biol, 2018. 104(1): p. 69-83.

307. O'Hurley, G., et al., *Garbage in, garbage out: a critical evaluation of strategies used for validation of immunohistochemical biomarkers.* Mol Oncol, 2014. 8(4): p. 783-98.

308. Prost, S., et al., *Choice of Illumination System & Fluorophore for Multiplex Immunofluorescence on FFPE Tissue Sections.* PLoS One, 2016. 11(9): p. e0162419.

309. Donaldson, J.G., *Immunofluorescence Staining.* Curr Protoc Cell Biol, 2015. 69: p. 4 3 1-7.

310. Dixon, A.R., et al., *Recent developments in multiplexing techniques for immunohistochemistry.* Expert Rev Mol Diagn, 2015. 15(9): p. 1171-86.

311. Koh, J., et al., *High-Throughput Multiplex Immunohistochemical Imaging of the Tumor and Its Microenvironment.* Cancer Res Treat, 2019.

312. Anyaegbu, C.C., et al., *Optimisation of multiplex immunofluorescence for a non-spectral fluorescence scanning system.* J Immunol Methods, 2019. 472: p. 25-34.

313. Morton, J. and T.A. Snider, *Guidelines for collection and processing of lungs from aged mice for histological studies.* Pathobiol Aging Age Relat Dis, 2017. 7(1): p. 1313676.

314. Radulescu, R.T. and T. Boenisch, *Blocking endogenous peroxidases: a cautionary note for immunohistochemistry.* J Cell Mol Med, 2007. 11(6): p. 1419.

315. Garba, M.T. and P.J. Marie, *Alkaline phosphatase inhibition by levamisole prevents 1,25-dihydroxyvitamin D3-stimulated bone mineralization in the mouse.* Calcif Tissue Int, 1986. 38(5): p. 296-302.

316. Kim, S.W., J. Roh, and C.S. Park, *Immunohistochemistry for Pathologists: Protocols, Pitfalls, and Tips.* J Pathol Transl Med, 2016. 50(6): p. 411-418.

317. Petersen, K.H., J. Lohse, and L. Ramsgaard, *Automated sequential chromogenic IHC double staining with two HRP substrates.* PLoS One, 2018. 13(11): p. e0207867.

318. Osman, T.A., et al., *Successful triple immunoenzymatic method employing primary antibodies from same species and same immunoglobulin subclass.* Eur J Histochem, 2013. 57(3): p. e22.

319. Shi, S.R., Y. Shi, and C.R. Taylor, *Antigen retrieval immunohistochemistry: review and future prospects in research and diagnosis over two decades.* J Histochem Cytochem, 2011. 59(1): p. 13-32.

320. Shi, S.R., M.E. Key, and K.L. Kalra, *Antigen retrieval in formalin-fixed, paraffin-embedded tissues: an enhancement method for immunohistochemical staining based on microwave oven heating of tissue sections.* J Histochem Cytochem, 1991. 39(6): p. 741-8.

321. Mahmoudian, J., et al., *Comparison of the Photobleaching and Photostability Traits of Alexa Fluor 568- and Fluorescein Isothiocyanate- conjugated Antibody.* Cell J, 2011. 13(3): p. 169-72.

322. Davis, A.S., et al., *Characterizing and Diminishing Autofluorescence in Formalin-fixed Paraffin-embedded Human Respiratory Tissue.* J Histochem Cytochem, 2014. 62(6): p. 405-423.

323. Lum, H. and W. Mitzner, *Effects of 10% formalin fixation on fixed lung volume and lung tissue shrinkage. A comparison of eleven laboratory species.* Am Rev Respir Dis, 1985. 132(5): p. 1078-83.

324. Limjunyawong, N., J. Mock, and W. Mitzner, *Instillation and Fixation Methods Useful in Mouse Lung Cancer Research.* J Vis Exp, 2015(102): p. e52964.

325. Boivin, G.P., et al., *Review of CO(2) as a Euthanasia Agent for Laboratory Rats and Mice.* J Am Assoc Lab Anim Sci, 2017. 56(5): p. 491-499.

326. Fisher, S., et al., *Interstrain Differences in CO2-Induced Pulmonary Hemorrhage in Mice.* J Am Assoc Lab Anim Sci, 2016. 55(6): p. 811-815.

327. Schoell, A.R., et al., *Euthanasia method for mice in rapid time-course pulmonary pharmacokinetic studies.* J Am Assoc Lab Anim Sci, 2009. 48(5): p. 506-11.

328. Van Hoecke, L., et al., *Bronchoalveolar Lavage of Murine Lungs to Analyze Inflammatory Cell Infiltration.* J Vis Exp, 2017(123).

329. Bass, B.P., et al., *A review of preanalytical factors affecting molecular, protein, and morphological analysis of formalin-fixed, paraffin-embedded (FFPE) tissue: how well do you know your FFPE specimen?* Arch Pathol Lab Med, 2014. 138(11): p. 1520-30.

330. Bogen, S.A., K. Vani, and S.R. Sompuram, *Molecular mechanisms of antigen retrieval: antigen retrieval reverses steric interference caused by formalin-induced cross-links.* Biotech Histochem, 2009. 84(5): p. 207-15.

331. Reichman, H., P. Rozenberg, and A. Munitz, *Mouse Eosinophils: Identification, Isolation, and Functional Analysis.* Curr Protoc Immunol, 2017. 119: p. 14 43 1-14 43 22.

332. Kajimura, J., et al., *Optimization of Single- and Dual-Color Immunofluorescence Protocols for Formalin-Fixed, Paraffin-Embedded Archival Tissues.* J Histochem Cytochem, 2016. 64(2): p. 112-24.

333. Isidro, R.A., et al., *Double immunofluorescent staining of rat macrophages in formalin-fixed paraffin-embedded tissue using two monoclonal mouse antibodies.* Histochem Cell Biol, 2015. 144(6): p. 613-21.

334. Ray, A., T.B. Oriss, and S.E. Wenzel, *Emerging molecular phenotypes of asthma.* Am J Physiol Lung Cell Mol Physiol, 2015. 308(2): p. L130-40.

335. Reichman, H., et al., *Activated Eosinophils Exert Antitumorigenic Activities in Colorectal Cancer.* Cancer Immunol Res, 2019. 7(3): p. 388-400.

336. Chojnacki, A., et al., *Intravital imaging allows real-time characterization of tissue resident eosinophils.* Commun Biol, 2019. 2: p. 181.

337. Barnig, C., et al., *Circulating Human Eosinophils Share a Similar Transcriptional Profile in Asthma and Other Hypereosinophilic Disorders.* PLoS One, 2015. 10(11): p. e0141740.

338. Levsky, J.M. and R.H. Singer, *Fluorescence in situ hybridization: past, present and future.* J Cell Sci, 2003. 116(Pt 14): p. 2833-8.

339. Ramos-Vara, J.A., *Principles and methods of immunohistochemistry.* Methods Mol Biol, 2011. 691: p. 83-96.

340. Raj, A., et al., *Imaging individual mRNA molecules using multiple singly labeled probes.* Nat Methods, 2008. 5(10): p. 877-9.

341. Levenson, R.M., A.D. Borowsky, and M. Angelo, *Immunohistochemistry and mass spectrometry for highly multiplexed cellular molecular imaging.* Laboratory Investigation, 2015. 95(4): p. 397-405.

342. Mondal, M., R. Liao, and J. Guo, *Highly Multiplexed Single-Cell Protein Analysis.* Chemistry, 2018. 24(28): p. 7083-7091.

343. Lin, J.R., et al., *Cyclic Immunofluorescence (CycIF), A Highly Multiplexed Method for Single-cell Imaging.* Curr Protoc Chem Biol, 2016. 8(4): p. 251-264.

344. Xiao, L. and J. Guo, *Multiplexed single-cell in situ RNA analysis by reiterative hybridization.* Analytical Methods, 2015. 7(17): p. 7290-7295.

345. Lubeck, E., et al., *Single-cell in situ RNA profiling by sequential hybridization.* Nat Methods, 2014. 11(4): p. 360-1.

346. Chen, K.H., et al., *RNA imaging. Spatially resolved, highly multiplexed RNA profiling in single cells.* Science, 2015. 348(6233): p. aaa6090.

347. Remark, R., et al., *In-depth tissue profiling using multiplexed immunohistochemical consecutive staining on single slide.* Science Immunology, 2016. 1(1).

348. Choi, H.M., V.A. Beck, and N.A. Pierce, *Next-generation in situ hybridization chain reaction: higher gain, lower cost, greater durability.* ACS Nano, 2014. 8(5): p. 4284-94.

349. Wang, F., et al., *RNAscope: a novel in situ RNA analysis platform for formalin-fixed, paraffin-embedded tissues.* J Mol Diagn, 2012. 14(1): p. 22-9.

350. Zhu, P., et al., *IL-13 secreted by ILC2s promotes the self-renewal of intestinal stem cells through circular RNA circPan3.* Nat Immunol, 2019. 20(2): p. 183-194.

351. Rosenberg, H.F., *Eosinophil-derived neurotoxin / RNase 2: connecting the past, the present and the future.* Current pharmaceutical biotechnology, 2008. 9(3): p. 135-140.

352. Cates, E.C., et al., *Intranasal Exposure of Mice to House Dust Mite Elicits Allergic Airway Inflammation via a GM-CSF-Mediated Mechanism.* The Journal of Immunology, 2004. 173(10): p. 6384.

353. Wong, D.T., et al., *Human eosinophils express transforming growth factor alpha.* J Exp Med, 1990. 172(3): p. 673-81.

354. Ohno, I., et al., *Granulocyte/macrophage colony-stimulating factor (GM-CSF) gene expression by eosinophils in nasal polyposis.* Am J Respir Cell Mol Biol, 1991. 5(6): p. 505-10.

355. Desreumaux, P., et al., *Interleukin 5 messenger RNA expression by eosinophils in the intestinal mucosa of patients with coeliac disease.* J Exp Med, 1992. 175(1): p. 293-6.

356. Finotto, S., et al., *TNF-alpha production by eosinophils in upper airways inflammation (nasal polyposis).* J Immunol, 1994. 153(5): p. 2278-89.

357. Bosse, M., et al., *Gene expression of interleukin-2 in purified human peripheral blood eosinophils.* Immunology, 1996. 87(1): p. 149-54.

358. Ying, S., et al., *Associations between IL-13 and IL-4 (mRNA and protein), vascular cell adhesion molecule-1 expression, and the infiltration of eosinophils, macrophages, and T cells in allergen-induced late-phase cutaneous reactions in atopic subjects.* Journal of Immunology, 1997. 158(10): p. 5050-5057.

359. Ellis, R.D., et al., *Selective binding of nucleotide probes by eosinophilic cationic protein during in situ hybridisation.* Histochem J, 2002. 34(3-4): p. 153-60.

360. Nitto, T., et al., *Characterization of the divergent eosinophil ribonuclease, mEar 6, and its expression in response to Schistosoma mansoni infection in vivo.* Genes & Immunity, 2004. 5(8): p. 668-674.

361. Domachowske, J.B., et al., *Eosinophil cationic protein/RNase 3 is another RNase A-family ribonuclease with direct antiviral activity.* Nucleic Acids Res, 1998. 26(14): p. 3358-63.

362. Hofman, P., et al., *Multiplexed Immunohistochemistry for Molecular and Immune Profiling in Lung Cancer-Just About Ready for Prime-Time?* Cancers, 2019. 11(3): p. 283.

363. Mosser, D.M. and J.P. Edwards, *Exploring the full spectrum of macrophage activation.* Nature Reviews Immunology, 2008. 8(12): p. 958-969.

364. Ortega-Gomez, A., M. Perretti, and O. Soehnlein, *Resolution of inflammation: an integrated view.* EMBO Mol Med, 2013. 5(5): p. 661-74.

APPENDIX A

[COPYRIGHT AND PERMISSIONS]

Chapter 3 has been submitted for publication in 2020. Material From: Christopher D. Nazaroff, William E. LeSuer, Mia Y. Masuda, Grace Pyon, Paige Lacy, Elizabeth A. Jacobsen, Assessment of Lung Eosinophils *in situ* using Immunohistological Staining, Methods in Molecular Biology, 2020, © 2020 Springer Nature Switzerland AG. Springer is part of Springer Nature.

Reproduced with permission from Springer.

From: Journalpermissions <journalpermissions@springernature.com>
Subject: RE: Re-use of authored content
Date: March 30, 2020 at 8:29:31 AM MST
To: Christopher Nazaroff <cnazarof@asu.edu>

Dear Chris,

Thank you for your recent email. Per your retained rights you can reuse your article in your thesis/dissertation without obtaining permission from us. **If the material is being reused prior to publication by us, please make your editor/editorial contact aware of your intended use.**

Copyright statement should read – 'Accepted and soon to be published; article name, journal, and publisher name'.

If you have any further questions, please contact me directly.

Best wishes,
Oda

Oda Siqveland
Rights Executive

SpringerNature
The Campus, 4 Crinan Street, London N1 9XW,
United Kingdom
T +44 (0) 207 014 6851

http://www.nature.com
http://www.springer.com
http://www.palgrave.com